

UNCLASSIFIED

AD NUMBER

AD841504

LIMITATION CHANGES

TO:

Approved for public release; distribution is unlimited.

FROM:

**Distribution authorized to U.S. Gov't. agencies and their contractors;
Administrative/Operational Use; AUG 1968. Other requests shall be referred to Rome Air Development Center, Griffiss AFB, NY.**

AUTHORITY

RADC ltr 31 Jan 1974

THIS PAGE IS UNCLASSIFIED

AD84150.4

RADC-TR-68-300
Final Report



RANGE AND ANGLE CALIBRATION FACILITY STUDY

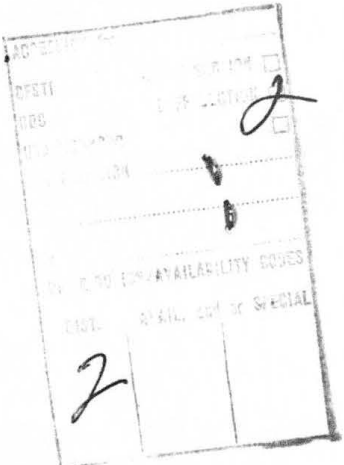
Dr. Robert L. Richardson
Syracuse University Research Corporation

TECHNICAL REPORT NO. RADC-TR-68-300
August 1968

THIS DOCUMENT IS SUBJECT TO SPECIAL
EXPORT CONTROLS AND EACH TRANSMITTAL
TO FOREIGN GOVERNMENTS, FOREIGN NA-
TIONALS OR REPRESENTATIVES THERETO
MAY BE MADE ONLY WITH PRIOR APPROVAL
OF RADC (EMASI), GAFB, N.Y.

226
227
228
229
230
231
232
233
234
235
236
237
238
239
240
241
242
243
244
245
246
247
248
249
250
251
252
253
254
255
256
257
258
259
260
261
262
263
264
265
266
267
268
269
270
271
272
273
274
275
276
277
278
279
280
281
282
283
284
285
286
287
288
289
290
291
292
293
294
295
296
297
298
299
300
301
302
303
304
305
306
307
308
309
310
311
312
313
314
315
316
317
318
319
320
321
322
323
324
325
326
327
328
329
330
331
332
333
334
335
336
337
338
339
340
341
342
343
344
345
346
347
348
349
350
351
352
353
354
355
356
357
358
359
360
361
362
363
364
365
366
367
368
369
370
371
372
373
374
375
376
377
378
379
380
381
382
383
384
385
386
387
388
389
390
391
392
393
394
395
396
397
398
399
400
401
402
403
404
405
406
407
408
409
410
411
412
413
414
415
416
417
418
419
420
421
422
423
424
425
426
427
428
429
430
431
432
433
434
435
436
437
438
439
440
441
442
443
444
445
446
447
448
449
450
451
452
453
454
455
456
457
458
459
460
461
462
463
464
465
466
467
468
469
470
471
472
473
474
475
476
477
478
479
480
481
482
483
484
485
486
487
488
489
490
491
492
493
494
495
496
497
498
499
500
501
502
503
504
505
506
507
508
509
510
511
512
513
514
515
516
517
518
519
520
521
522
523
524
525
526
527
528
529
530
531
532
533
534
535
536
537
538
539
540
541
542
543
544
545
546
547
548
549
550
551
552
553
554
555
556
557
558
559
560
561
562
563
564
565
566
567
568
569
570
571
572
573
574
575
576
577
578
579
580
581
582
583
584
585
586
587
588
589
590
591
592
593
594
595
596
597
598
599
600
601
602
603
604
605
606
607
608
609
610
611
612
613
614
615
616
617
618
619
620
621
622
623
624
625
626
627
628
629
630
631
632
633
634
635
636
637
638
639
640
641
642
643
644
645
646
647
648
649
650
651
652
653
654
655
656
657
658
659
660
661
662
663
664
665
666
667
668
669
670
671
672
673
674
675
676
677
678
679
680
681
682
683
684
685
686
687
688
689
690
691
692
693
694
695
696
697
698
699
700
701
702
703
704
705
706
707
708
709
710
711
712
713
714
715
716
717
718
719
720
721
722
723
724
725
726
727
728
729
730
731
732
733
734
735
736
737
738
739
740
741
742
743
744
745
746
747
748
749
750
751
752
753
754
755
756
757
758
759
760
761
762
763
764
765
766
767
768
769
770
771
772
773
774
775
776
777
778
779
770
771
772
773
774
775
776
777
778
779
780
781
782
783
784
785
786
787
788
789
790
791
792
793
794
795
796
797
798
799
800
801
802
803
804
805
806
807
808
809
8010
8011
8012
8013
8014
8015
8016
8017
8018
8019
8020
8021
8022
8023
8024
8025
8026
8027
8028
8029
8030
8031
8032
8033
8034
8035
8036
8037
8038
8039
8040
8041
8042
8043
8044
8045
8046
8047
8048
8049
8050
8051
8052
8053
8054
8055
8056
8057
8058
8059
8060
8061
8062
8063
8064
8065
8066
8067
8068
8069
8070
8071
8072
8073
8074
8075
8076
8077
8078
8079
8080
8081
8082
8083
8084
8085
8086
8087
8088
8089
8090
8091
8092
8093
8094
8095
8096
8097
8098
8099
80100
80101
80102
80103
80104
80105
80106
80107
80108
80109
80110
80111
80112
80113
80114
80115
80116
80117
80118
80119
80120
80121
80122
80123
80124
80125
80126
80127
80128
80129
80130
80131
80132
80133
80134
80135
80136
80137
80138
80139
80140
80141
80142
80143
80144
80145
80146
80147
80148
80149
80150
80151
80152
80153
80154
80155
80156
80157
80158
80159
80160
80161
80162
80163
80164
80165
80166
80167
80168
80169
80170
80171
80172
80173
80174
80175
80176
80177
80178
80179
80180
80181
80182
80183
80184
80185
80186
80187
80188
80189
80190
80191
80192
80193
80194
80195
80196
80197
80198
80199
80200
80201
80202
80203
80204
80205
80206
80207
80208
80209
80210
80211
80212
80213
80214
80215
80216
80217
80218
80219
80220
80221
80222
80223
80224
80225
80226
80227
80228
80229
80230
80231
80232
80233
80234
80235
80236
80237
80238
80239
80240
80241
80242
80243
80244
80245
80246
80247
80248
80249
80250
80251
80252
80253
80254
80255
80256
80257
80258
80259
80260
80261
80262
80263
80264
80265
80266
80267
80268
80269
80270
80271
80272
80273
80274
80275
80276
80277
80278
80279
80280
80281
80282
80283
80284
80285
80286
80287
80288
80289
80290
80291
80292
80293
80294
80295
80296
80297
80298
80299
80300
80301
80302
80303
80304
80305
80306
80307
80308
80309
80310
80311
80312
80313
80314
80315
80316
80317
80318
80319
80320
80321
80322
80323
80324
80325
80326
80327
80328
80329
80330
80331
80332
80333
80334
80335
80336
80337
80338
80339
80340
80341
80342
80343
80344
80345
80346
80347
80348
80349
80350
80351
80352
80353
80354
80355
80356
80357
80358
80359
80360
80361
80362
80363
80364
80365
80366
80367
80368
80369
80370
80371
80372
80373
80374
80375
80376
80377
80378
80379
80380
80381
80382
80383
80384
80385
80386
80387
80388
80389
80390
80391
80392
80393
80394
80395
80396
80397
80398
80399
80400
80401
80402
80403
80404
80405
80406
80407
80408
80409
80410
80411
80412
80413
80414
80415
80416
80417
80418
80419
80420
80421
80422
80423
80424
80425
80426
80427
80428
80429
80430
80431
80432
80433
80434
80435
80436
80437
80438
80439
80440
80441
80442
80443
80444
80445
80446
80447
80448
80449
80450
80451
80452
80453
80454
80455
80456
80457
80458
80459
80460
80461
80462
80463
80464
80465
80466
80467
80468
80469
80470
80471
80472
80473
80474
80475
80476
80477
80478
80479
80480
80481
80482
80483
80484
80485
80486
80487
80488
80489
80490
80491
80492
80493
80494
80495
80496
80497
80498
80499
80500
80501
80502
80503
80504
80505
80506
80507
80508
80509
80510
80511
80512
80513
80514
80515
80516
80517
80518
80519
80520
80521
80522
80523
80524
80525
80526
80527
80528
80529
80530
80531
80532
80533
80534
80535
80536
80537
80538
80539
80540
80541
80542
80543
80544
80545
80546
80547
80548
80549
80550
80551
80552
80553
80554
80555
80556
80557
80558
80559
80560
80561
80562
80563
80564
80565
80566
80567
80568
80569
80570
80571
80572
80573
80574
80575
80576
80577
80578
80579
80580
80581
80582
80583
80584
80585
80586
80587
80588
80589
80590
80591
80592
80593
80594
80595
80596
80597
80598
80599
80600
80601
80602
80603
80604
80605
80606
80607
80608
80609
80610
80611
80612
80613
80614
80615
80616
80617
80618
80619
80620
80621
80622
80623
80624
80625
80626
80627
80628
80629
80630
80631
80632
80633
80634
80635
80636
80637
80638
80639
80640
80641
80642
80643
80644
80645
80646
80647
80648
80649
80650
80651
80652
80653
80654
80655
80656
80657
80658
80659
80660
80661
80662
80663
80664
80665
80666
80667
80668
80669
80670
80671
80672
80673
80674
80675
80676
80677
80678
80679
80680
80681
80682
80683
80684
80685
80686
80687
80688
80689
80690
80691
80692
80693
80694
80695
80696
80697
80698
80699
80700
80701
80702
80703
80704
80705
80706
80707
80708
80709
80710
80711
80712
80713
80714
80715
80716
80717
80718
80719
80720
80721
80722
80723
80724
80725
80726
80727
80728
80729
80730
80731
80732
80733
80734
80735
80736
80737
80738
80739
80740
80741
80742
80743
80744
80745
80746
80747
80748
80749
80750
80751
80752
80753
80754
80755
80756
80757
80758
80759
80760
80761
80762
80763
80764
80765
80766
80767
80768
80769
80770
80771
80772
80773
80774
80775
80776
80777
80778
80779
80780
80781
80782
80783
80784
80785
80786
80787
80788
80789
80790
80791
80792
80793
80794
80795
80796
80797
80798
80799
80800
80801
80802
80803
80804
80805
80806
80807
80808
80809
80810
80811
80812
80813
80814
80815
80816
80817
80818
80819
80820
80821
80822
80823
80824
80825
80826
80827
80828
80829
80830
80831
80832
80833
80834
80835
80836
80837
80838
80839
80840
80841
80842
80843
80844
80845
80846
80847
80848
80849
80850
80851
80852
80853
80854
80855
80856
80857
80858
80859
80860
80861
80862
80863
80864
80865
80866
80867
80868
80869
80870
80871
80872
80873
80874
80875
80876
80877
80878
80879
80880
80881
80882
80883
80884
80885
80886
80887
80888
80889
80890
80891
80892
80893
80894
80895
80896
80897
80898
80899
80900
80901
80902
80903
80904
80905
80906
80907
80908
80909
80910
80911
80912
80913
80914
80915
80916
80917
80918
80919
80920
80921
80922
80923
80924
80925
80926
80927
80928
80929
80930
80931
80932
80933
80934
80935
80936
80937
80938
80939
80940
80941
80942
80943
80944
80945
80946
80947
80948
80949
80950
80951
80952
80953
80954
80955
80956
80957
80958
80959
80960
80961
80962
80963
80964
80965
80966
80967
80968
80969
80970
80971
80972
80973
80974
80975
80976
80977
80978
80979
80980
80981
80982
80983
80984
80985
80986
80987
80988
80989
80990
80991
80992
80993
80994
80995
80996
80997
80998
80999
80100
80101
80102
80103
80104
80105
80106
80107
80108
80109
80110
80111
80112
80113
80114
80115
80116
80117
80118
80119
80120
80121
80122
80123
80124
80125
80126
80127
80128
80129
80130
80131
80132
80133
80134
80135
80136
80137
80138
80139
80140
80141
80142
80143
80144
80145
80146
80147
80148
80149
80150
80151
80152
80153
80154
80155
80156
80157
80158
80159
80160
80161
80162
80163
80164
80165
80166
80167
80168
80169
80170
80171
80172
80173
80174
80175
80176
80177
80178
80179
80180
80181
80182
80183
80184
80185
80186
80187
80188
80189
80190
80191
80192
80193
80194
80195
80196
80197
80198
80199
80200
80201
80202
80203
80204
80205
80206
80207
80208
80209
80210
80211
80212
80213
80214
80215
80216
80217
80218
80219
80220
80221
80222
80223
80224
80225
80226
80227
80228
80229
80230
80231
80232
80233
80234
80235
80236
80237
80238
80239
80240
80241
80242
80243
80244
80245
80246
80247
80248
80249
80250
80251
80252
80253
80254
80255
80256
80257
80258
80259
80260
80261
80262
80263
80264
80265
80266
80267
80268
80269
80270
80271
80272
80273
80274
80275
80276
80277
80278
80279
80280
80281
80282
80283
80284
80285
80286
80287
80288
80289
80290
80291
80292
80293
80294
80295
80296
80297
80298
80299
80200
80201
80202
80203
80204
80205
80206
80207
80208
80209
80210
80211
80212
80213
80214
80215
80216
80217
80218
80219
80220
80221
80222
80223
80224
80225
80226
80227
80228
80229<br

When US Government drawings, specifications, or other data are used for any purpose other than a definitely related government procurement operation, the government thereby incurs no responsibility nor any obligation whatsoever; and the fact that the government may have formulated, furnished, or in any way supplied the said drawings, specifications, or other data is not to be regarded, by implication or otherwise, as in any manner licensing the holder or any other person or corporation, or conveying any rights or permission to manufacturer, use, or sell any patented invention that may in any way be related thereto.



Do not return this copy. Retain or destroy.

RANGE AND ANGLE CALIBRATION FACILITY STUDY

Dr. Robert L. Richardson
Syracuse University Research Corporation

THIS DOCUMENT IS SUBJECT TO SPECIAL
EXPORT CONTROLS AND EACH TRANSMITTAL
TO FOREIGN GOVERNMENTS, FOREIGN NA-
TIONALS OR REPRESENTATIVES THERETO
MAY BE MADE ONLY WITH PRIOR APPROVAL
OF RADC (EMAS), GAFB, N.Y. 13440

FOREWORD

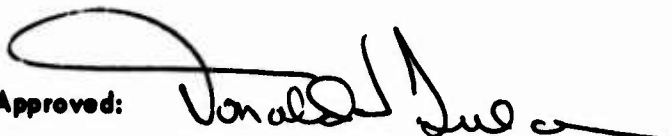
The investigation described in this Final Report was carried out by Syracuse University Research Corporation, Special Projects Laboratory, Merrill Lane, University Heights, Syracuse, New York, for Rome Air Development Center, Griffiss Air Force Base, New York, under Contract AF 30(602)-4215, and took place between April 1, 1966, and May 1, 1968. The report is Item 6 of the contract, dated May 1968.

Mr. Donald Zulch, EMASI, served as RADC Project Engineer, and the SURC Project Engineer was Dr. Robert L. Richardson. In addition to SURC personnel, three consultants assisted in the study. They were Dr. T.J. Kukkamaki, Director of the Finnish Geodetic Institute, Professor Ernest Muller of the Department of Geology, Syracuse University, and Professor Dean Merchant of the Geodetic Sciences Department of Ohio State University.

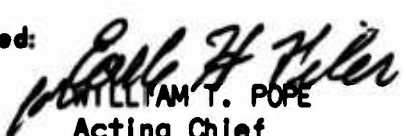
Distribution of this report is restricted to protect description of technical know-how, under the provisions of the U.S. Mutual Security Acts of 1949.

This Technical Report has been reviewed and is approved.

Approved:


DONALD I. ZULCH
Project Engineer

Approved:


WILLIAM T. POPE
Acting Chief
Surveillance and Control Division

FOR THE COMMANDER:


IRVING J. GABELMAN
Chief, Advanced Studies Group

ABSTRACT

This study was carried out to provide design criteria for a range and angle calibration facility to be built in the vicinity of Rome Air Development Center, Rome, New York. Sites for the facility are recommended together with means for constructing and calibrating the range and angle standards. Means for determining the refractive index of the atmosphere are suggested and experiments which were carried out on the Ohio State baseline at Mansfield, Ohio are described. These experiments were performed to test the techniques for determining the optical refractive index of the atmosphere and the accuracy of a Spectra Physics Model 3G Geodolite and an AGA Corporation Model 4D Geodimeter.

TABLE OF CONTENTS

SECTION	TITLE	PAGE
I	OBJECTIVES	1
II	INTRODUCTION	2
III	APPROACH	5
IV	RANGE CALIBRATION FACILITY	7
	1. GENERAL	7
	2. RANGE CONFIGURATION	9
	a. Pillar-Monument Structures	11
	3. BASELINE INSTRUMENTATION	15
	a. Temperature Measuring System	17
	b. Air Pressure Measurements	22
	c. Water Vapor Pressure Measurements	24
	d. Instrument Costs and Installation	26
	e. Summary	27
	4. BASELINE CALIBRATION	28
	a. Best Presently Available Method	29
	b. Improved Method for Calibrating the Baseline	31
	5. SPECIAL PURPOSE INTERFEROMETER	35
	a. General	35
	b. The Use of Two Wavelengths	41
	6. LABORATORY EXPERIMENTS	47
	7. SUMMARY	49
V	ANGLE CALIBRATION FACILITY	55
	1. GENERAL	55
	2. HORIZONTAL ANGLE CALIBRATION RANGE	56
	a. Range Configuration	56
	b. Method of Calibrating the Range	62
	c. Instructions	65

	3. VERTICAL ANGLE CALIBRATION RANGE	66
	a. Range Configuration	66
VI	SITE SURVEYS	72
	1. SITE REQUIREMENTS	72
	2. DISCUSSION OF POSSIBLE SITES	78
	a. Characteristics of the Forestport Site	79
	b. Characteristics of the Chase Lake Site	82
	c. Chase Lake Site and the Site Requirements	90
	d. Other Considerations	94
VII	MANSFIELD EXPERIMENTS	96
	1. INTRODUCTION	96
	2. DESCRIPTION OF THE EXPERIMENTAL PROGRAM	96
	a. Experimental Period and Personnel	96
	b. The Mansfield Site	97
	c. Weather	102
	d. Baseline Instrumentation	103
	e. Method of Taking Atmospheric Data	111
	f. Distance Measurements	126
	3. COMPUTER PROCESSING	127
	a. Determining the Average Refractive Index Along the Baseline	127
	b. Propagation Corrections for the Distance Measurements	134
	4. RESULTS AND CONCLUSIONS	136
	a. Geodimeter Measurements	137
	b. Geodolite Measurements	138
	c. Refractive Index Determination and Temperature Sampling	148
APPENDIX A	GEOLOGIST'S SITE EVALUATION REPORT-CHASE LAKE SITE	166
	1. INTRODUCTION	167
	a. Location of Area	167

b.	Site Evaluation Criteria	167
c.	Background	169
d.	Sources of Information	170
2.	GEOLOGY	171
a.	Physiographic Relationships	171
b.	Precambrian Geology	172
c.	Bedrock Topography	175
d.	Glacial Geology	175
3.	CHASE LAKE SITE	180
a.	Accessibility and Development	180
b.	Topography	181
c.	Vegetation	183
d.	Soil and Subsoil Materials	185
e.	Depth of Bedrock	186
f.	Other Considerations	187
APPENDIX B	REFRACTIVE INDEX CORRECTIONS FOR ELECTROMAGNETIC DISTANCE MEASUREMENTS	188
1.	INTRODUCTION	188
2.	TECHNIQUES FOR DETERMINING THE REFRACTIVE INDEX OF THE ATMOSPHERE IN THE VISIBLE RANGE	190
3.	DETERMINING THE REFRACTIVE INDEX OF THE ATMOSPHERE AT RADIO AND MICROWAVE FREQUENCIES	202
4.	APPLICATION OF REFRACTIVE INDEX FORMULAS	207
REFERENCES		209

LIST OF ILLUSTRATIONS

FIGURE	TITLE	PAGE
4-1	Baseline Pillar Layout	10
4-2	Zero Meter Pillar-Monument Configuration	12
4-3	Outlying Pillar-Monument Configuration	13
4-4	Baseline Thermometer System	18
4-5	Temperature Measuring and Recording Instrumentation	21
4-6	Water Vapor Pressure Constant as a Function of Temperature	25
4-7	Special Purpose Interferometer	37
4-8	Difference in Phase as a Function of Distance	43
4-9	Photograph of Interferometer Fringe Pattern	48
4-10	Experimental Model of Interferometer	50
4-11	Experimental Model of Interferometer	51
4-12	Experimental Model of Interferometer	52
4-13	Oscilloscope Display of Vidicon Video Signals	53
5-1	Optical Target	57
5-2	Layout of Horizontal Angle Calibrating Facility at the Chase Lake Site	59
5-3	Typical Pillar-Monument Configuration	61
5-4	Vertical Angle Measuring Facility	68
5-5	Geometrical Relationships Involved in the Facility Layout	68
6-1	Map of Forestport Area Showing Prospective Baseline Location	80
6-2	Road Map of Region from Rome to Chase Lake	83
6-3	Topographic Map of Chase Lake Area	84

6-4	Map of Chase Lake Area Showing Topographic Relationships and Proposed Baseline Alignment	86
6-5	Aerial Photograph of Region Just South and Southeast of Sand Pond	88
6-6	Pictures of the Proposed Chase Lake Calibration Facility Site	89
6-7	Map Showing Termination of Existing Electric Power Lines	91
6-8	Map Showing Land Owned by New York State	92
7-1	Map of the Region Surrounding the Mansfield Baseline	98
7-2	-3, 0, 1 and 5 Meter Pillars	99
7-3	-3, 0 and 1 Meter Pillars with Väisälä Comparator Equipment	99
7-4	5 Meter Pillar with Väisälä Equipment	100
7-5	View of Baseline Looking Eastward	100
7-6	View of Baseline Looking Westward	101
7-7	Histograms for Distance Measurements Made September 13, 1967	140
7-8	Histograms for Distance Measurements Made September 14, 1967	143
7-9	Histograms for Distance Measurements Made September 15, 1967	144
7-10	Histograms of September 13 Refractive Index Errors	154
7-11	Histograms of September 14 Refractive Index Errors	155
7-12	Histograms of September 15 Refractive Index Errors	156
7-13	Errors in Average Refractive Index as a Function of Time for September 13 Data	158

7-14	Errors in Average Refractive Index as a Function of Time for September 14 Data	159
7-15	Errors in Average Refractive Index as a Function of Time for September 15 Data	160
7-16	Errors in Average Refractive Index as a Function of Time for Three and Five Thermometer Combinations	163
A-1	Location Map Showing Topography and Highway Net Between Chase Lake Area and Rome	168
A-2	Geology of Chase Lake Area	174
A-3	Chase Lake Site	179
A-4	Map of Chase Lake Area Showing Topographic Relationships and Proposed Baseline Alignment	182
A-5	View Near Southeast End of Boggy Kettle	184
B-1	Partial Derivative of the Optical Refractivity with Respect to Temperature	196
B-2	Partial Derivative of the Optical Refractivity with Respect to Temperature	197
B-3	Partial Derivative of the Optical Refractivity with Respect to Pressure	198
B-4	Partial Derivative of the Optical Refractivity with Respect to Water Vapor Pressure	199
B-5	Partial Derivative of the Optical Refractivity with Respect to Wavelength	200

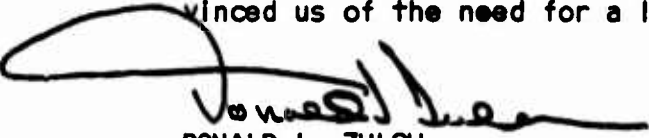
LIST OF TABLES

TABLE	TITLE	PAGE
6-1	Daily Values of the Variation of Heat Content of the Surface Layers of the Soil	76
7-1	Thermometer Identification Data	104
7-2	Thermometer Calibration Data	105
7-3	Temperature Corrections in Degrees Centigrade	107
7-4	Thermometer Position Data	109
7-5	Corrected and Converted Experimental Data Taken September 12, 1967	112
7-6	Corrected and Converted Experimental Data Taken September 13, 1967	113
7-7	Corrected and Converted Experimental Data Taken September 14, 1967	116
7-8	Corrected and Converted Experimental Data Taken September 15, 1967	121
7-9	Measured Distance, Corrected Distance and Average Refractive Index Values for September 12, 1967	126
7-10	Measured Distance, Corrected Distance and Average Refractive Index Values for September 13, 1967	128
7-11	Measured Distance, Corrected Distance and Average Refractive Index Values for September 14, 1967	130
7-12	Measured Distance, Corrected Distance and Average Refractive Index Values for September 15, 1967	132
7-13	Baseline Measurement Statistics	141
7-14	Baseline Measurement Statistics	146

7-15	Thermometer Combinations	150
7-16	Refractive Index Error Data for September 13, 1967	151
7-17	Refractive Index Error Data for September 14, 1967	152
7-18	Refractive Index Error Data for September 15, 1967	153
7-19	Average and Standard Deviation of the Errors in Refractive Index	157
B-1	Experimental Values for Radio Refractive Index	205

EVALUATION

The advent of the laser has made possible a capability to determine time delay or distance to greater precision over longer ranges than is currently possible with microwave or non-coherent optical distance measurement equipment. This has emphasized the need for adequate standards for calibration. Principal problems facing the designer of an adequate calibration range are the correlation of the field site standard of length with the international standard of length and the correction for the effects of the environment. In determining the technique to be used as a length standard, two constants were selected, first the value of the meter of 1,650,763.73 wavelengths of the orange red line of Krypton 86 and second, the constant for velocity of light in a vacuum was selected to be 2.997925×10^8 meters/sec. Early in our study we decided that the key instrument in our calibration system must be a laser, since wavelengths of certain lasers can be compared with Krypton 86 to an accuracy of at least one part in 10^8 . The configuration of the laser instrumentation chosen was an interferometer operating over 25 meters with initial calibrations being done in a vacuum. Laboratory measurements were performed on a laser interferometer of this type indicating that precision measurement of 2.5 microns can be obtained. Establishing the first 25 to 30 meters in a vacuum will eliminate the uncertainty in determining the propagation correction and assures well defined interference patterns. The problem of refraction correction does not have a convenient solution. The standard deviation in the determination of N is about .1 N units under the best of circumstances. No economical method was found for determining and recording temperature with the response time desired. Further work in the area of temperature determination will be undertaken. Considerable time was spent in site selection and we were fortunate in finding a site meeting our requirements. Additional experiments are being undertaken at the proposed site to determine the characteristics of temperature changes with a view toward verifying the utility of our refraction correction procedures. We were extremely fortunate to be able to make measurements of time delay on the 500 meter calibration line at Ohio State University. These tests provided basic data to verify our computer program for refraction correction and convinced us of the need for a long line for calibrating laser ranging systems.



DONALD I. ZULCH
Project Engineer

SECTION I

OBJECTIVES

The objective of the work described in this report is to provide requirement criteria for the design and construction of a highly accurate range and angle calibration facility in the vicinity of Griffiss Air Force Base, Rome, New York. The range shall provide the capability of evaluating the accuracy and stability of optical and microwave metric measuring equipment under various atmospheric conditions. The accuracy of length calibration shall be one part in 10^7 and that for angle calibration shall be ± 0.2 arc seconds.

SECTION II

INTRODUCTION

Until relatively recently, most distance measurements have been made using calibrated meter sticks, chains, tapes or wires and the standard for such measurements, the prototype meter, was kept in the International Bureau of Weights and Measures in Paris. During the last twenty years, however, technological advances have changed this situation somewhat. In 1960, the Eleventh General International Conference on Weights and Measures redefined the standard meter as 1,650,763.73 wavelengths, in a vacuum, of the orange-red radiation of Krypton 86 under certain conditions. This was done because the former international standard, being a metal bar, was subject to small changes in length with changes in temperature and age. The Krypton 86 radiation should theoretically have a wavelength which will not be significantly temperature sensitive or change with the passing of time. The wavelength is also relatively insensitive to source construction and environment and therefore, it is possible to build highly accurate laboratory standards at reasonable cost.

About forty years ago Dr. Y. Väisälä, Professor of Physics and Astronomy at Turku University in Finland, invented his now famous light interference comparator. This invention represented one of man's first attempts to accurately measure distances of the order of one kilometer by taking advantage of electromagnetic wave propagation. Since the nineteen forties, several other instruments have been developed, some using visible radiation and others operating in the microwave region of the spectrum. The Väisälä Comparator is still among the most accurate devices of this type but it is limited to maximum distances of approximately one kilometer. It also is not a portable system but rather requires that a series of stable concrete pillars be placed along the line being measured. The more recently developed systems are

mainly portable instruments with somewhat less inherent accuracy than the Väisälä equipment. With the advent of transistors, integrated circuits and lasers the size, weight and power requirements for such instruments have continuously decreased, while their maximum range of operation has increased to the point where it is now claimed that one instrument has a range of up to 100 kilometers under proper atmospheric conditions. Such a measurement can be made electromagnetically in a small fraction of the time that would be required if tapes or wires were used. Electromagnetic distance measuring instruments also have another advantage over the older tape, wire or chain systems. They are capable of measuring across water, valleys and other places where taping would not be possible. In many cases, they are more accurate and considerable work is presently being carried out to make even greater accuracy possible. It is reasonable to expect that in the future, all except the smallest distance measurement jobs will be carried out using electromagnetic equipment.

The rapid development of highly accurate electromagnetic distance measuring devices has resulted in a need for a facility where such devices may be calibrated and their limitations and characteristics studied. It was to meet this need that the study being described in this report was initiated. In addition, it was decided that the facility should have the capability of calibrating angle measuring devices and the accuracy requirements in both cases were set at consistent levels.

During the early phases of the study, considerable effort was directed toward ascertaining just what characteristics the facility ought to have. The present and future state-of-the-art for electromagnetic distance and angle measuring equipment was surveyed. It was found that relatively few new angle measuring devices are being developed and that a range satisfying the contract angular accuracy requirements will be more than adequate for their calibration. Furthermore,

it was found that existing optical equipment is sufficiently accurate to calibrate the angle range at the facility.

In contrast, the study revealed that there are several new types of distance measuring devices under development and that some of these are expected to require a calibration range with an accuracy equal to the specifications listed in the contract requirements. It was also found that while means for calibrating the distance standard at the facility with this accuracy, are presently available, new techniques are possible which show promise of producing even better results.

The study therefore consisted of three principle parts. First, the physical form of the calibration facility was determined together with means for calibrating the basic standards of length and angle. Sections IV and V cover this aspect of the work.

Secondly, it was found that the average refractive index of the atmosphere must be determined accurately along the ray paths of the devices being used at the facility. Appendix B presents techniques for determining this average index and Section VII contains the results of some associated experiments.

The third part of the study involved finding a site for the proposed facilities. This effort is described in Section VI and Appendix A.

SECTION III

APPROACH

This study was begun with a survey of existing literature to bring the personnel up-to-date on the "state-of-the-art" for distance and angle measuring equipment. This phase of the work was followed by visits to several laboratories, government agencies and Ohio State University. The purpose of these visits was to collect information on the current thinking of many people specializing in the field relative to several important questions. In addition, data was obtained on the performance of equipment under development together with predictions of what sort of characteristics the next generation of these devices would be likely to possess. This information was used to develop additional facility requirements and to pinpoint those areas in which the greatest effort would be needed.

It was found that there seemed to be relatively little interest in an angle calibrating facility possessing the accuracy required by the study. Only one new angle measuring device was found to be under development and it, being a microwave system, was considerably less accurate than the facility specification. In contrast, several new distance measuring devices were found. Those which were expected to provide the greatest accuracy operated at optical wavelengths and two used laser sources. On the basis of the expected performance characteristics of these devices, together with those of existing equipment, additional requirements for the length measuring part of the facility were developed and the study proceeded to the task of deciding how and where the calibration facility should be constructed. The results of this effort are presented in the next three sections.

During the course of the study, a number of ideas and techniques were developed for which experimental verification was highly desirable. An experimental aspect was therefore added to the project. These experiments, together with the results which they have provided are described in Sections IV and VII.

SECTION IV

RANGE CALIBRATION FACILITY

1. GENERAL

This aspect of the study program has received the most attention and shows promise of producing the most useful results. It has been found that there is considerable interest among people working in the fields of geology, surveying and electromagnetic propagation in the establishment of a relatively long baseline whose length is known with a probable error of not more than one part in 10^7 . Such a line could be used for equipment calibration, propagation studies and atmospheric studies.

Although the contract requirements mentioned a baseline of 800 meters in length, the study has shown that a baseline of 4000 meters would be considerably more useful. This length has therefore been adopted as an important facility requirement and prospective sites were not considered completely adequate unless they were capable of accomadating a line of this length. There are two reasons for increasing the required length. First, the dual wavelength distance measuring equipment currently under development is expected to require a distance of at least 2000 meters for calibration. Since this is a theoretical estimate, a considerable safety margin should be included in the specification of a baseline which will be used to calibrate such devices. Secondly, existing equipment like the Spectra-Physics Geodolite has a resolution rating of one millimeter or one part in 10^6 whichever is greater. If such an instrument is to be calibrated to convert the resolution rating into an accuracy rating, then a distance of more than one kilometer will be needed so that the one part in 10^6 limit prevails. Since it is anticipated that more accurate equipment of this type may be developed in the future the baseline should be significantly longer than one kilometer. Also, the widely used model 2A Geodimeter requires a distance of at least 3.2 kilometers for adequate calibration. It is entirely possible that the initial baseline length may be

only one kilometer in length, but its design should be such that it can be easily extended to the four kilometer length at a later time.

One of the most important aspects of the study was that of determining how the baseline could be calibrated with an accuracy of one part in 10^7 without resorting to prohibitively expensive techniques. Whenever calibration of an accurate baseline is considered, the Väisälä light interference technique immediately should come to mind since every highly accurate, out-of-doors standard baseline in the world has been calibrated using this technique. The technique was carefully examined and a baseline measurement method utilizing it was developed. In addition, a modified form of the technique was devised to serve as a means for obtaining even higher accuracy in the measurement of standard baselines.

Whenever electromagnetic distance measuring techniques are considered, two physical constants assume considerable importance. The first is the value of the meter which has been internationally defined as 1, 650, 763. 73 wavelengths of the orange-red line of Krypton 86 in a vacuum. The wavelength of this radiation is therefore 0.6057802 microns. The second constant is the velocity of light in a vacuum. For the purposes of this study, the value adopted as the international standard for geodetic work will be used. It is 2.997925×10^8 meters/sec. (1)

Another important parameter in most electromagnetic distance measuring systems is the average refractive index along the ray path. All such systems utilize the propagation of electromagnetic waves and most of them operate in such a way that the propagation time is actually measured. This time can be determined with very high accuracy but to convert the result into distance, the propagation velocity must be known. It is the error in the knowledge of this velocity that provides the principal limitation on the accuracy of such equipment. In most cases, the velocity of propagation is not constant but instead varies along the ray path. The relationship between distance and time therefore involves the average velocity of propagation and may be expressed as:

$$D = \bar{v} T$$

(4-1)

where D = the distance being measured

\bar{v} = the average velocity of propagation along the ray path

T = the time required for the wave to travel the distance D

The average velocity of propagation can be expressed as:

$$v = \frac{c}{\bar{n}}$$
 (4-2)

where c = the velocity of propagation in a vacuum

\bar{n} = the average refractive index with respect to
distance along the ray path

At present, c is known to a little better than one part in 10^6 and there are indications that this may be improved by an order of magnitude in the not too distant future. This leaves the knowledge of the average index of refraction, \bar{n} , as the principle source of error in many distance measuring systems. A number of means for determining the quantity are available and a detailed study of the present state of the art has been carried out. The results of this study are reported in Appendix B where specific means for determining the average index along the baseline are recommended.

2. RANGE CONFIGURATION

The recommended range configuration is shown in Figure 4-1 where it will be noticed that pillars are located at 0, 5, 25, 125, 250, 500, 1000, 1500, 2000, 3000, and 4000 meters. The recommended location of this baseline at the Chase Lake site is shown in Figure 6-4. Chapter 6 also contains a discussion of the sort of environment which must exist around the baseline so that optimum atmospheric conditions may be obtained. In Figure 4-1, the dashed lines enclose the area over which radiation from a microwave device with a 6° beamwidth would pass. It is recommended that trees and bushes be removed from the site if they lie within this region, or are within 25 meters of the baseline. If it should be decided that only visi-

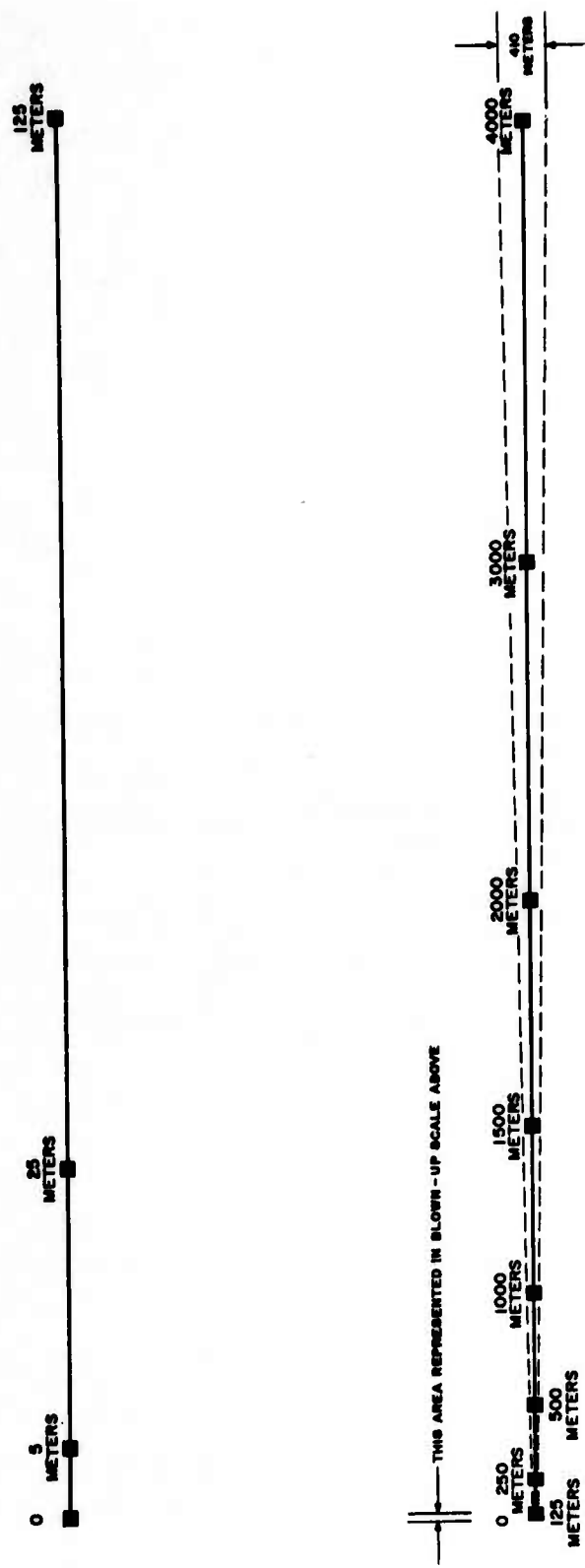


Figure 4-1 Baseline Pillar Layout

ble wavelength devices are to be used on the range, then a 50 meter corridor is all that needs to be cleared along the baseline.

The pillar structures along the baseline will take three different forms. That at the zero position will be the most elaborate while those at 5, 25, and 125 meters will be the simplest. Each of these structure types is described below.

a. Pillar-Monument Structures

The structures to be constructed along the baseline will hold the metal pieces upon which the terminal points of the various calibrated lengths are inscribed. The largest structure is shown in Figure 4-2, and will be located at the zero meter end of the baseline. It will consist of two above-the-ground pillars, an underground monument and a surrounding wooden platform. The top surface of the pillars will be approximately 1.5 meters above the ground and their bases will extend beneath the surface far enough to be well below the frost line. Surrounding the pillars will be a wooden platform whose upper surface is approximately 0.5 meters above the ground. This platform will have concrete footings as shown in the figure and should have a protecting canopy of the form shown in Figure 7-2. Below the zero meter pillar will be located a cylindrical concrete reference monument which is attached to three piles. The top of the cylinder should be approximately 0.75 meters below the surface of the earth. The monument constitutes a very stable underground reference structure. The pillar is less stable and serves as a table upon which calibration and measurement equipment may be placed. The wooden platform, which is not attached to either the monument or the pillar, is for the range personnel to walk on.

The pillar-monument arrangement for the 250, 500, 1000, 1500, 2000, 3000 and 4000 meter positions is shown in Figure 4-3. The underground monument is similar to that described for the zero meter position. At the 5, 25, and 125 meter positions no underground monument is required and only the pillar and platform section of the configuration shown in Figure 4-3 need be built.

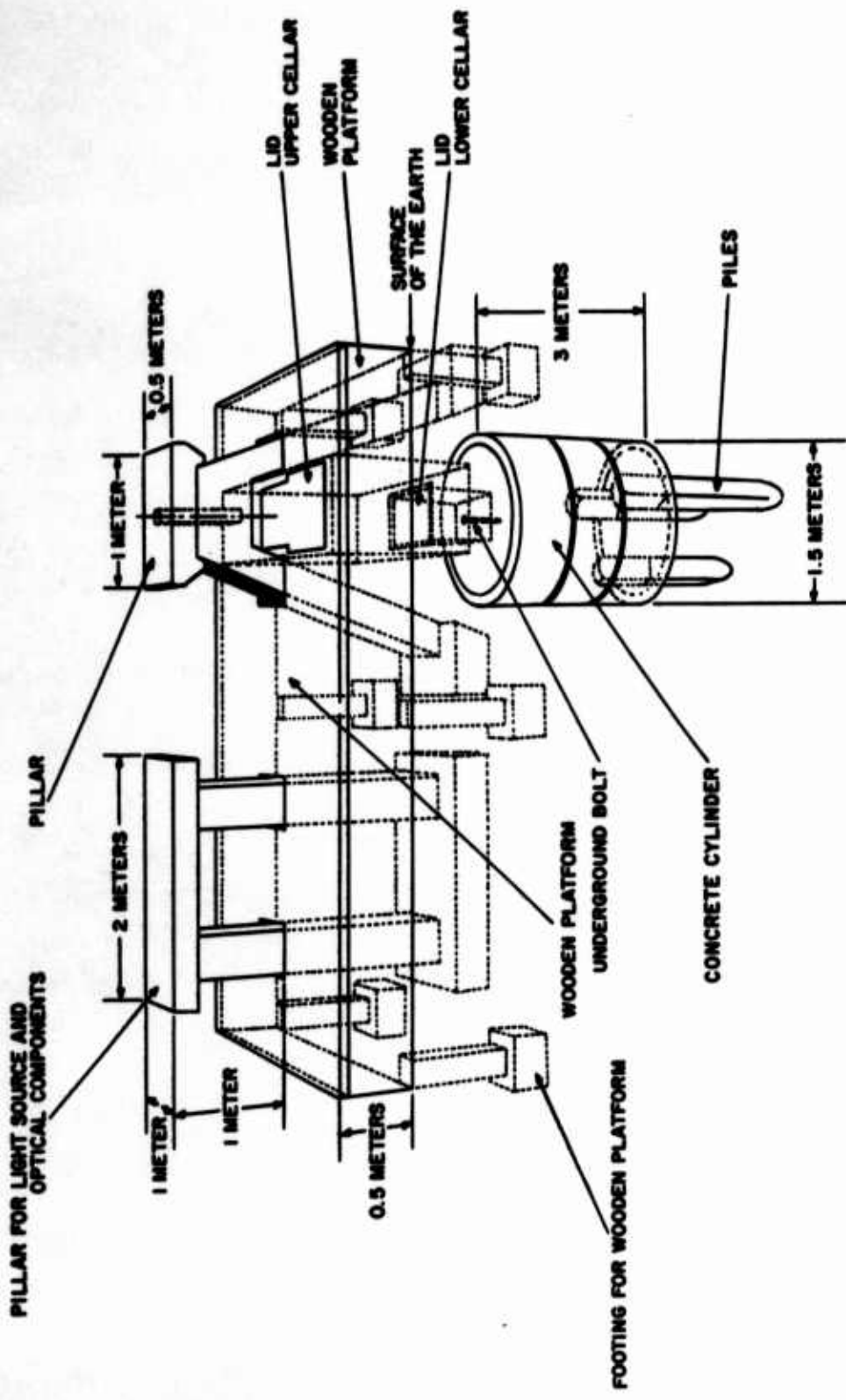


Figure 4-2 Zero Meter Pillar-Monument Configuration

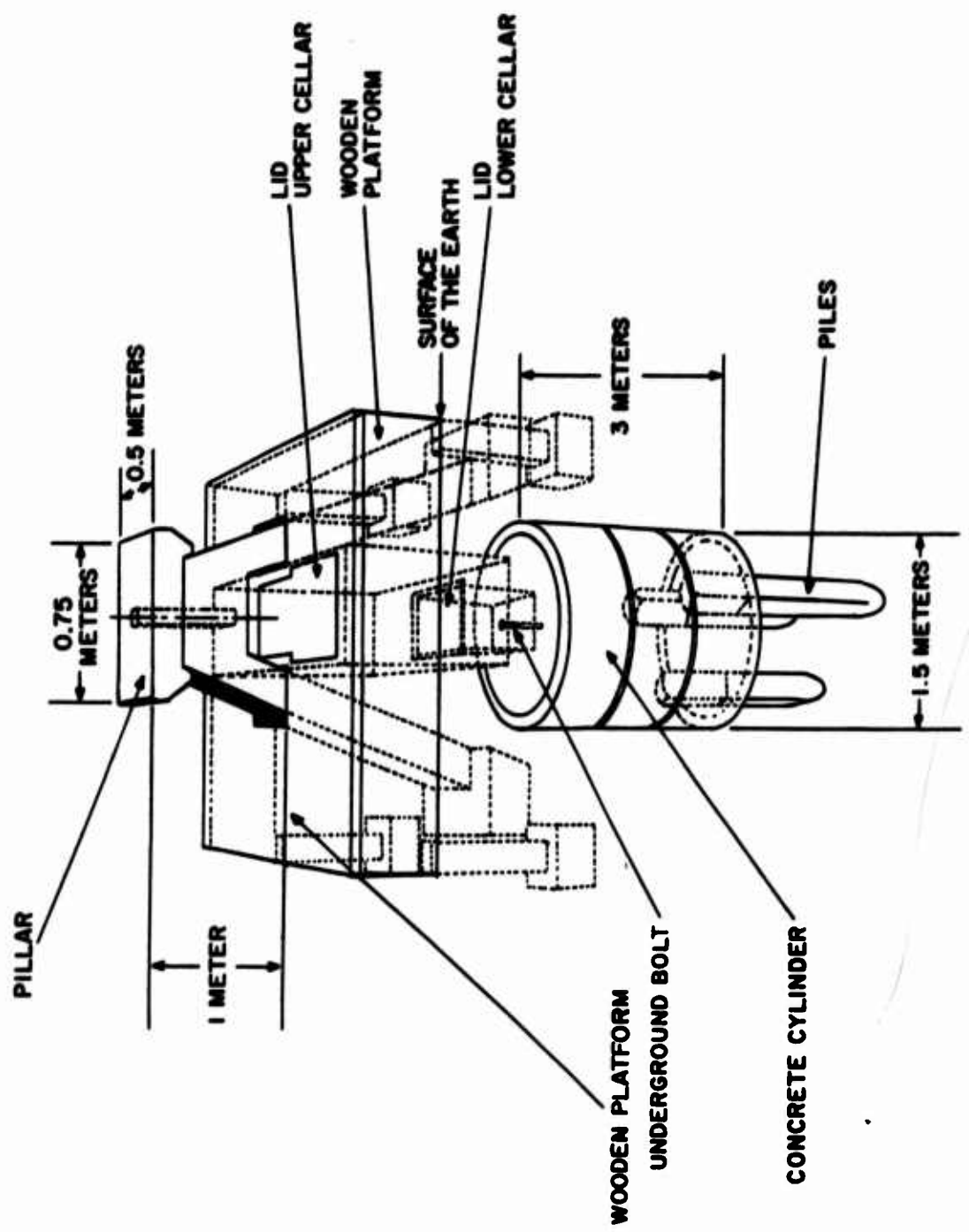


Figure 4-3 Outlying Pillar-Monument Configuration

The construction of a monument is begun by drilling a 1.5 meter diameter hole in the ground and then placing concrete rings, 1.5 meters in diameter, in it. The piles are then driven, after which the rings are filled with concrete. In this way there is a minimum of soil disturbance during construction. The pillar-monument configurations recommended here were obtained from the book "Standard Base Loenermark"(2) which contains an excellent description of important construction procedures and precautions. The top of each monument contains a brass reference bolt upon which the reference point is marked. Above the monument there is an upper and lower cellar and the pillar. None of these structures are in physical contact with the monument, and therefore any movement of these structures, and there may be some, is not transferred to the monument.

At the time of calibration the baseline length is measured between reference marks on the tops of the pillars. The locations of these marks are then projected downward through the holes in the pillars to the reference bolts. Periodically after this, the positions of the reference marks on the pillars are compared with those on the reference bolts so that the values of the various calibrated lengths can be adjusted to remove the effects of pillar movement. It has been found that for reasonably good soil conditions, underground monuments constructed in the manner suggested here require recalibration only every three years.

Normal practice dictates that the concrete for the monuments and pillars be poured and then at least six months be allowed to pass before calibration is begun. At the time of calibration, the monument brass bolts should be attached and the concrete contained in the upper five inches of the pillars poured. This surface layer will contain all of the desired mounting bolts and brackets. The upper surfaces of the pillars are made to lie in the same plane with their center lines collinear.

Each pillar should have a removable cover which will protect any equipment attached to it when the range is not in use. Each of the monument cellars also has a cover with that covering the upper cellar forming

part of the wooden platform. It is recommended that the above-the-ground surface of the pillars be covered with styrofoam sheets or other insulation. This material will prevent the massive concrete structures from absorbing large amounts of heat during a hot day and then reradiating it at night. Such reradiation cannot be tolerated because it causes severe local anomalies in the refractive index of the atmosphere along the baseline.

3. BASELINE INSTRUMENTATION

Whenever electromagnetic equipment is operated on the baseline, the average refractive index of the atmosphere along the ray path must be known. This average will be obtained by combining sample values of the index which have been obtained at many points. These values will be calculated using the technique suggested in Appendix B, and this requires that the air temperature, total pressure and water vapor pressure be determined at each sample point. The minimum number of sample points that will be required is difficult to predict because data taken at other sites cannot be depended upon to be meaningful for the Chase Lake site. It is therefore recommended that experimental tests, similar to those recently carried out at Mansfield, Ohio and reported in Section VII, be carried out at the proposed site before the baseline is constructed. The results of these tests will indicate the sort of sampling required along the baseline. It is the opinion of this author that the spacing of such samples at Chase Lake may be greater than that necessary at Mansfield for equivalent accuracy. This should result because the environment around the baseline at Chase Lake should be considerably more homogeneous and stable than that at Mansfield. For the purposes of this section however, it is assumed that the Chase Lake sampling intervals will be equal to those which the experimental data taken at Mansfield indicated would be required there.

At this point it should be mentioned that the average refractive index along the baseline can be obtained with considerably higher accuracy at optical wavelengths than in the microwave region. This occurs because means for determining the water vapor pressure of the atmosphere

with high accuracy do not exist. At optical wavelengths this presents no problem because the index is relatively insensitive to the water vapor content of the atmosphere. At microwave frequencies, however, the water vapor effect dominates all others and therefore the index cannot be determined with high accuracy. The study being reported here has produced the conclusion that it is feasible to construct a baseline where the average optical refractive index is known with a probable error of one part in 10^7 , but that at microwave frequencies the error will, at best, probably be about two parts in 10^6 . This larger error is due almost entirely to the water vapor effect.

When normal variations in air temperature, total pressure, and water vapor pressure are considered together with their effect on the optical refractive index, it is found that the maximum allowable distance between sample points is determined by the variation of temperature along the baseline. That is, temperature must be sampled much more frequently with respect to time and space than either of the other properties. In normal practice the temperature is measured at each sample point while the other two properties are measured only at a few, widely spaced, sample points. The effective values of these properties at all other sample points are obtained by interpolation.

It can be shown that if temperature, total air pressure and water vapor pressure are determined with errors whose standard deviations are given by:

$$\sigma_t = 0.05^\circ\text{C}$$

$$\sigma_p = 0.10 \text{ mm of H}_g$$

$$\sigma_e = 1.0 \text{ mm of H}_g$$

the standard deviation of the corresponding error in the refractive index is 0.0806×10^{-6} . This corresponds to a probable error of 5.44×10^{-8} which provides a margin of safety in meeting the one part in 10^7 accuracy requirement of the contract. Instruments capable of providing this level of ac-

curacy are available and particular devices will be specified in the following sections.

a. Temperature Measuring System

On the basis of the Mansfield data it is suggested that the maximum distance between temperature samples be 100 meters. The most common technique for measuring atmospheric temperature along a baseline consists of using mercury thermometers and having observers walk back and forth recording their indications. This is feasible for a 500 meter line of the type constructed at Mansfield but for a four kilometer line, this method would require too many people and too much walking. It is therefore suggested that an automated temperature measuring technique be used and a Hewlett Packard quartz thermometer system together with other control, indicating and recording equipment is recommended. Such a system will be quite expensive, but there is no low cost way of obtaining the necessary data. The layout of the system is shown in Figure 4-4 where each model 2850 temperature sensing probe has a model 2830 A temperature sensor oscillator associated with it. Probes located at 0, 100...1500 meters are connected through coaxial switches and a single coaxial cable back to a model 2801 A quartz thermometer located in a building near the zero meter end of the line. The switches are single pole, double throw types whose normal position is such that the coaxial line along the baseline is continuous. During system operation, d-c pulses are applied to the various switches in a sequential manner. When a given switch is energized it connects the sensor assembly associated with it to the coaxial line for a period which may be adjusted between 1.2 and 2.2 seconds. The first second will be needed for the sensor crystal to reach self-heating equilibrium and the temperature measurement should therefore be made after this period has elapsed. The switches could be Amphenol type DK-315 010002-3 or equivalent.

When the sensors are not connected to the coaxial line, they are not energized. This is important because an energized sensor tends to heat the air around it slightly and if the air is not moving, the thermometer will not give an accurate indication of the air temperature in the larger region

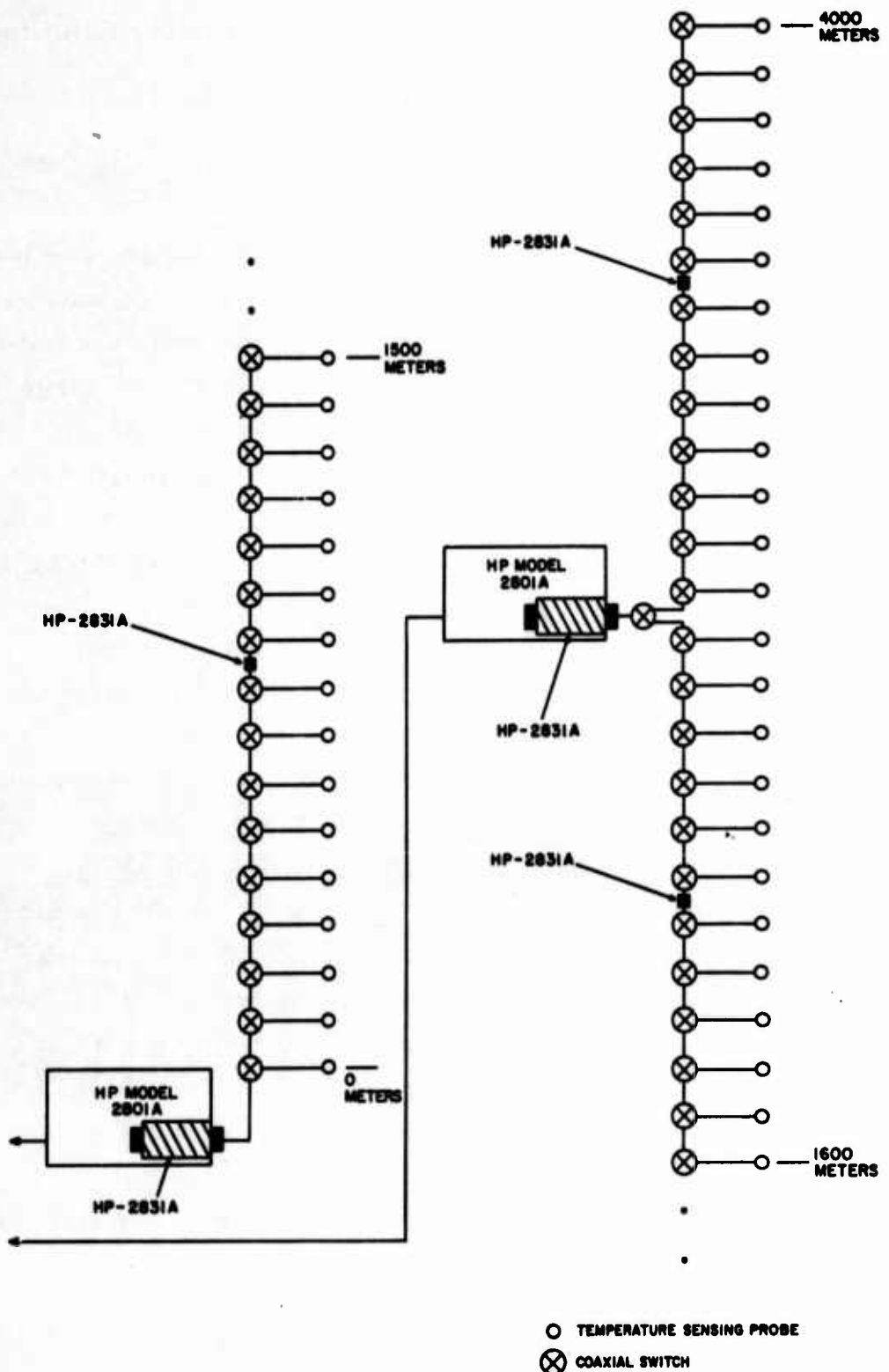


Figure 4-4 Baseline Thermometer System

around the probe. It will instead indicate the temperature of the small volume of heated air close to the sensing element. This problem is of enough significance that Hewlett-Packard recommends that the equipment should be used to sense the temperature of a gaseous medium "only after the thermodynamics of heat transfer for a particular application are investigated." This should be done for the baseline application but it is expected that since the sensor is energized only a small part of the time, no significant system limitation will occur.

The temperature sensing probes at 1600, 1700, . . . 3900 and 4000 meters will be connected to a similar system which has its model 2801 A unit located in an enclosure 2750 meters down the baseline from the zero meter point. The output of this unit is transmitted to the zero meter point where it is combined with that from the model 2801 A unit located there. This arrangement is necessary because with existing amplifiers, the maximum allowable distance between a temperature probe and the Model 2801 A unit is approximately 1600 meters. It should be mentioned that if amplifiers can be developed which make it possible to use 2000 meters of connecting cable (including the effects of the switches), then a single model 2801 A unit located at the 2000 meter point could be used.

The temperature sensors are connected to the thermometers by RG 59/U cable, or the equivalent. When the length of this cable exceeds 300 meters, an H-P Model 2831A oscillator amplifier must be used to compensate for line losses. If the distance exceeds 1000 meters, two amplifiers in cascade must be used. The locations of three such amplifiers are shown in Figure 4-4.

The coaxial switches are controlled from the zero meter end of the baseline in such a way that only one temperature sensing probe is being operated at any given instant of time. It is recommended that a special purpose controller be constructed for this purpose. This equipment should have the ability to select any given thermometer on command or to scan down the line a single time or continuously. It will also control the operation of

the other instrumentation shown in Figure 4-5. From the figure, it is seen that the system contains an H-P model 562A digital recorder with a digital clock. During the first second of each temperature sensing interval, the controller should cause the temperature sensor number and the time to be recorded. After the first second has elapsed, a read command should be applied to the thermometer. The length of the reading period which follows is determined by the resolution selected using the pushbuttons on the front of the quartz thermometer. If a resolution of 0.01 degrees is desired, then the thermometer must measure for 0.1 seconds. If a resolution 0.001 is desired, then the interval will be one second. The instrument can also provide a resolution of 0.001 degrees but this requires ten seconds which may be too long if a relatively rapid scan of 41 probes is desired. At the end of each measurement interval, the temperature is automatically displayed on the digital read-outs and printed by the recorder. It is suggested that most of the equipment shown in Figure 4-5 be located in an electronic equipment building which is sufficiently far from the baseline that it does not influence the atmospheric conditions along the line. The remote console and digital read out should be located under the canopy at the zero meter end of the baseline, however. In the future it may turn out that other recording devices will be required. The system suggested here can be expanded to include equipment which records on punched tape, punched cards or magnetic tape as desired.

The Hewlett-Packard temperature measuring system has a multitude of available probe shapes and sizes and no recommendation is made as to the particular unit to be used on the range. Instead, it is suggested that several of the most promising shapes be experimentally tested in a controlled atmosphere to determine which is best for the baseline application. The Mansfield baseline uses thermometer mounts which consist of two aluminum disks approximately ten inches in diameter. These disks are supported in a horizontal position about three inches apart, and the temperature sensing element is placed in the center of the region between them. The supports are made from 1" x 2" strips of wood. It seems that a similar disk arrangement would be best for the RADC baseline with the thermometers replaced by the appropriate probes. It is possible, however, that the probe-disc

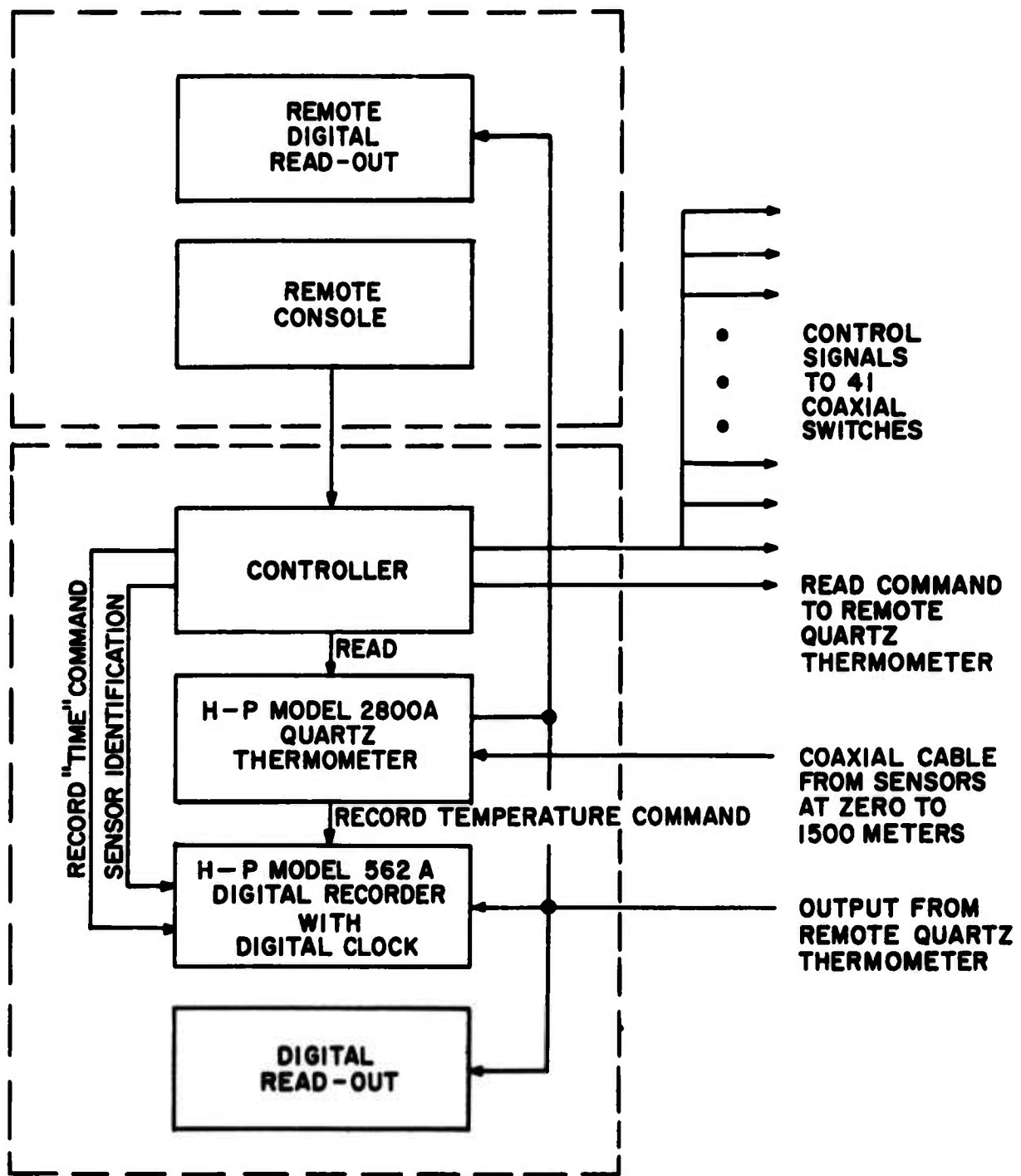


Figure 4-5 Temperature Measuring and Recording Instrumentation

configuration could produce significant un-wanted reflections when microwave devices are being used on the range. In such a case, it might be necessary to remove the disks and perhaps some of the probes. This will not be too serious however, because as mentioned earlier, it will not be possible to determine the refractive index with high accuracy at microwave frequencies anyway. The Mansfield data indicates that if errors of one N unit can be tolerated, then thermometer spacings of up to 300 meters can be used. Since the water vapor effect will probably produce errors of even greater magnitude the removal of the disks and some of the probes would be a reasonable step to take.

It may be desirable to have a special calibration of each probe carried out for the temperature region from -30° to + 40°C. In addition periodic recalibration of the sensors along the line will be required. This can be done by comparing the readings provided by the sensor with the readings a standard mercury thermometer which has been calibrated at NBS. This calibration should be carried out with the sensor in place along the baseline when the atmospheric conditions are as close to ideal as possible.

In this section a system for determining the temperature of the atmosphere at 41 points along a 4 kilometer baseline has been described. A quartz thermometer system has been suggested because this type of device converts the temperature into an equivalent radio frequency for transmission to a central point. Such a system is not affected by noise or lead resistance, both of which cause problems when temperature is measured at a great distance using most other techniques. The temperature will be measured to within 0.05 degrees centigrade and this is adequate to determine the group refractive index to within one part in 10^7 .

b. Air Pressure Measurements

To obtain the desired accuracy in the determination of the refractive index, air pressure must be measured with an error whose standard deviation is 0.1 millimeters of mercury. A survey of the var-

ious techniques and equipment available for making this measurement has resulted in the conclusion that there are no devices capable of this sort of accuracy which can be read remotely. The most accurate device commercially available for measuring pressure is the Wallace and Tiernan Model FA-187 Precision Calibrating Standard Mercury Manometer. This device has a guaranteed accuracy of 0.02% of full scale. If the 800 millimeter scale is used, this corresponds to an accuracy of ± 0.16 mm of Hg. Since this is a guaranteed value, it is reasonable to assume that the standard deviation of the error is probably less than 0.1 mm. One of the difficulties with this instrument is that the calibration is accurate only for the temperature range from 15° to 45° C. Since some operation of the facility at temperatures below this range is anticipated, it is recommended that the instrument be specially calibrated for use down to at least 0° C. If this cannot be done then a special temperature controlled enclosure must be provided for each of the manometers. The indication of the device must be read by an observer since no automatic reading and recording and recording technique is available. This is not a serious limitation, however, since it seems that only two or three air pressure measurements must be made along the baseline. The instruments should be located at the zero meter and 4000 meter points along the baseline and perhaps at the 2000 meter position also. Measurements should be made at the site to determine what sort of pressure variations exist along the line during periods of favorable atmospheric conditions. This data can then be used as a basis for determining the appropriate manometer spacing.

At Mansfield, air pressure was measured at each end of the line and the magnitude of this quantity varied very little from one observation to the next. There was a difference however, between the values measured at the two ends of the line with the pressure in the vicinity of the zero meter pillar being about 0.3 mb lower than that near the 500 meter pillar. This is to be expected since the baseline has a slight downward slope. At Chase Lake there will probably be very little slope, if any, and therefore the air pressure along the line will probably be more nearly constant. The pressure measurements which are made at a few sample points along the baseline can be used to determine the pressure at other points through interpolation.

Like all the other instruments on the range, the manometers must be periodically recalibrated. This is easily done using a standard bar which is provided by the manufacturer. The length of this bar is traceable to a standard length certified by NBS.

c. Water Vapor Pressure Measurements

It was stated earlier in this section that the standard deviation of the error in the measurement of the water vapor pressure must not exceed one millimeter of mercury. It turns out, however, that there is no commercially available instrument capable of measuring water vapor pressure. Instead, the percent relative humidity of the atmosphere is measured and the result converted to water vapor pressure using standard tables. It is recommended that the tables in the publication "Psychrometric Tables for Obtaining the Vapor Pressure, Relative Humidity and Temperature of the Dew Point" by C. F. Marvin be used for this purpose. This document is Weather Bureau publication No. 235 and may be obtained from the U.S. Government Printing Office.

The relationship between the error in the relative humidity and the error in the determination of the water vapor pressure is given by:

$$\Delta e = e_{\omega} \times \Delta(R.H.) \quad (4-3)$$

where e_{ω} is a temperature dependent constant whose value is given by the graph of Figure 4-6, Δe is the error in the water vapor pressure in millimeters of mercury and $\Delta(R.H.)$ is the error in the determination of the relative humidity in percent. For a typical temperature of 15°C, $e_{\omega} = 0.125$ and therefore, an error of 1 mm of Hg in e corresponds to an error of 8% in relative humidity. Accuracy of this sort presents no problem at all and it is recommended that an instrument capable of measuring relative humidity with an error of not more than 1.5% be used. Such a device is the Serdex Precision Indicating Hygrometer which is sold by MacAlaster Bicknell as item number 20724. This device is inexpensive, portable and could be placed in the vicinity of the manometers. It is expected that only two or

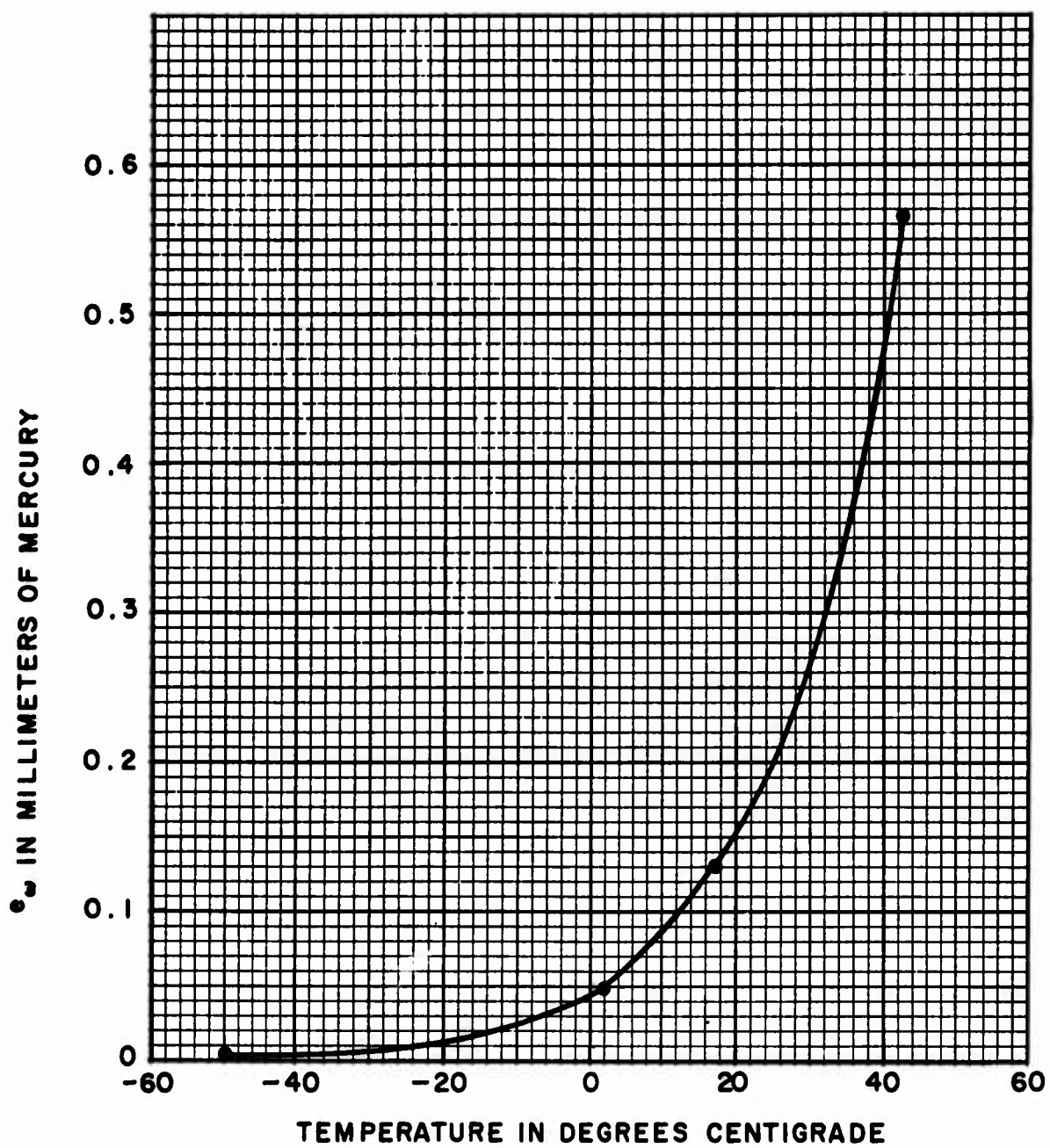


Figure 4-6 Water Vapor Pressure Constant as a Function of Temperature

three of these devices will be required to provide all of the necessary relative humidity information.

There are devices available which can measure humidity at remote locations but all are relatively expensive and less accurate than the device recommended above. In the future new devices capable of remote operation with considerably higher accuracy may become available. If this occurs and the cost is reasonable, it may become desirable to instrument the range with humidity sensors at relatively short intervals as is suggested for temperature. It may then be possible to determine the radio refractive index with an accuracy approaching the one part in 10^7 which can be obtained for optical wavelengths. For the present however, such radio frequency accuracy is not obtainable even if the most accurate and costly remote humidity sensing equipment is used.

d. Instrument Costs and Installation

The most expensive part of the baseline instrumentation is the temperature measuring system. The costs of the equipment are estimated to be as follows:

2 HP Model 2801A Quartz Thermometer	\$6500.
39 Additional H-P Model 2850 Probe and Model 2830 sensor oscillator combinations.	18,300.
5 H-P Model 2831A Oscillator Amplifiers	500.
42 Amphenol Coaxial Switches	610.
22,000 ft. RG 59/U Coaxial Cable	1,000.
1 H-P Model 562A Recorder with Model 571B Digital Clock	2,700.
<hr/>	
Total	\$29,610.

In addition to these items, the special purpose controller, remote console and digital read-outs must be obtained. No estimate of the cost of these items is made.

Of course, the system will require that many wires and cables be run along the baseline. It is suggested that a waterproof, underground pipe (conduit, or channel) be constructed to accomodate these wires. This pipe should have above-the-ground openings near each probe location and if necessary, also between these locations. It should be sufficiently deep in the ground that the wires do not affect microwave devices being used on the range. The electronic equipment building located near the zero meter end of the line and the remote instrument enclosure which is located at the 2750 meter point should be covered on the outside with a material which does not absorb large amounts of heat. The building should be located at least 100 meters from the baseline and should also be heavily insulated so that its internal temperature does not affect the temperature along the baseline. At the present time, it is expected that air conditioning of this building will not be necessary. If this should become necessary in the future due to the addition of equipment with large power dissipation, the system should have a heat exchanger which is sufficiently remote from the baseline that it does not influence the temperature along the line.

The manometers which are recommended sell for \$800. each and the associated calibrating bar for \$134. The hygrometers are \$75. each. During range operation, these devices must be mounted at a number of points along the baseline and some sort of enclosures should be provided. In the case of the manometer, the enclosure may have to be heated during range operation at temperatures below 15°C. When the range is not used for long periods of time, these instruments should be returned to the electronic equipment building for storage.

e. Summary

In this section means for measuring air temperature, total pressure and water vapor pressure have been recommended. A complicated and expensive remote temperature sensing system has been suggested because such a system is necessary if the optical refractive index of the atmosphere along the baseline is to be determined with the desired

accuracy. In contrast, it has been found that considerably less expensive means will suffice for providing the corresponding air pressure and water vapor pressure information. It may turn out that eventually these relatively unsophisticated devices will be replaced by automated remote sensing systems. For the time being, however, these simpler devices should provide information whose accuracy is compatible with the temperature data for achieving the desired accuracy in determining the optical refractive index.

Once the range is in operation, it may be found desirable to make measurements of other meteorological quantities in addition to those required for determining the refractive index. Such parameters would be wind velocity, wind direction, solar radiation, rainfall and snowfall. These quantities would be measured at a single point and there are numerous devices commercially available for the purpose.

At this point a word of caution should be stated, however. The selection of the various devices and equipment has been made strictly on the basis of data and specifications published by the various manufacturers. No equipment was actually tested to determine whether it satisfied the specifications or not.

In this section particular devices have been recommended for measuring air temperature, pressure and water vapor content. For a complete discussion of the characteristics of the wide variety of devices which are available for the measurement of meteorological quantities, the reader is referred to the report, "Meteorological Measurement System" by Martin Katzin, et al. This report was written for RADC in March of 1967 and carries the Defense Document Center Number AD 650 790.

4. BASELINE CALIBRATION

Two somewhat different approaches to the problem of baseline calibration are presented in this section. If the baseline has to be calibrated in the near future with the accuracy specified in the contract then an already proven technique must be used. This technique, however, does

have some limitations and considerable effort has been devoted to finding ways for ultimately improving it. Therefore, a modified calibration technique which has not been completely tested, is also described. This technique will take advantage of recently developed methods and devices and its complete implementation may have to await small advances in the state-of-the-art in certain areas. The ultimate implementation of this technique, however, will represent a significant advance in the state-of-the-art for baseline calibration. The already proven technique which could be used to calibrate the baseline involves the use of the Väisälä light interference comparator to measure the first 500 meters with the remainder of the line being measured using invar tapes. The tapes would be calibrated on the first 500 meters of the baseline. Both methods are described in the following sections.

a. Best Presently Available Method

1) The Väisälä Light Interference Comparator Technique

One of the most desirable attributes of the Väisälä technique is its independence of man's knowledge of the velocity of light in a vacuum. In fact, if the refractive index along the baseline is uniform, the operation of this technique is independent of propagation velocity. In that which follows, the details of the Väisälä technique will not be presented and instead the reader is referred to references (2), (3), (4), (5), (6), and (7) for excellent descriptions of the method and how it is used.

In practice the propagation velocity is not a constant, and the effect must be compensated for. This is done by determining the refractive index variation along the baseline and then appropriately adjusting the length measurements. This variation is due almost entirely to variations in the temperature along the line unless the terrain slopes significantly. The correction, therefore, is somewhat insensitive to air and water vapor pressure and these characteristics do not have to be determined with extremely high accuracy.

Another important characteristic of the Väisälä technique is its dependence on the obtaining interference fringes. These fringes are produced by two non-coherent white light beams which are combined in a telescope. The beams, are obtained from the same source by beam splitting and travel different paths through the atmosphere along the baseline. Since white, non-coherent light is used, the propagation times of the two beams must be such that their total phase shift is not more than two or three wavelengths for a frequency in the middle of the visible region. If the shift is more than this, no fringes will be seen. If the fringes are to be stable enough to be seen, the average refractive index of the atmosphere must be relatively stable also. This is normally the same condition which makes it possible to determine the average index along the baseline accurately while using a reasonable number of temperature samples. The system therefore has a built-in mechanism for telling the operators when atmospheric conditions are sufficiently stable for accurate distance measurements to be made.

In the section on baseline instrumentation it was suggested that temperature be measured every 100 meters during normal baseline operation. During baseline calibration however, it is suggested that more temperature samples be taken. This is most easily done by placing mercury thermometers between the Hewlett-Packard temperature sensing probes. This will require observers to walk up and down the line recording temperature, but such a procedure is not too inconvenient for a 500 meter measurement which is not frequently made.

The Väisälä system has been used to measure standard baselines in many countries and most recent measurements have been made with an accuracy of at least one part in 10^7 . Reference (3) contains a discussion of some of these measurements together with data on the accuracy which was achieved. People around the world have found that the best way to measure baselines using the Väisälä technique is to have experts from Finland participate in the design of the line and then come to the site and carry out the calibration at the appropriate time. This is recommended for the baseline being proposed here. The best person to contact for help of this sort would be our consultant, Dr. T.J. Kukkamäki, Director of the

Finnish Geodetic Institute, Hämeentie 31, Helsinki, 50, Finland. A second source of assistance would be Mr. Sol Cushman of the Geodetic Sciences Department of Ohio State University. Ohio State has a Väisälä Comparator and Mr. Cushman is skilled in its operation. He worked with Dr. Kukkamäki during the calibration of the baseline at Mansfield, Ohio.

2) Extension Beyond 500 Meters

The Väisälä technique is limited by atmospheric conditions to distances of not more than 900 meters for most locations. If it should turn out that conditions at the proposed site are unusually good then perhaps extension to 1000 meters would be possible. This should be done if feasible and the design of the 1000 meter pillar should be such as to accomodate the possibility. For the purposes of this section, however, it will be assumed that only the first 500 meters can be measured using the comparator.

Extension beyond 500 meters can be carried out in a number of ways. The Finns have found that the use of invar tapes constitutes a very desirable way of accomplishing this. Our consultant, Dr. T. J. Kukkamäki, has suggested that extension be carried out using ten tapes which have been calibrated on the first 500 meters of the line. In practice, the tapes would be calibrated at the beginning, in the middle and at the end of the measurement program. The measurements should be made by people experienced in making first order surveys and extreme precautions should be taken. Each measurement would be made many times and a statistical average obtained. The Finns have extended their Vihti baseline in this manner to a total length of 6,049 meters with an accuracy of one part in twelve million. It is recommended that Dr. Kukkamäki be consulted in developing techniques and field procedures for such invar tape calibration and length measurements.

b. Improved Method for Calibrating the Baseline

Although a means for calibrating the baseline with the accuracy required by the contract had been found, considerable effort was devoted to finding even better methods for obtaining the desired calibration.

This effort was carried out because it seemed that recently developed devices such as lasers could be used to provide improved means for calibrating baselines. Also, although most people accept the degree of accuracy claimed by the Finns, a few do not. These people point to the possibility of certain systematic errors in the Väisälä technique and feel that the Finns may actually be achieving precision rather than accuracy. The improved technique is designed to remove the most significant possible sources of systematic error.

The improved measurement system consists of three steps. The first 25 meters of the baseline would be measured using a special purpose interferometer. This distance would then be multiplied up to 500 meters (1000 meters if possible) using the Väisälä technique and then the remainder of the line would be measured by multiplying the 500 meters upward using Geodolite-type equipment in a Väisälä-type manner. These methods, together with their advantages will be described in the following paragraphs. The interferometer will be described in the next section.

The Väisälä system as presently used has two principle weaknesses. One is that its reference for distance measurements is a quartz meter bar which has been compared with the former international standard bar kept in Paris. Since the standard is now in terms of wavelengths of light from Krypton, this is a rather indirect route to obtaining true accuracy. Furthermore, the length of the bar is a function of its temperature and probably also changes with age. If the temperature of the bar is accurately known its expansion or contraction can be determined but one can never be sure how accurately he knows the effective internal temperature of a solid object.

The second weak point has to do with the variation of the refractive index along the baseline. The Väisälä system must be used at night and it turns out that under good atmospheric conditions the temperature is quite uniform. An exception to this sometimes occurs however, in the vicinity of the zero meter pillar. Here the temperature is somewhat higher because the massive concrete structure is reradiating heat absorbed during the day.

This condition is most serious for the first five meters along the line. To reduce the effect and to eliminate the first limitation, it is recommended that the first 25 meters be measured using a special purpose interferometer whose ray path is in an evacuated tube. This interferometer will permit the distance to be measured in terms of laser wavelengths which can be compared accurately with the wavelength of Krypton 86.

After the distance has been measured, the evacuated tube is removed and the 25 meter distance is multiplied up to 500 meters using the Väisälä system. Since the entire 25 meter distance is being multiplied, the temperature effects in the first five meters are of considerably less importance.

Extension beyond 500 meters can probably best be obtained by using a special purpose Geodolite-type instrument in a Väisälä-type manner. That is, a laser beam could be amplitude modulated with a sine wave whose frequency is four gigahertz. This beam would be broken into two parts with one part being reflected back and forth between 0 and 500 meters twice while the other part travels out to 1000 meters and back. The phase of the modulation on these two beams would then be compared. If the average refractive indexes along the two ray paths are the same, then the two signals should be exactly in phase. If the indexes are not equal, then a difference in phase will occur. The difference to be expected, if any, can be determined from the atmospheric data which is obtained along the paths. During baseline calibration, the atmospheric data would be collected and used to determine the average refractive index of the atmosphere along the ray path between 0 and 500 meters and that between 500 and 1000 meters. This information would then be used to calculate the amount of phase shift which should exist between the two modulation signals. The position of the 1000 meter mirror could then be adjusted until the phase shift reaches the desired value.

The accuracy with which this can be done depends upon the accuracy with which the phase shifts can be measured. The Rantec Model ET-210 test equipment can measure phase shift with a probable error of ± 0.75 degrees, and this corresponds to a probable error in the round trip distance of ± 0.156 millimeters. This is 0.78 parts in 10^7 and, therefore, provides the required accuracy. The advantage of this technique lies in the fact that it does not require that the modulating signal be extremely stable or that its wavelength be known with very great accuracy. It does depend upon the system's ability to resolve small phase differences but the requirement is within the state-of-the-art.

The greater distances of 1500, 2000, 3000 and 4000 meters could be measured using the same equipment and multiplying upward by factors of 2, or 3 from appropriate smaller distances. Of course, a technique of this sort will be limited by the variation of the refractive index of the atmosphere and many measurements of each length should be made with the final value in each case obtained by standard statistical techniques. The method has not been tried but seems to have enough inherent advantages that it should be experimentally tested.

(5) SPECIAL PURPOSE INTERFEROMETER

a. General

The interferometer described in this section can be used to measure distances up to at least 40 meters in length with very great accuracy. It does this by taking advantage of the long coherence length associated with the light obtained from certain very stable lasers. The distance is measured in terms of laser wavelengths which can then be converted to Krypton 86 wavelengths. The basic unit of length is now defined in terms of Krypton 86 wavelength and since wavelengths can be compared with an accuracy of at least one part in 10^8 , this approach has significant appeal. The principle problem therefore was how to measure a given distance in terms of laser wavelengths. One technique which is widely used consists of building an interferometer containing a movable mirror. As the mirror is moved, the fringe pattern changes in a manner such that a phototube can be used to obtain a voltage pulse every time the mirror moves a distance equal to $\lambda/2$. These pulses are counted and the result converted into distance. The technique is called fringe counting and has been used to measure distances up to 40 meters in length. In every case known to this author, the technique has been used in the open atmosphere and therefore although the number of wavelengths is known exactly, the average value of the wavelength is probably not known with an accuracy much greater than one part in 10^6 . Therefore the total distance is measured with comparable accuracy. To achieve accuracies of one part in 10^7 or better, the moving mirror must be in a vacuum or an accurately controlled atmosphere. Creating such an environment for a mirror which must be moved along a path many meters long is a substantial engineering problem. Furthermore, since the distance which can be measured using this technique seems to be relatively limited, the remainder of the baseline must be measured by comparing it with the distance measured with the fringe counter. The Väisälä technique is well

.suited for this application but the structure necessary to create the vacuum or controlled atmosphere would most certainly interfere with its operation. Another method was therefore sought.

Several other approaches to the problem were made and finally the special purpose interferometer shown in Figure 4-7 was conceived. This interferometer is capable of measuring the distance between the two mirrors with an accuracy of at least one part in 10^7 . The Väisälä technique can then be used to multiply this distance up to 500 meters as described in an earlier part of this Section.

The two mirrors shown in Figure 4-7 are rigidly attached to concrete pillars in the manner of the Väisälä equipment. The laser is a Spectra Physics Model 119 which has a greater coherence length than any other laser commercially available today. It is thought that a mirror spacing of up to at least 50 meters is possible with this laser. To be conservative however, it is recommended that the mirror spacing be set at 25 meters.

The evacuated tube is placed between the mirrors in such a manner that it does not touch the mirrors or the concrete pillars to which they are attached. The ends of the tube are slightly tilted so that light reflected by the surfaces of the glass end plates does not enter the telescope.

The fringes which appear on the screen are circular in shape and are due to interference between the beams reflected by the partially reflecting and the totally reflecting mirrors. By measuring where the fringe intensity minimums occur it is possible to determine the phase shift between the wavefronts of the two beams. Since the two beams travel the same path except for the region between the two mirrors, the phase shift measured using the fringes can be utilized to determine the mirror separation. If d is the separation

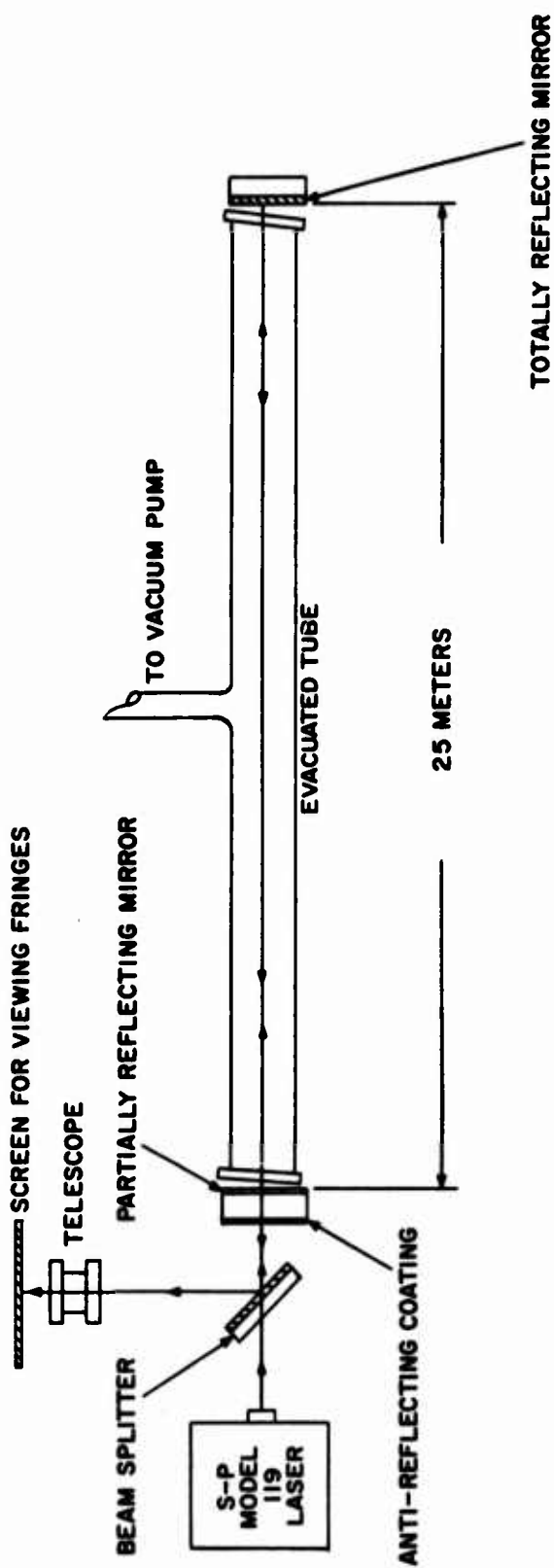


Figure 4-7 Special Purpose Interferometer

between the mirrors, then the phase shift between the two beams is given by:

$$\begin{aligned}\phi_t &= \frac{d}{\lambda} (360^\circ) \\ &= k (360^\circ) + \phi\end{aligned}\tag{4-4}$$

where λ is the wavelength of the radiation and k is an integer. The fringes can be used to determine ϕ but the value of k and therefore ϕ_t remains unknown. Actually some limits can be placed on the value of k by measuring the distance, d , by independent means. The accuracy of this measurement will determine the range of values of k which are possible.

It is well known that all but one of the possible values of k can be eliminated if ϕ is determined for each of several, specially chosen, different wavelengths. This technique is known as the "Method of Exact Fractions" and is described in Reference (8).

Unfortunately, when one is attempting to obtain interference fringes with a 50 meter difference in ray path length only two visible region wavelengths are presently available. One of these is the 0.63299 micron wavelength at which the Model 119 laser normally operates. The other is at 0.64028 microns and can be obtained from a Model 119 laser using a special set of mirrors. It is recommended that a Model 119 operating at each of these wavelengths be obtained.

The partially reflecting mirror should be approximately 80% transmitting and 20% reflecting. This allows for a loss of 55% of the original intensity between the two mirrors. Such a loss is desirable so that second go-round reflections are of negligible amplitude. Much of the loss is obtained at the surfaces of the glass end plates which are attached to the evacuated tube. In practice, the loss between the two mirrors should be measured and the reflectivity of the partially reflecting mirror adjusted so that the two beams

striking the screen have equal intensity.

An analysis of the effects of the evacuated tube on the accuracy of the system has been carried out. Of course the ideal system would be entirely enclosed by a vacuum but as mentioned earlier the achievement of such an environment is a substantial engineering task. Therefore, it seems far more desirable to evacuate only that region between the two mirrors where the laser beam travels. This is done with an evacuated tube which does not touch the mirrors or the concrete pillars upon which they rest. The tube has its own supports and although it is subjected to very large air pressure forces, no force is applied to the pillars or mirrors. Such a tube may be evacuated from the center thereby keeping the vacuum pump with its associated vibration at least 12.5 meters from either pillar. It is estimated that an adequate vacuum can be obtained in a 2 inch diameter tube by pumping with an ordinary mechanical roughing pump for a period of five hours. Once the desired vacuum is obtained, the pump could be shut down for a short time, if necessary, to allow the precise fringe measurements to be made.

The characteristics of the glass end plates and the air gaps between these plates and the mirrors must be accurately known. An error analysis of this part of the system has been carried out and the results are as follows. Let the true distance between the two mirrors, d , be given by:

$$d = s - 2d_1(n_1 - 1) - 2d_2(n_2 - 1) \quad (4-5)$$

where s is the electrical distance as measured using the interferometer

d_1 is the length of each of the air gaps.

d_2 is the effective thickness of each glass end plate.

n_1 is the refractive index of the air between the glass plates and the mirrors.

n_2 is the refractive index of the glass plates.

The error in d is given by:

$$\Delta d = \frac{\partial d}{\partial s} \Delta s + \frac{\partial d}{\partial d_1} \Delta d_1 + \frac{\partial d}{\partial d_2} \Delta d_2 + \frac{\partial d}{\partial n_1} \Delta n_1 + \frac{\partial d}{\partial n_2} \Delta n_2$$

(4-6)

For typical values of

$$d_1 = 3 \text{ millimeters}$$

$$d_2 = 6 \text{ millimeters}$$

$$n_1 = 1.000285$$

$$n_2 = 1.500$$

The derivatives are given by:

$$\frac{\partial d}{\partial s} = 1.0$$

$$\frac{\partial d}{\partial d_1} = -2(n_1 - 1) = -570 \times 10^6$$

$$\frac{\partial d}{\partial d_2} = -2(n_2 - 1) = -1.0$$

$$\frac{\partial d}{\partial n_1} = -2d_1 = -6 \times 10^{-3} \text{ meters}$$

$$\frac{\partial d}{\partial n_2} = -2d_2 = -12 \times 10^{-3} \text{ meters}$$

It can be assumed that the error Δs is negligibly small. Therefore

$$\Delta d = -570 \times 10^{-6} \Delta d_1 - 1.0 \Delta d_2 - 6 \times 10^{-3} \Delta n_1 - 12 \times 10^{-3} \Delta n_2 \quad (4-8)$$

Since d is 25 meters and an error of less than one part in 10^7 is desired, Δd must be somewhat less than 2.5 microns. Also, since the errors are independent, random, and can be assumed to have zero average

value we may write Equation (4-8) in terms of standard deviations:

$$\sigma_d = [3.25 \times 10^{-7} \sigma_{d_1}^2 + \sigma_{d_2}^2 + 36 \times 10^{-6} \sigma_{n_1}^2 + 144 \times 10^{-6} \sigma_{n_2}^2]^{\frac{1}{2}} \quad (4-9)$$

Typical values for the standard deviations are:

$$\sigma_{n_1} = 10^{-6}$$

$$\sigma_{n_2} = 10^{-5}$$

$$\sigma_{d_1} = 0.3 \text{ millimeters}$$

$$\sigma_{d_2} = 1 \text{ micron}$$

When these values are substituted into the above equation, it is found that $\sigma_d = 1.02$ microns which is one part in 25 million and well within the accuracy limits existing for this application.

It should be pointed out that in the example presented above, the error is almost entirely due to the error in determining the effective thickness of the glass end plates. The thickness of such plates can be measured with an accuracy of one micron and since the plates are not perpendicular to the laser beam, the effective thickness must be calculated. This can be easily done when the slant angle is known. Of course, the effects of air pressure on the thickness of the glass must be determined and used in determining d_2 and Δd_2 . The error in d is relatively insensitive to changes in all of the quantities except n_2 and Δd_2 . Therefore, the typical values of these quantities chosen above could be significantly increased, if necessary, without producing a substantial change in σ_d .

(b) The Use of Two Wavelengths

Let it be assumed that the distance between the two mirrors is approximately 25 meters. If the distance were exactly 25 meters, the total phase shift between the two beams at a wavelength of 0.63299μ

would be 78,990,189 complete cycles plus 151 degrees and that at 0.64028μ would be 78,090,835 complete cycles plus 93 degrees. If the distance between the mirrors is 25 meters plus $x/2$ then the phase shift at the two wavelengths would be:

$$\phi_1 = \frac{x}{0.63299} 360^\circ + 151^\circ \quad (4-11)$$

$$\phi_2 = \frac{x}{0.64028} 360^\circ + 93^\circ$$

where x is measured in microns and the number of complete wavelengths in the 50 meter path have been ignored. Let us now define two new phase shift quantities as:

$$\phi'_1 = \phi_1 - 360 k_1 \text{ degrees} \quad (4-12)$$

$$\phi'_2 = \phi_2 - 360 k_2 \text{ degrees}$$

where k_1 and k_2 are positive or negative integers which are selected such that ϕ'_1 and ϕ'_2 are greater than or equal to zero and less than 360° . ϕ'_1 and ϕ'_2 are therefore the angles which can be measured using the interferometer. To see how a knowledge of the magnitudes of ϕ'_1 and ϕ'_2 can be used to measure distance consider how their difference varies as a function of x :

$$\phi'_1 - \phi'_2 = 6.475 x + 58 + 360(k_2 - k_1) \text{ degrees} \quad (4-13)$$

A plot of this difference as a function of x is given in Figure 4-8. Although the figure covers only the interval from $x = 0$ to $x = 12.5$ microns, it is easy for one to visualize how the envelope of the function behaves outside this interval. From Equation (4-13) it can be seen that this envelope will repeat everytime $6.475 x$ increases by 360° . The function therefore has a period given by:

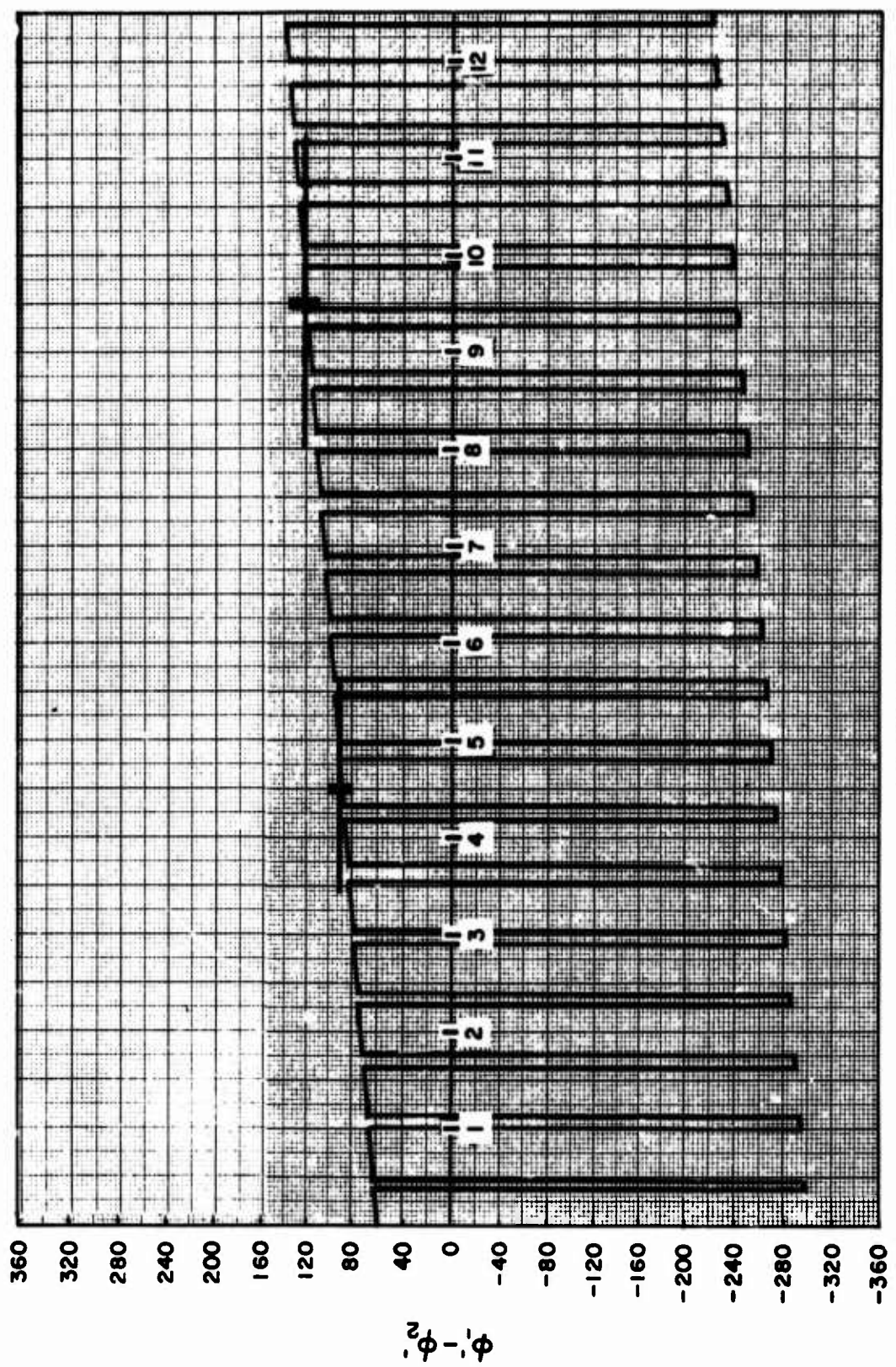


Figure 4-8 Difference in Phase as a Function of Distance

$$x = \frac{360^\circ}{6.475} = 55.6 \text{ microns} \quad (4-14)$$

If ϕ_1' and ϕ_2' are measured using the interferometer, then the quantity $\phi_1' - \phi_2'$ can be determined. From this the total round trip distance between the mirrors can be determined with an ambiguity distance of 55.6 microns and other means must be found for resolving this ambiguity.

To understand what has been said here, consider the following example. Let the measured values be:

$$\phi_1' = 172^\circ \quad (4-15)$$

$$\phi_2' = 69^\circ$$

Assume that each angle has been measured using the interferometer to within $\pm \frac{\lambda}{45} = \pm 8^\circ$.

Then $\phi_1' - \phi_2'$ will be equal to 103° and this will be known with an accuracy of $\pm 16^\circ$. Therefore $\phi_1' - \phi_2'$ will lie between 87° and 119° . From Figure 4-8 it can be seen that this range of angles occurs for values of x between 4.5 and 9.5 microns. If a value of 7 microns is chosen for x , then the round trip distance will be known with a probable error of 2.5 microns which is 0.5 parts in 10^7 . This measurement places the distance at the proper place within the 55.6 micron interval and the problem now becomes that of determining which interval is being used. At the present time there is no easy way of resolving the 55.6 micron ambiguity that arises in the distance measurements. What is needed is a means for determining which 55.6 micron interval the total ray path falls in. Therefore the round trip path length (twice the mirror spacing) must be measured by other means to an accuracy of ± 27.8 microns. In the future more

laser wavelengths will probably become available for interferometer use and some will probably be of such a magnitude that their use, together with the two already available will allow the ambiguity interval to be increased to the point where a relatively crude initial measurement of mirror spacing will be sufficient for ambiguity removal. Until this happens however, the 27.8 micron requirement will prevail and this is 5.4 parts in 10^7 for the 50 meter total path length.

At present it seems that the best way of measuring the total round trip path length between the mirrors with an accuracy of \pm 27.8 microns involves amplitude modulation of the laser beam. A measurement of the phase shift between the modulation on the beams reflected by the two mirrors can be used to determine the round trip path length with an ambiguity distance equal to the modulation wavelength. The phase shift must be measured with an accuracy sufficiently great that the distance will be known to within \pm 27.8 microns. To get an idea of what is required here, let the laser beam be amplitude modulated at a frequency of 10 gigahertz. This corresponds to a wavelength of 3 centimeters. To determine the round trip path length with the desired accuracy, the phase shift must be measured with an accuracy of \pm 0.32 degrees. This distance measurement will be ambiguous every 3 centimeters and the ambiguity can be removed by measuring the distance with a tape. In this application a very stable modulating source, whose wavelength can be determined with an accuracy of at least five parts in 10^7 , must be used.

It is realized that some aspects of this technique lie near the edge of what is possible due to state of the art limitations. In particular, the means of modulating the laser beam at such a high frequency and determining the phase shift with such accuracy fall in this category. The phase shift could be determined by removing the modulation from the light wave carrier with a phototube and then applying the output signal to an electric phase shift measuring system. Another technique

for determining the modulation phase shift involves a measurement of the intensity of the fringe pattern as a function of modulation wavelength. When the laser beam is modulated at microwave frequencies, no movement of the fringe pattern occurs. That is, the positions of the nulls and points of maximum brightness remain fixed. It is true however, that as the phase shift of the modulation on the two beams varies, the intensity of the fringe pattern changes. If twice the mirror spacing is exactly an integral number of wavelengths at the modulating frequency, then the intensity at the nulls is minimum and that at the maximums is maximum. In this condition, the modulation on the two interfering beams is in phase and the fringe contrast is greatest. For other mirror spacings the two modulation envelopes are out of phase and the intensity at the nulls is greater and that at the maximum points is less. Therefore, a means for detecting when twice the mirror spacing is an integral number of modulation wavelengths can be developed by using phototubes to determine the intensity of the radiation at a null and at a maximum. In practice, the mirrors can be positioned and then the wavelength of the modulation varied until the output of one phototube is a maximum and that at the other is a minimum. The modulation frequency can then be measured and the wavelength calculated. Since the number of wavelengths can be determined from an independent measurement, the distance will be known with an accuracy which is dependent on the sensitivity of the phototube measurements. No experimental measurements of the sensitivity of this system have been made but the technique appears to be very promising.

In summary it can be said that the special purpose interferometer shows considerable promise of providing a significant increase in the accuracy of distance measurements. An experimental model of this interferometer was constructed in the RADC Coherent Optics Laboratory and the results of this work are discussed in the next section. Two means for resolving the distance ambiguity which

presently exists when the interferometer is used have been suggested but time has not permitted an intensive study of their relative usefulness. It would be highly desireable to carry out such a study in the future so that a complete system can be specified.

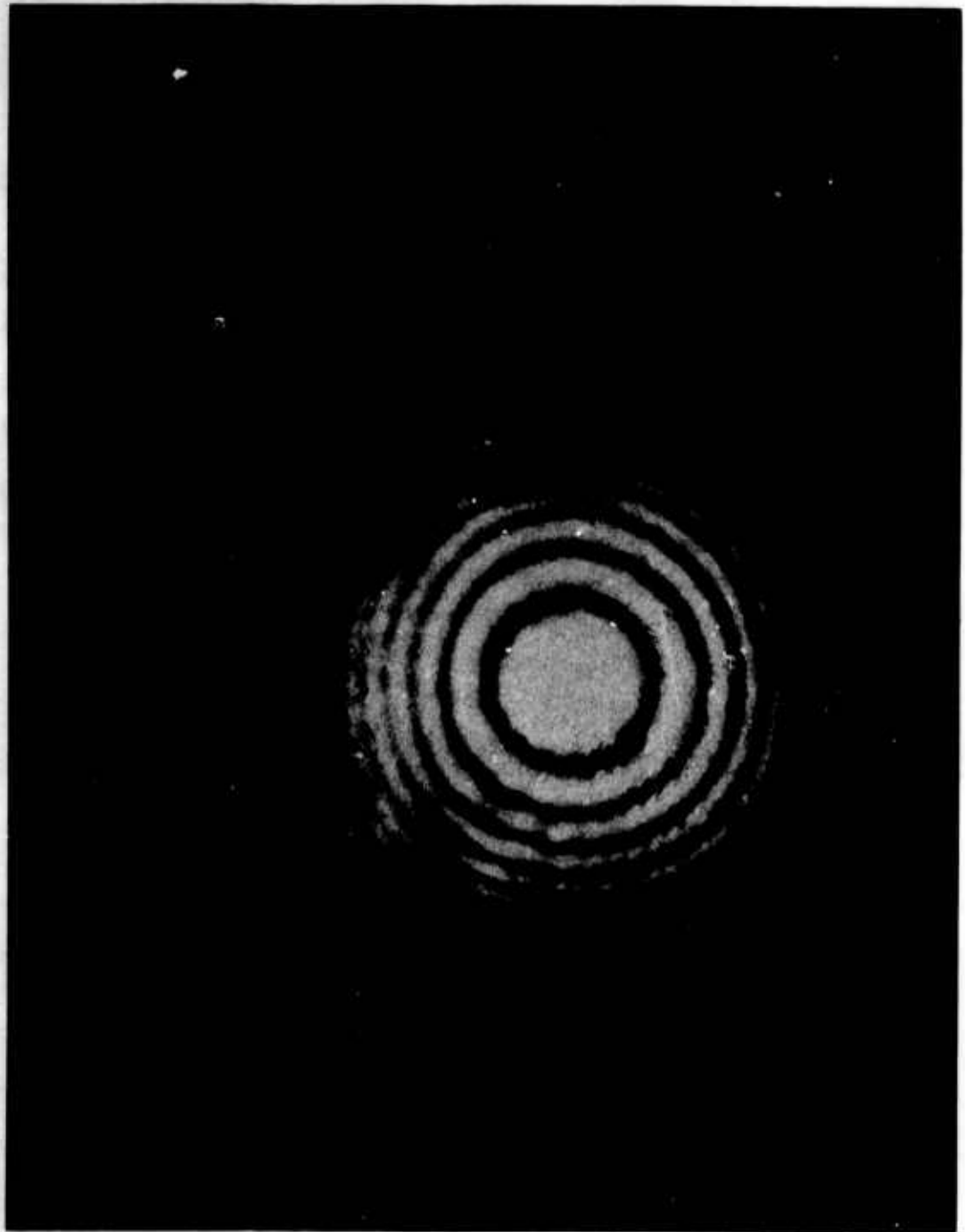
6. LABORATORY EXPERIMENTS

The idea of using the special-purpose interferometer appeared so promising that arrangements were made to construct such a system in the Coherent Optics Laboratory at RADC. This was done on a standard optical bench placed on a granite table. Standard optical components were used and the distance between the mirrors set at 243 centimeters. At first no tube was placed between the mirrors and the effect of air movement in the room made the fringe pattern relatively unstable. This effect was eliminated by placing a two inch glass tube between the mirrors and covering its ends with glass plates. The tube was not evacuated.

A Spectra-Physics model 119 laser was used as the source of radiation. This device was operated at 0.63299 microns wavelength without servo control and was found to have very high wavelength stability after a reasonable warm-up period. When the air filled tube was used, the fringes were stable to the extent that no fringe movement could be observed with the eye for periods of 10 minutes or more.

The fringes obtained with the interferometer were displayed in a number of ways. In every case the telescope shown in Figure 4-7 consisted merely of a concave-concave diverging lens which spread the pattern out. At first, the pattern was displayed on a white screen so that its characteristics could be studied. The pattern was later focused on a piece of film for photographing. The result is shown in Figure 4-9. It will be noticed that this picture contains many smaller patterns which are due to particles of dust on the mirrors, lenses, in the air and on the glass end plates. These rings were not noticed during the course of the experiments and were discovered only after the photographs were processed.

Figure 4-9 Photograph of Interferometer Fringe Pattern



When using the interferometer to measure distance, the positions of the fringe nulls must be determined. To do this the fringe pattern was focused on the photocathode of a General Electric home entertainment type Vidicon camera. Figures 4-10, 4-11, and 4-12 show the interferometer together with a monitor for displaying the fringe pattern. The video signal from the camera was applied to the vertical input of a Tektronix 547 oscilloscope. Using the delayed sweep feature of this instrument, the raster line passing through the center of the fringe pattern was displayed. Figure 4-13a shows a typical oscilloscope pattern where it will be noticed that the nulls (lower edges) of the waveform are relatively pointed while the upper edges are more rounded. Theoretically the shapes of the two extremities should be similar but non-linearities in the Vidicon light to voltage transfer function produce the distortion. In this case, the distortion is quite helpful since it allows the positions of the nulls to be more accurately located. To illustrate the sharpness of the nulls, the oscilloscope waveform was amplified and moved upward. The resulting waveform is shown in Figure 4-13b. From the picture it can be seen that the positions of the nulls can be obtained with relatively high accuracy even with this unsophisticated system. The phase relationship at the center of the fringe pattern must be determined with an accuracy of $\pm \lambda/45$ in order that the distance be measured with the desired accuracy. The experimental evidence presented here indicates that this can certainly be done.

The experiment described in this section has shown that a scaled down model of the special purpose interferometer can be used to measure the phase shift between the laser beams reflected by the two mirrors with an accuracy great enough to allow the distance between the mirrors to be determined with a probable error of ± 2.50 microns. Therefore, this portion of the distance measuring system is considered feasible.

7. SUMMARY

In this section several means have been presented for calibrating the baseline. One method could be used immediately while the others all need

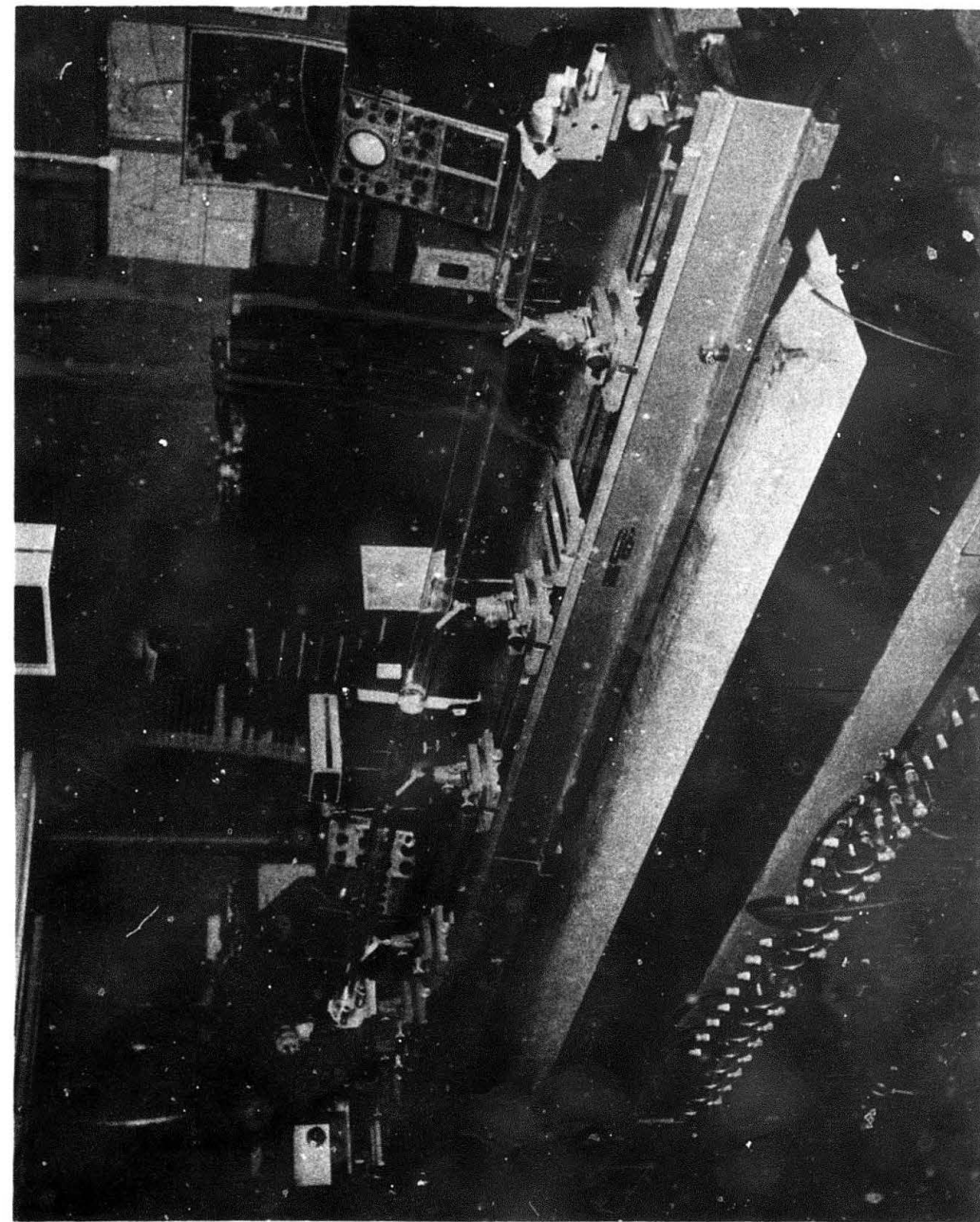


Figure 4-10 Experimental Model of Interferometer

Figure 4-11 Experimental Model of Interferometer

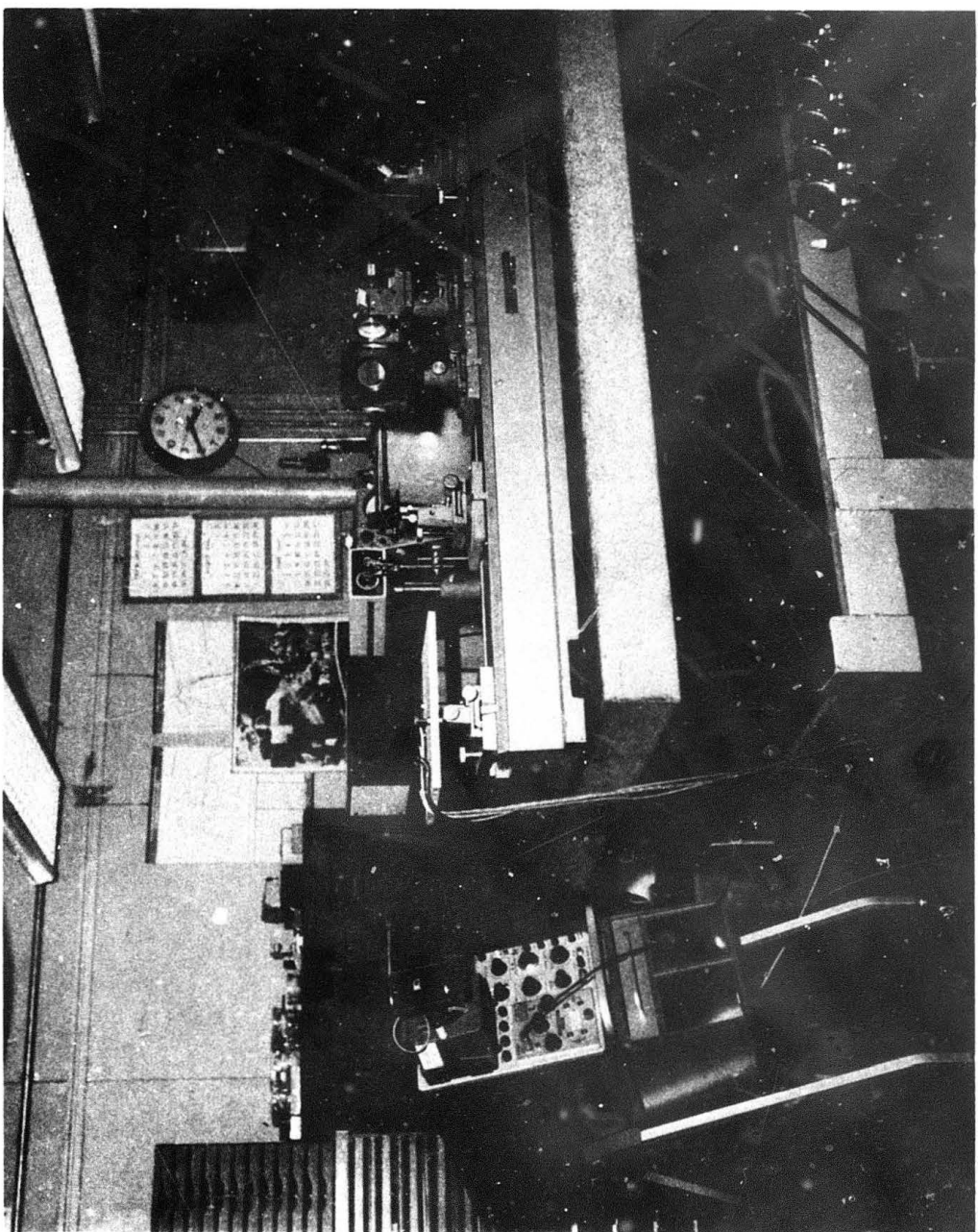
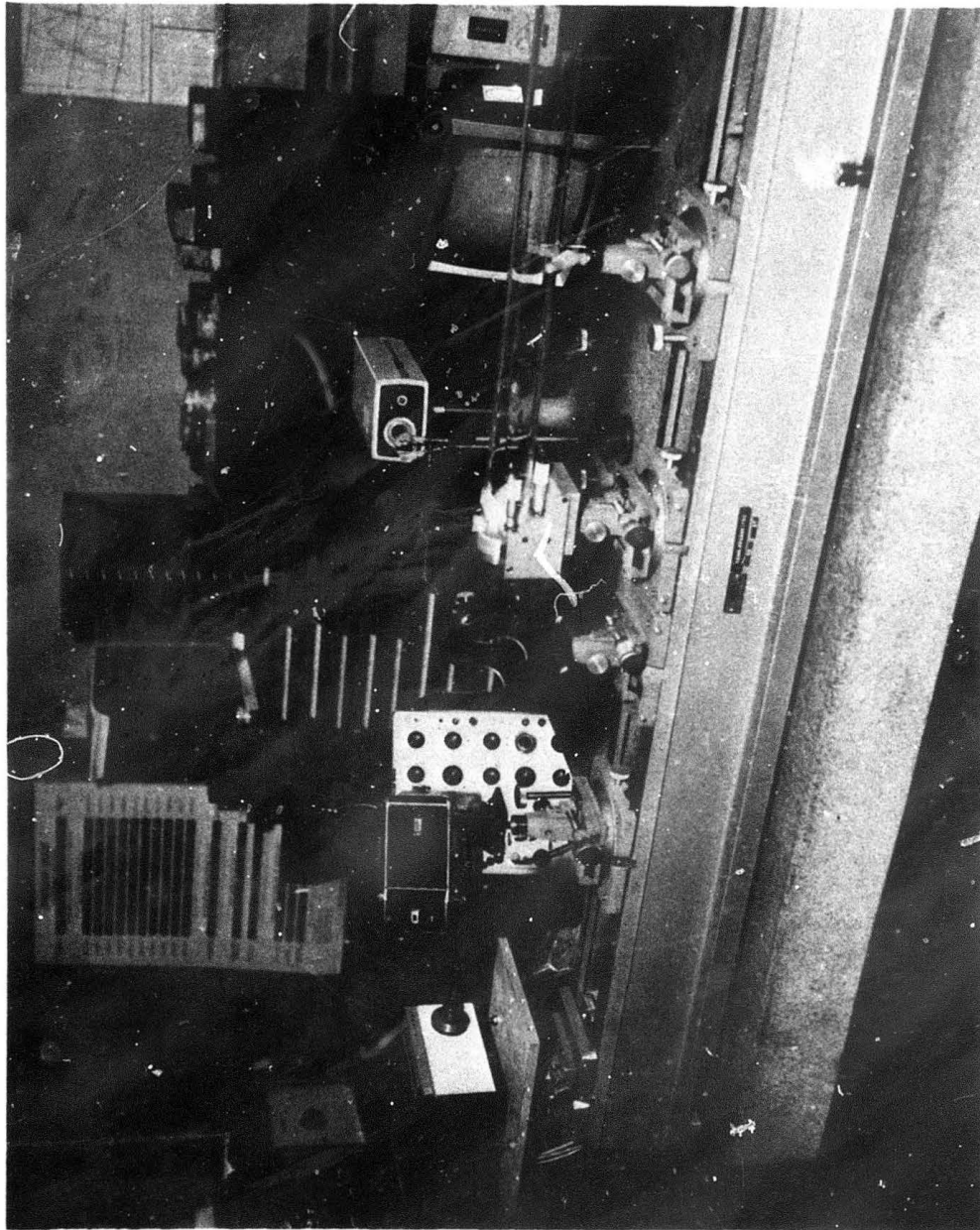
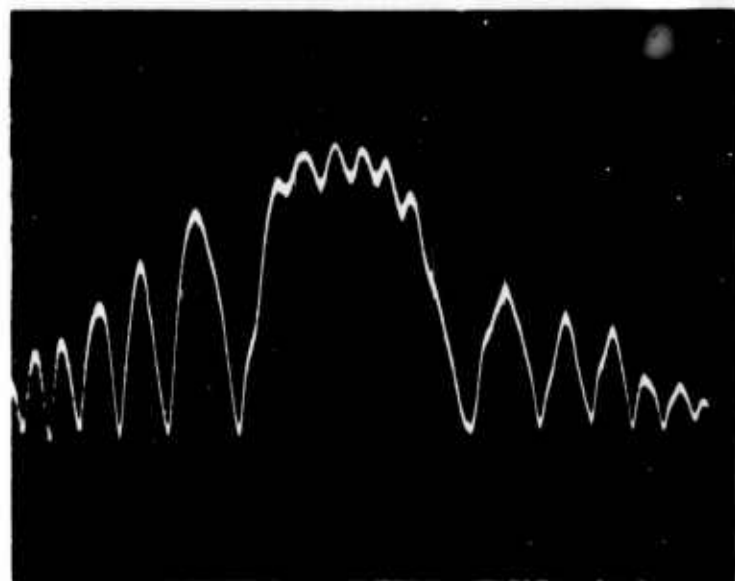
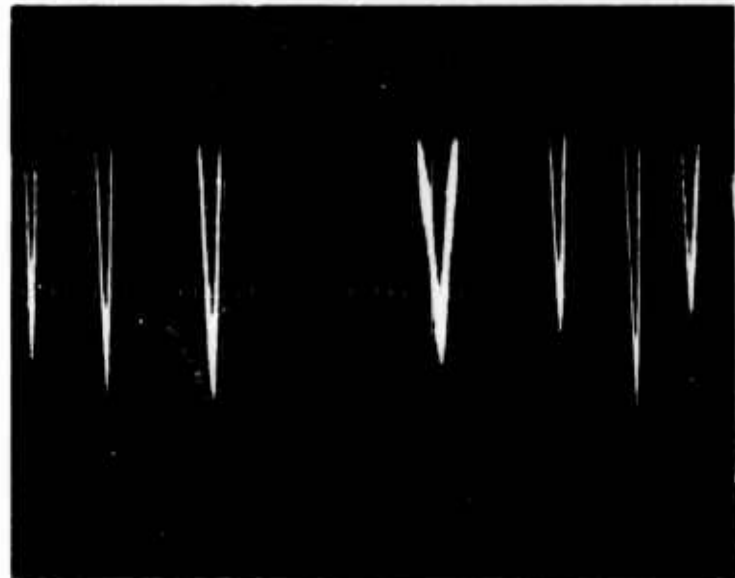


Figure 4-12 Experimental Model of Interferometer





(a) VIDICON VIDEO WAVEFORM



(b) LOWER EDGE OF VIDICON VIDEO WAVEFORM MAGNIFIED

Figure 4-13 Oscilloscope Display of Vidicon Video Signals

further development. These latter methods however, show promise of being capable ultimately of achieving increased accuracy. In particular, the special purpose interferometer seems to have exciting prospects and should be developed further. This technique could be used to make precise measurements in many applications.

As this report was being completed, it was learned that a group working at the Boeing Scientific Research Laboratories has developed a similar interferometer for use in the observation of earth tides. Although their system is quite similar, they do not use it to measure distance. Instead, they use it to measure changes in length due to earth tides. To accomplish this they use fringe counting techniques. References (9), (10), and (11) describe the Boeing work, where it is claimed that displacements of the completely reflecting mirror as small as 1/100 of a fringe can be resolved. Other experimental data are also presented in these references and all indicate that the idea of measuring distance in this manner is very feasible indeed.

SECTION V

ANGLE CALIBRATION FACILITY

1. GENERAL

The facility angle requirements fall into two categories, those related to vertical angles and those for horizontal angles. The study requirements state that the baseline and horizontal angle facility must be in the same physical location, but that the vertical angle facility may be located elsewhere. It has been found however, that there is no advantage in placing the vertical facility elsewhere, and therefore, all three facilities should be located at the same site.

In the previous section, a discussion of the effects of variations in refractive index on the accuracy of electromagnetic distance measurements was presented. It turns out that this phenomenon also provides a limitation on the accuracy with which angles may be measured. The effect is especially severe for vertical angle measurements because the temperature, and therefore the refractive index of the atmosphere, ordinarily varies significantly in the first 30 feet above the ground. Constant temperature surfaces are often parallel to the surface of the earth and therefore the ray path of an electromagnetic vertical angle measuring device must pass through these surfaces, usually at an angle other than 90°. In such a case, ray bending occurs in a somewhat unpredictable way. Highly accurate angle measurements cannot be made because although the angle of arrival of the radiation at the measuring instrument can be determined accurately, the angle between the horizontal and a straight line leading to a particular elevated point cannot be accurately determined. A similar effect occurs for horizontal angle measurements but, as mentioned in the next section, its magnitude is ordinarily sufficiently small that it will not prevent the contract requirements from being met. Of course, when the air is turbulent, the ray path is bent in a

fluctuating, random way and the image of a distant point tends to dance around. Under such conditions, no accurate angle or distance measurements can be made.

During the course of the study, no other out-of-doors angle calibration facility was found and as far as unclassified equipment is concerned, there seems to be no present need for vertical and horizontal angle calibrating facilities with the ± 0.2 second accuracy specified in the study requirements. It is therefore recommended that until a need for such facilities exists, they not be built. To meet the study requirements, however, design criteria for such facilities are presented in this section along with a suggested location at the Chase Lake site.

2. HORIZONTAL ANGLE CALIBRATION RANGE

a. Range Configuration

The horizontal angle calibration range consists of a central point surrounded by a number of outlying markers. A particular calibrated angle is obtained by using the separation between the lines-of-sight to a particular pair of markers. The marker locations were selected such that an angle of any integral number of degrees between 0° and 360° can be obtained. These angles will be accurate to within 0.2 seconds of arc (probable error). The markers will be attached to monuments which are located generally on the perimeter of a circle whose center is at the central point. It should be emphasized that the idea of placing the monuments on a circle is merely one of convenience and if the terrain dictates otherwise, they may be put at varying ranges. Each marker should be an optical target of the form shown in Figure 5-1 having a translucent, flat white cross on a solid black background. Rear illumination should be provided so that day or night operation is possible. The center of the target must be positioned to within 0.2 seconds of arc which corres-

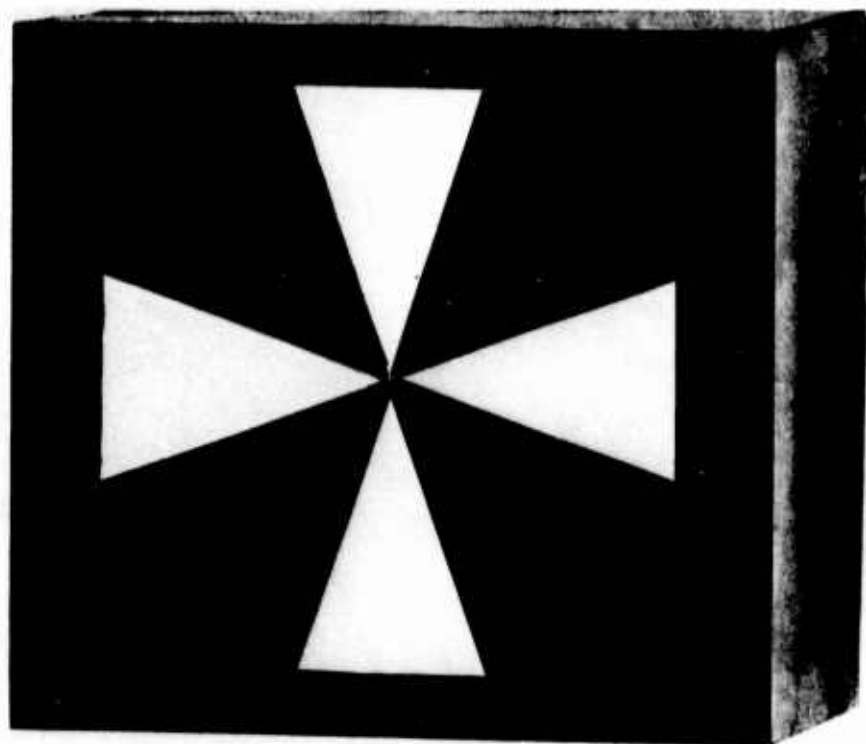


Figure 5-1 Optical Target

ponds to a tolerance of \pm 0.97 millimeters (probable error) in the transverse direction if the target is one kilometer away. This is a relatively small tolerance and therefore, the range of the markers should be at least one kilometer. A greater radial distance would be more desirable since it would result in an increased transverse distance tolerance.

The facility must be placed at the Chase Lake site and the layout shown in Figure 5-2 is suggested. This location was chosen because it results in the largest possible radial distance (1.5 kilometers) to the markers while staying on the flat part of the plain and away from those areas where a significant number of trees would have to be cut. The markers should be located 0° , 1° , 2° , 3° , ..., 21° , 22° , 23° , 45° , 90° , 135° , 158° , 180° , 270° , and 315° for a total of 31 monuments. This layout is subject to some modification if a detailed survey of the area should show that the topography of the region exhibits small depressions or rises at the points where the monuments are supposed to be located. In such a case the range of the markers could be adjusted to place them at the proper elevation. The forest will have to be removed wherever it blocks the line-of-sight to a given marker.

It should also be pointed out that if a facility with reduced accuracy requirements were built, then the radial distances to the markers could be shortened thereby decreasing the range dimensions. In such a case, a somewhat different orientation of the facility might be more desirable.

Each marker will be attached to a poured concrete pillar which extends approximately 1.5 meters above the surface of the earth. Below the pillar is a reference monument which extends sufficiently deep into the ground to be stable. For the purposes of this range, pillars and monuments similar to those used on the Loenermark (2) baseline in the Netherlands are recommended. These

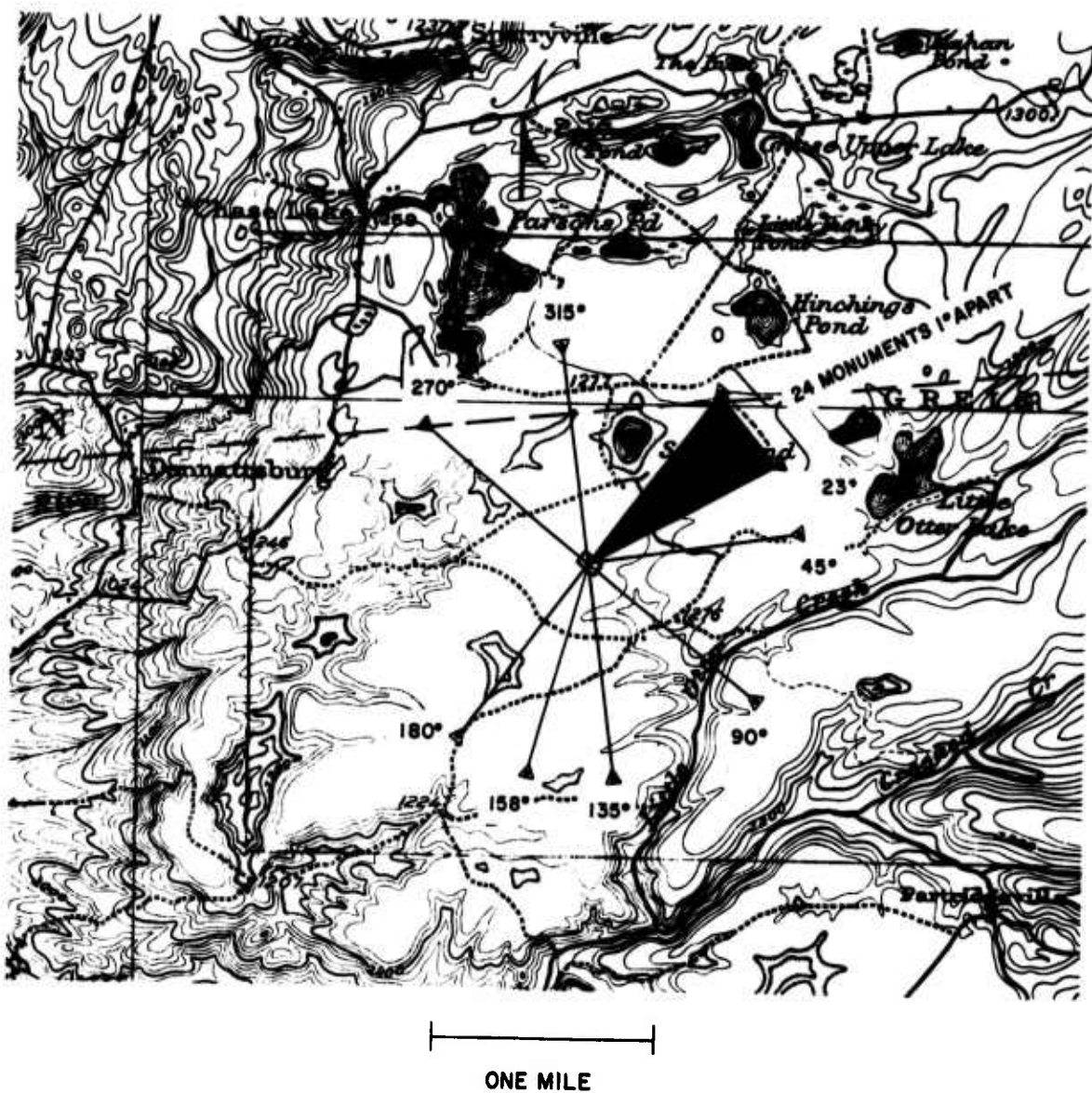


Figure 5-2 Layout of Horizontal Angle Calibrating Facility at the Chase Lake Site

structures are shown in Figure 5-3 where it should be noted that the pillar and monument are not attached. The pillar holds the marker and at the time of calibration the marker position is projected downward and inscribed on a brass plate placed in the top of the monument. The monument is a poured concrete cylinder, one meter in diameter and 1.5 meters deep, which is attached to three piles that have been driven into the ground. The hole for the monument is drilled into the soil and then completely filled with concrete. In this way, there is a minimum of soil disturbance during construction. The monument, whose upper surface is approximately one meter below the surface, forms a very stable reference which will not require frequent recalibration.

The pillar is not nearly as stable as the monument and, therefore, the position of the marker should be periodically checked to be sure that it is directly above the monument reference point. Removable covers should be provided to protect the markers and monuments when the range is not being used.

There will also be a pillar-monument structure at the central point. It should be covered by an open canopy similar to that shown in Figure 7-2, but with the uprights located in such a way that they do not interfere with any of the desired lines-of-sight. The canopy will protect equipment and personnel using the range. Mountings for such equipment, if necessary, must be provided on adjacent pillars whose design will be determined by the type of equipment to be calibrated on the range. As in the case of the outlying structures, the underground reference monument is not attached to the pillars. It is recommended that this monument be constructed in a manner similar to that for the outlying units but that it be somewhat larger having a diameter of 1.5 meters and a length of three meters.

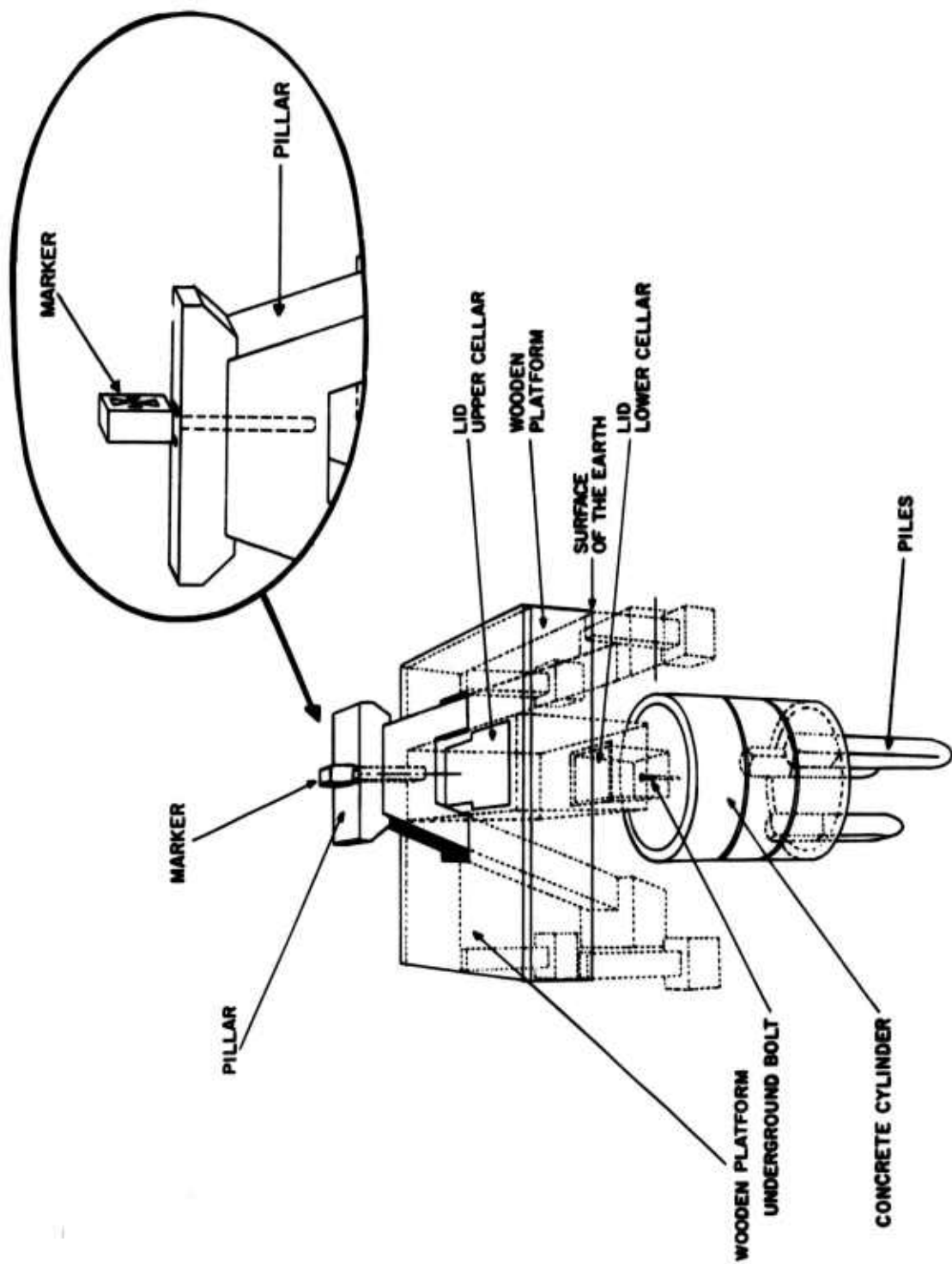


Figure 5-3 Typical Pillar-Monument Configuration

Normal practice dictates that the concrete for the monuments and pillars be poured and then at least six months be allowed to pass before calibration is begun. At the time of calibration, the monument brass plates should be attached and the upper five inches of the pillars be poured. This surface layer of concrete will contain all of the desired mounting bolts and brackets. For an excellent description of important construction procedures, the reader is referred to the "Loenermark" reference which was cited earlier in this section.

b. Method of Calibrating the Range

A theoretical analysis has been performed regarding the attainment of the contract angular accuracy requirements of 0.2 arc seconds (sexagesimal) in the measurement of horizontal angles. An accuracy of 0.1 arc seconds is a desired design goal. The results of the analysis for horizontal angles are verified from published results of a recent high accuracy survey performed by the USC and GS (12)

Little technical difficulty is anticipated in achieving the accuracy objective. The Kern Instrument Co. of Switzerland indicates that their theodolite DKM-3 provides a least count of 0.5 seconds and estimation of 0.05 seconds. This, however, may be misleading in some cases since the justification for such refined read-out lies in the use of proper field procedures coupled with suitable data reduction techniques. For this purpose, the USC and GS has established specifications for several levels of survey accuracy. The best of these levels of survey is termed "First Order." Recently, this has been further broken down into accuracy or order classes. For the purposes of this analysis, the old classification will be used permitting use of the actual field results obtained by the USC and GS while engaged in "First Order" triangulation over a period of thirty years.

The "First Order" specification states, "...the average closure of the triangles shall seldom exceed one second."(13) This may be taken to mean that ± 1 second of arc is twice the probable error representative of triangle closure using first order procedures. Assuming the facility specification of 0.2 seconds is also in terms of probable error, an analysis may be made of the errors in horizontal angle measurement which will indicate tentatively the necessary level of field effort to achieve the required accuracy.

Triangle closure error in triangulation is defined as:

$$W_e = 180^\circ - \alpha - \beta - \gamma + e$$

where:

α, β, γ ~ interior spherical angles

e ~ spherical excess

W_e ~ triangle misclosure

For the purposes of this analysis it is the error in any one of the spherical angles that is of interest. Assuming all angles of the triangle are measured with equal precision and taking the probable error of misclosure (PEW) from the experience of the USC and GS, the probable error in the angle (PEA) may be computed from:

$$PEA = \frac{PEW}{\sqrt{3}} = \frac{\pm 0.5}{\sqrt{3}} = \pm 0.29 \text{ seconds}$$

This result may be expected for one complete station occupation as accomplished by the field crews of the USC and GS usually during the course of one evening. For this purpose, a Wild T-3 or equivalent theodolite is used employing the mean values of sixteen sets of direct

and reverse observations. For achieving the accuracy required here, an estimate may be made as to the number of reoccupations of the station that will be required.

$$\text{Required accuracy} = \frac{\text{PEA}}{N}$$

where: N ~ number of required reoccupations

Based on the above assumptions, the station would require reoccupation two times preferably with different instruments and on different nights to achieve the required 0.2 arc seconds. To achieve the goal of 0.1 arc seconds may require nine reoccupations with perhaps six different theodolites on as many nights. All errors are in terms of probable errors.

The foregoing analysis has been developed from the specifications and general experience of the USC and GS. It is also of interest to compare the above general procedural recommendations to the results obtained by a specific survey and the methods that were used to obtain the results. During the spring and summer of 1960, the Coast Survey, at the request of AFMTC (Patrick), performed a survey with the unique accuracy specification of one part in 400,000 over an area of 45 by 90 miles. For this task the Geodimeter Model 2A and the Wild T-3 were used. Of particular interest here are the accuracy estimates after adjustment of the observed angles.(12) The probable error of one observation was found to be ± 0.21 seconds which agrees favorably with the above estimate of ± 0.29 seconds derived from general experience. It is recognized that the actual result is aposteriori and has been subject to some refinement due to observational procedures. For instance, due to horizontal refraction, horizontal angles cannot be depended on to an accuracy in excess of ± 0.5 seconds. Accordingly, several nights of observations are required.

Using the field observation instructions for triangulation that were prepared especially for the AFMTC requirements and extending them to the task at hand, a set of field instructions are presented below designed to achieve the \pm 0.2 seconds and \pm 0.1 seconds requirements.

c. Instructions

In general, lines-of-sight should be at least one mile in length. Collimation of both the instrument and the targets should be checked both before and after each observational set to assure \pm 2.0 mm accuracy for the 0.2 seconds task and \pm 1.0 mm accuracy for the 0.1 seconds task.

Field notes should contain a listing of party members, instrument numbers, description of weather including wind direction and magnitude, temperature and general sight conditions. All observations should be made at a time when there is relatively little heat transfer between the earth's surface and the atmosphere. This will often occur on a cloudy night following a cloudy day. On clear days it will occur near sunrise and sunset. Not more than one set of observations is to be made during any one night. A set will consist of at least sixteen positions. Special care should be taken in leveling the instruments.

Quoting from the USC and GS instructions (12) "The observers should be cautioned not to hurry their observations, but to be particularly careful in obtaining precise pointings. Everything that may work against precision in observations shall be avoided and nothing reasonable that will be favorable to accuracy of results shall be overlooked."

To achieve the angle measurements to within a probable error of \pm 0.2 arc seconds, two sets of sixteen positions, each using

different instruments, will be required. If the difference of the means of the sets exceeds \pm 0.5 seconds, a third set will be observed which will be meaned with the set in best agreement, or with both if appropriate. A final angle will be determined from the weighted mean.

To achieve the angle measurements to within a probable error of \pm 0.1 seconds, nine sets of sixteen positions each are required. At least three and perhaps six different first order type theodolites should be used on six different days. Sets which disagree with the mean in excess of 0.4 seconds are to be rejected and reobserved. A weighted mean of the sets will be used as the final adjusted angle.

3. VERTICAL ANGLE CALIBRATION RANGE

a. Range Configuration

During the course of the study a number of possible implementations for the vertical angle calibration facility were considered. At one point it was thought that a system which used the star field as its standard would be best. Further analysis indicated, however, that this scheme had several significant defects.

Of course, all systems are limited by the effects of the variation in the refractive index of the atmosphere. There seems to be no way of accurately predicting the magnitude of this limitation for the Chase Lake site since data obtained at other places may not apply to the area. Therefore, the facility configuration being suggested here, ignores the index effects and it is suggested that before any implementation is carried out, a study of the Chase Lake atmospheric characteristics be made. By measuring air temperature, pressure and water vapor content at appropriate places for relatively long periods of time, data can be obtained, from which refractive index

variations can be calculated. With this information available, it will then be possible to determine the sort of limitations these variations impose on vertical angle measurements.

The angle calibrating configuration to be recommended here consists of an accurately measured baseline and a vertical tower as shown in Figure 5-4. Optical targets similar to those suggested for the horizontal angle facility are placed at various places up the side of the tower. These markers lie along a straight line extending upward from point B on the ground. This line is perpendicular to the baseline A-B. The position of a particular marker relative to point A is determined by accurately measuring the baseline length, R, and the height to the marker, d. An error in positioning the marker will result from errors in measuring R and d and the departure from strict perpendicularity of the lines A-B and B-C. To get an idea of the sort of tolerances which must be placed upon these quantities, consider the situation shown in Figure 5-5 where the departure from 90° of the angle between A-B and B-C has been exaggerated. The error in the vertical angle, α , can be derived as follows:

$$\alpha = \arctan \frac{d \sin \theta}{R - d \cos \theta} \quad (5-1)$$

$$\frac{\partial \alpha}{\partial d} = \frac{R \sin \theta}{R^2 + d^2 - 2Rd \cos \theta} \quad (5-2)$$

$$\frac{\partial \alpha}{\partial R} = \frac{d \sin \theta}{R^2 + d^2 - 2Rd \cos \theta} \quad (5-3)$$

$$\frac{\partial \alpha}{\partial \theta} = \frac{d^2 - Rd \cos \theta}{R^2 + d^2 - 2Rd \cos \theta} \quad (5-4)$$

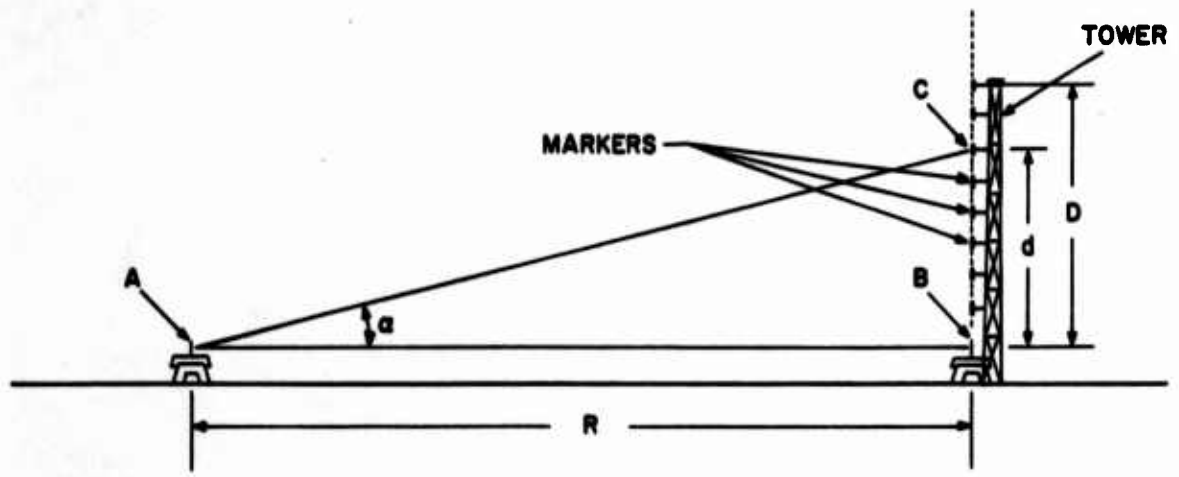


Figure 5-4 Vertical Angle Measuring Facility

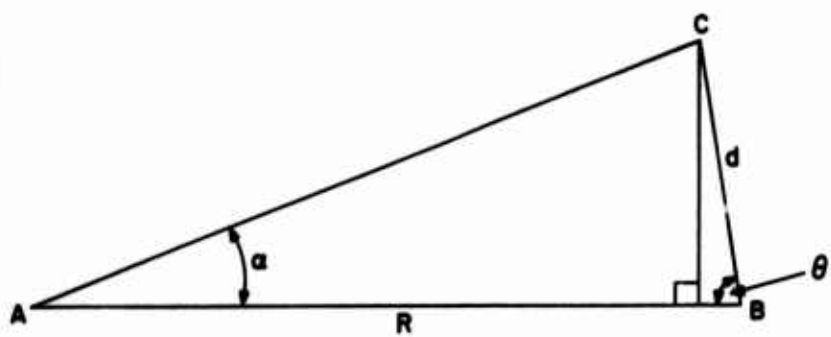


Figure 5-5 Geometrical Relationships Involved in the Facility Layout

For $\theta = 90^\circ$ these become:

$$\frac{\partial \alpha}{\partial d} = \frac{R}{R^2 + d^2} = \frac{\cos^2 \alpha}{R} \quad (5-5)$$

$$\frac{\partial \alpha}{\partial R} = \frac{d}{R^2 + d^2} = -\frac{\sin^2 \alpha}{d} \quad (5-6)$$

$$\frac{\partial \alpha}{\partial \theta} = -\frac{d^2}{R^2 + d^2} = -\sin^2 \alpha \quad (5-7)$$

The total error in α can be expressed in terms of the errors in d , R and θ by the following equation:

$$m_\alpha = \frac{\partial \alpha}{\partial d} m_d + \frac{\partial \alpha}{\partial R} m_R + \frac{\partial \alpha}{\partial \theta} m_\theta \quad (5-8)$$

where m_α , m_d , m_R , and m_θ are the errors in the determination of the respective quantities. If the errors are independent, with zero average values, then the mean squared error in α is given by:

$$\overline{m_\alpha^2} = \left(\frac{\partial \alpha}{\partial d}\right)^2 \overline{m_d^2} + \left(\frac{\partial \alpha}{\partial R}\right)^2 \overline{m_R^2} + \left(\frac{\partial \alpha}{\partial \theta}\right)^2 \overline{m_\theta^2} \quad (5-9)$$

In terms of probable errors this equation may be written as:

$$(PE\alpha)^2 = \left(\frac{\partial \alpha}{\partial d}\right)^2 (PEd)^2 + \left(\frac{\partial \alpha}{\partial R}\right)^2 (PER)^2 + \left(\frac{\partial \alpha}{\partial \theta}\right)^2 (PE\theta)^2 \quad (5-10)$$

To get an idea of what sort of limitation this places upon the range of angles for which the facility may be used, let it be assumed that the probable error in d is one part in 500,000 and that in R is one part in a million. Therefore:

$$(PEd) = 2 \times 10^{-6} \times d \text{ meters}$$

$$(PER) = 1 \times 10^{-6} \times R \text{ meters}$$

After some manipulation, Equation 5-10 becomes:

$$(PE\alpha)^2 = 1.25 \times 10^{-12} \sin^2 2\alpha + (PE\theta)^2 \sin^4 \alpha \quad (5-11)$$

If it is further assumed that the probable error in θ is 0.5 seconds ($\approx 2.5 \times 10^{-6}$ radians), then the above equation becomes:

$$(PE\alpha)^2 = 1.25 \times 10^{-12} \sin^2 \alpha + 6.25 \times 10^{-12} \sin^4 \alpha \quad (5-12)$$

The probable error in α must not exceed 0.2 seconds and therefore:

$$(PE\alpha)^2 = 0.941 \times 10^{-2} \text{ radians}^2$$

When this value is substituted into Equation (5-12) and the result solved for α , it is found that maximum angle is approximately 25° . Therefore, the range can be used to calibrate vertical angle measuring equipment with an accuracy of 0.2 seconds only for angles between 0° and 25° . If a larger calibration interval is desired, then more accurate means must be used to measure R , d and the angle θ . It should be emphasized again that variations in the refractive index of the atmosphere will probably provide even further limitations on the range of angles which can be measured with such high accuracy.

Another limitation on the vertical angle range can result from practical constraints on the maximum tower height. For example, if it is assumed that the tower height is limited to 100 meters, and if the measuring equipment being calibrated has a minimum range of

500 meters, then the maximum obtainable angle will be limited to only 11.3 degrees.

During calibration of the range, the markers on the side of the tower will be precisely positioned and then rarely moved. Different elevation angles will be obtained both by using different markers and by changing the distance R. A number of pillar-monument combinations should be installed for this purpose at increasing distances from the base of the tower so that a change in elevation angle can be obtained by moving the equipment under test from one point to another.

The measurement technique being recommended here uses a baseline, R, whose length has been measured with an accuracy of one part in 10^6 . It is not suggested however, that this be the same line used in the distance measuring facility. This facility should be placed sufficiently far away from the distance measuring baseline that it does not interfere with the homogeneous environment which must be achieved in that region. Since it is anticipated that the vertical angle baseline will not exceed one kilometer in length, there are many places at the Chase Lake site where it could be placed. No specific recommendation on location is made here but rather, this decision should be made when such a facility is constructed.

The vertical angle measuring facility will have a number of pillars and underground monuments and a large tower. The tower should be designed in such a way that its wind resistance and effect on the refractive index of the atmosphere are a minimum. Of course, it should be as stable as possible. The pillars and underground monuments should be similar to those suggested for the horizontal angle facility.

SECTION VI

SITE SURVEYS

The material presented in this section was written by both Dr. Ernest Muller, Professor of Geology at Syracuse University and Dr. Robert Richardson of Syracuse University Research Corporation. In addition, see Appendix A for a complete report by Dr. Muller of the surface geology of the Chase Lake Site.

1. SITE REQUIREMENTS

At the beginning of this study it was thought that the calibration facility baseline would be approximately one kilometer in length and could be located relatively close to Rome, New York. It soon became apparent however that a considerably longer baseline would be recommended. This decision resulted principally from the fact that although all existing, electromagnetic distance measuring devices could be calibrated on a one kilometer baseline, the dual wavelength optical, distance measuring devices, which are currently under development, are expected to require a minimum calibration distance of two to three kilometers. Since these devices are expected to produce more accurate distance measurements than presently available equipment, they will probably be widely used in the future and the calibration facility being proposed here must be able to accomodate them. As a result, a baseline length requirement of at least 4 kilometers (2.5 miles) was established thereby eliminating all prospective sites which were close to RADC.

As the study progressed other site requirements were determined and the final selection was based upon those which are listed below:

SITE REQUIREMENTS

- 1) Location within 50 miles of Rome.
- 2) The facility must be capable of expansion to 2.5 miles in length

if it is not constructed this long initially.

- 3) The terrain must be flat or capable of being graded to a flat condition. It does not necessarily have to be level and a small slope can be tolerated.
- 4) The area surrounding the baseline should be homogeneous; forested if possible.
- 5) The surface layer of the soil and existing vegetation should be of such a character, that large daily changes in surface temperature do not take place.
- 6) The area must be remote from sources of vibration, extreme electromagnetic interference, fog and industrial air pollution.
- 7) The ground must be geologically stable, preferably consisting of gravel or coarse grained sand to a depth of 20 or 30 meters. The area must be well-drained with the local water table well below the surface.
- 8) The line should run in the direction of the prevailing winds.

These requirements may be collected into the three general categories:

- (a) Requirements set by RADC.
- (b) Requirements determined by the devices to be calibrated at the facility.
- (c) Requirements resulting from the study of what characteristics an ideal calibration facility ought to have.

The requirements of categories (a) and (b) must be met, those of category (c) should be met as nearly as possible. Each requirement will now be discussed.

The first requirement belongs in category (a) and was established by RADC personnel as the maximum distance which it would be feasible to travel to get to the facility. Anything beyond this would require unreasonable amounts of travel time and significantly reduce the usefulness of the facility.

The second requirement belongs in category (b) and the considerations upon which it is based were discussed above.

All of the remaining requirements are in category (c) and have resulted from a study of just what characteristics an ideal calibration facility site ought to have. It has been concluded that an ideal location for an outdoor range and angle calibration facility would be in a place remote from civilization, where the ground is stable and the above-the-ground environment is uniform with respect to time and space. The ground stability is required so that the underground monuments remain in fixed positions thereby maintaining range calibration. The uniform environment will result in a constant value of refractive index whose amplitude can be determined with a minimum of range instrumentation. A constant value of refractive index is necessary for optimum comparator performance. In practice, of course, such an ideal site is not obtainable and one must content himself with approaching the ideal as nearly as possible under existing circumstances.

The third requirement is related to the desire for both a homogeneous environment above the ground and stable underground monuments. A level or slightly sloped region will help produce both. If the slope becomes large, however, the environment will not be homogeneous and air pressure and temperature will generally not be uniform along the range. Furthermore, such a slope usually produces significant underground water flow and this phenomena causes underground reference monuments to move. The ground water flow problem is also serious in narrow valleys which lie between large hills and therefore this sort of location is to be avoided.

The satisfying of requirements four and five will help to make the baseline a place where temperature changes and therefore refractive index changes with respect to distance and time are minimized. It is a matter of human observation that daily temperature variations are usually considerably less in a forest than in an open

field. This phenomenon is particularly noticeable on a hot summer day or a cool spring or autumn evening. Furthermore, trees provide protection from the wind. On the other hand, since the range is intended for the calibration of microwave as well as optical equipment, trees cannot be allowed to exist too close to the baseline or multipath reflections will interfere with equipment operation. Ideally, the baseline should be located in a corridor through a forest of large trees. The width of the corridor should be the minimum value allowable without reducing the ability of the facility to handle microwave equipment. If a site without surrounding forests is used, the periods of time when the line may be calibrated and used may be more limited than for a forested site.

It should also be mentioned, that cutting a reasonably wide, 2.5 mile corridor, through a dense forest of large trees can be a very costly job. The Finns have constructed some of their baselines in such an environment where they took advantage of tree plantations with trees already growing in long, straight rows. Since they were interested principally in calibrating invar tapes, a corridor of minimum width was cut. The well-known Nummela baseline is placed in a corridor which is only about four meters wide.

If the prospective site is forested, then requirement five normally will be satisfied. If an acceptable forested region cannot be found, and that is what has happened for this study, then requirement five becomes quite important. In such a case we must rely on the surface layer of soil and the existing vegetation to help minimize temperature variations of the atmosphere. This will occur when the daily temperature variation of the surface layer is as small as possible. Since the temperature of a body is proportional to its heat content, we would like to have the daily variation of heat content of the soil be as small as possible. This characteristic for various surface conditions has been investigated by micrometeorologists and the following table published in the literature (14):

Table 6-1.

DAILY VALUES OF THE VARIATION OF HEAT CONTENT
OF THE SURFACE LAYERS OF THE SOIL

Type of country	ΔH , g-cal cm ⁻²
Woods, sandy or moorland soil (summer)	15-24
Moorland meadow (summer)	33-43
Sandy soil, bare (summer)	95-105
Sandy soil, bare (fall)	27-42
Sandy soil, grass-covered (summer)	52-67
Rock (granite)	128

On the basis of this data, rock or bare sand would be least desirable and woods with sandy or moorland soil the most desirable. The seasonal variation should be noted. A range with bare sand in the fall would be better than a grass covered sandy surface in the summer. It is to be expected however, that a grass covered surface would be better than a bare sandy surface when compared at the same time of year.

The sixth requirement has two parts. Earth shock and vibration must be avoided so that, once measured, the baseline remains in calibration for a reasonable amount of time. Also, stable conditions are a necessity during line calibration operations. Fog must be avoided so that the line may be used to calibrate devices operating in the visible range. Air pollution will cause a variation in the refractive index of the atmosphere which cannot be easily measured and corrected for. It therefore cannot be tolerated. Since the facility will be used to calibrate devices operating in the microwave region, it must be located in an area remote from sources which produce interfering signals.

The seventh requirement is based almost completely on the experience of the Finns. Heiskanen has written (3):

"The location of standard base line must be chosen carefully. For instance rock ground can not be considered stable, when distances are to be measured with a very high degree of accuracy. This is easy to understand when we think that the rock is always split up into blocks and that stone has a relatively high temperature dilation coefficient. Thus, the direction in which the mark moves depends on the corner of the block in which the bolt is fastened. Clay soil is most unsuitable. The marks move after rain and during winter because of frost. The best would be horizontal gravel soil of 10 m thick or so. The Nummela standard base line is on 25 m thick moraine gravel bed." The undesirability of clay soil is confirmed by the experience at Mansfield, Ohio baseline where the poor drainage of the clay soil has produced flooding around the underground monuments at certain times of the year. The monuments have been observed to move during such flooding. Our consultant, Dr. T. J. Kukkamaki, has stated that sand is excellent for baseline construction if sufficiently coarse that water can easily penetrate. This statement is true from a stability of the soil point of view. Since the Finns have used their baselines mainly for the calibration of invar tapes, they have not been concerned with refractive index variations except during calibration which is carried on at infrequent, specially selected times. For a baseline to be used for the calibration of electromagnetic distance measuring equipment, the deleterious effects of a sandy surface layer on the stability of the refractive index of the atmosphere must be considered.

The eight requirement, which is probably the least important, is also based on the experience of the Finns. They have found that the refractive index is most uniform when atmospheric conditions are optimum and there is a slight breeze travelling down the baseline. Such a breeze tends to prevent local anomalies in temperature

from developing and is most likely to occur on a baseline oriented in the direction of the prevailing winds.

In this section the requirements for the ideal calibration facility site have been presented. In the next section we will discuss the two sites which have been found to most nearly satisfy these requirements.

2. DISCUSSION OF POSSIBLE SITES

The amount of time and effort required to find sites, which satisfy the requirements presented in the preceding section, was substantial and considerably greater than anticipated at the beginning of the study. Initial efforts toward location of one or more sites suitable for establishment of the facility were localized in close proximity to Rome. Potential sites were sought on the Rome Sand Plains, along the right of way of the abandoned New York, Ontario and Western Railroad, and near Camden. Particular attention was directed to an area directly northwest of the RADC Camden Test Annex.

When all sites near Rome proved unsuitable for one reason or another, the area of search was extended to include all of the region lying in a circle centered at RADC and having a radius of 50 miles. All of the U.S. Geological Survey topographical maps covering this area were carefully examined. The contour lines on these maps made it possible to locate flat areas where 2.5 mile baselines might be constructed. In all, sixteen additional prospective sites were found and each was subsequently visited. All but two of the sites were unacceptable. The two which showed promise were located near Chase Lake in Lewis County and near Forestport in Oneida and Herkimer Counties. It turned out however, that further investigation showed the Chase Lake site to be considerably more desirable than the Forestport site. For this reason, most of the effort in the final stages of site

selection was directed toward learning as much as possible about the Chase Lake site. Since it is felt however, that an alternative location should be described, we will briefly discuss the Forestport location before proceeding to a comprehensive treatment of the Chase Lake region.

a. Characteristics of the Forestport Site

This area is located about six miles east of Forestport, New York and about one mile south of the Forestport Loran Station which is operated by RADC. One of the attractive characteristics of the site is its proximity to this Air Force facility which is approximately 24 miles from RADC. The possible baseline location is shown on the map* of Figure 6-1 and consists of a long, narrow plateau which is between two valleys. At the northeast end of the plateau there is a steep hill which rises 160 ft above the flat area. This site satisfies requirements 1, 4 and 5 very well. It will not meet requirement 2, however, since it is not large enough to accomodate a 2.5 mile baseline. How well it meets the "flat terrain" requirement is still not definitely known. The forest in the area is very dense and only a small part of the region can be observed at any one time. Therefore, although the plateau appears to be quite flat, significant departure from such a condition could exist over a distance of a mile or more and not be detected by the human eye. If this site were to be given serious consideration, an accurate survey should be carried out to determine its flatness characteristics.

From the point of view of requirement 4, the forest is desirable, but the trees are large and it would be a relatively costly job to cut a corridor through them for the baseline. The homogeneous environment part of this requirement could be fully met providing the baseline is not allowed to closely approach the steep hill at the northeast end of the plateau.

*Copied from NORTH WILMURT 7-1/2' topographic map,
USGS, 1:24,000 Series.

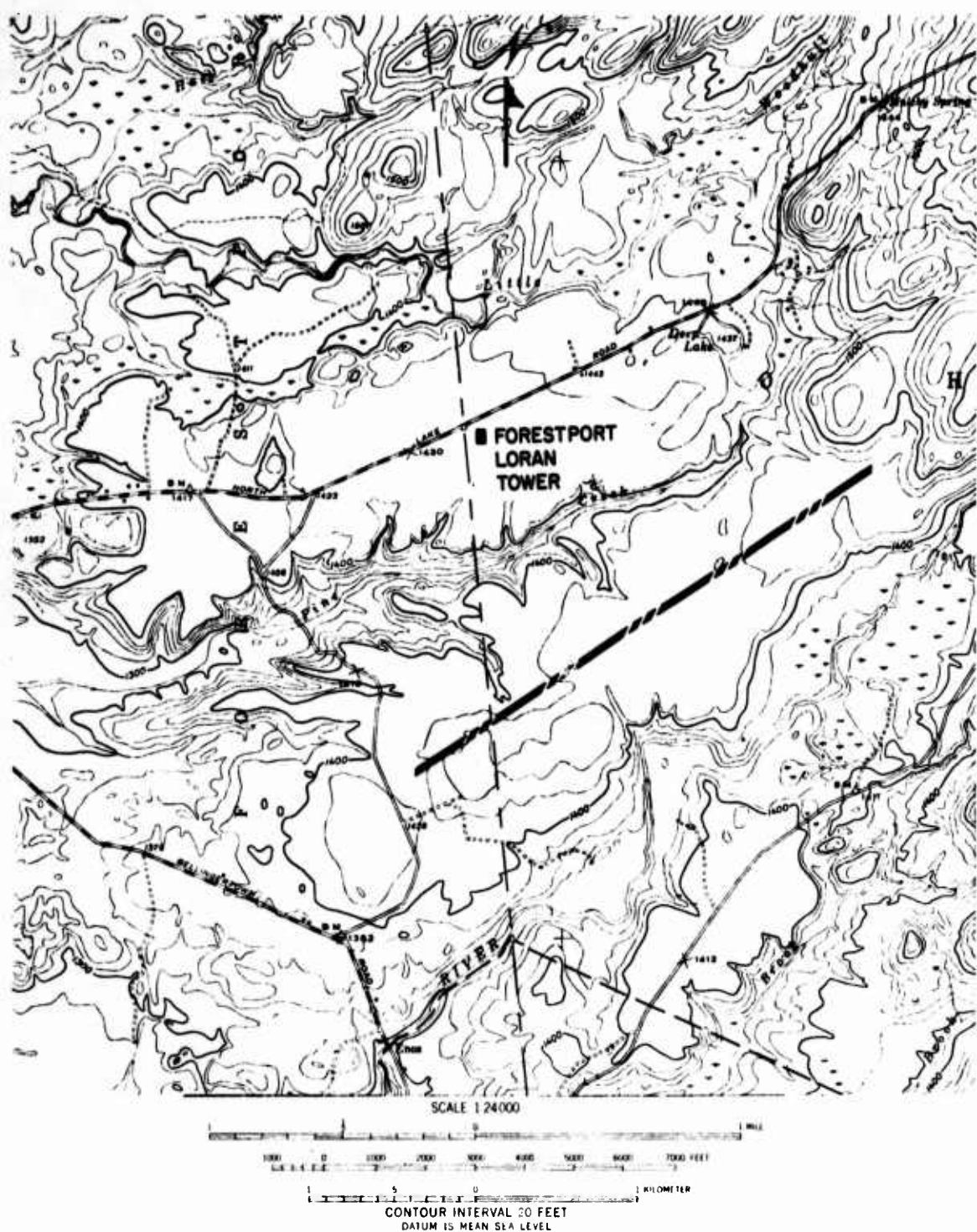


Figure 6-1 Map of Forestport Area Showing Prospective Baseline Location

With the exception of the electromagnetic interference portion, all of requirement 6 is easily met at this location. The effect of signals being radiated by the Forestport Loran facility on baseline instrumentation and microwave devices under test is difficult to predict but it is expected that they could cause undesirable interference. The characteristics of these radiations together with their periods of transmission are well-known to our sponsor who operates the facility. We therefore have not investigated this aspect of the problem to any great degree.

Requirement 7 is met by this site providing the baseline is not allowed to extend too close to the road on the southwest end or to the steep hill on the northeast end. Both of these regions are poorly drained and surface water puddles have been found there. The northeast end is particularly vulnerable to this effect when the snow melts in the spring and large amounts of water flow down the steep hill and onto this end of the plateau.

Since the proposed line runs at an approximate azimuth of 45° and the prevailing winds are at 90° , requirement 8 is partially met at this location.

To sum up, the principle attributes of this prospective site are:

- a) Relatively close to RADC.
- b) Within one mile of an existing RADC facility.
- c) Satisfies some of the site requirements established in the preceding section.

The deficiencies of this site are:

- a) The baseline length is limited to a maximum of 1.6 miles (2.6 kilometers).
- b) Degree of surface flatness is not definitely known.
- c) Cost of clearing forest could be large.
- d) Electromagnetic interference from the Forestport Loran station could be serious.

In the judgment of this author, the Chase Lake site is a far better choice and the remainder of this section will be devoted to a discussion of this area.

b. Characteristics of the Chase Lake Site

(1) Accessibility and Development

The Chase Lake site is 36 airline miles north of Rome and just over 40 miles by way of West Leyden, Constableville, Lyons Falls and Greig (Figure 6-2). It is in the southeastern corner of the Lowville quadrangle and the northeastern corner of the Port Leyden quadrangle of the U.S. Geological Survey 1:62,500 topographic map series. The area has not yet been covered by the current U.S. Geological Survey 1:24,000 map series. Because the maps date from surveys of 1910-1911 and 1904-1905, respectively, the culture is partly outdated and the maps are less accurate than recent maps based on air photography. A composite map of the area, obtained by copying parts of four geological survey maps is shown in Figure 6-3. It has been found that many errors exist in the topography presented on these maps. For example, the large kettle shown 1.1 miles southwest of Sand Pond does not exist. There is a slight depression along the southeastern edge of this particular region but nothing with the area or depth indicated on the map. Also, the relatively large pond shown close to the northwest edge of Little Otter Lake, was not indicated on the map but was added by SURC personnel. The pond is located in a kettle of significant depth which also was not shown on the map.

Presently access to the site is by unpaved, single lane auto trail from the Chase Lake Road toward Sand Pond, or by similar trail from the end of the Nortonville Road. In places trails not shown on the map lace the flat woodland of the sand plain which in the dry months can be traversed quite readily with or without trail.

The area is almost completely undeveloped and parts are under state ownership. Many farm dwellings shown on the Lowville and Port Leyden sheets at the time of survey, 50 years ago, no

GRAPHIC NOT REPRODUCIBLE

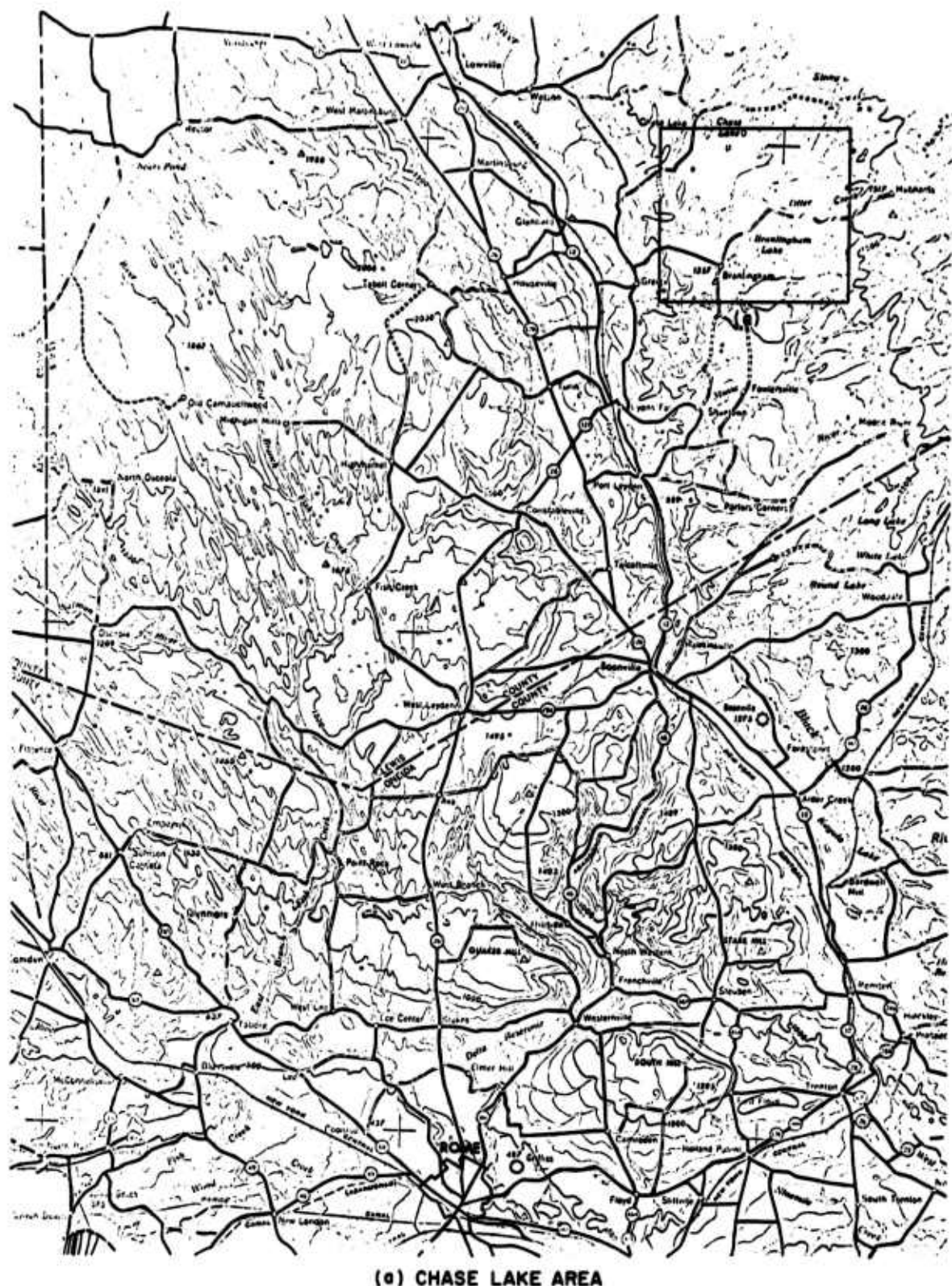


Figure 6-2 Road Map of Region from Rome to Chase Lake

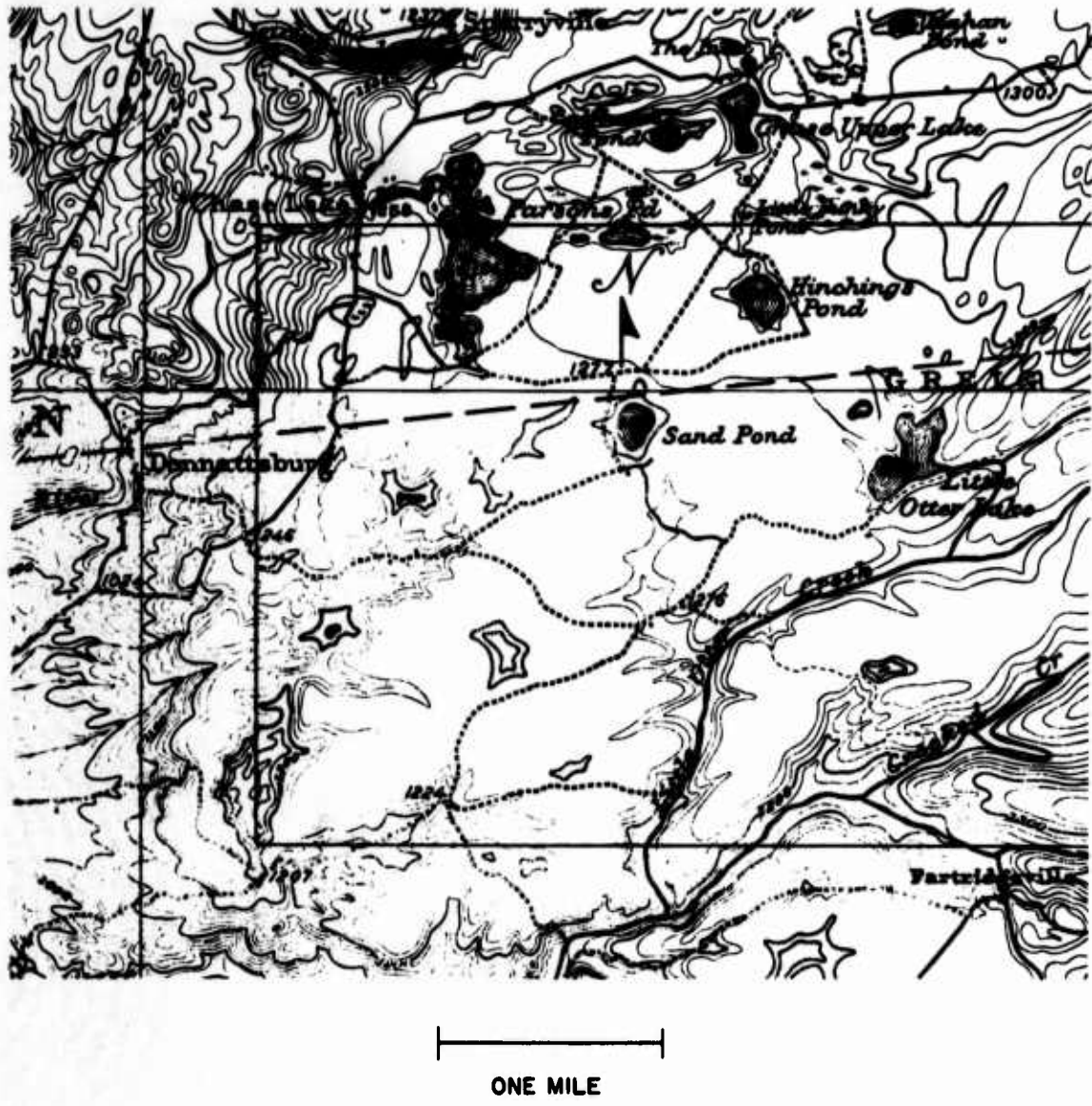


Figure 6-3 Topographic Map of Chase Lake Area

longer exist. On the other hand, resort development has commenced around some of the larger and more attractive lakes. The area in the immediate vicinity of the proposed alignment is essentially devoid of year around habitation and with very few summer cabins. Single cabins exist on Hinchings Pond, and Little Otter Lake and a larger number on Sand Pond where a Boy's Club from Carthage, New York operates Camp Mohawk as a summer camp. Other clusters of resort cabins have been built in the vicinity of Chase Lake and the Hiawatha Lakes within a mile of the southwest end of the proposed alignment.

(2) Topography

The Chase Lake site is located in an essentially undissected remnant of the Port Leyden lacustrine sand plain, bounded on the southeast and south respectively by Little Otter and Otter Creeks, on the west by the Chase Lake kettle alignment, on the north by an area of kettle-pitted sand plain, and on the east by the Adirondack foot-hills projecting above the plain.

An optimal alignment for the proposed baseline, selected on 14 September 1967 by Dr. Robert Richardson (SURC) and Mr. Donald Zulch (RADC), trends N 55 E, passing within 200 yards of Sand Pond as shown in Figure 6-4. At its southwest end the alignment is at an elevation of approximately 1270 feet. For two miles northeastward the plain is almost horizontal along the proposed baseline. A broad, shallow depression, less sharply defined than is suggested by the contours, is centered southeast of the baseline 0.4 miles from its southwest end. A broad, open swale draining south to Little Otter Creek heads within 200 yards of the kettle occupied by Sand Pond, but is relatively shallow and narrow at the proposed alignment. Approximately 2 miles from the southwest end of the alignment the regional slope increases to 15 to 20 feet per mile, but without marked irregularity.

Extension of the proposed alignment southwestward is prevented by gully dissection toward the Hiawatha-Chase Lake kettle

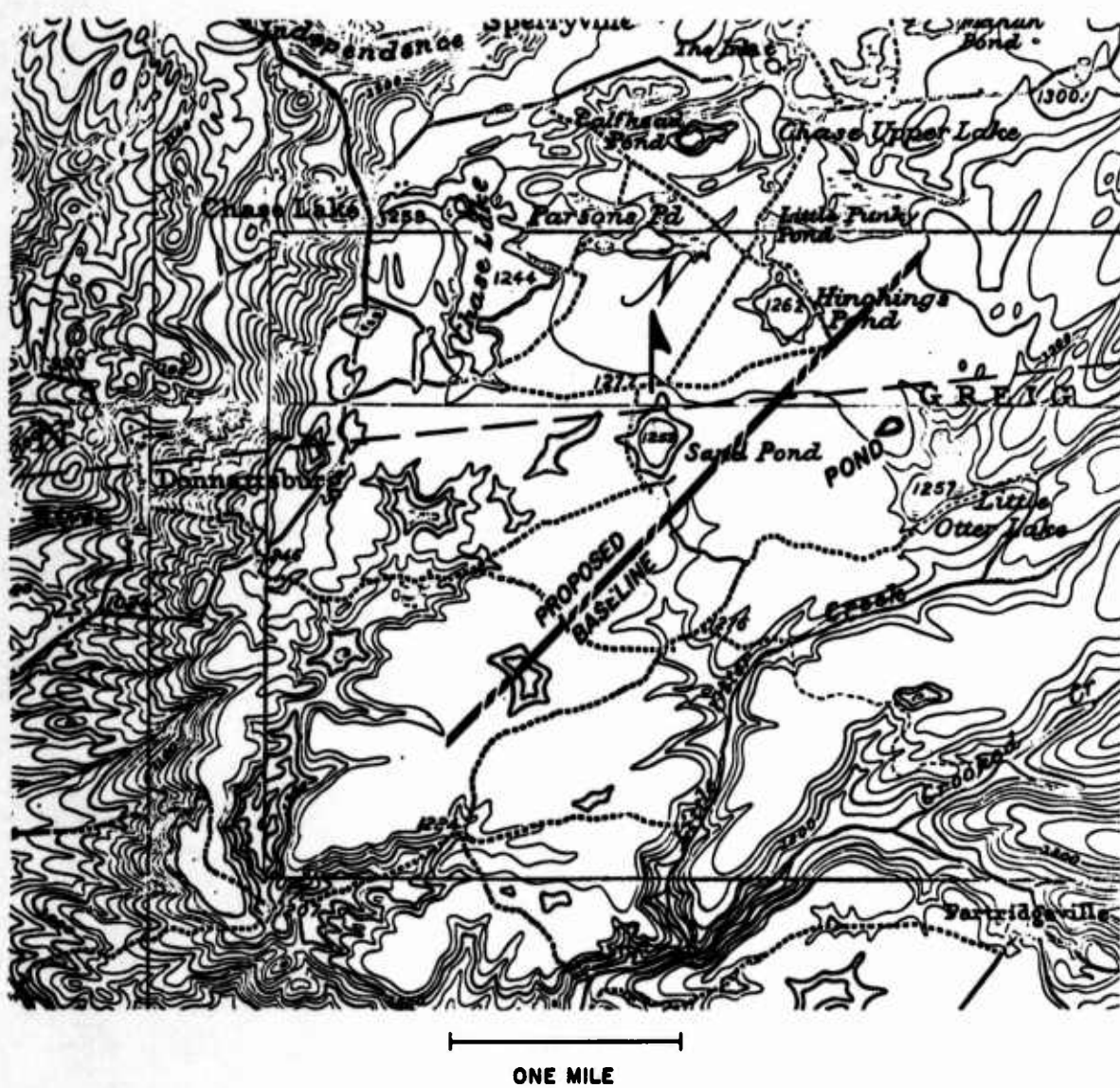


Figure 6-4 Map of Chase Lake Area Showing Topographic Relationships and Proposed Baseline Alignment

alignment. Northeastward extension of the alignment beyond a length of 3.0 miles encounters minor topographic irregularity. With the exception of the swale near Sand Pond, the area being considered for the baseline is relatively flat and should make a fine baseline location.

(3) Soil and Subsoil Materials

This aspect of the site is treated in considerable detail in Appendix A. The dominant surface soil material is medium to coarse sand. The area is well drained and geological studies indicate that bedrock is probably more than 20 to 30 meters below the surface over most, if not all, of the proposed line.

(4) Vegetation

Low brush and second growth cover most of the Chase Lake area, apparently taking over from abandoned farm and pastureland or after the forest fire which occurred about 1917. Mature forest is completely lacking although very old, charred stumps as much as six feet in diameter have been found in the immediate area. Patches of open forest and park land are composed of scattered spruce and pine among dominant aspen, maple, cherry and other hardwoods. Soft-wood plantation, of the cover type that would assure maximum homogeneity, is of very limited extent in the area.

In the immediate area of the proposed facility, the vegetation consists principally of grass, low bushes and Bracken Ferns. The area is dotted with spruce, White Pines, a few small clumps of aspens, maples and other hardwoods. A typical aerial photograph of the area is shown in Figure 6-5. It was taken during the winter and covers the region south and southeast of Sand Pond. The pictures of Figure 6-6 show some of the same area and were taken from the ground during the summer.

For most of the length of the proposed baseline, homogeneous vegetation conditions can be easily obtained by removing the few scattered trees. The exception to this statement occurs at the extreme southwest end of the line where a light forest of medium sized hard-

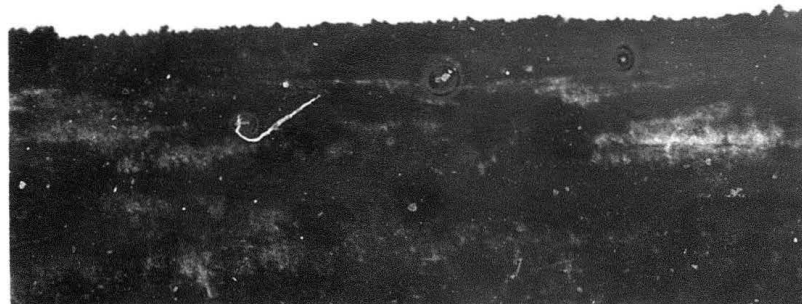


220 FT

Figure 6-5 Aerial Photograph of Region Just South and Southeast of Sand Pond.



AREA BETWEEN HITCHINGS POND AND LITTLE OTTER LAKE NEAR
HITCHINGS POND LOOKING SOUTHEAST



OPEN AREA WEST OF LITTLE OTTER LAKE

Figure 6-6 Pictures of the Proposed Chase Lake Calibration Facility Site

woods, principally Black Cherry, Beech and maple, exists. For a 2.5 mile baseline, very little of this area would be used.

(5) Other Characteristics of the Site

Electric power lines presently extend to Sand Pond and to the Hiawatha Ponds. Facility power would have to be obtained from one of these two places and present Niagara Mohawk price schedules for such service provide for 500 feet per customer of free transmission lines. For all line length beyond this there is a charge of \$1.50 per foot initially plus \$0.18 per foot in annual surcharge. These are average rates for installation of low revenue lines in ordinary territory. If large amounts of power are used, then the surcharge is reduced. If dense forests must be cleared, or if rights of way become expensive, then the cost to the customer is increased. The map of Figure 6-7 shows the termination points of existing power lines together with the locus of points which are a half mile and one mile from them. Of course, a customer may run his own lines over territory which he owns or leases. In this case he pays the power company for service only up to his property line. If great distances are involved, however, the transmission must be carried out at high voltage.

An investigation of state land ownership was carried out and the results are shown by the map of Figure 6-8. It can be seen from the figure that much of the land being considered belongs to New York State and lies within the Adirondack Park Forest Preserve. Therefore, the use of this region will depend upon making adequate arrangements with the state. It is the understanding of the author that in the past RADC has been able to acquire state owned land for construction of remote installations. The remainder of the land is privately owned and since it is of relatively little value, it should not be expensive to acquire.

c. Chase Lake Site and the Site Requirements

In part 1 of this Section a group of eight site requirements were described. In this portion of the report we will consider how well the Chase Lake site meets these requirements.

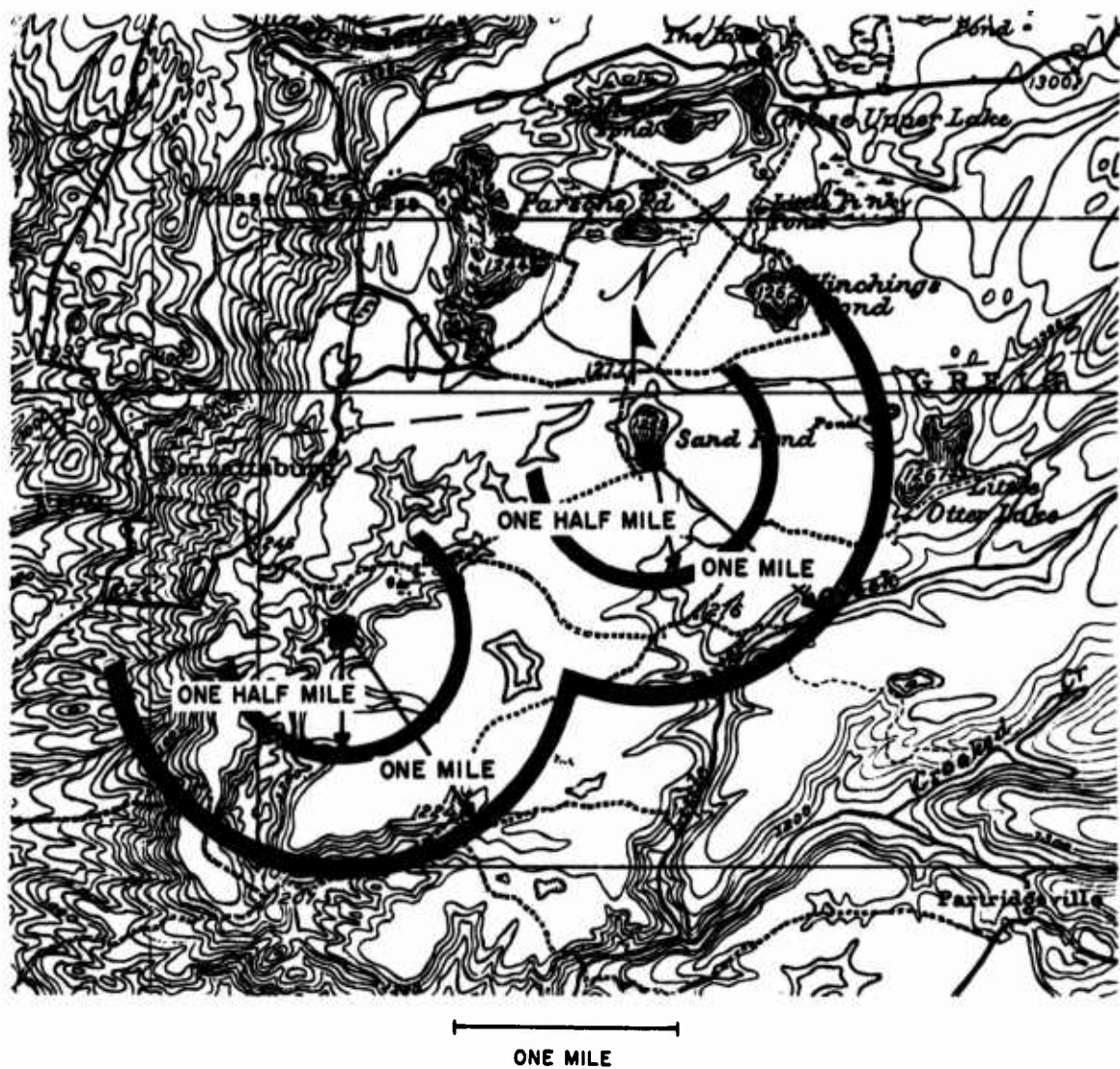


Figure 6-7 Map Showing Termination of Existing Electric Power Lines

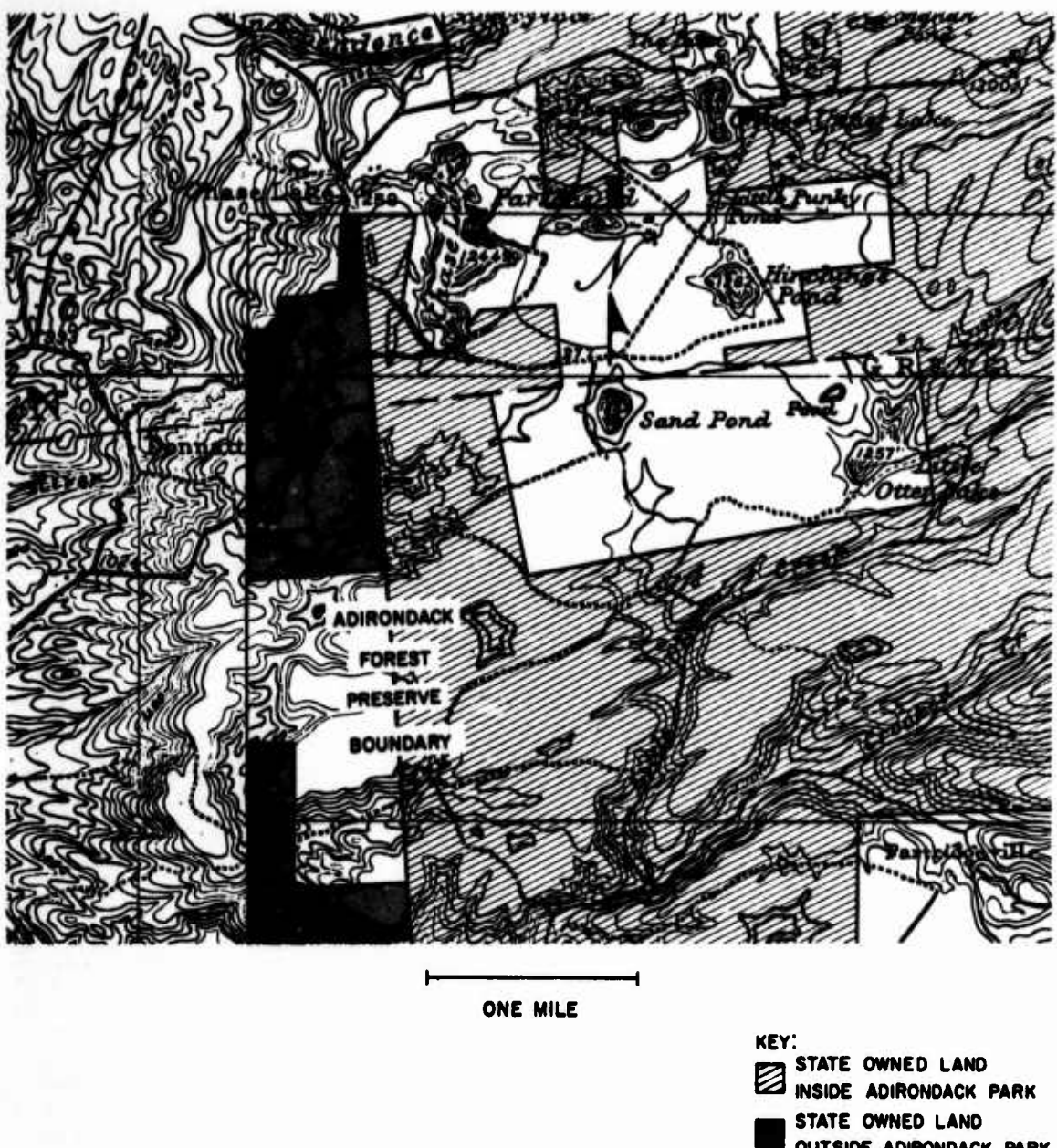


Figure 6-8 Map Showing Land Owned by New York State

Requirement 1 is satisfied since the site is located approximately 40 highway miles from RADC.

There are a number of possible baseline alignments which could be made 2.5 miles long thereby satisfying requirement 2. Up to 4.0 miles could be used if necessary, with some departure from maximum surface flatness and vegetation homogeneity.

The flatness of the terrain is one of the region's most desirable attributes. With the exception of the small depression near Sand Pond, it is very flat, a characteristic which is clearly observable because of the lack of forests over most of the area.

The region around the proposed line is a large plain which can be made quite homogeneous by removing the small number of scattered trees. The desire for forested surroundings must be abandoned for this site and instead the homogeneity demanded by the fourth requirement must be established by removing the sparse tree population.

Requirement 5 is not well satisfied by this site. The sandy soil covered by grass, bushes and ferns will exhibit relatively large daily variations in temperature which may somewhat reduce the usefulness of the line. During the final site survey trip, significant air turbulence was noticed to exist in the area when under the hot sun. At the time, some of the surface vegetation in the area had been killed by frost and consisted of dried leaves and ferns. Of course, precise measurements are never attempted under such atmospheric conditions and it is not known to what extent daytime heating of the surface would be likely to cause intolerable air turbulence at night as well. Perhaps this situation could be somewhat remedied by planting a different form of vegetation along the line. Of course, this effect would not occur on cloudy days.

Since the area is dry and relatively remote from civilization it satisfies requirement 6 very well.

The Geologist's report in Appendix A indicates that requirement 7 is satisfied. Also, SURC and RADC personnel visited the area during the spring snow thaw and found absolutely no evidence of flooding. The area is very well drained and no water table problems are likely to occur.

Since the prevailing winds are westerly, requirement 8 is not completely satisfied. For an open area, such as we have here, this requirement is of relatively little importance, however.

At the outset it was agreed that any existing site would probably not meet all site requirements completely. As discussed above, the Chase Lake site meets most of them in an adequate way and the remainder to a tolerable extent. The most serious shortcoming of the site is the unforested sandy soil and its effect upon air turbulence when illuminated by the hot sun. The worst that this phenomena can do is to make the site unusable for precise measurements on some sunny summer days and perhaps the following nights. On the other hand, since such days constitute only a relatively small part of the year, this limitation, if it exists at all, is not thought to be too serious and the Chase Lake site described herein is recommended as the best choice within 50 miles of RADC.

d. Other Considerations

It will be noted that relatively little has been said in this section about the angle calibration part of the facility. From the beginning of the study, it was obvious that the baseline and the distance measuring aspects of the project were by far the most important. As a result, the site selection criteria was based to a large extent upon baseline considerations. Of course, the need for a place for the angle facility was not completely ignored and it turns out that there is adequate space at the Chase Lake site for an angle calibration facility. The requirements for this facility, together with a suggested lay-out at Chase Lake, are included in Section V which is devoted entirely to the angle aspects of the study.

To make this Section complete, it should be acknowledged, that considerable help in making the site selection was provided by Mr. Robert Cracknell of RADC. His geodetic and geological knowledge and experience in work of this kind were brought to bear on the problem. His patience in examining a large number of sites, most of which has to be rejected, prevented this aspect of the job from becoming unpleasant.

SECTION VII

MANSFIELD EXPERIMENTS

1. INTRODUCTION

At the beginning of this contract, no experimental work was anticipated, but as the study progressed, a number of ideas and techniques were developed for which experimental verification was highly desirable. In the summer of 1967, Mr. Donald Zulch of RADC directed that an experimental aspect be added to the project and arranged for the collection of data by university and government geodesists. SURC undertook the analysis and interpretation of the results of the experiments which were conducted on the Ohio State baseline at Mansfield. The objective of this work was to evaluate the optical environmental correction techniques and procedures, which had been developed during the course of the study, using air-pressure, temperature, water vapor pressure and distance measurements. The data was also to be used to evaluate the performance of an RADC Model 4D Geodimeter and a Spectra Physics Model 3G Geodolite.

2. DESCRIPTION OF THE EXPERIMENTAL PROGRAM

a. Experimental Period and Personnel

The experiments were carried out on the evenings of September 12-15, 1967 by Professor Dean Merchant and Mr. Sol Cushman of the Geodetic Sciences Department of Ohio State University, Mr. Dolan Mansir, and Mr. John Motsinger of Spectra Physics, Inc., Mr. Lawrence Crouth and Sgt. George Ferguson of RADC and Professor Robert Gunn of the Department of Civil Engineering, University of Toronto. On September 12, Crouth and Ferguson made distance measurements using the RADC Geodimeter while Merchant observed and recorded air temperature, pressure and water vapor values. On September 13 - 15, Mansir and Motsinger made

distance measurements using a Geodolite while Merchant, Cushman, Crouth and Ferguson observed and recorded the atmospheric characteristics. In addition, on September 14, Gunn also participated in the latter activity.

b. The Mansfield Site

The Ohio State University baseline is located on a slightly inclined piece of land adjacent to its branch just outside of Mansfield, Ohio. The terrain has been graded to a flat condition in the immediate vicinity of the line. A map of the area, derived from sketches made by Dr. Merchant, is shown in Figure 7-1. The baseline is 500 meters long with above-the-ground pillars located at 0, 1, 5, 25, 125, 250 and 500 meters. There is also a table-like pillar located at -3 meters upon which distance measuring equipment may be placed. This pillar, together with those at 0 and 1 meter are covered by a canopy as shown in Figure 7-2. The Figure also shows the pillar at 5 meters which is outside the canopy. Each pillar has a removable aluminum cover to protect any equipment which may be attached to it. Another view of the pillars under the canopy, with the covers removed, is presented in Figure 7-3. The equipment on the pillars is part of the Väisälä Light Interference Comparator.

The 5 meter pillar, with cover removed, is shown in Figure 7-4. The pillars and equipment at 25, 125, 250, and 500 meters are similar. Figure 7-5 shows a view looking down the range with the 25 meter pillar in the foreground and the 125, 250, and 500 meter pillars in the background. Figure 7-6 is a view looking in the opposite direction where the truck in the picture is on the highway which passes the site. The tall wooden slats are thermometer holders which are located at 25 meter intervals along the line.

Each of the pillars has a large concrete monument deep in the ground beneath it. The monuments are cylindrical in shape with a 10 ft. length and a 4 ft. diameter. The line was calibrated by

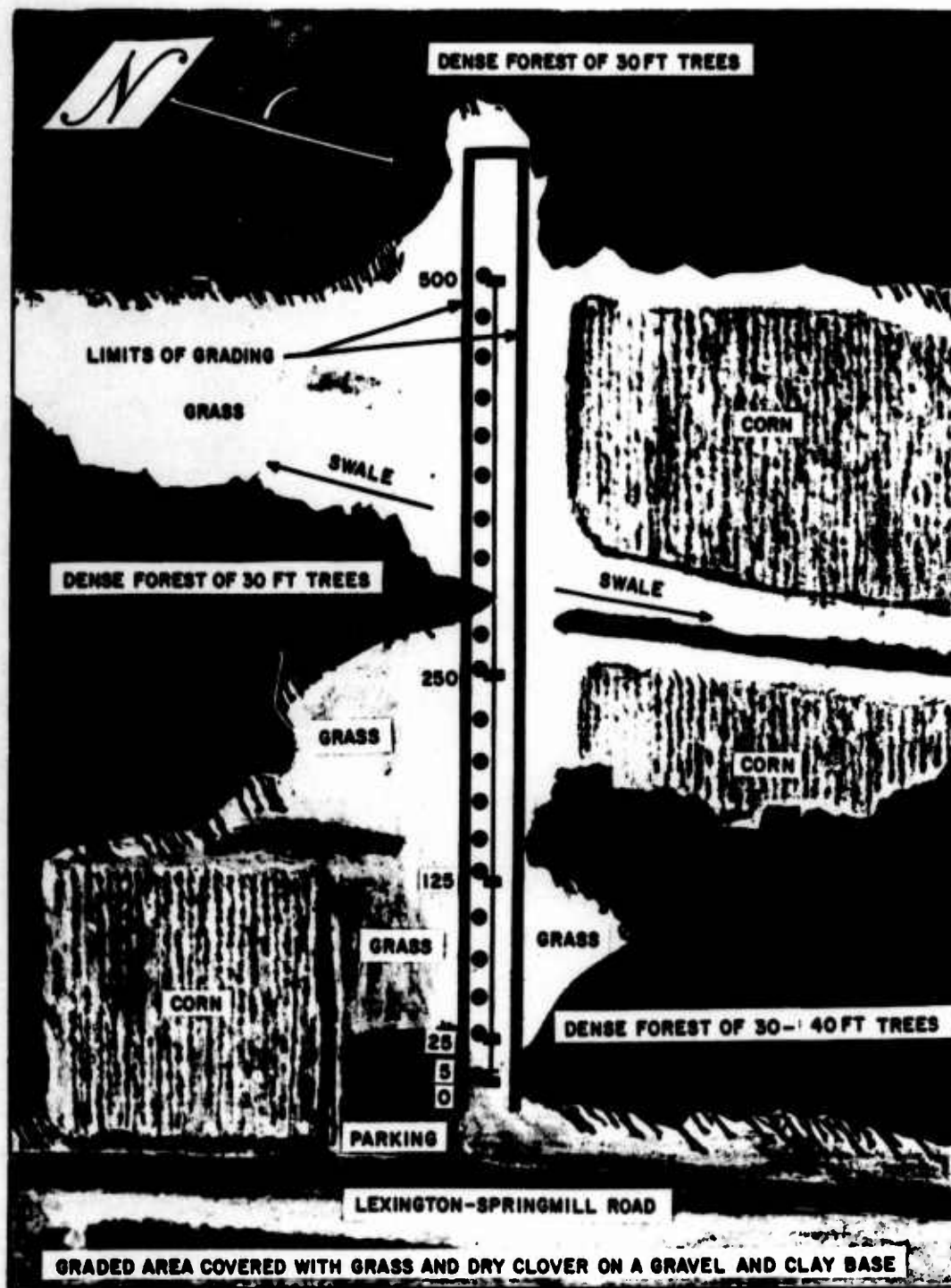


Figure 7-1 Map of the Region Surrounding the Mansfield Baseline

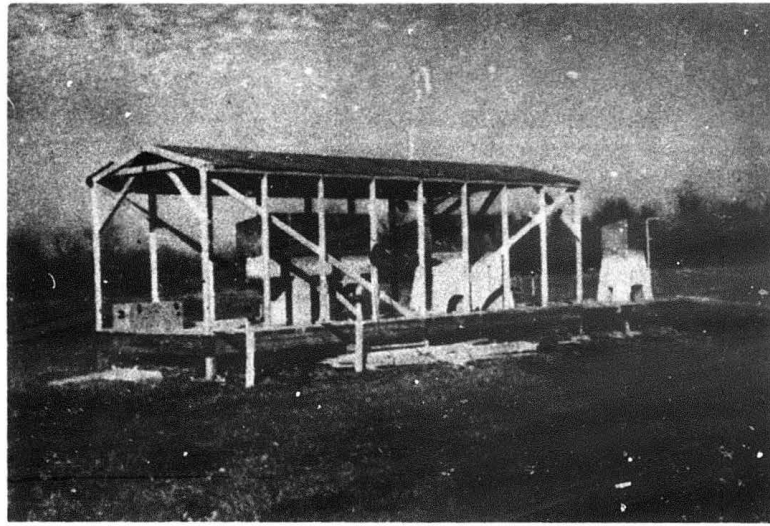


Figure 7-2 - 3, 0, 1 and 5 Meter Pillars

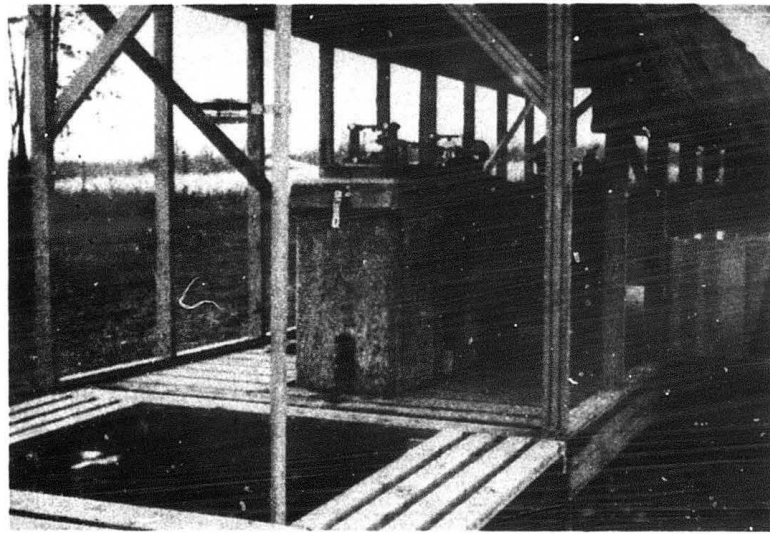


Figure 7-3 1, 0 and -3 Meter Pillars with Väisälä Comparator Equipment

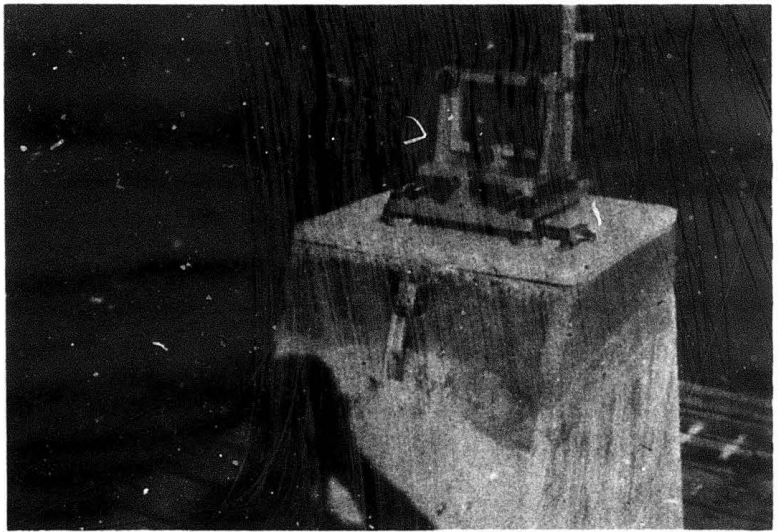
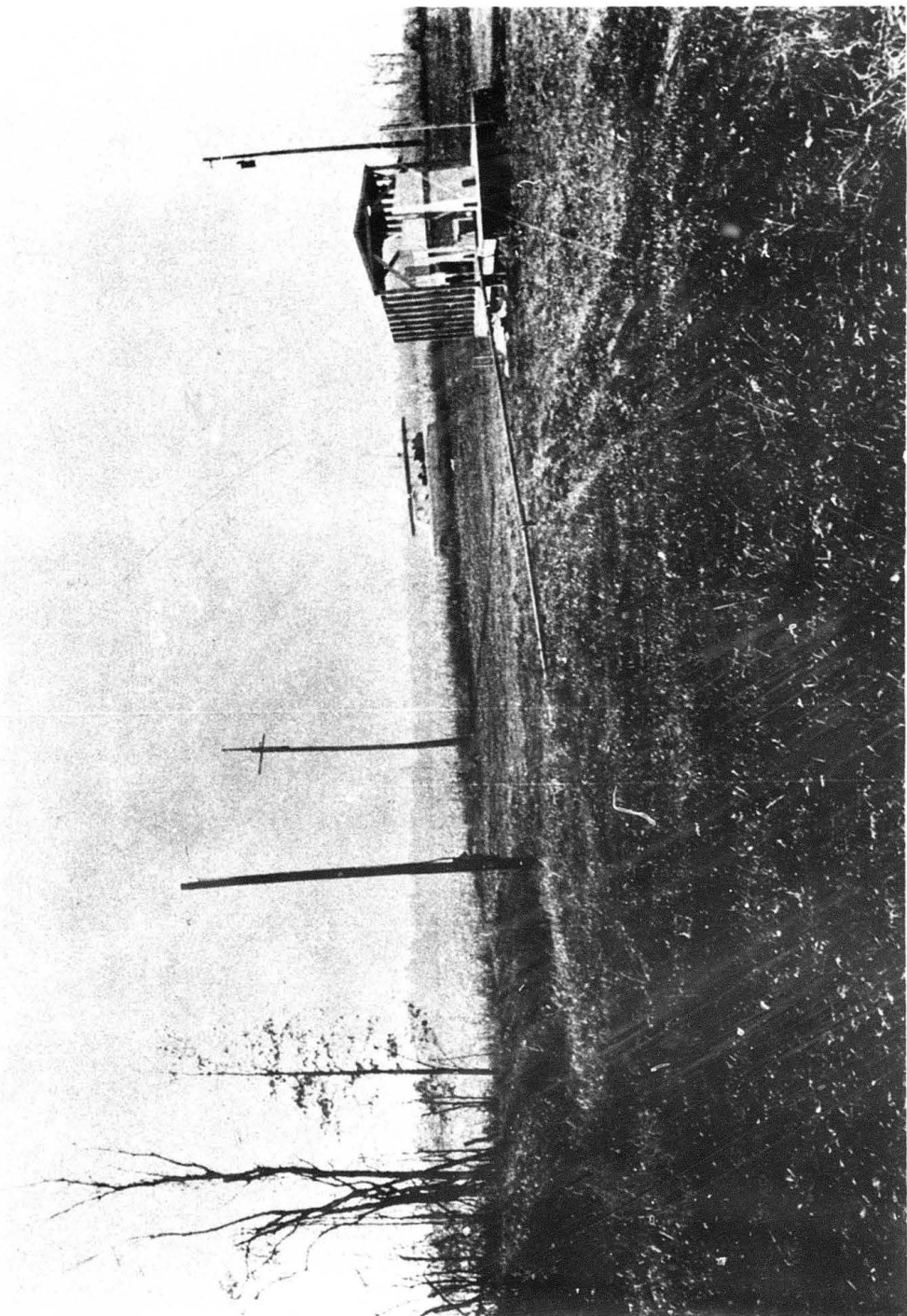


Figure 7-4 5 Meter Pillar with Väisälä Equipment



Figure 7-5 View of Baseline Looking Eastward

Figure 7-6 View of Baseline Looking Westward



first determining the distance between bars that are securely fastened to the tops of the pillars and then projecting the measurements down to brass bolts imbedded in the tops of the below-ground monuments. These monuments are considerably more stable than the pillars.

Referring to the map of Figure 7-1, the forest shown just beyond the 500 meter end of the line is relatively narrow and on land that drops steeply. The main building of the Ohio State Branch is located just beyond the forest.

c. Weather

The weather existing at the time when electromagnetic distance measurements are being made will have an important effect on the accuracy and precision of the measurements. Optimum weather conditions occur when air temperature, pressure and water vapor content are as stable as possible over relatively long periods of time and large intervals of space. It has been found that this usually occurs on a cloudy night following a cloudy day in the Fall of the year. A light rain and slight breeze are also desirable.

Unfortunately, relatively little weather data was recorded on September 12-15 but on the basis of that which is available, it is concluded that the weather during the experiment periods was rather far from the ideal. The available data is presented below.

September 12 -- Wind calm, visibility good.

September 13 -- Clear and calm during observing period. Horizontal temperature variations were so great that they were felt by the observers as they walked along the line.

September 14 -- Clear, calm. Variations in temperature were reduced in magnitude as compared to the previous night.

September 15 -- 10% coverage of high clouds. Slight wind (1 to 2 knots) from the northeast at 8:30 P.M. E.D.T. At 10:00 P.M. a light ground fog began to develop near the center of the line. By 12:00 P.M. it was visible on the line and by 1:00 A.M. it

extended along the whole line and adjustment of the neutral density filter in the Geodolite was necessary. At 2:00 A.M. only a threshold return was sensed. During the process of securing the equipment for the night, it was noticed that a great deal of moisture had condensed on the reflectors accounting for much of the attenuation of the returning signal. Sundown occurred at:

September 12 -- 7:44 P.M. E.D.T.

September 13 -- 7:43 P.M. E.D.T.

September 14 -- 7:41 P.M. E.D.T.

September 15 -- 7:40 P.M. E.D.T.

d. Baseline Instrumentation

During the course of the experiments, the baseline length was measured using both a Geodimeter and a Geodolite. The atmospheric characteristics were sensed using 21 thermometers, three barometers and a hygrometer.

The Geodimeter was a model 4D, serial number 306, owned by RADC. This instrument has a rated average error of \pm one centimeter plus two millionths of the distance being measured. For the 500 meter line, this corresponds to \pm 11 millimeters (\pm 0.434 inches) which is \pm twenty-two parts per million. The reflector was a single prism with a 75 second wedge attached.

The Geodolite was the property of Spectra Physics, Inc. and had a rated resolution of \pm 1 millimeter (\pm 0.003 ft) or one part in 10^6 whichever is greater. For the 500 meter line the \pm 1 millimeter rating predominates and this corresponds to \pm two parts per million. As noted later, however, this sort of performance was not achieved. On September 13, a single prism reflector was used and on the 14th and 15th a three prism reflector was utilized.

Each of the thermometers was given an identification number between one and twenty-one. These numbers, together with the corresponding thermometer serial numbers are given in Table 7-1.

TABLE 7-1
Thermometer Identification Data

Thermometer Number	Serial Number	Thermometer Number	Serial Number
1	9A8429	12	9A6933
2	60095	13	69087
3	812672	14	812728
4	60026	15	812676
5	812667	16	812705
6	812649	17	812645
7	9A2488	18	72994
8	812724	19	53998
9	812651	20	60014
10	812661	21	9A4245
11	72885		

Thermometers 1, 7, 12 and 21 are Fisher Scientific Company, liquid in glass types which belong to RADC. These devices have a range from -1 to + 51°, with 0.1°C. graduations and have been calibrated at the National Bureau of Standards. Thermometers 2, 4, 11, 13, 18, 19 and 20 have 0.1°C. graduations and belong to Ohio State University. The remaining thermometers belong to SURC and are Princo, -5 to + 50° C., 0.1°C. graduation types.

The calibration of the thermometers was checked by placing them in a constant temperature environment and recording their respective readings. The results of four such tests are given in Table 7 - 2. During the course of these comparisons, it was noticed that thermometer #21 exhibited a separation and the readings obtained from it were not recorded. The separation was removed and the thermometer was used during the September 13- 15 experiment periods. After the experiments were completed however, it was compared with thermometer # 12 and found to give inconsistent results.

TABLE 7-2
Thermometer Calibration Data

Thermometer Number	Temperature Readings in Degrees Centigrade			
1	10.42	10.54	13.74	13.88
2	10.38	10.50	13.74	13.88
3	10.28	10.40	13.62	13.78
4	10.38	10.50	13.72	13.84
5	10.30	10.42	13.62	13.74
6	10.30	10.40	13.60	13.74
7	10.40	10.52	13.74	13.88
8	10.24	10.38	13.60	13.70
9	10.28	10.40	13.62	13.76
10	10.30	10.42	13.68	13.80
11	10.34	10.44	13.68	13.80
12	10.40	10.50	13.72	13.86
13	10.40	10.50	13.74	13.86
14	10.30	10.42	13.66	13.78
15	10.26	10.40	13.60	13.72
16	10.30	10.42	13.62	13.74
17	10.28	10.40	13.62	13.76
18	10.40	10.50	13.70	13.80
19	10.38	10.50	13.72	13.82
20	10.40	10.50	13.74	13.88
21	-----	-----	-----	-----

Therefore, all of the data obtained from this device were discarded and replaced by the readings of Thermometer # 20 during data reduction and analysis.

Using the data of Table 7-2 together with Bureau of Standards calibration data which was available, corrections for each thermometer reading were computed. These corrections are given in Table 7-3. Since the Mansfield comparison data gives relative values of temperature only in the vicinity of 10.5°C. and 13.8°C., interpolation and extrapolation of the correction data had to be made. Interpolation was obtained by fitting a step function to the straight line characteristic which was assumed to exist between the end points. Outside the data interval, i.e. below 10°C. and above 14°C., it was assumed that the best corrections could be obtained by using the adjacent experimental values. An exception to this occurs for thermometers #1 and #12 for which NBS correction data at 20°C. was available thereby making it possible to obtain a step function approximation to the linear variation which was assumed to exist between the +10°C. and +20°C. values.

As shown in Figure 7-1 there are twenty-one places along the baseline where temperature can be measured. At each of these points there is a specially designed support which holds the thermometer close to the ray path of the distance measuring equipment thereby allowing it to sense the effective temperature of the surrounding atmosphere. Each thermometer position was given an identifying number, between one and twenty-one, beginning at the 0 meter end and extending to the 500 meter end of the line. The location of each thermometer position, together with the identifying number of the thermometer used there during the experiment periods, is given in Table 7-4. It should be noticed that only eleven thermometers were used on September 12.

There were three barometers used during the course of the experiments and all are the property of RADC. Barometer #1 is

TABLE 7-3
TEMPERATURE CORRECTION IN DEGREES CENTIGRADE

Thermometer Number	Temperature Reading			
	Below 11°C	11° - 12°C	12° - 13°C	Above 13°C
1	-.06	-.06	-.06	See below
2	-.02	-.02	-.03	-.04
3	+.08	+.08	+.07	+.07
4	-.02	-.02	-.01	-.01
5	+.06	+.07	+.08	+.09
6	+.07	+.08	+.09	+.10
7	-.04	-.04	-.04	-.04
8	+.11	+.11	+.12	+.12
9	+.08	+.08	+.08	+.08
10	+.06	+.05	+.04	+.03
11	+.03	+.03	+.03	+.03
12	-.03	-.02	-.02	See below
13	-.03	-.03	-.03	-.03
14	+.06	+.06	+.05	+.05
15	+.09	+.09	+.10	+.11
16	+.06	+.07	+.08	+.09
17	+.08	+.08	+.08	+.08
18	-.03	-.02	0	+.02
19	-.02	-.02	-.01	0
20	-.03	-.03	-.04	-.04

TABLE 7-3 CONTINUED

Thermometer Number	Temperature Reading			
	13-14°C	14-15°C	15-16°C	16-17°C
1	-.05	-.05	-.05	-.05
12	-.01	-.01	+.01	+.01
<hr/>				
	17 - 18°C	18 - 19°C	19 - 20°C	
1	-.04	-.04	-.04	
12	+.02	+.02	+.03	

TABLE 7-4
THERMOMETER POSITION DATA

Thermometer Position No.	Distance From Beginning of the Baseline in Meters	Thermometer Number on Sept. 12	Thermometer Number on Sept. 13-15.
1	3	8	1
2	27		2
3	50	13	3
4	75		4
5	100	17	5
6	127		6
7	150	6	7
8	175		8
9	200	14	9
10	225		10
11	252	10	11
12	275		12
13	300	9	13
14	325		14
15	350	15	15
16	375		16
17	400	5	17
18	425		18
19	450	16	19
20	475		20
21	502	3	21

a Wallace and Tiernan Type ML102, Serial number 2704, which has an accuracy of \pm 0.35 millibars. Barometers #2 and #3 are actually very sensitive altimeters and read in feet. They are Wallace and Tiernan Model FA 185 types having a maximum error of \pm 8 feet. The instruction manual which accompanies them also states that: "The majority of their elevation indications will be correct to \pm two or three feet." They carry the serial numbers 10102 and 10103 respectively. It is assumed that these instruments are actually Wallace and Tiernan Model FA 185 precision aneroid barometers with an appropriate scale. These devices have a dial diameter of six inches and a scale length of 30 inches through two pointer revolutions. When calibrated to read in millibars, the scale extends from 745 to 1065 mb. According to the manufacturer, these instruments are accurate to within \pm 0.1% of full scale or 0.133 mb. These devices have built-in temperature compensation which limits temperature error to \pm 0.05% of full scale per 10°C change in temperature above or below 25°C .

All of these instruments were calibrated against the standard barometer located at the Mansfield airport weather bureau. It is assumed that when this calibration data is used to correct the data obtained from the Model 185 barometers, the results have an accuracy somewhat greater than that indicated by the manufacturer. All experimental values of air pressure were corrected and converted to millibars if necessary, by RADC personnel using the Mansfield calibration data and instructions provided by the manufacturer.

On September 12 barometer #3 was located near the 0 meter pillar and barometer #2 near the 500 meter pillar; barometer #1 was not used. On September 13, 14, and 15, barometer #1 was located near the 0 meter pillar and barometers #2 and #3 were both located near the 500 meter pillar.

During all four experiment periods a dry and a wet bulb hygrometer was located in the vicinity of the 0 meter pillar. It was a type ML-436-A, serial number 10, psychrometer. The wet and dry bulb temperature information obtained from this device, was subsequently used to determine the water vapor pressure by means of the technique presented in "Psychrometric Tables for Obtaining the Vapor Pressure, Relative Humidity and Temperature of the Dew Point" by C. F. Marvin, Weather Bureau publication No. 235, 1941.

(e.) Method of Taking Atmospheric Data

The data taken during each experiment period can be collected into the two categories of distance measurements and atmospheric characteristic measurements. On September 12, four separate measurements of baseline length were made using the RADC Geodimeter. On September 13, 14 and 15 the same length was measured a very large number of times using the Geodolite. While the distance measurements were being made, simultaneous readings of air pressure, temperature and water vapor content were also being made. This atmospheric data was subsequently used to determine the average refractive index along the ray path and thereby provide corrections for the distance measurements.

The procedure for making the atmospheric measurements was as follows, starting at the beginning of the baseline:

- (1) Read barometer
- (2) Read hygrometer
- (3) Record the time
- (4) Walk down the line recording the reading of each of the 21 thermometers.
- (5) After reading the thermometer in position #21 record the time.
- (6) Read the barometer(s) located at the 500 meter end of the line.
- (7) Return to the beginning of the line

On September 12 only five passes down the line were made but on September 13, 14 and 15 the number was considerably larger

TABLE 7-5
CORRECTED AND CONVERTED EXPERIMENTAL DATA
TAKEN SEPTEMBER 12, 1967

Barometer # 3	974.6	974.9	974.9	974.9	974.9
Hygrometer	.402	.373	.334	.347	.322
Time	0:12	0:43	1:49	2:12	2:34
1	13.57	13.57	12.22	11.63	11.61
3	14.17	13.99	13.17	11.85	11.84
5	15.94	15.68	14.68	14.30	14.18
7	15.50	15.48	14.67	14.10	13.90
9	15.40	15.40	14.45	13.93	13.73
11	15.41	15.14	14.22	13.68	13.69
13	15.30	15.30	14.26	13.59	13.63
15	15.46	15.61	14.26	14.18	13.61
17	15.54	15.38	14.30	14.28	14.00
19	15.29	14.67	14.11	13.59	13.91
21	14.95	14.49	13.35	13.12	12.91
Time	0:31	0:55	2:03	2:23	2:47
Barometer #2	975.0	975.3	975.3	975.3	975.2

TABLE 7-6
CORRECTED AND CONVERTED EXPERIMENTAL DATA
TAKEN SEPTEMBER 13, 1967

Barometer #1	974.4	974.7	974.7	974.9	974.9	974.9	974.9
Hygrometer	0.322	0.316	0.310	0.316	0.331	0.318	0.308
Time	1:40	1:53	2:14	2:29	2:39	2:47	2:58
1	10.74	10.59	10.20	10.39	10.41	9.52	9.16
2	10.08	10.66	11.36	10.28	10.03	9.09	8.26
3	10.12	10.68	11.14	10.18	10.02	9.06	9.04
4	9.58	9.93	10.54	10.20	10.13	9.06	9.24
5	9.38	10.54	9.90	9.86	10.08	9.26	8.86
6	9.49	10.55	9.77	8.92	9.27	8.17	7.65
7	10.01	10.46	9.80	9.01	9.28	8.16	7.80
8	10.09	10.61	9.11	8.51	8.91	8.17	8.23
9	10.36	10.38	9.48	8.33	8.80	7.66	8.12
10	10.66	10.48	9.64	8.98	8.41	7.71	7.98
11	10.45	10.23	9.81	8.53	8.08	8.13	8.11
12	10.66	10.47	10.33	8.17	7.62	8.42	8.11
13	10.95	10.50	10.57	7.97	8.12	8.09	8.05
14	11.11	10.48	10.56	8.56	9.21	8.26	8.30
15	10.69	9.64	10.11	9.19	9.11	8.19	8.29
16	10.10	9.56	9.64	8.26	8.64	8.18	8.26
17	10.73	9.98	9.16	8.98	8.30	8.13	8.10
18	10.85	9.69	9.05	9.77	8.49	8.09	8.09
19	10.73	9.46	10.06	9.08	8.58	8.36	8.38
20	11.22	10.32	11.01	9.17	9.35	8.75	8.93
21	11.22	10.32	11.03	9.17	9.35	8.75	8.93
Time	2:05	2:20	2:27	2:46	2:53	3:08	3:09
Barometer #2	975.0	975.4	975.4	975.6	975.4	975.6	975.6
Barometer #3	975.0	975.2	975.2	975.3	975.4	975.5	975.5

TABLE 7-6 CONTINUED

Barometer #1	975.0	975.0	975.1	975.1	975.0	974.9	975.0
Hygrometer	0.293	0.296	0.331	0.341	0.347	0.293	0.290
Time	3:01	3:18	3:31	3:41	3:54	4:14	4:15
	1	9.34	9.34	9.30	9.24	9.42	8.52
	2	8.23	8.88	8.38	8.96	9.08	9.02
	3	8.48	8.86	9.26	9.24	9.23	9.10
	4	8.53	8.98	8.90	8.46	9.14	9.48
	5	8.41	9.36	8.44	8.26	9.14	9.80
	6	7.94	8.62	7.97	8.22	8.32	8.25
	7	8.36	8.34	8.14	7.94	8.16	9.94
	8	8.46	8.46	7.65	9.91	8.39	11.31
	9	8.68	8.04	7.48	8.96	7.93	11.38
	10	8.71	8.11	7.76	9.34	8.36	11.15
	11	8.63	8.38	7.53	8.12	8.73	9.69
	12	8.87	8.34	7.75	8.09	9.42	11.06
	13	8.87	7.92	8.13	7.85	9.17	9.47
	14	8.51	7.81	8.40	9.44	10.47	9.92
	15	8.74	8.11	7.79	9.55	10.57	10.49
	16	8.96	8.11	7.62	8.48	10.06	11.02
	17	8.78	7.73	7.76	8.20	9.73	11.86
	18	8.92	7.87	7.77	8.57	8.97	11.64
	19	9.63	8.48	8.08	9.96	8.58	11.52
	20	9.17	8.82	8.95	10.07	8.95	9.91
	21	9.17	8.82	8.95	10.07	8.95	10.47
Time	3:18	3:34	3:41	4:02	4:09	4:24	4:32
Barometer #2	975.6	975.6	975.6	975.6	975.7	975.6	975.5
Barometer #3	975.4	975.5	975.5	975.4	975.4	975.3	975.3

TABLE 7-6 CONTINUED

Barometer #1	975.0	974.9	974.8	974.8	974.6	974.6	974.6
Hygrometer	0.300	0.300	0.287	0.308	0.277	0.310	0.334
Time	4:25	4:46	4:54	5:01	5:15	5:27	5:41
1	9.29	8.40	8.42	8.59	8.34	8.60	8.36
2	9.03	7.94	8.60	8.58	8.33	7.94	7.96
3	9.23	9.04	9.10	8.92	8.68	8.10	8.66
4	9.34	8.14	8.60	7.80	8.48	8.52	9.19
5	8.46	9.54	8.66	8.58	8.56	8.36	9.74
6	7.97	8.49	7.59	7.55	7.97	8.17	10.34
7	9.76	10.10	8.51	10.96	9.96	8.92	12.34
8	11.61	10.87	11.63	12.92	11.01	10.07	12.33
9	11.48	11.78	11.96	13.06	12.38	11.76	13.03
10	11.70	12.24	11.55	12.64	12.54	12.30	12.86
11	11.23	11.85	10.05	11.41	12.13	12.49	12.33
12	11.83	10.81	10.35	11.48	12.23	12.52	12.29
13	11.12	11.27	9.67	10.97	12.27	11.97	11.55
14	11.81	12.15	11.26	11.86	12.55	12.73	12.15
15	11.69	12.68	12.42	12.42	13.11	13.19	12.28
16	12.28	12.22	13.11	12.36	13.39	13.23	12.48
17	12.23	12.28	12.46	12.44	13.40	13.08	12.08
18	11.23	11.80	12.10	12.25	13.22	12.46	11.50
19	10.98	10.34	10.98	12.19	13.00	12.05	10.93
20	10.62	10.25	8.67	11.49	12.36	12.10	10.94
21	10.62	10.25	8.67	11.49	12.36	12.10	10.94
Time	4:40	4:56	5:10	5:20	5:31	5:38	5:57
Barometer #2	975.4	975.3	975.3	975.3	975.1	975.1	975.1
Barometer #3	975.3	975.2	975.1	975.1	975.0	975.0	974.9

TABLE 7-7
 CORRECTED AND CONVERTED EXPERIMENTAL DATA
 TAKEN SEPTEMBER 14, 1967

Barometer #1	974.4	974.4	974.4	974.4	974.5	974.4	974.4
Hygrometer	0.387	0.390	0.402	0.398	0.407	0.387	0.380
Time	1:00	1:02	1:13	1:26	1:36	1:42	1:51
1	13.19	13.17	13.20	12.49	12.42	12.09	12.14
2	12.55	12.87	12.57	12.98	12.83	12.92	12.22
3	13.87	13.87	13.55	12.62	12.85	12.82	13.27
4	13.59	13.69	12.01	11.96	12.17	12.27	11.88
5	13.33	13.09	12.78	12.53	12.26	12.38	11.99
6	12.06	11.78	11.46	11.88	11.28	11.43	11.18
7	14.14	13.88	13.24	13.34	13.46	13.26	13.36
8	12.66	14.07	14.34	14.47	14.52	14.84	14.22
9	13.94	14.53	14.96	15.00	14.50	14.93	13.66
10	13.83	13.63	14.73	14.58	14.43	14.48	14.11
11	12.83	14.03	14.03	14.54	13.85	13.58	14.13
12	13.25	13.57	14.09	14.04	14.47	13.19	13.74
13	14.05	14.07	13.79	13.89	13.67	13.82	12.87
14	14.73	14.55	15.14	15.30	15.23	14.70	14.50
15	15.93	15.71	15.49	15.66	15.23	15.31	14.83
16	16.29	16.01	16.41	15.91	16.05	15.58	14.99
17	15.98	15.63	16.18	15.96	16.36	15.58	14.78
18	15.70	15.12	15.52	15.07	16.06	14.52	14.50
19	15.36	14.60	14.80	14.68	15.84	14.15	14.50
20	14.62	14.36	14.94	14.44	15.44	13.61	13.86
21	14.62	14.36	14.94	14.44	15.44	13.61	13.86
Time	1:10	1:14	1:31	1:39	1:46	1:55	2:03
Barometer #2	974.8	974.9	974.9	974.9	974.9	975.0	975.0
Barometer #3	974.7	974.8	974.8	974.8	974.8	974.8	974.9

TABLE 7-7 CONTINUED

Barometer #1	974.5	974.5	974.6	974.5	974.6	974.6
Hygrometer	0.395	0.373	0.370	0.367	0.365	0.360
Time	2:02	2:13	2:22	2:29	2:36	2:45
1	12.76	12.89	12.72	12.87	12.29	12.92
2	12.35	12.32	12.35	11.88	12.17	12.65
3	13.15	12.45	13.41	13.07	11.88	12.55
4	12.49	12.41	12.23	12.24	11.23	12.44
5	11.89	12.60	11.93	11.27	11.01	11.87
6	11.38	11.38	10.99	10.82	10.27	12.03
7	12.71	13.21	13.76	12.53	11.04	12.54
8	13.46	13.77	15.14	14.32	11.21	11.86
9	14.63	14.98	13.88	14.11	11.88	11.58
10	13.88	14.47	14.43	14.93	12.64	12.99
11	13.13	13.31	13.71	14.93	13.05	12.03
12	14.51	13.39	14.95	15.96	13.29	11.58
13	13.67	12.92	12.87	15.07	12.97	10.97
14	14.15	14.50	14.05	14.95	12.55	12.20
15	14.91	14.51	14.55	14.76	12.55	12.65
16	15.15	14.44	14.01	14.84	13.54	13.39
17	14.86	14.08	13.84	14.73	13.63	13.06
18	14.07	13.77	13.84	14.77	13.92	12.85
19	14.48	13.65	13.08	14.90	13.05	12.95
20	13.46	12.96	13.34	14.11	14.44	12.74
21	13.46	12.96	13.34	14.11	14.44	12.74
Time	2:20	2:27	2:33	2:42	2:50	3:04
Barometer #2	975.1	974.9	975.0	975.0	975.1	975.2
Barometer #3	974.9	974.9	974.9	974.9	974.9	975.0

TABLE 7-7 CONTINUED

Barometer #1	974.6	974.6	974.5	974.4	974.5	974.4	974.3
Hygrometer	0.366	0.360	0.347	0.352	0.360	0.343	0.347
Time	2:56	3:03	3:14	3:21	3:36	3:46	3:59
1	12.64	12.50	12.17	12.22	11.69	12.12	12.16
2	12.22	11.48	11.32	11.66	11.20	11.58	11.28
3	11.83	12.43	12.12	11.58	11.66	11.62	11.53
4	12.44	11.46	11.66	11.38	11.63	11.52	11.83
5	11.82	10.24	11.55	11.07	11.07	10.56	11.42
6	11.48	10.97	10.27	10.37	9.82	10.05	9.99
7	12.68	12.50	12.26	11.28	11.72	12.08	12.41
8	12.42	13.90	14.27	13.42	14.58	14.66	13.82
9	13.46	14.18	14.78	14.68	14.68	14.08	12.83
10	13.56	13.89	14.63	14.11	14.73	14.21	12.44
11	12.28	13.15	13.93	13.73	13.63	12.95	11.85
12	13.41	14.35	15.26	15.69	14.79	12.18	11.63
13	12.29	13.19	14.19	14.17	12.27	11.23	10.97
14	12.77	13.27	13.85	14.45	11.76	12.05	12.00
15	13.11	13.69	14.71	14.51	12.85	12.66	12.80
16	13.51	14.17	14.69	13.59	13.34	13.63	13.74
17	13.16	13.94	14.43	14.01	12.94	13.14	13.96
18	12.82	13.08	14.07	13.52	13.77	13.62	14.12
19	13.32	13.56	14.00	13.90	12.94	13.00	11.56
20	12.66	13.08	13.93	13.06	11.12	11.01	11.92
21	12.66	13.08	13.93	13.06	11.12	11.01	11.92
Time	3:08	3:13	3:26	3:35	3:54	3:56	4:09
Barometer #2	975.1	975.0	974.9	974.9	974.8	974.8	974.8
Barometer #3	975.0	974.9	974.8	974.8	974.6	974.6	974.5

TABLE 7-7 CONTINUED

	Barometer #1	974.2	974.2	974.0	974.2	974.1	974.1
	Hygrometer	0.347	0.339	0.347	0.347	0.347	0.344
	Time	4:06	4:14	4:23	4:28	4:37	4:46
	1	11.76	11.54	11.34	11.66	11.49	11.94
	2	11.08	10.93	10.92	11.56	11.99	11.58
	3	11.66	11.64	11.44	11.64	11.96	10.98
	4	12.01	11.03	11.54	11.96	12.24	11.33
	5	11.01	12.48	11.91	12.28	12.28	11.17
	6	9.67	11.65	12.41	11.23	11.33	10.07
	7	13.16	14.81	14.96	14.26	13.58	10.68
	8	13.92	14.42	14.92	14.88	14.42	10.51
	9	12.38	14.08	14.64	14.68	14.40	10.88
	10	10.56	14.43	14.25	14.13	13.75	10.96
	11	11.68	13.63	13.75	13.05	13.53	10.83
	12	11.80	12.83	12.78	13.49	13.49	10.87
	13	13.17	13.02	12.85	13.12	13.37	10.37
	14	14.20	14.05	14.19	13.23	13.00	10.96
	15	13.90	14.21	14.31	13.71	13.36	11.09
	16	13.57	14.19	14.45	13.59	13.47	11.47
	17	13.88	14.08	14.06	13.90	13.60	11.18
	18	11.18	11.68	11.12	13.76	13.42	11.48
	19	10.18	10.88	10.78	13.55	13.50	11.78
	20	11.22	11.92	11.89	12.46	12.08	11.57
	21	11.22	11.92	11.89	12.46	12.08	11.57
	Time	4:17	4:26	4:33	4:45	4:48	4:57
	Barometer #2	974.6	974.6	974.5	974.6	974.6	974.5
	Barometer #3	974.4	974.5	974.4	974.5	974.6	974.4

TABLE 7-7 CONTINUED

Barometer #1	974.0	974.1	974.2	974.1	974.2	974.3	974.4
Hygrometer	0.352	0.330	0.367	0.334	0.340	0.334	0.340
Time	4:59	5:06	5:12	5:24	5:32	5:44	5:48
1	11.69	11.28	10.89	10.54	10.74	10.48	10.72
2	10.95	10.86	10.28	10.46	10.28	9.62	10.53
3	11.14	10.60	10.30	10.58	9.88	10.28	10.56
4	10.73	10.32	10.78	10.49	10.08	10.36	10.86
5	10.61	10.56	10.54	10.56	10.16	10.26	11.12
6	10.27	10.23	10.15	9.45	9.57	9.53	9.27
7	11.01	11.78	11.64	10.61	10.08	10.54	9.71
8	11.21	10.81	9.65	9.41	9.51	9.29	9.09
9	12.18	10.82	10.66	9.50	9.10	8.84	8.48
10	12.09	11.02	10.21	10.08	9.86	8.62	8.64
11	11.83	11.37	9.68	9.73	9.78	8.73	9.01
12	12.99	11.32	10.65	9.35	10.02	8.97	9.97
13	12.97	11.73	10.95	10.56	10.59	9.79	9.72
14	12.95	12.19	11.38	12.01	11.56	11.36	10.94
15	13.71	13.41	13.26	12.87	10.69	11.37	10.67
16	13.64	13.67	13.64	13.54	11.87	11.00	9.86
17	13.88	13.96	13.96	14.18	11.78	11.48	10.00
18	13.72	14.12	13.67	14.17	12.30	11.06	10.15
19	12.89	13.62	13.28	13.82	12.69	11.22	10.56
20	13.31	13.50	13.28	13.71	11.37	11.55	11.27
21	13.31	13.50	13.28	13.71	11.37	11.55	11.27
Time	5:09	5:15	5:28	5:36	5:45	5:53	6:02
Barometer #2	974.6	974.5	974.7	974.8	974.7	974.9	974.9
Barometer #3	974.5	974.4	974.7	974.5	974.6	974.7	974.8

TABLE 7-8
 CORRECTED AND CONVERTED EXPERIMENTAL DATA
 TAKEN SEPTEMBER 15, 1967

Barometer #1	973.1	973.3	973.4	973.5	973.5	973.5	973.4
Hygrometer	0.408	0.448	0.432	0.417	0.417	0.417	0.409
Time	0:36	0:42	0:54	1:00	1:09	1:18	1:30
1	18.46	17.06	16.60	16.41	14.89	14.70	14.05
2	19.08	18.16	16.78	17.24	15.68	14.76	13.78
3	18.99	18.25	17.27	17.32	14.93	15.42	13.87
4	18.95	17.99	16.79	16.74	15.31	15.04	13.54
5	18.77	17.53	16.99	16.81	15.11	14.74	13.39
6	17.66	16.26	16.20	16.09	14.30	14.02	13.70
7	17.96	17.40	16.86	15.87	15.20	13.51	13.16
8	17.32	16.57	15.92	14.77	15.40	12.78	12.72
9	16.32	16.56	15.53	14.13	14.26	12.70	12.68
10	15.81	16.05	14.93	14.13	13.79	12.62	13.13
11	16.01	16.38	15.08	14.43	14.43	13.01	12.85
12	16.27	16.17	15.21	14.81	14.53	13.49	12.83
13	16.29	16.17	14.92	14.55	14.97	13.91	12.37
14	17.47	16.77	15.65	15.16	15.35	14.00	12.65
15	17.47	16.29	15.46	14.61	15.13	14.19	13.26
16	17.53	15.89	14.99	14.04	14.91	14.05	13.19
17	17.28	16.36	14.88	14.38	15.22	14.30	12.98
18	16.10	16.86	14.97	14.82	14.94	13.82	13.32
19	16.32	16.08	15.25	14.62	15.10	14.45	13.20
20	16.30	17.01	15.16	14.76	15.24	14.84	13.11
21	16.30	17.01	15.16	14.76	15.24	14.84	13.11
Time	0:46	0:57	1:07	1:12	1:19	1:33	1:43
Barometer #2	973.7	973.9	973.9	973.9	973.9	973.9	973.9
Barometer #3	973.7	973.9	974.0	974.0	973.8	973.8	973.8

TABLE 7-8 CONTINUED

Barometer #1	973.4	973.5	973.5	973.5	973.6	973.6
Hygrometer	0.417	0.402	0.417	0.406	0.400	0.364
Time	1:38	1:46	1:56	2:10	2:20	2:28
1	13.66	13.85	13.95	13.35	12.79	12.09
2	14.17	14.28	13.56	13.21	13.17	12.55
3	13.82	13.91	13.85	13.07	13.19	12.71
4	13.61	13.33	13.99	13.04	13.09	12.87
5	13.37	13.15	13.49	13.19	12.90	12.84
6	13.28	12.99	11.93	12.89	12.70	12.61
7	13.46	12.36	12.86	12.76	12.21	11.90
8	13.07	12.60	13.02	12.32	12.09	12.52
9	12.93	12.62	12.46	12.28	12.13	12.12
10	12.84	12.78	12.42	12.42	11.93	12.34
11	12.83	12.91	12.43	12.63	12.04	12.51
12	12.83	13.07	12.40	12.43	12.10	13.05
13	13.19	12.87	12.05	12.37	12.09	12.87
14	13.67	13.01	13.11	12.07	12.10	13.21
15	13.19	12.68	12.76	12.41	12.04	13.33
16	13.03	12.76	12.68	12.88	11.89	13.09
17	12.96	12.88	12.66	12.63	12.08	12.92
18	13.02	13.40	12.05	12.30	11.78	12.00
19	13.05	13.22	12.79	12.49	12.00	12.07
20	13.51	13.74	13.91	12.86	12.38	12.66
21	13.51	13.74	13.91	12.86	12.38	12.66
Time	1:49	1:53	2:11	2:22	2:32	2:37
Barometer #2	973.9	973.9	974.2	974.0	974.0	974.2
Barometer #3	973.9	973.8	974.0	974.0	974.0	974.1

TABLE 7-8 CONTINUED

Barometer #1	973.7	973.7	973.8	974.0	973.9	973.9	973.7
Hygrometer	0.387	0.373	0.387	0.365	0.373	0.364	0.395
Time	2:37	2:52	3:01	3:10	3:20	3:34	3:45
1	12.55	12.45	12.68	11.72	11.64	12.45	13.17
2	12.57	11.98	11.48	10.12	11.98	12.17	12.89
3	12.45	11.88	11.98	11.54	11.88	12.07	12.79
4	12.35	11.78	12.53	12.07	11.53	12.59	12.28
5	12.54	11.97	12.30	11.59	11.04	11.07	11.72
6	12.34	11.53	11.20	10.57	11.16	10.49	11.48
7	12.26	11.51	10.91	11.00	11.32	10.41	11.16
8	11.99	11.51	11.10	11.45	10.81	10.69	10.91
9	12.28	11.48	10.70	11.10	10.78	10.88	10.80
10	12.04	11.55	10.53	10.78	10.94	10.58	10.83
11	12.03	11.73	11.42	11.29	11.07	10.65	11.01
12	12.28	11.53	11.16	11.44	11.38	10.37	10.77
13	12.31	11.27	10.72	10.97	10.81	10.57	10.77
14	12.13	11.56	12.01	12.51	11.81	11.21	11.46
15	12.28	11.89	11.91	11.87	11.91	11.79	11.31
16	11.75	11.47	11.04	11.09	12.18	11.62	10.98
17	11.58	11.43	10.99	11.28	11.94	11.03	10.96
18	11.86	11.63	11.06	11.22	11.63	11.10	10.75
19	11.68	12.04	11.39	11.56	11.53	10.96	10.88
20	12.56	12.38	12.16	12.18	11.85	11.82	11.87
21	12.56	12.38	12.16	12.18	11.85	11.82	11.87
Time	2:50	3:03	3:12	3:19	3:33	3:45	3:57
Barometer #2	974.4	974.3	974.3	974.3	974.3	974.2	974.3
Barometer #3	974.3	974.2	974.2	974.2	974.2	974.1	974.2

TABLE 7-8 CONTINUED

Barometer #1	973.9	973.8	973.6	973.8	973.7	973.7
Hygrometer	0.357	0.383	0.369	0.393	0.370	0.366
Time	3:55	4:09	4:24	4:33	4:42	4:53
1	12.45	11.86	11.74	11.36	11.50	11.22
2	12.57	11.42	10.93	10.73	11.46	11.18
3	12.43	11.63	11.88	11.16	11.62	12.07
4	11.98	11.53	11.53	11.09	12.25	12.37
5	11.89	11.17	10.36	11.39	11.65	11.95
6	10.65	10.45	10.67	10.27	10.57	10.62
7	10.82	10.74	10.68	10.45	10.10	11.04
8	10.51	9.91	9.71	9.66	11.43	13.12
9	10.36	9.88	9.88	9.58	11.52	13.12
10	10.30	9.44	9.66	9.61	11.09	12.54
11	10.27	10.18	10.28	10.18	10.51	12.38
12	10.21	11.06	9.57	11.03	10.37	12.02
13	10.15	10.25	10.27	10.65	10.83	11.35
14	11.56	11.92	11.36	12.33	12.17	12.70
15	11.09	11.19	11.49	11.67	12.20	13.26
16	10.18	10.94	11.67	11.32	11.87	13.11
17	11.10	10.86	11.98	10.88	12.20	13.23
18	12.04	11.63	12.42	11.58	12.06	12.52
19	13.00	12.51	11.58	12.01	11.64	11.36
20	12.40	12.02	12.66	12.59	11.51	11.39
21	12.40	12.02	12.66	12.59	11.51	11.39
Time	4:04	4:22	4:35	4:44	4:51	5:07
Barometer #2	974.3	974.2	974.1	974.0	974.1	974.1
Barometer #3	974.2	974.0	974.0	974.0	974.1	974.0

TABLE 7-8 CONTINUED

Barometer #1	973.6	973.5	973.5	973.6	973.4
Hygrometer	0.360	0.345	0.379	0.398	0.384
Time	5:13	5:18	5:29	5:40	5:52
1	10.99	11.66	12.49	12.79	12.10
2	11.30	11.88	12.25	12.27	11.93
3	11.18	11.73	12.49	12.65	12.07
4	12.39	12.29	12.73	12.94	12.54
5	12.58	11.69	12.88	12.54	12.78
6	10.97	11.30	12.53	11.50	11.98
7	14.16	14.97	15.36	13.46	11.56
8	14.02	14.22	14.82	14.68	11.51
9	13.68	14.27	14.94	13.78	12.18
10	13.73	13.75	14.81	13.81	12.54
11	12.93	13.31	14.65	13.63	11.43
12	13.44	13.57	14.11	12.88	12.08
13	12.57	14.25	14.57	13.39	11.47
14	14.25	14.43	15.17	13.85	12.65
15	14.21	14.59	15.19	14.17	12.80
16	13.69	14.30	14.71	14.49	12.23
17	13.68	14.46	14.78	14.60	12.18
18	13.92	13.42	14.86	14.22	12.40
19	12.19	12.11	13.88	13.36	12.39
20	11.12	12.16	12.52	12.18	12.31
21	11.12	12.16	12.52	12.18	12.31
Time	5:24	5:30	5:39	5:55	6:03
Barometer #2	973.8	973.9	974.0	974.0	973.7
Barometer #3	973.8	973.8	973.9	973.8	973.8

with an observer starting down the line approximately every twelve minutes. Since it normally took more than twelve minutes to obtain all of the required data, two people were recording data much of the time. Those taking the data made an effort to move along the line at a constant speed and therefore the approximate time at which any given temperature measurement was made, can be obtained by interpolating between the starting and ending times of the particular pass. The atmospheric information was corrected in the manner described in the preceding section and converted into different units where desirable. The results are presented in Tables 7-5, 7-6, 7-7 and 7-8, where air pressure is given in millibars, temperature in degrees centigrade, water vapor pressure (hygrometer) in inches of mercury, and time in hours and minutes after 8:00 P. M.

E. D. T. on the day in which the particular experiment period began.

(f) Distance Measurement

On September 12, four separate measurements of the base-line were made using the RADC Geodimeter. The magnitude of the results, together with the approximate times at which they were obtained, are given in Table 7-9. Time is measured in the manner described in the previous section.

TABLE 7-9

Measured Distance, Corrected Distance And
Average Refractive Index Values
For September 12, 1967

Time	Measured Distance in Meters	Measured Distance in Feet	Average Refractive Index	Corrected Distance in Feet
0:37	499.892	1640.0656	1.00027698	1640.1182
0:58	499.885	1640.0427	1.00027726	1640.0948
1:59	499.878	1640.0197	1.00027821	1640.0702
2:28	499.882	1640.0328	1.00027866	1640.0826

On September 13, 14, and 14 a very large number of distance measurements were made using the Spectra Physics Geodolite. Each measurement was the result of averaging over a ten second period. The measurements were made in groups of about ten calibration measurements followed by approximately ten baseline length measurements followed by ten more calibration measurements, followed by ten length measurements, etc. At the suggestion of Mr. Mansir, the first two measurements in each group were ignored and the rest were averaged. The average of each calibration group was used to determine the equipment correction to be applied to the average of the baseline measurement group which followed it. In a few cases, entire measurement groups were thrown out because notes on the original data sheets indicated that they might not be reliable. The average of each measurement group, corrected as described above is given in Tables 7-10, 7-11 and 7-12 under the heading "Measured Distance". The average time at which the measurements in the group were made is also given. Here again, time is measured from 8:00 P.M. E.D.T. on the day in which the experiment period began.

3. COMPUTER PROCESSING

(a) Determining the Average Refractive Index Along the Baseline

All the temperature, air pressure, water vapor pressure, distance measurement and identifying time data were fed into the SURC, SDS Model 930 computer. Using the formula given by Equation (B - 11), the refractive index of the atmosphere was computed for each thermometer position at the instant of each length measurement. For the Geodimeter, an effective vacuum wavelength of 0.550 microns was used and for the Geodolite 0.63299146 microns. Since a complete description of the computer program used to accomplish this is given in the separate report "Documentation for Distance Measurement Program," only a brief description of some of the more important aspects of the processing will be given here.

TABLE 7-10
Measured Distance, Corrected Distance and
Average Refractive Index Values
for September 13, 1967

Time	Measured Distance in Feet	Average Refractive Index	Corrected Distance in Feet.
2:06	1640.1380	1.00027768	1640.1412
2:11	1640.1261	1.00027788	1640.1290
2:14	1640.1326	1.00027798	1640.1353
2:17	1640.1370	1.00027810	1640.1396
2:21	1640.1341	1.00027821	1640.1365
2:25	1640.1357	1.00027836	1640.1378
2:27	1640.1374	1.00027845	1640.1394
2:30	1640.1364	1.00027862	1640.1381
2:33	1640.1318	1.00027878	1640.1332
2:39	1640.1384	1.00027900	1640.1395
2:45	1640.1363	1.00027924	1640.1370
2:51	1640.1354	1.00027958	1640.1355
2:58	1640.1340	1.00027980	1640.1338
3:06	1640.1387	1.00027986	1640.1384
3:09	1640.1363	1.00027970	1640.1362
3:14	1640.1362	1.00027953	1640.1364
3:17	1640.1199	1.00027953	1640.1201
3:21	1640.1233	1.00027960	1640.1234
3:27	1640.1525	1.00027981	1640.1522
3:29	1640.1465	1.00027989	1640.1461
3:35	1640.1404	1.00028004	1640.1398
3:37	1640.1404	1.00028001	1640.1398
3:41	1640.1446	1.00027989	1640.1442
3:45	1640.1284	1.00027971	1640.1283
3:52	1640.1457	1.00027943	1640.1461
3:55	1640.1570	1.00027935	1640.1575
3:57	1640.1510	1.00027929	1640.1516
4:01	1640.1483	1.00027910	1640.1492
4:04	1640.1529	1.00027894	1640.1541
4:07	1640.1425	1.00027885	1640.1438
4:13	1640.1463	1.00027849	1640.1482
4:16	1640.1443	1.00027824	1640.1466
4:19	1640.1470	1.00027803	1640.1497
4:23	1640.1567	1.00027783	1640.1597
4:26	1640.1463	1.00027777	1640.1494
4:30	1640.1448	1.00027775	1640.1479

TABLE 7-10 CONTINUED

Time	Measured Distance in Feet	Average Refractive Index	Corrected Distance in Feet
4:34	1640.1501	1.00027765	1640.1534
4:37	1640.1471	1.00027760	1640.1505
4:40	1640.1449	1.00027759	1640.1483
4:44	1640.1470	1.00027759	1640.1504
4:48	1640.1448	1.00027757	1640.1482
4:57	1640.1391	1.00027774	1640.1422
5:00	1640.1368	1.00027781	1640.1398
5:04	1640.1331	1.00027775	1640.1331
5:07	1640.1584	1.00027759	1640.1618
5:15	1640.1425	1.00027738	1640.1462
5:19	1640.1487	1.00027721	1640.1527
5:23	1640.1451	1.00027710	1640.1493
5:26	1640.1469	1.00027703	1640.1512
5:30	1640.1527	1.00027701	1640.1570
5:35	1640.1484	1.00027691	1640.1529
5:39	1640.1498	1.00027683	1640.1544

TABLE 7-11
**Measured Distance, Corrected Distance and
 Average Refractive Index Values**
for September 14, 1967

Time	Measured Distance in Feet	Average Refractive Index	Corrected Distance in Feet
1:11	1640.1052	1.00027393	1640.1146
1:13	1640.1066	1.00027398	1640.1159
1:17	1640.1007	1.00027397	1640.1100
1:20	1640.1005	1.00027394	1640.1099
1:24	1640.0996	1.00027391	1640.1090
1:27	1640.0994	1.00027389	1640.1089
1:33	1640.1108	1.00027391	1640.1202
1:37	1640.1103	1.00027399	1640.1196
1:40	1640.1101	1.00027397	1640.1194
1:42	1640.1093	1.00027393	1640.1187
1:45	1640.1103	1.00027389	1640.1197
1:48	1640.1108	1.00027406	1640.1200
1:51	1640.1130	1.00027425	1640.1219
1:55	1640.1077	1.00027443	1640.1163
2:04	1640.1145	1.00027447	1640.1230
2:07	1640.1164	1.00027449	1640.1249
2:10	1640.1145	1.00027450	1640.1230
2:14	1640.1156	1.00027449	1640.1241
2:18	1640.1142	1.00027453	1640.1226
2:22	1640.1147	1.00027460	1640.1230
2:25	1640.1155	1.00027464	1640.1237
2:28	1640.1162	1.00027469	1640.1243
2:31	1640.1151	1.00027468	1640.1233
2:35	1640.1198	1.00027461	1640.1281
2:46	1640.1125	1.00027536	1640.1195
2:50	1640.1107	1.00027543	1640.1176
2:53	1640.1100	1.00027554	1640.1167
2:56	1640.1084	1.00027560	1640.1150
3:10	1640.1140	1.00027515	1640.1214
3:13	1640.1138	1.00027502	1640.1214
3:16	1640.1136	1.00027490	1640.1214
3:20	1640.1155	1.00027479	1640.1235
3:24	1640.1149	1.00027479	1640.1229
3:28	1640.1156	1.00027486	1640.1235
3:32	1640.1154	1.00027496	1640.1231
3:36	1640.1139	1.00027507	1640.1214
3:41	1640.1150	1.00027520	1640.1223
3:45	1640.1164	1.00027532	1640.1235
3:49	1640.1158	1.00027554	1640.1225

TABLE 7-11 CONTINUED

Time	Measured Distance in Feet	Average Refractive Index	Corrected Distance in Feet
3:52	1640.1175	1.00027568	1640.1240
3:56	1640.1197	1.00027575	1640.1261
3:59	1640.1174	1.00027577	1640.1238
4:09	1640.1137	1.00027580	1640.1200
4:14	1640.1168	1.00027559	1640.1235
4:18	1640.1163	1.00027530	1640.1234
4:22	1640.1138	1.00027511	1640.1213
4:26	1640.1138	1.00027502	1640.1214
4:30	1640.1139	1.00027504	1640.1215
4:35	1640.1158	1.00027501	1640.1234
4:41	1640.1142	1.00027501	1640.1218
4:44	1640.1169	1.00027529	1640.1241
4:51	1640.1174	1.00027657	1640.1225
4:55	1640.1162	1.00027671	1640.1210
5:19	1640.1184	1.00027641	1640.1237
5:23	1640.1140	1.00027656	1640.1191
5:26	1640.1202	1.00027666	1640.1251
5:30	1640.1159	1.00027673	1640.1207
5:34	1640.1202	1.00027679	1640.1249
5:37	1640.1202	1.00027696	1640.1246
5:44	1640.1107	1.00027750	1640.1205
5:48	1640.1242	1.00027761	1640.1276

TABLE 7-12
Measured Distance, Corrected Distance and
Average Refractive Index Values
for September 15, 1967

Time	Measured Distance in Feet	Average Refractive Index	Corrected Distance in Feet
0:48	1640.1172	1.00027107	1640.1313
0:51	1640.1121	1.00027123	1640.1259
0:55	1640.1144	1.00027150	1640.1278
1:03	1640.1209	1.00027227	1640.1330
1:06	1640.1241	1.00027267	1640.1356
1:09	1640.1187	1.00027294	1640.1297
1:12	1640.1158	1.00027301	1640.1267
1:17	1640.1201	1.00027310	1640.1309
1:20	1640.1234	1.00027331	1640.1338
1:24	1640.1225	1.00027366	1640.1323
1:28	1640.1227	1.00027390	1640.1321
1:31	1640.1257	1.00027408	1640.1348
1:35	1640.1206	1.00027428	1640.1294
1:39	1640.1185	1.00027444	1640.1271
1:42	1640.1175	1.00027449	1640.1260
1:45	1640.1186	1.00027454	1640.1270
1:48	1640.1183	1.00027462	1640.1266
1:52	1640.1182	1.00027463	1640.1264
1:56	1640.1264	1.00027468	1640.1346
2:00	1640.1252	1.00027476	1640.1332
2:06	1640.1288	1.00027489	1640.1366
2:10	1640.1257	1.00027496	1640.1334
2:13	1640.1270	1.00027501	1640.1346
2:16	1640.1259	1.00027507	1640.1334
2:19	1640.1249	1.00027514	1640.1323
2:23	1640.1262	1.00027531	1640.1333
2:26	1640.1200	1.00027544	1640.1269
2:29	1640.1235	1.00027547	1640.1304
2:32	1640.1164	1.00027532	1640.1235
2:35	1640.1220	1.00027525	1640.1292
2:39	1640.1202	1.00027540	1640.1272
2:42	1640.1209	1.00027553	1640.1277
2:46	1640.1190	1.00027574	1640.1254
2:49	1640.1205	1.00027586	1640.1267
3:06	1640.1349	1.00027641	1640.1302
3:09	1640.1284	1.00027651	1640.1336
3:12	1640.1216	1.00027652	1640.1267
3:23	1640.1292	1.00027638	1640.1346
3:27	1640.1235	1.00027638	1640.1289

TABLE 7-12 CONTINUED

Time	Measured Distance in Feet	Average Refractive Index	Corrected Distance in Feet
3:43	1640.1184	1.00027642	1640.1237
3:47	1640.1212	1.00027638	1640.1266
3:51	1640.1220	1.00027646	1640.1272
3:55	1640.1276	1.00027663	1640.1326
4:01	1640.1290	1.00027667	1640.1339
4:04	1640.1291	1.00027664	1640.1340
4:08	1640.1246	1.00027668	1640.1295
4:12	1640.1258	1.00027672	1640.1306
4:16	1640.1308	1.00027673	1640.1356
4:19	1640.1301	1.00027676	1640.1348
4:23	1640.1291	1.00027678	1640.1338
4:32	1640.1277	1.00027676	1640.1324
4:35	1640.1310	1.00027674	1640.1358
4:38	1640.1331	1.00027667	1640.1380
4:43	1640.1342	1.00027645	1640.1395
4:46	1640.1332	1.00027633	1640.1386
4:49	1640.1294	1.00027623	1640.1350
4:53	1640.1309	1.00027605	1640.1368
4:57	1640.1281	1.00027585	1640.1343
5:08	1640.1320	1.00027540	1640.1390
5:11	1640.1286	1.00027528	1640.1358
5:15	1640.1259	1.00027510	1640.1334
5:23	1640.1235	1.00027470	1640.1316
5:26	1640.1230	1.00027450	1640.1315
5:30	1640.1309	1.00027421	1640.1398
5:35	1640.1312	1.00027397	1640.1405

The time at which each air pressure and water vapor pressure observation was made is presented in the data. The time at which each temperature observation was made was obtained by interpolating between the beginning and ending times of the respective passes down the baseline assuming that the observer moved at constant speed.

To obtain the refractive index at any particular thermometer location and any particular instant, it was necessary to determine the prevailing values of temperature, air pressure, and water vapor pressure. The temperature was obtained by interpolating between the value of temperature observed immediately before and immediately after the time being considered.

The air pressure was obtained by a double interpolation. The pressure at each end of the line, at the instant being considered, was obtained by interpolating, with respect to time, between the values of pressure observed just before and just after that instant. The second interpolation was with respect to distance between the values calculated to exist at the ends of the baseline.

Water vapor pressure was assumed to be constant with respect to distance. Therefore, the effective value of water vapor pressure at a particular time and location was obtained by a single interpolation with respect to time between the appropriate recorded values.

The average refractive index along the baseline was computed using Equation (B-16) which assumes that this quantity varied linearly between the various thermometer positions. The results of computing this average for each time of interest are given in Tables 7-9, 7-10, 7-11, and 7-12.

(b) Propagation Corrections for the Distance Measurements

(1) The Geodimeter

This instrument produces amplitude modulated radiation which is centered at 0.550 microns and is calibrated at an air pressure of 760 mm, a temperature of -4°C and zero water vapor pressure. The

formula for the corrected distance, D , is obtained by substituting these calibration conditions into Equation (B-23). The result is:

$$D = \frac{n_G (t = -4^\circ\text{C}, P = 760 \text{ mm}, e = 0)}{\bar{n}_G} S$$

$$= \frac{1.0003090353}{\bar{n}_G} S \quad (7-1)$$

where S is the distance indicated by the Geodimeter and \bar{n}_G is the average group refractive index along the ray path. It should be mentioned that the 0.550 micron wavelength is approximate to the extent that it is close enough to the correct value to produce measurements which are accurate to one part in 10^6 . This wavelength applies to Geodimeters which use either the tungsten or mercury lamp.

(2) The Geodolite

This equipment uses an amplitude modulated laser beam as its radiated signal and is calibrated to produce accurate measurements for a temperature of 20°C , air pressure of 760 mm and zero water vapor pressure. The laser vacuum wavelength is 0.63299146 microns. If S denotes the distance as measured using the Geodolite, then the correct value for the distance, D , is:

$$D = \frac{n_G (20^\circ\text{C}, 760 \text{ mm}, 0\text{mm})}{\bar{n}_G} S$$

$$= \frac{(1.0002796568)}{\bar{n}_G} S \quad (7-2)$$

where 1.0002796568 is the group refractive index obtained by substituting the calibration conditions into Equation (B-11) and solving for n_G . \bar{n}_G is obtained by averaging the values calculated for the various points along the line.

The results of correcting the distance measurements obtained on September 12-15 are presented in Tables 7-9, 7-10, 7-11, and 7-12 under the heading "Corrected Distance."

4. RESULTS AND CONCLUSIONS

At the time that the Mansfield experiments were carried out, the length of the baseline was not known with high accuracy. It was anticipated however, that by the time the data was reduced and analyzed, the baseline length would be known with high accuracy. This information was expected to come from two measurement programs. First, the line had been measured in the Fall of 1966 using the Väisälä technique and it was expected that the results of this work would be available. Unfortunately, the processing of this data has not been completed and the results are not known. Even when they do become available their usefulness may be somewhat reduced because of the possibility that the pillars and monuments on the line could have moved during the intervening period.

It was also expected that Ohio State personnel, under the direction of Sol Cushman, would remeasure the line using the Väisälä equipment soon after the experiments described here were completed. This was attempted but unfavorable weather conditions produced variations in the refractive index of the atmosphere which were so great that interference fringes could not be obtained over the longer distances. Therefore, no baseline length data was obtained and the only information presently available concerning the length of the line was obtained using less accurate techniques. It is estimated by Mr. Cushman that the line is 499.9064 meters (1640.113 ft) long and that this result is accurate to \pm two parts per million. This error corresponds to ± 1 millimeter = ± 0.00328 ft = ± 0.0394 inches, and therefore, the line length must be somewhere between 1640.110 ft and 1640.116 ft.

Although the more accurate length data would have been more

useful, the available data does allow many meaningful conclusions to be drawn.

(a) The Geodimeter Measurements

The Geodimeter length measurements, corrected for refractive index effects, are given in Table 7-9. These values vary from 1640.0702 to 1640.1182 and this spread is about what one would expect. As listed in Part 2d of this section, the Geodimeter has a rated average error of one centimeter plus two millionths of the distance being measured. For the 500 meter line, this corresponds to an error of \pm 11 millimeters which is equivalent to \pm 0.434 inches or \pm 0.0362 ft. If this error and the error assumed to exist in the known length of the line are combined, it is found that the Geodimeter measurements should have been between 1640.074 ft and 1640.152 ft. Three of the four values fall within this range but the fourth is slightly below it. The average of the four measurements is 1640.0915 which is within the lower portion of the range. On the basis of this small amount of information it is concluded that the Geodimeter under test may be slightly out of calibration, producing measurements which are, on the average, a little less than the correct values.

For the measurements being considered, we have a spread of 0.0481 ft, in the corrected values and 0.0460 ft. in the measured values. The corrected values have a greater spread than the measured values and this is contrary to theory. That is, if the spread in the measured values is partly due to variations in the refractive index then since this effect is removed during correction, the resulting values should have a smaller spread. The reason for this disagreement with theory can be found by considering the various sources of error in the measurement. The instrumental error has been shown to be \pm 11 millimeters which is \pm twenty two parts per million. This source of error could result in measurements which are as far apart as 44 parts per million.

Now consider the variation in the refractive index. According to Table 7-9 this quantity varied from 1.00027698 to 1.00027866 for the four measurements being considered. This is a variation of only 1.68 parts per million in the velocity of propagation. Therefore, the error in the measuring equipment completely obscures the variation of atmospheric propagation effects and it is no surprise that the corrected values have a greater spread than the measured values when only four samples are used. In addition, since only five groups of atmospheric measurements were made during the 155 minute interval when the distance measurements were made, there is a very real possibility that the calculated average refractive index values are somewhat in error. This would not be more than one or two parts per million, however.

(b) The Geodolite Measurements

One of the primary objectives of the experiments was the evaluation of the visible wavelength refractive index correction technique developed during the course of this study. In the original planning it was assumed that the average refractive index would probably vary by at least ten parts per million during the experiment period. It was expected that the line length would be known to better than \pm one part per million and that the Geodolite would operate at its rated accuracy of \pm two parts per million. On the basis of these requirements, the spread of the actual measured lengths could be expected to be approximately fourteen parts per million and if the correction technique is valid, the spread of the corrected values should be within \pm two parts per million of the known line length.

The refractive index did vary by about ten parts per million but the line length is known only with an accuracy of \pm two parts per million. Furthermore, it turned out that the operators had difficulty in obtaining proper operation of the Geodolite for a measuring distance as short as 500 meters. They found that the error in the instrument under the existing conditions was \pm 0.01 ft, which

is \pm six parts per million. Errors of this magnitude can obscure some of the effects of the correction formula. As a result the original objective of evaluating the environmental correction technique was not completely achieved. In spite of this several significant conclusions can be reached from the data which was obtained.

It has turned out that the data obtained on each of the three evenings during which Geodolite measurements were made has its own distinctive characteristics. We will therefore consider the data obtained during each experimental period separately.

(1) Measurements made on September 13, 1967

This night produced distance measurement results which were relatively useless. It was the first night of Geodolite operation and a single reflecting prism was used. Several difficulties were experienced because of the limited length of the range. Also as described in Part 2(c) the atmospheric conditions were very poor. When the actual length measurements are plotted in histogram form, then result is that shown in Figure 7-7a. The measured values cover a range from 1640.1190 to 1640.1585 ft. When these values are corrected for variations in the refractive index, the result is a set whose histogram is given in Figure 7-7b. This procedure has caused the average distance to increase slightly and the spread of the values to increase. This latter effect is just the opposite of what should have occurred. As in the Geodimeter case it is reasonable to expect that measurements taken over an extended period of time will have a significant spread since the atmospheric characteristics, and therefore the refractive index, were varying. When the correction formula is applied however, the effect should be to remove that part of the spread in the distance measurements which was due to variations in propagation velocity. Since in this case, the spread was increased, it seems that the data probably contained very large random errors. Furthermore, the spread in measured values is equivalent to more than twenty-three parts per million while the spread in the calculated refractive index values

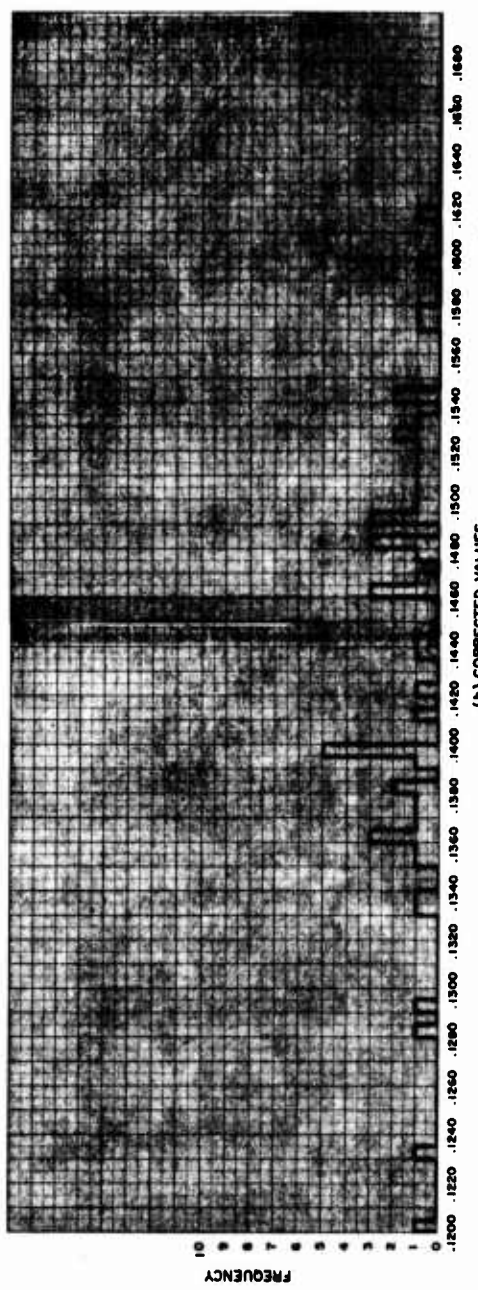
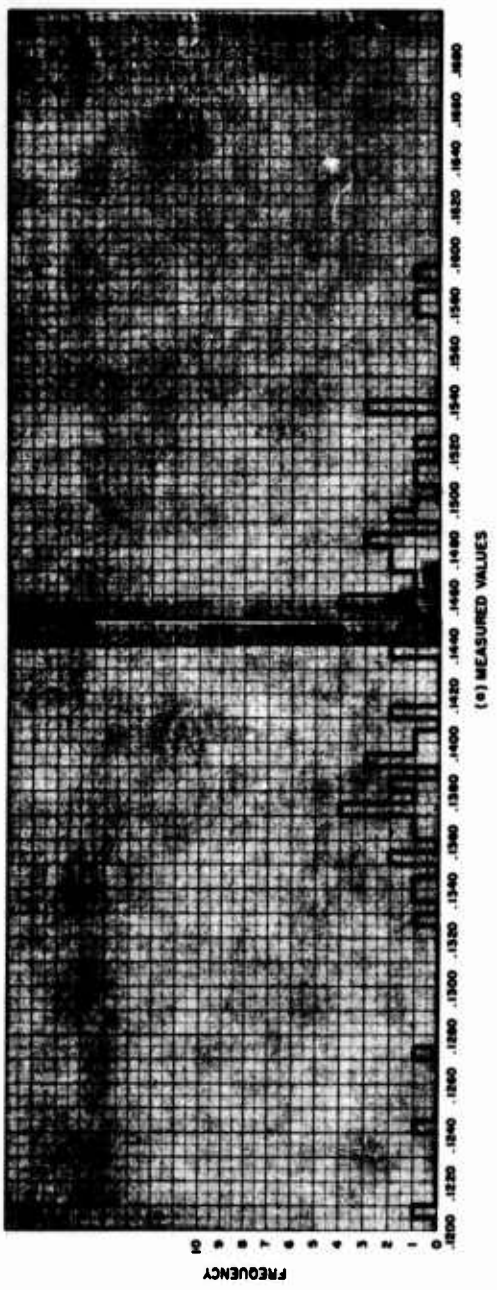


Figure 7-7 Histograms for Distance Measurements Made
September 13, 1967

for the period is only 3.2 parts per million. It therefore appears that on this evening the range of errors in the Geodolite measurements approached twenty parts per million which is considerably greater than the modified accuracy specification presented in the preceding section. In terms of numbers, the average and the standard deviation of the measured and corrected lengths, together with the correlation coefficient between the average refractive indexes and the measured lengths were calculated. The results are presented below along with the corresponding data for September 14 and 15.

TABLE 7-13
Baseline Measurement Statistics

	<u>Sept. 13</u>	<u>Sept. 14</u>	<u>Sept. 15</u>
Average Measured Length (S)	1640.1419 ft.	1640.1136 ft.	1640.1245 ft.
Average Corrected Length (D)	1640.1438 ft.	1640.1210 ft.	1640.1317 ft.
Standard Deviation of Measured Lengths	0.0083 ft.	0.0050 ft.	0.0052 ft.
Standard Deviation of Corrected Lengths	0.0090 ft.	0.0041 ft.	0.0042 ft.
Correlation Coefficient between average refractive index (n) and measured values (S)	-0.312	0.668	0.587

The inaccuracies and anomalies of the September 13th data are clearly illustrated by these numbers. The average corrected length (D) is nineteen parts per million (0.0308 ft.) away from the known value of baseline length. The standard deviation of the corrected lengths is greater than that of the measured lengths and therefore the correlation coefficient is negative. The negative correlation coefficient implies that the dependence of the distance measurements upon refractive index is just the opposite of that which theory predicts. Such data is clearly not of much use in satisfying the objectives which were listed at the beginning of this section.

(2) Measurements made on September 14, 1967.

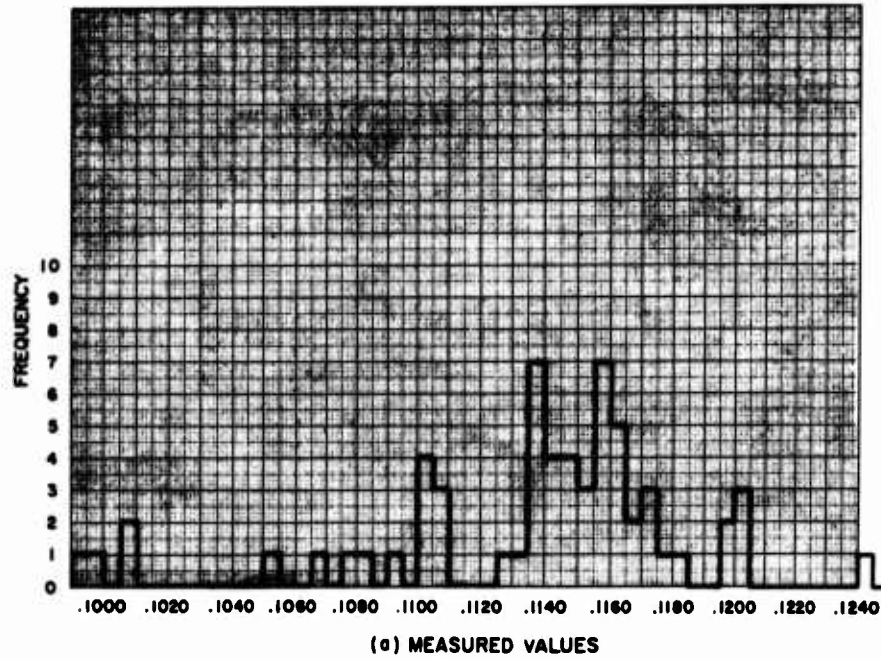
The weather on this night was considerably more favorable for distance measuring than that of the preceding evening. Three reflecting prisms were used. The important characteristics of the data are presented in the manner used in the preceding section. The histograms of the measured and corrected values of baseline length are presented in Figures 7-8a and 7-8b where it will be noticed that a significant reduction in the dispersion of the values is obtained through refractive index correction. The values of Table 7-13 express this effect in a numerical way since the standard deviation of the corrected values is significantly less than that of the measured values. This results from the fact that there is significant correlation between the average refractive index and the measured values of distance. This characteristic of the data is in accordance with theory.

(3) Measurements made on September 15, 1967

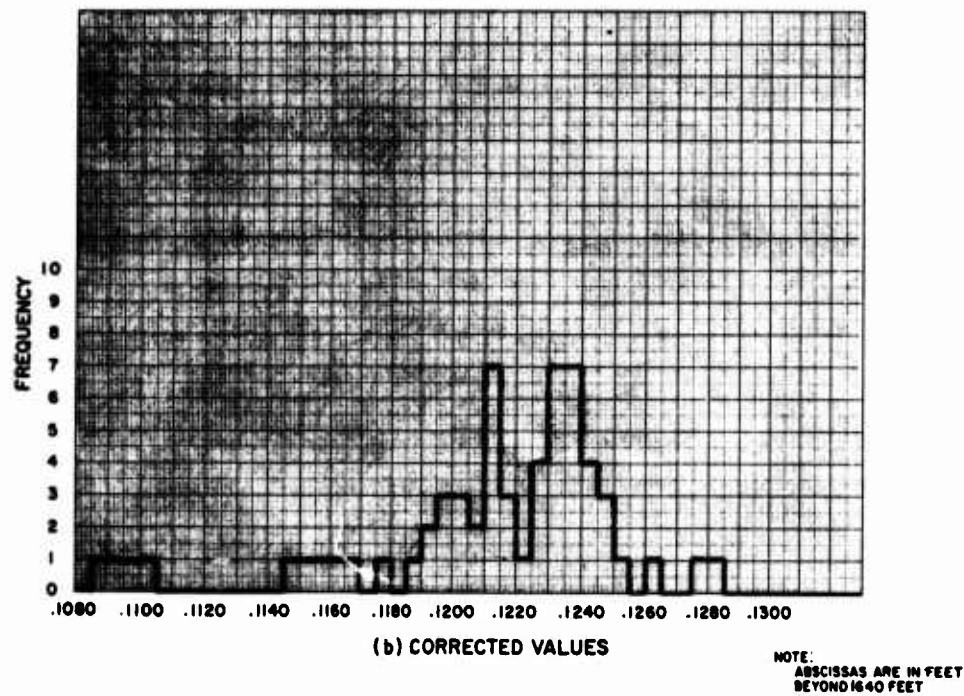
The histograms of the data obtained during this period are presented in Figures 7-9a and 7-9b and the numerical data in Table 7-13. Here as for the preceding night, three reflecting prisms were used and the spread of the data points is significantly less after correction than before. The corresponding standard deviation and correlation coefficients are also comparable. The weather on this evening, while far from ideal, was similar to that of September 14, and much better for the purposes of the experiments than that of September 13.

(4) Comparison of Geodolite Measurements

The distance measurements obtained on September 13, have a large dispersion which becomes even greater after correction. Since just the opposite should occur, it is concluded as mentioned above, that this data contains large random errors and is not useful in reaching any meaningful conclusions. The data obtained on the following two nights is quite useful, however. After correction, each



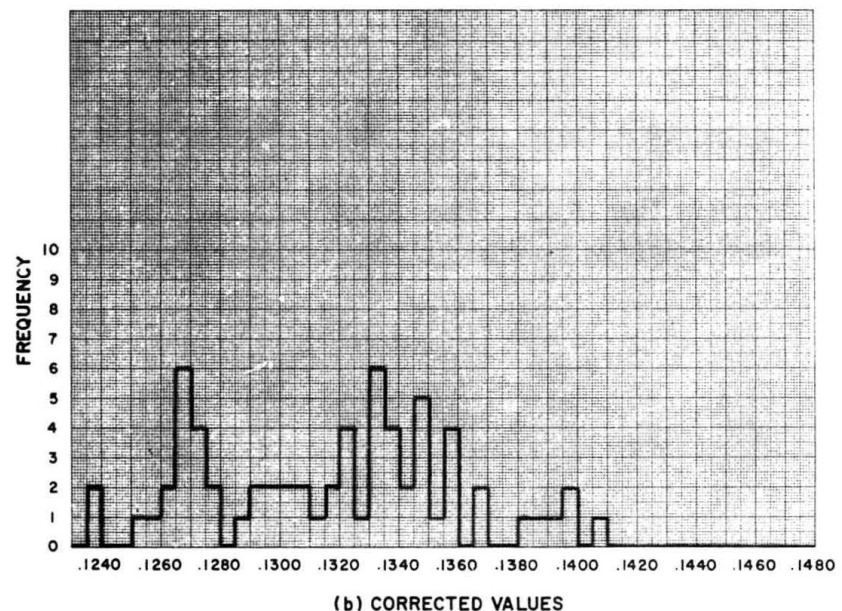
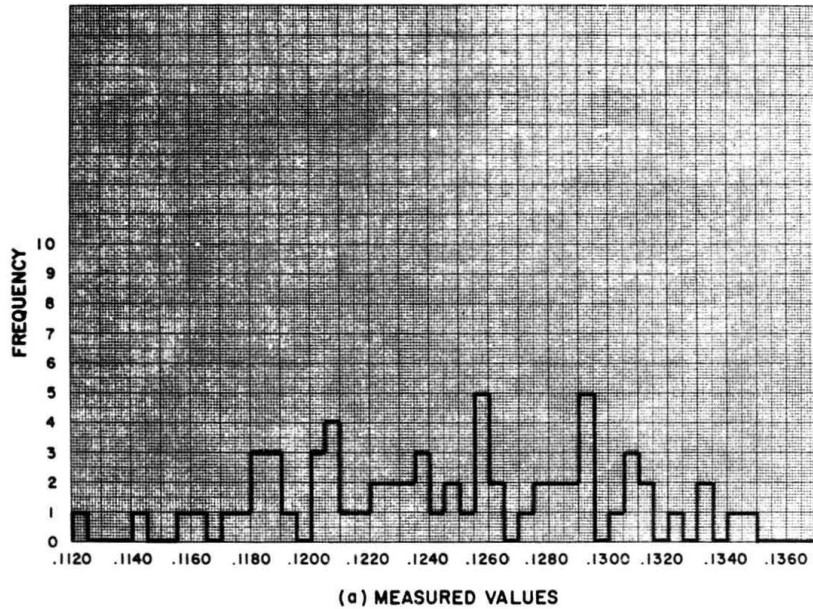
(a) MEASURED VALUES



(b) CORRECTED VALUES

NOTE:
ABSCISSAS ARE IN FEET
BEYOND 1640 FEET

Figure 7-8 Histograms for Distance Measurements Made September 14, 1967



NOTE
ABSCISSAS ARE IN FEET BEYOND
1640 FEET

Figure 7-9 Histograms for Distance Measurements Made September 15, 1967

set has a rather well-behaved distribution with a standard deviation of approximately 0.0041 ft. which is 2.5 parts in 10^6 for the 1640 ft. baseline. The range of the corrected lengths for each set is given in Table 7-14 where it is seen that the dispersion is just about what would be expected from an instrument having an accuracy of ± 0.01 ft. (± 6 ppm.) There is a discrepancy, however, in the average of the corrected lengths for the two experiment periods. That is, while the values of corrected length for the 14th and 15th are clustered around particular points with reasonable standard deviations, the centers of the distributions (Average Corrected Length) for the two nights are separated by 0.0107 ft. Effectively, data collected on September 14 indicates that the distance being measured was 0.0107 ft. (0.128 inches) shorter than the distance measured on September 15. This is equivalent to 6.5 parts per million and none of those participating in the experiments can provide an explanation for such a result. When one looks at the temperature data, for the two nights he finds that there were some significant differences, however. For example, at the beginning of the experiment period and in the vicinity of the Geodolite, the temperature was approximately 13°C on September 14th and 19°C on September 15th. An initial calibration of the instrument is made at this time and place. This author, however, does not see any way in which these different calibration conditions can explain the difference in the centers of the point distributions.

Of course, it is possible that the length of the line did change. Since the geodolite was moved between the two measuring periods and a cover was placed over the reflecting prisms, either one or both could have moved a total of 0.128 inches. Also, since three reflecting prisms were used, it is possible that the geodolite alignment was such that the return from one prism dominated on September 14 while that from one of the others had the greatest effect on the 15th. These suggestions are presented only as possibilities since the source of the differences cannot be positively ascertained.

TABLE 7-14
Baseline Measurement Statistics

	<u>Sept. 14</u>	<u>Sept. 15</u>
Average Corrected Length	1640.1210 ft.	1640.1317 ft.
Deviation of Average Corrected Length from the True Value of Line Length	0.0080 ft 4.9 ppm	0.0187 ft 11.4 ppm
Maximum Corrected Length	1640.1281 ft.	1640.1405 ft.
Maximum Positive Deviation from the Average Line Length	0.0071 ft 4.3 ppm	0.0088 ft. 5.4 ppm
Minimum Corrected Length	1640.1089 ft	1640.1235 ft.
Maximum Negative Deviation from the Average Line Length	0.0121 ft. 7.4 ppm	0.0082 ft. 5.0 ppm

(5) Determining the Length of the Baseline from the Geodolite Measurements.

Because of the peculiar way in which the two sets of usable Geodimeter data were distributed, we will not combine them, but rather will determine the baseline length indicated by each set. The easiest way of doing this is merely to use the average of the corrected lengths which are presented in Table 7-14. One is led to inquire however, if a mean square fit to the data might not provide a more accurate way of interpreting the Geodimeter measurements. Therefore, it was assumed that the true distance and measured distance were related by the formula:

$$S = \left(\frac{D}{n_o} \right) \bar{n} + \epsilon \quad (7-3)$$

where S is the measured length

D is the true length

n_o is the refractive index under calibration conditions

\bar{n} is the average refractive index along the line

ϵ is the error.

We are interested in determining the value of D which will minimize the mean squared value of the error ϵ . When this is done the result is:

Date	D (minimum mean squared error)	D (average)
Sept. 14	1640.12105 ft.	1640.1210 ft.
Sept. 15	1640.13190 ft.	1640.1317 ft.

where the average value of corrected distance is included for comparison. The differences in the corresponding values are negligible.

Other attempts were made to extract more information from the recorded data. For example, the mathematical model was changed and the measured distance was represented by the equation

$$S = \left(\frac{D}{n_0} \right) \bar{n} + b + \epsilon \quad (7-4)$$

where in this case b is a constant error and ϵ is a random error. When one tries to determine both D and b such that ϵ is minimized, he obtains completely unrealistic results.

Next, Equation (7-4) was again used together with the value of D obtained in the first case above. The equation was solved to see if there was a value for b which would make the mean square value of ϵ less than that in the first case where b was set equal to zero. The values of b which were obtained from this procedure were negligibly small thereby indicating that there was no significant constant error in the data.

The mathematical model used above is based on the assumption that the error in \bar{n} is negligible when compared to the error in S . When the approach to the problem is changed and instead it is assumed that the major source of error is that in \bar{n} , the values of D calculated to minimized the mean squared errors, are within one part in 10^{10} of those presented in Table 7-15. Therefore, it is concluded that for the purpose of these experiments nothing is gained by a minimum mean square error approach and the average corrected values may as well be used.

(c) Refractive Index Determination and Temperature Sampling

Although not anticipated at the beginning of the experimental program, it has turned out that the temperature sampling data which was obtained is of considerable interest all by itself. One of the questions which always arises when highly accurate electromagnetic distance measurements are made is, "How many temperature samples along the ray path must be taken?" A similar problem usually does not occur for the air pressure and water vapor pressure parameters

because normal variations of these quantities with respect to time and space produce relatively small variations in the average refractive index. One or two measurements of each of these quantities is usually sufficient even for relatively long ray paths. This is borne out by the experimental data obtained in September where the magnitude of the variations in these quantities was such as to produce a negligible effect upon the refractive index.

Temperature, however, must be treated differently. Normal variations in temperature with respect to both time and distance can cause variations in the refractive index of many parts per million. This also is born out by the data obtained in September. For example, on the 15th the highest temperature recorded during the five hour experiment period was 19.08° and the lowest was 9.57°C . This produces a variation in refractive index of approximately nine parts per million. Also, for any given pass down the baseline, the differences in the temperature observations were often of such a magnitude as to produce a variation in the refractive index of three parts per million. It therefore becomes apparent that the temperature must be sampled at numerous points along the ray path if a highly accurate value for the average refractive index is to be obtained.

During the course of the experiment described here, thermometers were located every 25 meters along the line for a total of 21 samples in 500 meters. At the instant of each distance measurement the refractive index was calculated for each thermometer location and then an average value obtained as described earlier in this section. To determine the effect fewer temperature samples would have had on the computed average index, one merely needs to use only part of the recorded data. This sort of investigation was anticipated when the computer program was written and it is possible for the computer operator to select any desired combination of temperature samples in determining the average index. The results of using all twenty one temperature samples have already been presented in Tables 7-10, 7-11, and

7-12. For each value included in these tables, the corresponding average index was also calculated using only 11, 6, 5, 3, 2, and 1 temperature samples. The particular thermometer locations which were used for each combination are given below:

TABLE 7-15

<u>Number of Thermometers Used</u>	<u>Locations which were used</u>
11	1, 3, 5, 7, 9, 11, 13, 15, 17, 19, 21
6	1, 5, 9, 13, 17, 21
5	1, 6, 11, 16, 21
3	1, 11, 21
2	1, 21
1	1
1	21

It will be noticed that in each case the thermometers were equally spaced. The use of unequally spaced samples was considered but examination of the recorded data indicated that there seemed to be no advantage in such a procedure.

Although the Geodolite data obtained on September 13 was not useful, the atmospheric data obtained that evening was useful and therefore we have significant refractive index information for three different experiment periods. The data taken on September 12 was not used because of its limited quantity.

In analyzing the results of using fewer than 21 thermometers, it was assumed that the average refractive index values calculated using all 21 were accurate. The values obtained using fewer samples were therefore subtracted from the accurate values to determine the error which had resulted. This was done for each thermometer combination and each experiment period. The results of these subtractions are presented in Tables 7-16, 7-17, 7-18 and the histograms of Figures 7-10, 7-11 and 7-12. It will be noticed that no histograms are presented

TABLE 7-16
Refractive Index Error Data for September 13

Time	11 thermo-meters	6 thermo-meters	5 thermo-meters	3 thermo-meters	2 thermo-meters	Thermometer at position #1	Thermometer at position #21
2:06	3	- 1	18	- 4	- 30	9	- 50
2:11	4	1	18	- 6	- 29	- 20	- 62
2:14	4	2	19	- 5	- 26	- 25	- 67
2:17	3	2	15	- 8	- 30	- 36	- 51
2:21	1	5	14	- 9	- 38	. 44	- 32
2:25	- 1	6	8	- 19	- 77	- 50	- 42
2:27	- 1	4	7	- 27	- 95	- 54	- 48
2:30	- 1	4	9	- 26	- 99	- 74	- 39
2:33	- 1	4	11	- 24	- 101	- 92	- 44
2:39	- 2	4	12	- 12	- 95	- 118	- 43
2:45	- 3	- 3	19	13	- 55	- 110	- 13
2:51	- 2	- 1	3	- 11	- 73	- 128	- 44
2:58	- 2	- 4	5	- 23	- 74	- 122	- 63
3:06	- 4	- 9	- 1	- 31	- 69	- 109	- 55
3:09	- 4	- 11	- 3	- 30	- 57	- 69	- 41
3:14	- 4	- 8	- 3	- 16	- 48	- 57	- 26
3:17	- 5	- 5	- 2	- 16	- 54	- 61	- 27
3:21	- 4	- 4	- 7	- 19	- 57	- 69	- 33
3:27	- 4	4	- 10	- 30	- 72	- 91	- 52
3:29	- 5	4	- 8	- 29	- 78	- 99	- 60
3:35	- 3	1	5	- 16	- 88	- 113	- 94
3:37	0	- 1	10	- 12	- 87	- 109	- 105
3:41	5	3	14	- 9	- 78	- 95	- 119
3:45	8	10	18	- 7	- 74	- 80	- 95
3:52	8	17	21	- 6	- 71	- 58	- 58
3:55	5	20	19	- 10	- 70	- 49	- 51
3:57	3	21	18	- 10	- 64	- 37	- 53
4:01	1	17	14	- 3	- 46	- 8	- 55
4:04	3	7	18	16	- 9	14	- 32
4:07	4	- 1	24	33	32	27	- 5
4:13	4	- 4	50	63	86	88	22
4:16	2	- 6	61	66	82	102	9
4:19	4	- 6	48	71	88	126	17
4:23	- 1	- 6	47	38	88	151	21
4:26	1	- 3	50	25	82	153	15
4:30	4	5	44	11	78	151	6
4:34	2	1	32	10	87	160	11
4:37	- 3	- 7	26	11	95	164	15
4:40	- 7	- 10	24	9	99	165	15
4:44	- 12	- 15	21	8	112	184	23
4:48	- 15	- 18	19	7	122	200	50
4:57	1	- 9	38	37	113	199	45
5:00	2	- 7	43	59	118	187	- 6
5:04	- 3	2	46	77	148	194	- 7
5:07	- 7	5	55	79	183	213	17
5:15	- 8	0	55	38	159	237	138
5:19	- 7	- 5	39	13	115	245	- 74
5:23	- 7	- 11	25	- 5	94	252	- 87
5:26	- 5	- 11	16	- 12	84	257	- 90
5:30	- 3	- 8	5	- 27	71	263	- 92
5:35	- 4	- 4	- 1	- 18	87	270	- 60
5:39	- 3	- 3	- 1	- 3	105	275	- 28

TABLE 7-17
Refractive Index Error Data for September 14

Time	11 thermometers	6 thermometers	5 thermometers	3 thermometers	2 thermometers	Thermometer at position #1	Thermometer at position #21
1:11	-20	-12	22	15	22	88	-56
1:13	-18	-15	19	13	24	84	-60
1:17	-12	-13	23	19	34	96	-52
1:20	-7	-11	23	24	40	106	-49
1:24	-2	-7	19	24	47	120	-45
1:27	0	-6	14	20	50	127	-49
1:33	-4	-2	19	8	50	136	-80
1:37	-3	2	32	23	58	149	-75
1:40	2	8	43	41	68	169	-30
1:42	4	7	46	47	64	179	-10
1:45	0	2	50	46	47	184	-30
1:48	-7	-6	42	41	42	173	-38
1:51	-9	0	34	30	52	157	-31
1:55	-8	17	25	13	62	135	-3
2:04	-4	11	27	12	28	108	0
2:07	-4	1	29	22	28	100	9
2:10	-7	-10	34	34	30	93	18
2:14	-9	-16	37	38	36	87	30
2:18	-12	-10	41	36	41	81	23
2:22	-5	14	47	28	48	73	18
2:25	-1	29	48	19	50	62	7
2:28	5	34	44	4	45	53	-11
2:31	9	28	38	-17	44	65	-28
2:35	6	14	28	-37	54	91	-43
2:46	6	4	-12	-43	-81	0	-74
2:50	11	13	-21	-34	-91	12	-87
2:53	12	18	-15	-22	-81	-2	-79
2:56	10	16	-9	-13	-66	-10	-67
3:10	-2	2	30	4	39	51	-25
3:13	-4	-6	36	3	44	72	-36
3:16	-5	-14	42	1	46	87	-26
3:20	-2	-15	38	-9	42	100	-5
3:24	2	-16	37	-9	33	109	6
3:28	1	-16	49	-6	36	111	27
3:32	-1	-12	61	-3	51	107	61
3:36	1	-5	62	0	66	103	94
3:41	4	3	58	-4	67	86	108
3:45	8	14	48	-9	67	71	118
3:49	8	20	39	-2	61	52	105
3:52	6	22	32	16	61	40	95
3:56	3	16	33	22	68	14	89
3:59	3	10	33	26	54	10	66
4:09	-6	-10	45	42	39	27	48
4:14	-19	-32	34	51	87	67	69
4:18	-17	-24	16	40	127	106	105
4:22	-10	-11	3	29	134	133	108
4:26	-8	-7	-3	25	121	140	87
4:30	-7	-14	11	28	116	139	79
4:35	-6	-17	40	50	118	147	87
4:41	-7	-13	44	28	97	132	89
4:44	-9	-13	33	9	55	93	63
4:51	-4	-2	8	-5	-49	-36	-68
4:55	-3	0	6	-20	-50	-58	-99
5:19	-13	-11	17	58	-50	61	-188
5:23	-12	-8	17	58	-53	59	-204
5:26	-12	-8	13	49	-61	54	-184
5:30	-7	-4	6	37	-75	50	-137
5:34	-2	-4	1	25	-92	52	-126
5:37	0	0	0	13	-98	42	-138
5:44	-7	5	13	36	-55	-11	-108
5:48	-8	-1	25	46	-67	-28	-94

TABLE 7-18
Refractive Index Error Data for September 15

Time	11 thermometers	6 thermometers	5 thermometers	3 thermometers	2 thermometers	Thermometer at position #1	Thermometer at position #21
0:48	- 7	1	25	27	12	- 71	47
0:51	- 6	0	24	16	- 6	- 62	45
0:55	- 4	2	23	11	- 36	- 56	34
1:03	1	14	11	21	- 32	- 73	15
1:06	2	15	18	24	- 21	- 83	- 6
1:09	1	11	29	17	- 8	- 80	- 24
1:12	1	7	30	16	0	- 78	- 14
1:17	- 5	- 1	18	19	- 22	- 32	- 29
1:20	- 5	- 3	12	16	- 42	- 26	- 40
1:24	- 6	- 5	2	12	- 61	- 48	- 42
1:28	- 4	- 4	- 4	7	- 70	- 59	- 36
1:31	- 2	1	- 10	- 3	- 76	- 68	- 32
1:35	2	10	- 11	- 7	- 68	- 72	- 47
1:39	3	15	- 3	- 2	- 45	- 70	- 38
1:42	3	11	5	5	- 27	- 67	- 21
1:45	3	6	6	1	- 32	- 65	- 27
1:48	6	3	1	- 15	- 52	- 65	- 47
1:52	5	3	9	- 21	- 67	- 63	- 64
1:56	2	1	15	- 23	- 79	- 84	- 77
2:00	0	0	21	- 20	- 79	- 83	- 71
2:06	0	1	4	- 22	- 81	- 84	- 63
2:10	0	- 2	- 9	- 28	- 80	- 82	- 57
2:13	- 1	- 2	- 17	- 26	- 68	- 74	- 45
2:16	- 1	- 2	- 18	- 23	- 52	- 63	- 30
2:19	0	- 1	- 15	- 10	- 36	- 54	- 16
2:23	1	- 1	- 5	2	- 20	- 43	- 18
2:26	2	- 2	1	9	- 11	- 34	- 27
2:29	3	- 2	5	3	0	- 21	- 25
2:32	5	0	0	7	13	- 6	- 2
2:35	2	- 5	- 5	10	6	14	- 1
2:39	- 1	- 8	- 4	0	- 17	6	- 17
2:42	- 2	- 9	- 1	- 4	- 27	- 10	- 26
2:46	- 2	- 8	- 1	- 17	- 44	- 35	- 42
2:49	- 1	- 5	- 2	- 23	- 53	- 50	- 50
3:06	- 5	3	- 4	- 39	- 78	- 88	- 79
3:09	- 4	4	3	- 35	- 66	- 84	- 84
3:12	- 3	4	11	- 29	- 58	- 83	- 78
3:23	6	20	0	- 8	- 47	- 28	- 49
3:27	6	17	- 3	- 7	- 54	- 38	- 43
3:43	3	8	- 9	- 23	- 104	- 118	- 47
3:47	2	8	- 11	- 24	- 99	- 135	- 49
3:51	1	5	- 5	- 28	- 90	- 137	- 64
3:55	0	1	9	- 18	- 90	- 148	- 88
4:01	- 4	9	33	- 5	- 99	- 128	- 101
4:04	- 4	14	35	- 5	- 102	- 105	- 106
4:08	- 2	17	29	- 4	- 94	- 96	- 103
4:12	- 1	21	24	- 4	- 94	- 92	- 109
4:16	- 2	26	18	- 3	- 90	- 85	- 115
4:19	0	27	11	- 5	- 89	- 83	- 121
4:23	- 2	24	1	- 8	- 89	- 79	- 132
4:32	- 3	0	- 7	- 10	- 93	- 57	- 151
4:35	- 1	- 2	0	- 11	- 98	- 53	- 144
4:38	5	7	9	- 1	- 93	- 42	- 118
4:43	9	5	23	13	- 69	- 11	- 70
4:46	7	- 5	31	29	- 37	6	- 41
4:49	2	- 10	33	35	0	17	- 6
4:53	1	- 7	35	36	39	40	31
4:57	2	- 7	33	31	62	66	54
5:08	2	0	43	49	127	125	110
5:11	2	3	49	58	132	140	126
5:15	2	7	57	65	141	148	127
5:23	- 5	12	56	69	146	152	132
5:26	- 10	- 3	50	66	143	153	135
5:30	- 12	- 11	35	47	136	154	138
5:35	- 11	- 2	34	30	131	148	147

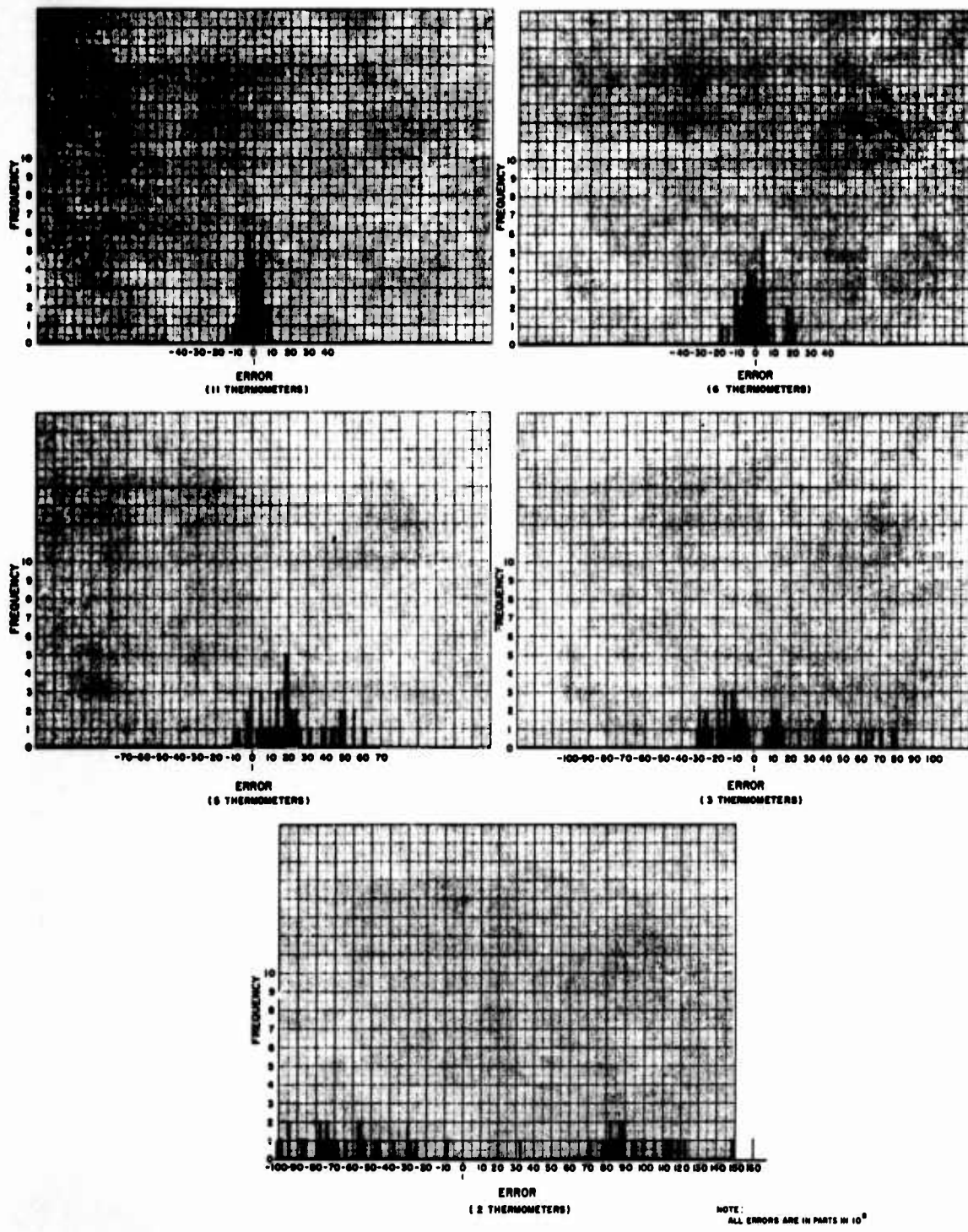


Figure 7-10 Histograms of September 13 Refractive Index Errors

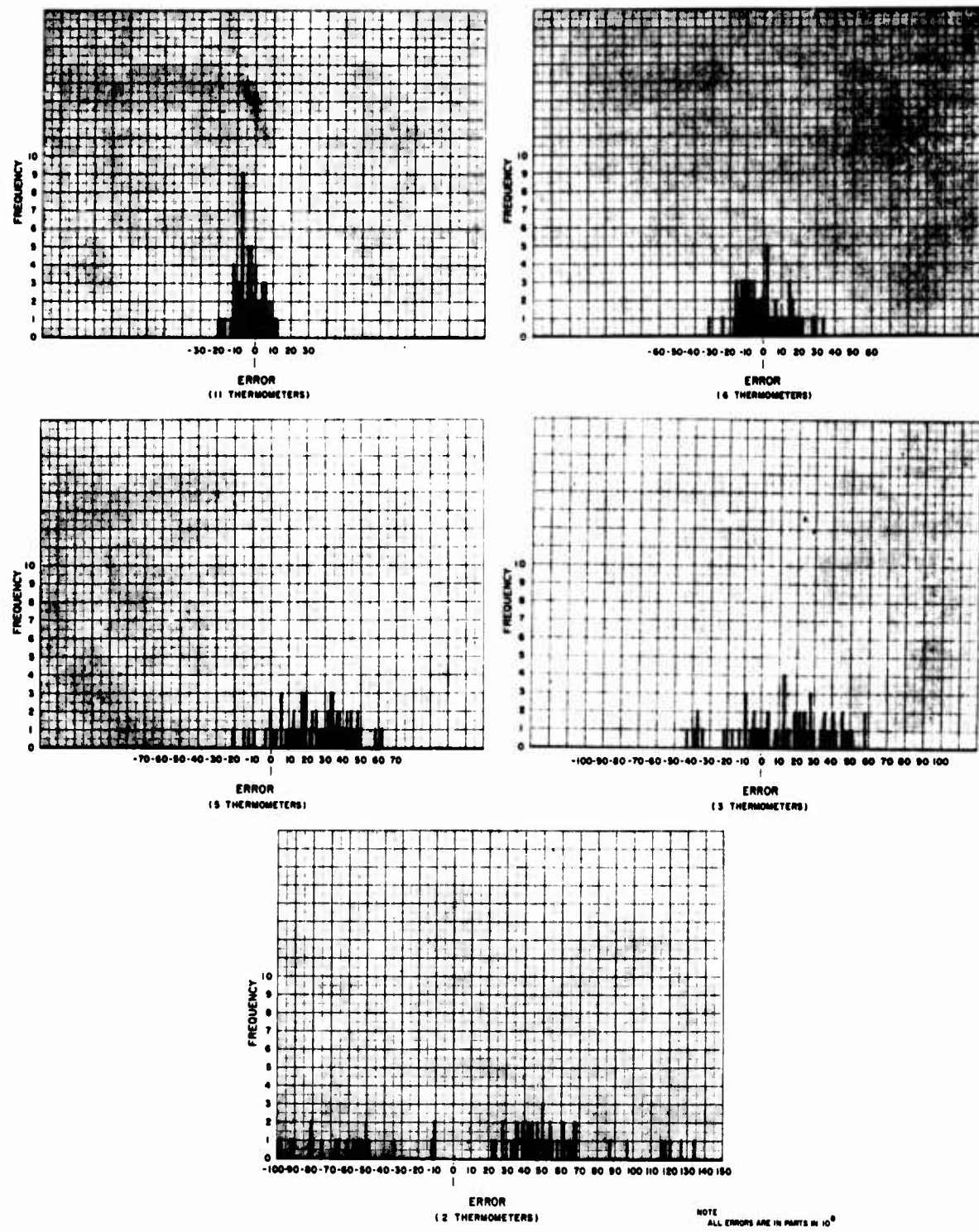


Figure 7-11 Histograms of September 14 Refractive Index Errors

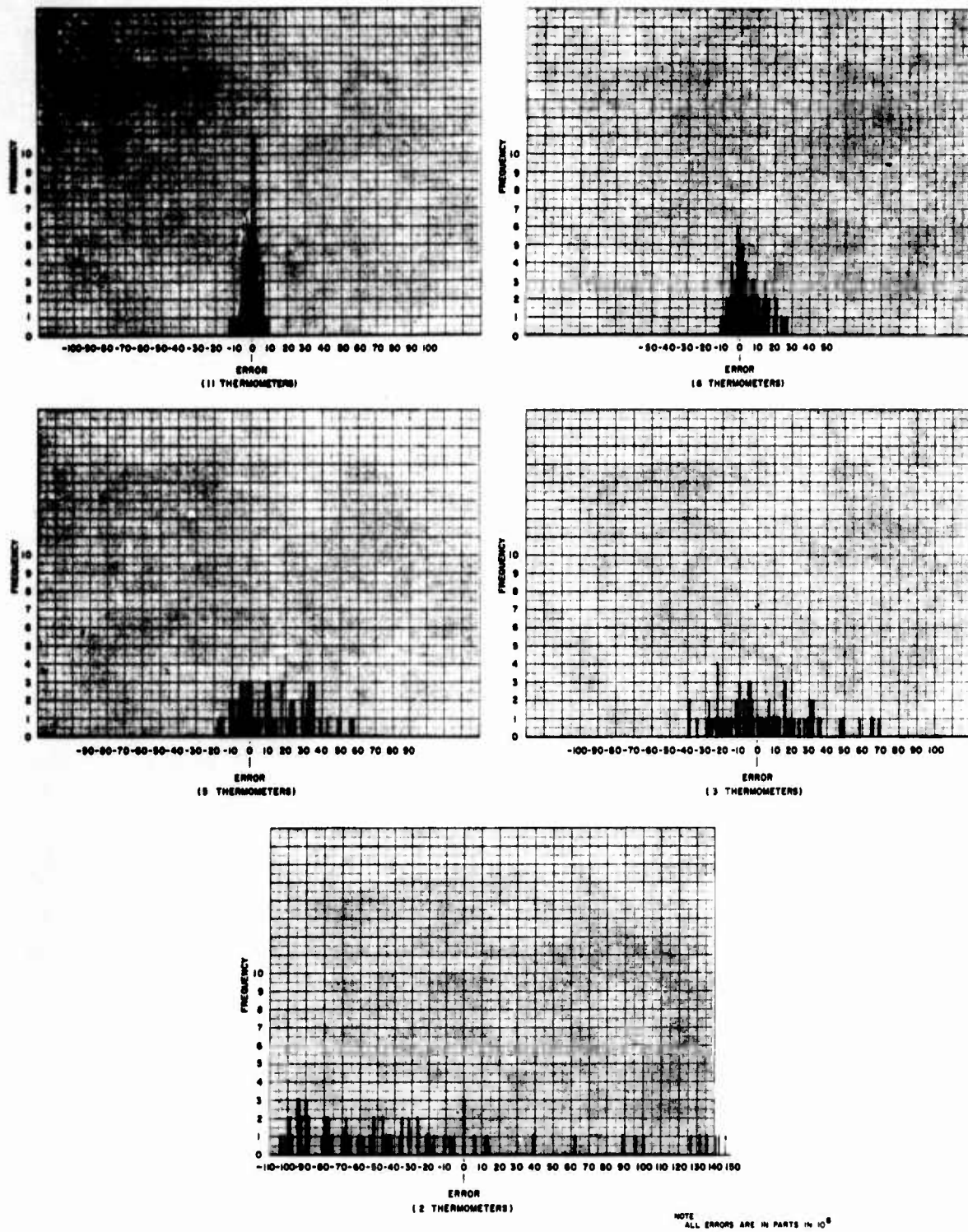


Figure 7-12 Histograms of September 15 Refractive Index Errors

for a single thermometer at positions 1 or 21. Instead, the errors for these situations are plotted as a function of time in Figures 7-13, 7-14, and 7-15.

It also was deemed desirable to obtain a numerical measure of the sort of error that had resulted from increasing the spacing of the temperature samples. Therefore, the average and standard deviation of each error distribution was computed. The results are presented in Table 7-19.

TABLE 7-19
Average and Standard Deviation of the Errors in Refractive Index

	Sept. 13	Sept. 14	Sept. 15
11 Thermometers Avg.	-1.1×10^{-8}	-3.3×10^{-8}	-0.4×10^{-8}
σ	4.7×10^{-8}	7.3×10^{-8}	4.1×10^{-8}
6 Thermometers Avg.	-0.6×10^{-8}	-1.0×10^{-8}	3.6×10^{-8}
σ	8.1×10^{-8}	13.6×10^{-8}	8.8×10^{-8}
5 Thermometers Avg.	19.8×10^{-8}	27.1×10^{-8}	12.0×10^{-8}
σ	18.3×10^{-8}	18.7×10^{-8}	18.6×10^{-8}
3 Thermometers Avg.	3.9×10^{-8}	16.7×10^{-8}	3.7×10^{-8}
σ	29.5×10^{-8}	23.6×10^{-8}	25.1×10^{-8}
2 Thermometers Avg.	9.3×10^{-8}	28.3×10^{-8}	-30.1×10^{-8}
σ	86.2×10^{-8}	58.8×10^{-8}	68.4×10^{-8}
Single Thermometer at Position #1			
Avg.	44.1×10^{-8}	80.3×10^{-8}	-36.6×10^{-8}
σ	135.3×10^{-8}	54.6×10^{-8}	74.6×10^{-8}
Maximum Positive Error	275×10^{-8}	184×10^{-8}	154×10^{-8}
Maximum Negative Error	128×10^{-8}	58×10^{-8}	148×10^{-8}
Single Thermometer at Position #21			
Avg.	-34.1×10^{-8}	-13.5×10^{-8}	-27.6×10^{-8}
σ	39.6×10^{-8}	79.6×10^{-8}	70.2×10^{-8}
Maximum Positive Error	50×10^{-8}	118×10^{-8}	147×10^{-8}
Maximum Negative Error	119×10^{-8}	204×10^{-8}	151×10^{-8}

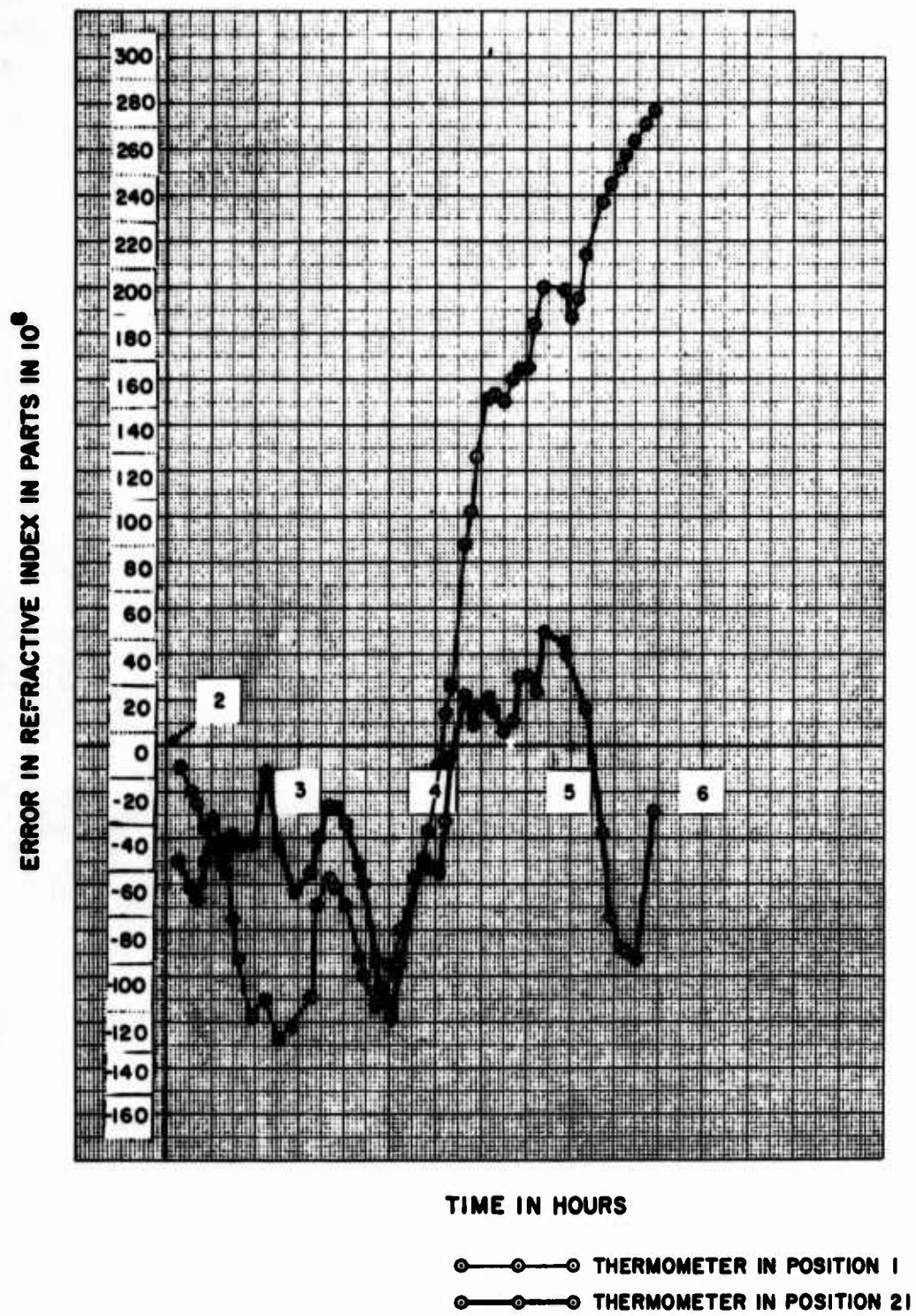


Figure 7-13 Errors in Average Refractive Index as a Function of Time for September 13 Data

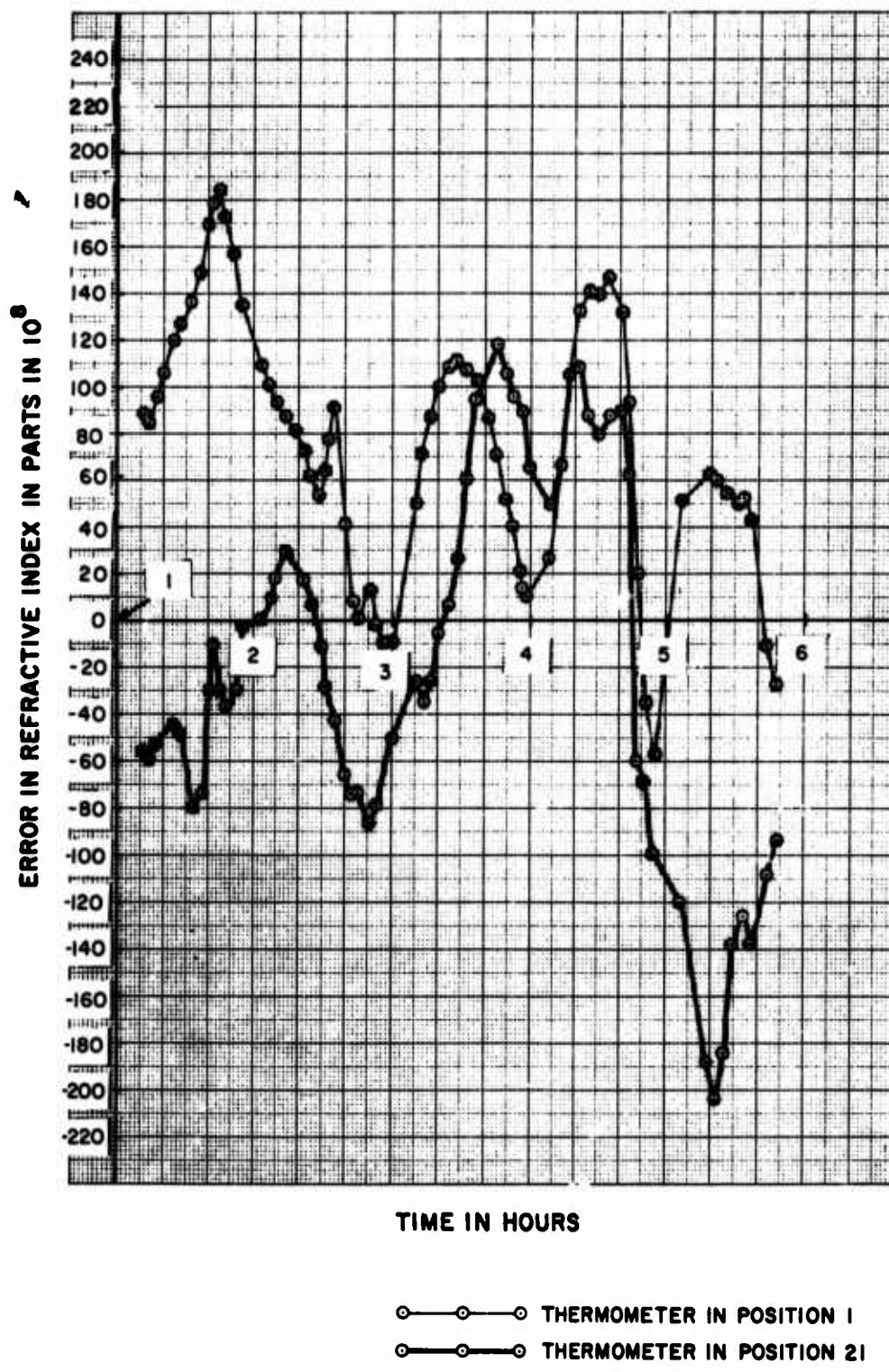


Figure 7-14 Errors in Average Refractive Index as a Function of Time for September 14 Data

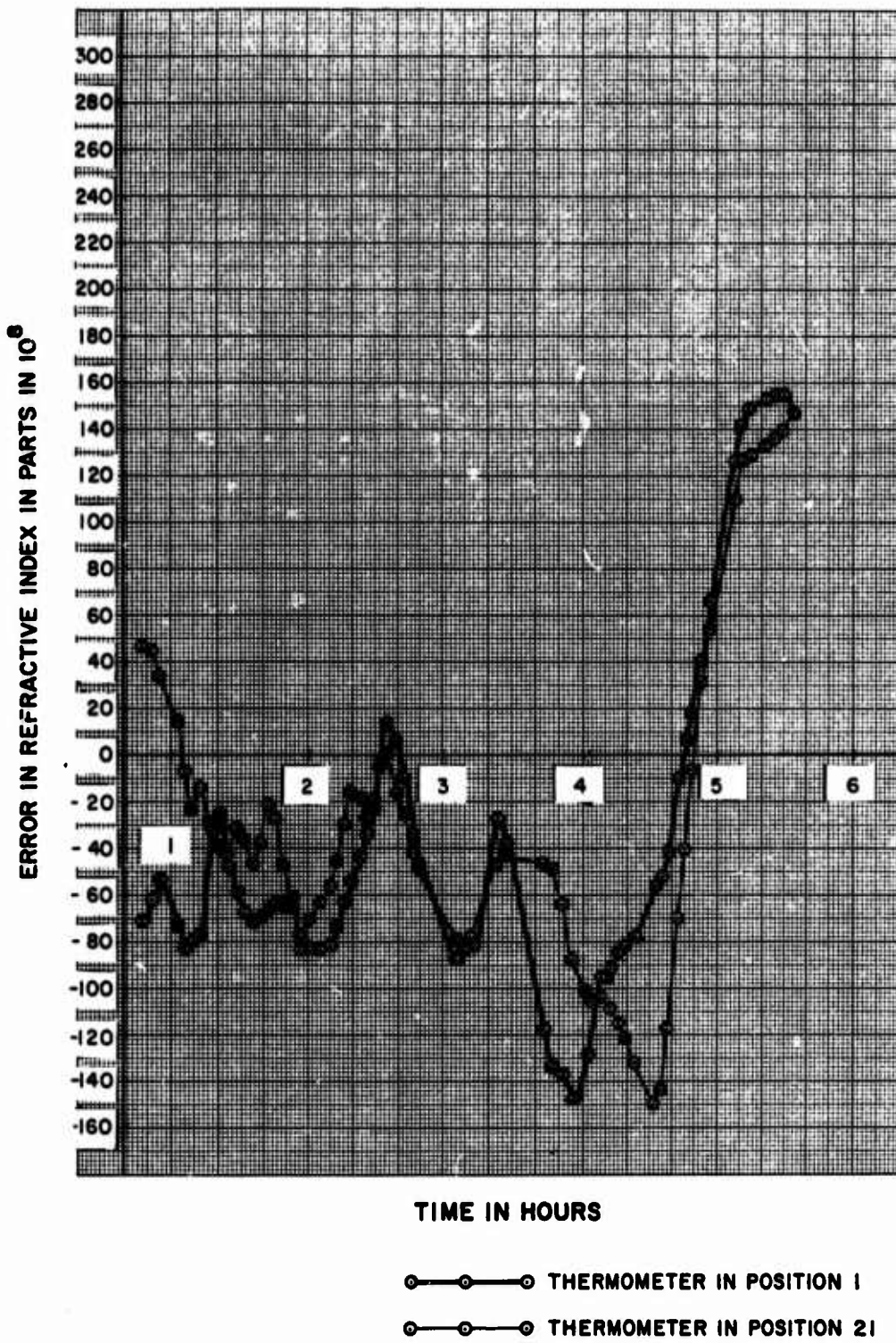


Figure 7-15 Errors in Average Refractive Index as a Function of Time
for September 15 Data

On the basis of the data provided by these tables and histograms a number of conclusions can be reached. First, it is clearly evident that the fewer the thermometers, the larger the error in the calculated average refractive index along the baseline. The use of 11 thermometers produced an error which was always less than 20 parts in 10^8 . The use of 6 thermometers produced errors of less than 40 parts in 10^8 . The use of only three thermometers produced errors which were never greater than 80 parts in 10^8 (0.8 parts in 10^6). These are the worst case values, and the histograms show that most of the values calculated using the respective thermometer combinations were considerably less in error.

If the increase in error with respect to decrease in the number of temperature samples is extrapolated in the reverse direction it is found that the use of 21 thermometers should produce a value of average refractive index along the line which is never in error, relative to the true value, by as much as 10 parts in 10^8 . For a series of measurements taken over a relatively long period of time and favorable atmospheric conditions, the average error is probably less than two or three parts in 10^8 . Therefore, the contribution to the error in a distance measurement, resulting from an error in the determination of the average refractive index along the ray path, can be made relatively small if enough temperature samples are taken.

If an average refractive index accuracy of one part in 10^6 had been required, then thermometers located only at positions 1, 11 and 21 would have been sufficient. If only two thermometers had been used, at position #1 and # 21, the maximum error would have been 1.83 parts in 10^6 and a significant number of cases would have been in error by more than one part in 10^6 .

When a single thermometer at one end of the baseline is used, the accuracy is degraded even further. The errors for several such cases are plotted in Figures 7-13, 7-14, and 7-15. The maximum error in average refractive index for these cases was 2.76 parts in

10^6 . The plots show that not only is the error relatively large much of the time, but that it remains a monotonic function for rather long periods. This characteristic also occurs when more thermometers are used as shown in Figure 7-16 where the errors for the three and the five thermometer combinations are plotted. The plots indicate that the magnitudes of the errors in these cases are smaller than the corresponding single thermometer situations, but that they vary with respect to time in much the same way. These results indicate that although the average error for a large number of calculations may be relatively small, one cannot be sure that a few calculations made over a short period will not have a relatively large error. For example, consider the case of a single thermometer at position # 21 on September 14. The average error for the entire experiment period was 13.5 parts in 10^6 , and yet if measurements were made during the one hour period from 12:50 to 1:50 AM (4:50 to 5:50 on Figure 7-14) the average error in the calculated average refracted index would have been approximately 130 parts in 10^8 or ten times as great. It is therefore concluded that a trade-off can be made between the number of temperature samples made along a ray path and the length of the time interval over which it is repeatedly measured. If many temperature samples are taken, then a relatively few length measurements made over a relatively short period of time may be sufficient. If fewer temperature observations are made, more length measurements should be made over a longer period of time.

The errors plotted in Figures 7-13, 7-14, and 7-15 can be related to the temperature data presented in Tables 7-6, 7-7 and 7-8 when it is recognized that the refractive index and temperature at a point are related in a reciprocal way. When the corresponding data of September 15 is compared, it is found that at the beginning of the evening, the temperature at thermometer # 1 was considerably above the average along the line while that at position # 21 was considerably below the average. At the end of the experiment period,

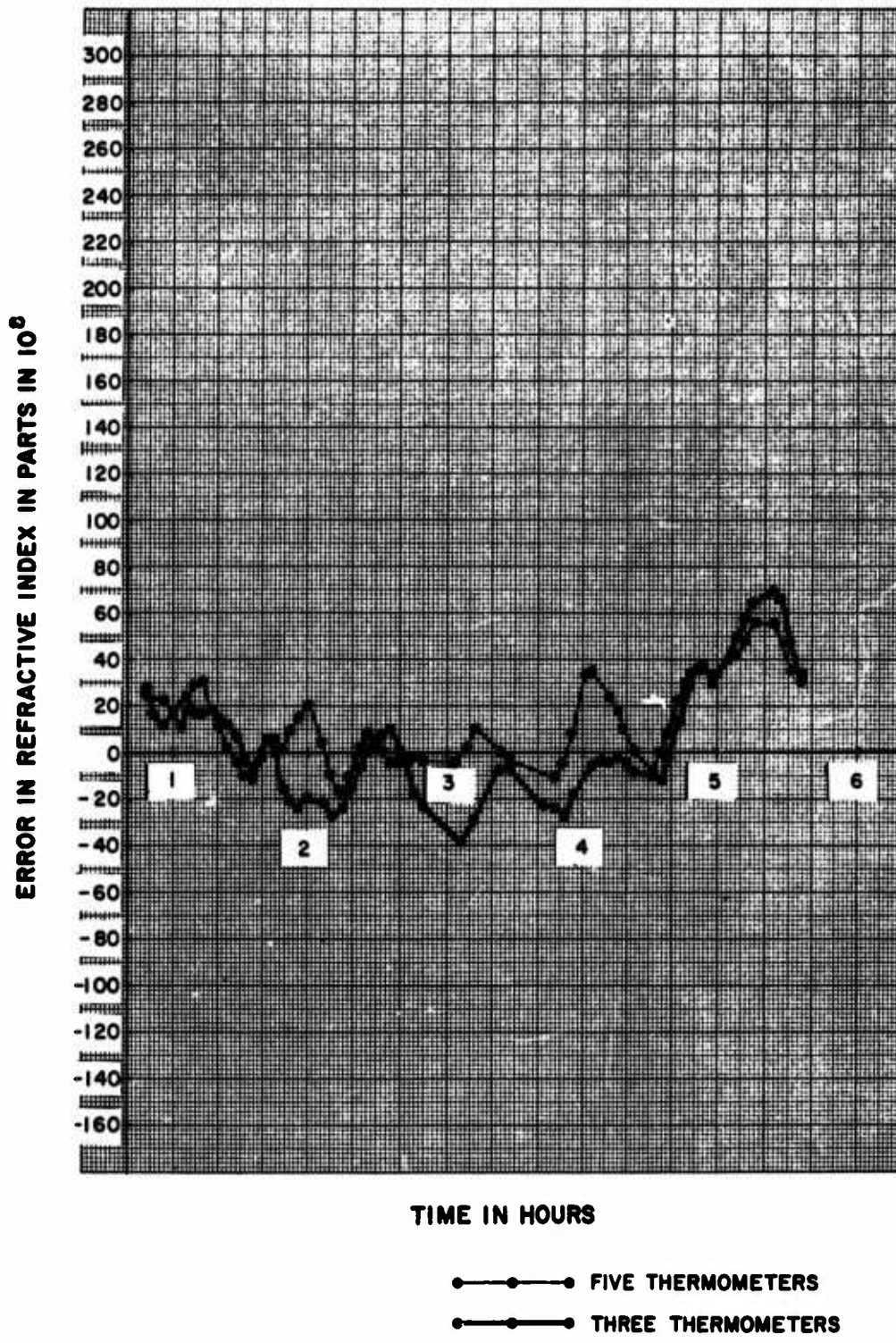


Figure 7-16 Errors in Average Refractive Index as a function of Time for Three and Five Thermometer Combinations--September 15, 1967

the temperature at both locations was significantly below the average for the line. This is reflected in the plots of Figure 7-15 where at the beginning of the experiment period, the error in refractive index, calculated using only the #1 position temperature data, is -72 parts in 10^8 while that obtained using only the #21 position data is +47 parts in 10^8 . At the end of the experiment period the error is approximately +145 parts in 10^8 for both thermometer positions.

The results for all three nights indicate that relatively small masses of air were moving along the line in such a way that relatively large temperature differences existed simultaneously at the various thermometers. When a warm mass of air was in the vicinity of a given thermometer, the refractive index at this point was significantly below the average for the entire ray path. When a cool air mass was around the thermometer, just the opposite occurred.

If an average refractive index error less than one part in 10^6 is required in all cases then at least three thermometers are required. If one part in 10^7 is desired then one should use six thermometers and take many measurements over a relatively long period of time or use eleven thermometers and take the average of several measurements. Of course, these errors are relative to the index values obtained using 21 temperature samples. It was pointed out above that the 21 sample case is probably in error by two or three parts in 10^8 .

The data presented here applies to the 500 meter Mansfield baseline for the evenings of September 13-15, 1967, and no completely general conclusions can be drawn on the basis of such a small amount of information. It does seem reasonable, however, that many of the conclusions would apply to other baselines, which are in reasonably homogeneous environments, when the weather conditions are not too unfavorable for the making of electromagnetic distance measurements. The results certainly shed some doubt on

the claims of some electromagnetic distance measuring equipment manufacturers, that their devices are accurate to one part in 10^6 when only one temperature measurement is made along the ray path.

When baselines longer than 500 meters are considered, it seems that more thermometers would be required to maintain a given level of accuracy. This author does not think, however, that the number of thermometers required is a linear function of baseline length. It is likely that a smaller number than that indicated by a linear extrapolation will provide a given desired level of accuracy.

APPENDIX A

RANGE AND ANGLE CALIBRATION FACILITY STUDY

SITE EVALUATION REPORT

CHASE LAKE SITE

Prepared by

**Dr. Ernest H. Muller
Professor of Geology at Syracuse University**

for

**Syracuse University Research Corporation
Special Projects Laboratory
December, 1967**

1. INTRODUCTION

a. Location of Area

This appendix describes geologic and environmental conditions that bear on the suitability of a site near Chase Lake in the Black River Valley, 36 miles north of Rome, for development of a Range and Angle Calibration Facility satisfying basic requirements presented in RADC purchase request number A-6-1621 dated 25 October 1965.

The Chase Lake Site (Figure A-1) is located in the towns of Greig and Watson, in Lewis County, at $43^{\circ} 45' N$, $75^{\circ} 17' W$ approximately 10 miles east-southeast of Lowville. The southwestern edge of the area under specific consideration is 4 miles east-northeast of Glenfield and a similar distance northeast of Greig.

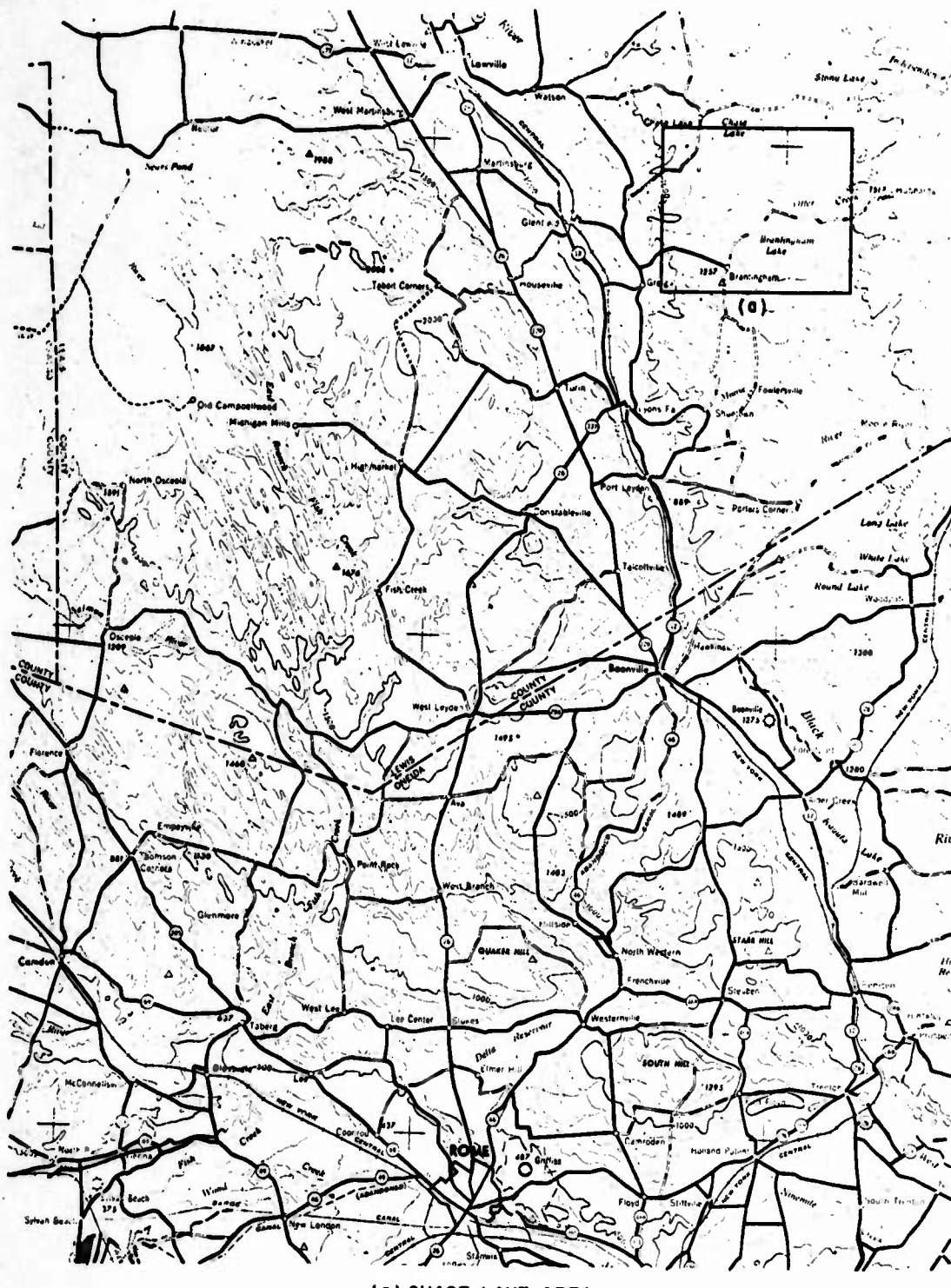
b. Site Evaluation Criteria

As listed in the body of this report, site evaluation criteria employed in the present study are as follows:

Site Requirements

- (1) Location within 50 miles of Rome.
- (2) The baseline must be capable of expansion to 2.5 miles in length if it is not constructed this long initially.
- (3) The terrain must be flat or capable of being graded to a flat condition. It does not necessarily have to be level and a small slope can be tolerated.
- (4) The area surrounding the baseline should be homogeneous; forested if possible.
- (5) The surface layer of the soil and existing vegetation should be of such a character, that large daily changes in surface temperature do not take place.
- (6) The area must be remote from sources of vibration, extreme electromagnetic interference, fog and industrial air pollution.

GRAPHIC NOT REPRODUCIBLE



(a) CHASE LAKE AREA

Figure A-1 Location Map Showing Topography and Highway Net Between Chase Lake Area and Rome

- (7) The ground must be geologically stable, preferably consisting of gravel or coarse grain sand to a depth of 20 or 30 meters. The area must be well-drained with the local water table well below the surface.
- (8) The line should run in the direction of the prevailing winds.

c. Background

Initial efforts toward location of one or more sites suitable for establishment of a Range and Angle Calibration Facility were localized in close proximity to Rome. Potential sites were sought on the Rome Sand Plain, along the right of way of the abandoned New York, Ontario and Western Railroad, and near Camden. Particular attention was directed to an area directly northwest of the RADC Camden Test Annex. When all sites near Rome proved unsuitable for one reason or another, the radius of search was extended and attention was directed to the "sand plains" bordering the Black River Valley on the east.

Two sites on the Black River "sand plains" were singled out for further study following mid-winter reconnaissance visits by Dr. Richardson and Mr. Robert Cracknell of RADC. Because of its proximity to the Forestport Loran Tower, a site in the towns of Forestport and Ohio (North Wilmurt 7-1/2' topographic map, U.S.G.S. 1:24,000 series) was given careful attention during the course of several subsequent visits. Topographically, the Forestport site was deemed less suitable than a second site, the Chase Lake site, farther north on the "sand plains."

In terms of all criteria except proximity to Rome and lack of homogeneous forest cover, the Chase Lake site is considered the most suitable location evaluated in the present studies.

d. Sources of Information

Following the preliminary midwinter reconnaissance, the Chase Lake Site was revisited on 6 June 1967 by Richardson, Cracknell and the writer. It was subsequently examined on several occasions by Richardson and the writer independently.

Certain aspects of the geology of the Chase Lake area are discussed in the following published works:

Broughton, John G., et al., 1961, Geological Map of New York. Map and Chart Series No. 5, New York State Museum and Science Service, Albany.

Buddington, A. F., 1934, Geology and Mineral Resources of the Hammond, Antwerp and Lowville Quadrangles. New York State Museum Bull. 296, 251 p.

Fairchild, H. L., 1912, The Glacial Waters in the Black and Mohawk Valleys. New York State Museum Bull. 160, 47 p.

Hanefeld, Horst, 1960, Die Glaziale Umgestaltung der Schichtstufenlandschaft am Nordrand der Alleghenies. Schriften des Geographischen Instituts, Kiel University, Kiel, Germany, 170 p.

Miller, W. J., 1910, Geology of the Port Leyden Quadrangle, Lewis County, New York. New York State Museum Bull. 135, 61 p.

Taylor, F. B., 1924, Moraines of the St. Lawrence Valley; Jour. Geol. 32:641-667.

The Chase Lake Site is in the southeastern corner of the Lowville quadrangle and the northeastern corner of the Port Leyden quadrangle of the U.S. Geological Survey 1:62,500 topographic map series. Because these sheets date from surveys of 1910-1911 and 1904-1905, respectively, the culture is partly outdated and the maps are less accurate than recent maps based on air photography. The

area has not yet been covered by the current U. S. Geological Survey 1 : 24,000 map series.

2. GEOLOGY

a. Physiographic Relationships

The Chase Lake Site is located on the eastern margin of the Black River Valley bordering the low western foot-hills of the Adirondack Mountains. Beneath a cover of Pleistocene sediments, Adirondack Mountain structures and metamorphic rocks pass beneath Paleozoic strata exposed in the Black River Valley about 4 miles west of the site. Topographically, the area may be considered part of the Black River Valley, but in terms of the underlying rock structure it is more closely related to the adjacent Adirondack Province.

The Black River occupies a structurally-controlled, glacially-scoured trough along the western margin of the Adirondacks. Paleozoic sedimentary strata, deposited under marine conditions were subsequently domed as a result of Adirondack mountain-building. Subsequent denudation stripped sedimentary cover from most of the Adirondack dome, leaving the strata truncated in a peripheral ring dipping gently away from the center of the uplift. The oldest and lowermost beds are exposed against the metamorphic and igneous rocks that comprise the Adirondack massif, whereas younger strata crop out at greater distance from the crystalline rocks of the Adirondacks.

Because the lowest exposed strata in the Paleozoic sequence flanking the Adirondacks are relatively non-resistant carbonate rocks, they have been deeply eroded first by running water and subsequently by glaciation. It is through this trough between the crystalline rocks of the Adirondacks and the elastic sediments capping the

Tug Hill that the Black River flows northward before curving westward to Lake Ontario. In the latitude of Lowville, only crystalline rocks are exposed on the east side of the Black River Valley.

b. Precambrian Geology

Precambrian crystalline rocks are only locally exposed on knobs, eroded slopes and in stream courses, but are also continuously presented beneath the cover of unconsolidated sediments which comprise Map Unit 1 (Figure A-2). The crystalline rocks comprise parts of the Adirondack massif that was formed more than a billion years ago under high confining pressures and temperatures at considerable depth within the crust. Rocks that covered them were subsequently removed by erosion before the beginning of Paleozoic sedimentation.

The most widespread rock type beneath the sedimentary cover is hornblende-bearing granitic gneiss. This rock is typically composed of perthitic feldspar comprising 60 to 80% of the rock, quartz 15 to 30%, plagioclase 0 to 19% with minor hornblende (Miller, 1910). It is uniformly coarse textured and relatively uniform in composition. Where quartz is essentially lacking the rock is mapped as syenitic gneiss. Where hornblende is the dominant mineral the rock is mapped as amphibolite.

Garnetiferous sillimanite gneiss that crops out west of Chase Lake indicates the high rank of metamorphism to which these rocks were subjected. These rocks (Map Unit 7) are referred to as paragneiss to indicate the apparent sedimentary nature of the parent rocks prior to metamorphism. Although the nature of the parent rocks is less conclusive for some of the other map units, their conformability and lack of cross-cutting relationships suggests that most of the rocks in the Chase Lake area are metasedimentary in origin.

KEY TO FIGURE A-2*

Map Unit	Identification
1	Glacial and alluvial deposits concealing underlying geology. See Figure A-3.
2	Pyroxene-Hornblende syenitic gneiss.
3	Hornblende granitic gneiss.
4	Pyroxene-hornblende granitic gneiss.
5	Leucogranitic gneiss, biotitic and hornblende-bearing in part.
6	Interlayered amphibolite and granitic, charnockitic or syenitic gneiss.
7	Quartz-feldspar paragneiss with variable amounts of garnet, sillimanite, biotite.
8	Amphibolite, commonly biotitic

* after Broughton, et al., 1961.

A5343

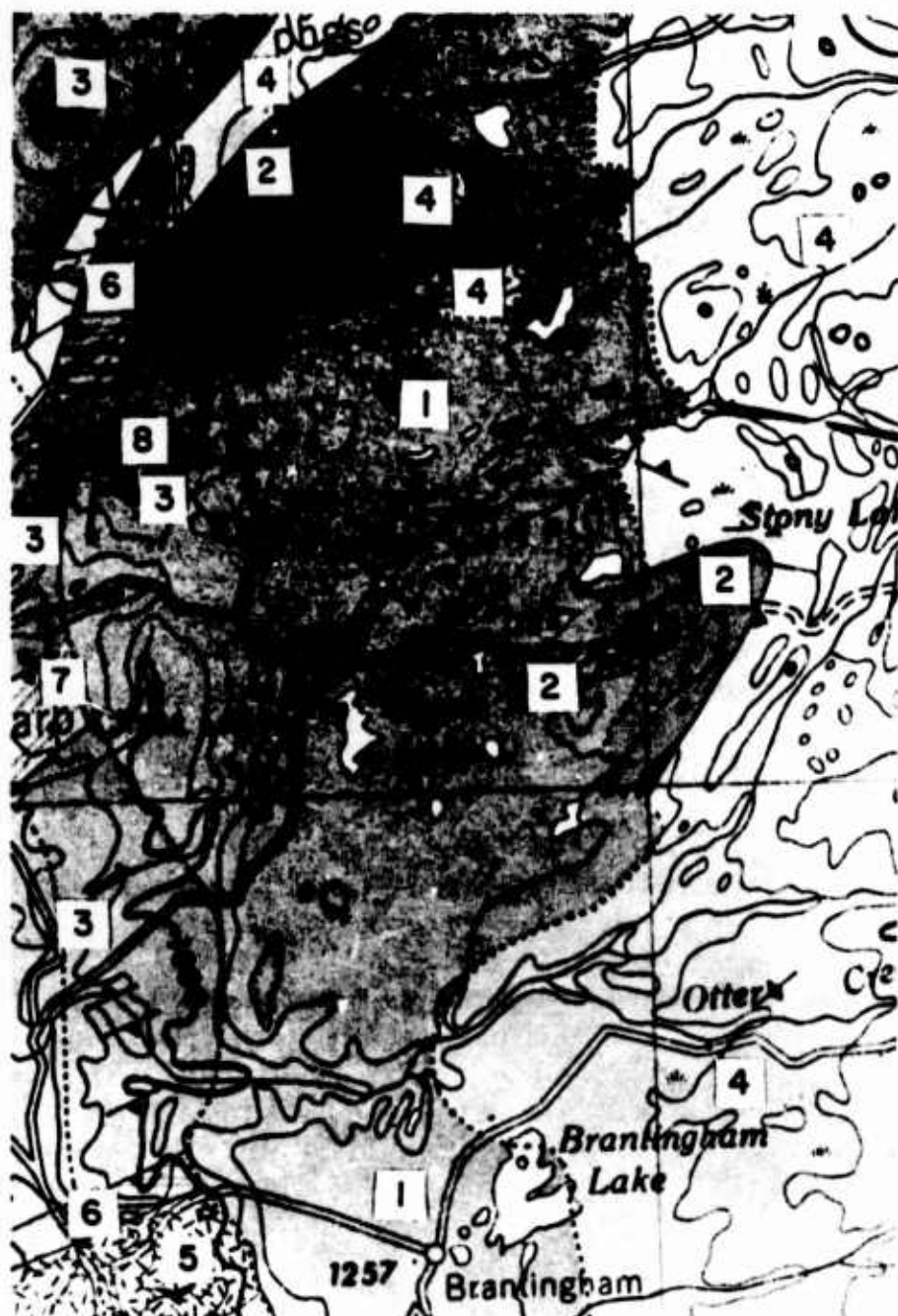


Figure A-2 Geology of Chase Lake Area

The planes of foliation that characterize these gneissic rocks are oriented generally with northeasterly strike (e.g. N60E across the street from the church in Greig) with steep angles of dip. Buddington infers the existence of an anticlinal axis trending northeast beneath the Chase Lake area on the basis of measured foliation attitudes.

c. Bedrock Topography

The contrast between gneissic Adirondack rocks and the compacted but unmetamorphosed sedimentary rocks that lie upon them west of the Black River indicates that a great thickness of rocks must have been eroded before Paleozoic sedimentation began. In places outside of the Chase Lake map area, the surface of the crystalline rocks directly beneath overlying sediments is deeply weathered and the surface of contact possesses very low relief. This has been interpreted as evidence that the Precambrian rocks were peneplaned, or eroded essentially to base level before being covered by sediments deposited in Paleozoic seas.

Subsequent denudation that initiated the Black River Valley as a topographic feature stripped the Paleozoic sediments east of the river and exhumed the once-buried Precambrian surface. Subsequent stream dissection and glacial scour of projecting knobs produced an irregular surface on the crystalline rocks which was once again buried by sediments deposited during deglaciation. In the absence of seismic profiles to detail the buried bedrock topography, an assumption of regional westward slope with minor irregularities and relief of one hundred feet or more may be utilized for an approximation of the thickness of unconsolidated drift in the Chase Lake area.

d. Glacial Geology

Most of the unconsolidated drift and the principle topographic features of the Chase Lake area were produced about 12,000 years ago

during melting of the last ice sheet, late in the Port Huron substage of Wisconsin glaciation.

At that time, glacial meltwaters impounded between the wasting ice margin and higher land of the Adirondack foot-hills and the Tug Hill Plateau formed a pro-glacial lake in the Black River Valley. Initially draining southward over stagnant debris-covered ice into the headwaters of West Canada Creek near Remsen, this lake was short-lived and limited in extent. Referred to as Forestport Lake (Fairchild, 1912), this stage ceased to exist as such when the retreating ice margin exposed a lower outlet southwest into the Lansing Kill near Booneville.

The Lansing Kill outlet controlled the level of impounded waters in the Black River Valley long enough for development of extensive terrace deposits aggraded approximately to the level of the threshold southwest of Booneville. Along the east side of the Black River Valley, the receding ice margin in the latitude of Port Leyden and Lowville trended north-northeast to south-southwest. As a result, a long arm of the so-called Port Leyden Lake (Fairchild, 1912, Buddington, 1934) spread northward between the receding ice margin and the Adirondack foot-hills. It was into this lake that the sand plains of which the Chase Lake area is a part were deposited. Deposition appears to have been partly as a complex delta deposited primarily by streams draining the ice-free Adirondack foot-hills, and also by streams flowing from the surface of the glacier. The lack of surface channels suggests that accumulation of the sand plain took place not primarily by subaerial distribution of outwash, but rather by lacustrine sedimentation.

Successive positions of the receding ice margin are interpretable from ill-defined and discontinuous moraine remnants. One such moraine, the Dicob moraine (Buddington, 1934) accounts for the abrupt southward deflection of Independence River about a mile west

of Sperryville, south to Donnattsburg (Figure A-3). In the Chase Lake area, the moraine is largely covered by lacustrine sand and lies generally at or below the level of the Port Leyden lake terrace. Northwest of Sperryville, however, one of its moraine ridges rises nearly 100 feet above the sand plain. The till is sandy, poorly compacted and contains numerous boulders of metamorphic origin. Locally it is marked by weak platy structure which can be mistaken for true bedding. Coarse-textured ice contact stratified drift is now widely exposed, being generally overlain by lacustrine sand.

Less marked than the Dicob moraine, but probably of similar origin, is the north-south alignment of kettle depressions resulting from the melting out of sediment-covered stagnant ice remnants buried at the waning ice margin. Among kettles in this alignment is the depression that contains Chase Lake, the several basins of the small Hiawatha Lakes directly south of Chase Lake, and others. The deeper basins and those more remote from the incised stream valleys of Independence River and Little Otter Creek contain small lakes while other kettles are dry. These basins are inset below the level of the sand plain in a manner which suggests essentially complete burial of the glacial ice blocks before they melted. Nevertheless, a mixture of coarser washed drift and sandy gravel may be encountered on the lower slopes of the basin walls.

Other kettles are scattered within the sand plain. Sand Pond and Hinchings Pond occupy two such relatively isolated basins which though shallow are sufficiently far from the nearest drainage line that they contain water-table controlled lakes. A large number of kettle basins in the area north and east of Hinchings Pond seem to be related to the rapid burial of stagnant ice which took place where Independence River debouched into Port Leyden Lake.

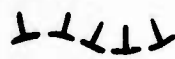
As the ice margin melted away from the north slope of the Tug Hill Plateau northwest of Lowville, meltwater outlets lower than

KEY TO FIGURE A-3

- 1 Medium to coarse sand of Port Leyden Lake terrace.
- 2 Coarse sand to gravel and sand of Port Leyden Lake terrace.
- 3 Dominantly glacial till and coarse stratified drift.
- 4 Dominantly Precambrian rock with discontinuous patches of drift



Dicob moraine (ice marginal alignment)



Chase Lake-Hiawatha inferred ice marginal alignment.

All contacts inferred or approximate.

Base map enlarged from McKeever, Number Four, Lowville and Port Leyden sheets, U. S. Geological Survey 1:62,500 series.



Figure A-3 Chase Lake Site

the Lansing Kill were uncovered. The level of impounded waters in the Black River Valley dropped progressively as each successive outlet was abandoned in favor of the next lower channel. The level of Glenfield Lake (Fairchild, 1912), controlled by these outlets, lay below the Chase Lake sand plain. Instead of debouching at the level of the sand plain, Independence River and Little Otter Creek set about downcutting toward the dropping base level, an incision which continues at the present time. Thus Independence River occupies a gorge 120 feet deep west of Sperryville and the floor of Otter Creek is 200 feet below the level of the sand plain at the southwest edge of the Chase Lake Site. Displaced from the valleys they occupied prior to the last glaciation, both of these streams now expose bedrock in places, thus affording evidence of the buried bedrock topography and facilitating inferences as to thickness of unconsolidated sediment cover.

With disappearance of the continental ice sheet, the diminished load on the earth's crust permitted rebounding or regional upwarping. As a result, features initially aggraded toward a lake level or other datum plane were tilted from the horizontal. Thus, the Port Leyden sand plain controlled by the rock threshold southwest of Booneville at about 1130 feet above sea level was warped upward about 5 feet per mile toward the north and stands now about 1280 feet above sea level at the latitude of Chase Lake.

3. CHASE LAKE SITE

a. Accessibility and Development

The Chase Lake Site is 36 air miles north of Rome and just over 40 miles by way of West Leyden, Constableville, Lyons Falls and Greig (Figure A-1). Presently access to the site is by unpaved, single lane auto trail from the Chase Lake Road toward Sand Pond, or by similar trail from the end of Nortonville Road. In places trails

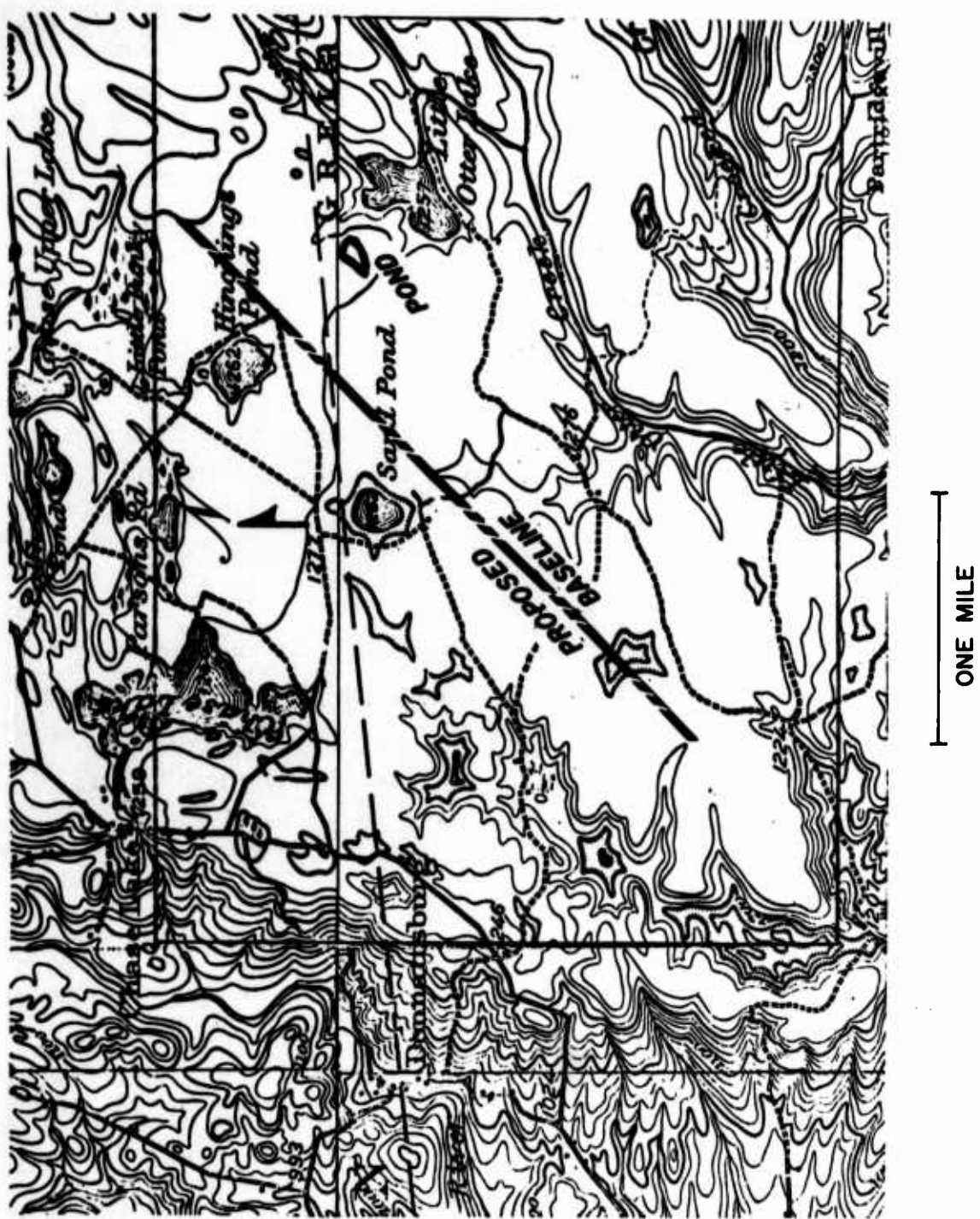
not shown on the map lace the flat woodland of the sand plain which in dry months can be traversed quite readily with or without trail.

The area is almost completely undeveloped and parts are already under state ownership. Many farm dwellings shown on the Lowville and Port Leyden sheets at the time of survey, 50 years ago, no longer exist. On the other hand, resort development has commenced around some of the larger and more attractive lakes. The area in the immediate vicinity of the proposed alignment is essentially devoid of year around habitation and with very few summer'cabins. Single cabins exist on Hinchings Pond, and Little Otter Lake and a larger number on Sand Pond where a boys club from Carthage, New York operates Camp Mohawk as a summer camp. Other clusters of resort cabins have been built in the vicinity of Chase Lake and the Hiawatha Lakes within a mile of the southwest end of the proposed alignment.

b. Topography

The Chase Lake Site is located in essentially undissected remnant of the Port Leyden lacustrine sand plain (Figure A-3), bounded on the southeast and south respectively by Little Otter and Otter Creeks, on the west by the Chase Lake kettle alignment, on the north by an area of kettle-pitted sand plain, and on the east by the Adirondack foot-hills projecting above the plain.

An optimal alignment for the proposed range and angle calibration facility, selected on 14 September 1967 by Dr. Robert Richardson (SURC) and Mr. Donald Zulch (RADC) trends N 55 E, passing within 200 yards of Sand Pond. At its southwest end the alignment is at an elevation of approximately 1270 feet. For two miles northeastward the plain is almost horizontal along the proposed base line. A broad, shallow depression less sharply defined than is suggested by the contours (Figure A-4) is centered southeast of the base line 0.4



miles from its southwest end. A broad, open swale draining south to Little Otter Creek heads within 200 yards of the kettle occupied by Sand Pond, but is relatively shallow and narrow at the proposed alignment. Approximately 2 miles from the southwest end of the alignment, the regional slope increases to 15 to 20 feet per mile, but without marked irregularity.

Extension of the proposed alignment southwestward is prevented by gully dissection toward the Hiawatha-Chase Lake kettle alignment. Northeastward extension of the alignment beyond a length of 3.0 miles encounters minor topographic irregularity. For short distance such features can be avoided, as for example the boggy kettle near Little Otter Lake. Although not previously mapped, it was discovered by Richardson during site reconnaissance. In this area, too, bedrock is at shallow depth and locally exposed (Figure A-5). Should a base line longer than 3 miles become desirable, the most favorable alignment would be gained on an azimuth N 48 E from a point 4000 feet south-southwest of the optimal alignment under present site criteria.

c. Vegetation

Low brush and second growth cover most of the Chase Lake area, apparently taking over from abandoned farm and pastureland. Mature forest is completely lacking. Patches of open forest and park land are composed of scattered spruce and pine among dominant aspen, maple and other hardwoods. Softwood plantation, the cover type that would assure maximum homogeneity is of very limited extent in the immediate area.

The nature and variety of cover at the Chase Lake Site would facilitate clearing and preparation of a base line. The lack of homogeneity is, however, a negative factor in terms of possible optical



Figure A-5 View Near Southeast End of Boggy Kettle which is Located Next to Little Otter Lake, Showing Open and Varied Vegetation. Precambrian Rock, Exposed at this Point, Underlies the Sand Plane at Depths of as much as One Hundred and Fifty Feet

variability due to disturbance and temperature difference within the ground level atmosphere.

d. Soil and Subsoil Materials

The dominant surface soil material in the Chase Lake area is medium to coarse sand. The grains are sub-angular to sub-rounded, somewhat loosely packed and lacking interstitial colloidal material to serve as binder.

Although no soil survey of Lewis County has been published, the soils are considered best assigned to the Adams series, ranging from well-drained to excessively drained brown podzolic soils developed on non-calcareous deltaic sands and showing weak tendency to iron oxide accumulation in the subsoil.

Accordingly the soils afford little problem in the way of drainage. High infiltration capability limits runoff. When the site was examined on 27 March by Richardson and Cracknell, no standing water was observed even though snow melt during the preceding week had been considerable. Poor drainage is limited to near water table situations encountered in kettles which are avoided by the proposed base line alignment. Because of their texture and permeability, these soils are not particularly subject to destructive frost action. Although not close-packed they are stable under reasonable loads. Extensive removal of vegetation cover might make such a surface subject to deflation or wind erosion.

Coarser sand and gravelly sand may underlie the sand below the soil zone and may be encountered near some of the deeper kettle depressions. A dug well at the intersection of trails 3500 feet south-southeast of the southwest end of the proposed base line encountered only medium to coarse sand to depth of 16 feet below the surface.

Glacial till which crops out west of the sand plain in the Dicob moraine area, and probably discontinuously lies between the sand plain deposits and underlying solid rock, is itself sandy and less tight and impermeable than most glacial till.

e. Depth to Bedrock

Without seismic survey, the depth to bedrock in the Chase Lake area can only be inferred by interpolation of presumed topography between areas of present rock exposure. Considerations involved in such interpolation were discussed under "Bedrock topography" (Section 2c).

Near the western end of the small pond shown next to Little Otter Lake, rock crops out at 1300 feet above sea level (Figure A-5). Rock exposures in the bed of Little Otter Creek, south-southeast of Sand Pond are about 40 feet below the level of the sand plain. Westward, bedrock lies below even the deepest kettles in the Chase Lake-Hiawatha alignment. At the western edge of the sand plain the general level of bedrock exposure is near or below 1000 feet above sea level. Buddington (1934) describes the sand plains along their western edge as composed of "sand up to 150 feet in thickness, thinning to zero at the eastern edge where they abut against the mountains."

Accordingly, it is probable that the site evaluation criterion calling for 20 to 30 meters of cover over solid rock is probably safely met below most of the base line. Northeastward, however, beyond 2.5 miles a concealed bedrock knoll if such exists could mean cover less than the desired limit. As part of a development program on this site, seismic survey is recommended, even though it has not been considered essential to the initial site evaluation.

f. Other Considerations

Crustal recovery from unloading due to deglaciation continues to take place in northeastern United States and Canada. In the Chase Lake area recovery rates may be as high as a few tens of centimeters per century. The effect is regional, however and the component of differential uplift within the Chase Lake area should have negligible effect on operation of the proposed facility.

The geologic map (Figure A-2) shows a north-south trending fault contact within 5 miles of the Chase Lake Site but activity along this fault is presumed to have ceased in the geologic past. On the other hand occasional seismic events centered in the St. Lawrence Lowlands may affect the Chase Lake area. Nevertheless this area is considered to be seismically relatively stable.

The Chase Lake site is remote from highways, railroads and population concentrations. No significant sources of noise, vibration or undue air contamination are recognized in the vicinity. Because of location in the snowbelt in the lee of Lake Ontario, the Chase Lake Site experiences an average of more than 4 feet of snowfall per year.

In view of the low level of development, land acquisition problems should be minimal.

APPENDIX B

REFRACTIVE INDEX CORRECTIONS FOR ELECTROMAGNETIC DISTANCE MEASUREMENTS

1. INTRODUCTION:

All electromagnetic distance measuring devices utilize the propagation of electromagnetic waves and most of them operate in such a way that the propagation time is actually measured. This time can be determined with very high accuracy but to convert the result into distance the propagation velocity must be known. It is the error in the knowledge of this velocity that provides the principal limitation on the accuracy of such equipment. In most cases, the velocity of propagation is not constant but instead varies along the ray path. The relationship between distance and time, therefore, involves the average velocity of propagation and may be expressed as:

$$D = \bar{v} t \quad (B-1)$$

where D = the distance being measured

\bar{v} = the average velocity of propagation with respect to time along the ray path

T = the time required for the wave to travel the distance D

The average velocity of propagation can be expressed as

$$\bar{v} = \frac{c}{\bar{n}} \quad (B-2)$$

where c = the velocity of propagation in a vacuum

\bar{n} = the average refractive index with respect to distance along the ray path.

At present, c is known to at least one part in 10^6 and there are indications that this may be improved by an order of magnitude in the not too distant future. This leaves the knowledge of the average index of refraction, n , as the principle source of error in many distance measuring systems.

In practice, there are actually two refractive indexes which must be considered. One, known as the phase refractive index, will be denoted by n_ϕ . It is the average value of this quantity which should be used in Equation (B-2) when the wave contains only a single frequency component. In most cases, however, the radiation will contain components in a narrow frequency band and the group refractive index, n_G , must be used. The group refractive index is related to the phase value by the equation:

$$n_G = n_\phi + \sigma \frac{dn_\phi}{d\sigma} \quad (B-3)$$

where $\sigma = \frac{1}{\lambda}$

λ = the mean wavelength of the radiation in a vacuum

It should be noted that if the medium is not dispersive, n_ϕ is a constant independent of frequency and the group and phase indexes are equal. This occurs in the microwave frequency region.

It has been found for air that the magnitudes of n_ϕ and n_G depend principally upon the temperature, pressure, water vapor content, CO_2 content and the wavelength of the radiation. The actual change of these indexes as a function of the above parameters is quite small for normal environmental variations. For example, if radiation in the visible region is considered, then n_ϕ and n_G will be in the range from 1.000250 to 1.000350 for all normal environmental conditions. Because the variation is in the fourth decimal place, it is convenient to define a new constant, N , called the refractivity:

$$N = (n - 1) \times 10^6 \quad (B-4)$$

The relationship between N_G and N_ϕ , corresponding to Equation (B-3), is therefore:

$$N_G = N_\phi + \sigma \frac{dN_\phi}{d\sigma} \quad (B-5)$$

Since in the visible range N_ϕ decreases with wavelength, the above derivative is positive and N_G is larger than N_ϕ . For the ordinary environmental conditions mentioned above, N_ϕ and N_G will be in the range from 250 and 350.

2. Techniques for Determining the Refractive Index of the Atmosphere in the Visible Range

In the preceding section, it was pointed out that accurate electromagnetic distance measurements require an accurate determination of the refractive index along the ray path, which is normally in the out-of-doors. In many cases, one would like to determine the average index with an accuracy of one part in 10^6 or better in such an environment. For many years people have been working on this problem and numerous solutions have been presented. A number of techniques for directly measuring the phase index in a small region have been developed, but all highly accurate systems require equipment which is physically large and expensive. Such systems are not well suited for use along a lengthy ray path in the out-of-doors. A pair of systems presently under development by Dr. James Owens and Dr. Moody Thompson at ESSA, Boulder, Colorado, take advantage of the dispersion of the atmosphere to make direct measurements of the average refractive index along a lengthy ray path. These systems, when perfected, should provide a very convenient means for determining n with relatively high accuracy. For the time being however, other techniques must be

used.

The best results have been obtained using indirect methods for determining the index. That is, the temperature, pressure and constituents of the atmosphere are measured at a number of points along the ray path and then this data is used to calculate discrete values for the refractive index. These values are then averaged, using standard statistical methods.

A number of formulas have been developed which express the phase refractive index in terms of the quantities upon which it depends. In every case, the expression is based upon data taken in the laboratory, and in some cases, an idealized model was used. At the present time, most people prefer the experimental results reported by Barrell and Sears(15) in 1939. At the same time, these investigators presented a formula relating the index to the various parameters upon which it depends:

$$N_{\phi} = (n_{\phi} - 1) \times 10^6 = \left[0.378125 + 0.00214140^2 + 0.000017930^4 \right] x \\ P \left[\frac{1 + (1.049 - 0.0157t) P \times 10^{-6}}{1 + 0.003661t} \right] - \frac{(0.0624 - 0.00068 \sigma^2) e}{1 + 0.003661t}$$

(B-6)

where P is the total air pressure in mm of Hg

t is the temperature in degrees Centigrade

e is the water vapor pressure in mm of Hg

σ is the reciprocal of the vacuum wavelength
in microns.

This formula applies to air containing 0.03% CO_2 whose pressure lies between 720 and 800 mm of Hg and whose temperature is between 10° and 30°C . It is valid for the range of wavelengths from 0.4358 to 0.6438 microns and forms the basis for the correction procedure presently suggested by the AGA Company for use with

Geodimeters.

It should be noted that the equation can be written in the form:

$$N_{\phi} = [\text{Dispersion Relationship}] [\text{Density Factor}] + [\text{Water Vapor Correction Term}] \quad (B-7)$$

The dispersion relationship contains the dependence upon wavelength and the density factor the dependence upon air pressure and temperature.

Since 1939, considerable effort has been directed toward obtaining more experimental data and better mathematical representations. It turns out however, that the Barrell and Sears density factor and water vapor correction term are still the most widely accepted mathematical relationships covering these aspects of index variation. In the case of the dispersion relationship, an improved formula has been developed by Edlen.(16) This formula is included in the following expression for the refractivity of standard air which he published in 1951:

$$N_{\phi} = 64.328 + \frac{29498.1}{146 - 0^2} + \frac{255.4}{41 - 0^2} \quad (B-8)$$

Standard air is, by definition, dry air containing 0.03% by volume of CO_2 at normal pressure (760 mm Hg at 0°C and $g = 980.665 \text{ cm/sec}^2$) and a temperature of 15°C . When the Barrell and Sears density factor for standard conditions is divided out of the constants 64.328, 29498.1 and 255.4, we obtain the following expression:

Edlen Dispersion Relationship =

$$0.0892351 + \frac{40.9194}{146 - 0^2} + \frac{0.354288}{41 - 0^2} \quad (B-9)$$

When the dispersion relationship portion of Equation (B-6) is replaced by that of Equation (B-9), the following formula results:

$$\begin{aligned}
 N_{\phi} &= (n_{\phi} - 1) \times 10^6 = \\
 &\left[0.0892351 + \frac{40.9194}{146 - \sigma^2} + \frac{0.354288}{41 - \sigma^2} \right] \times \\
 &P \left[\frac{1 + (1.049 - 0.0157t) P \times 10^{-6}}{1 + 0.003661t} \right] \\
 &- \frac{(0.0624 - 0.000680 \sigma^2)e}{1.0 + 0.003661t} \quad (B-10)
 \end{aligned}$$

This formula is widely accepted as the most accurate expression available and it will be used whenever the phase quantities, n_{ϕ} and N_{ϕ} , are required.

It was pointed out earlier that in most practical cases the group refractive index must be used and Equations (B-4) and (B-5) indicate how it may be obtained from the expression for the phase refractivity. The group relationship, corresponding to Equation (B-10) is given by:

$$\begin{aligned}
 N_G &= (n_G - 1) \times 10^6 \\
 &\left[0.0892351 + 40.9194 \frac{146 + \sigma^2}{(146 - \sigma^2)^2} + 0.354288 \frac{41 + \sigma^2}{(41 - \sigma^2)^2} \right] \times \\
 &P \left[\frac{1 + (1.049 - 0.0157 t) P \times 10^{-6}}{1 + 0.003661t} \right] \\
 &- \frac{(0.0624 - 0.00068 \sigma^2)e}{1.0 + 0.003661t} \quad (B-11)
 \end{aligned}$$

This formula will be used to calculate the group quantities, n_G and N_G , whenever they are required. It should be emphasized

that for Equations (B-10) and (B-11):

P = total air pressure, in millimeters of mercury (Hg)
t = temperature in degrees centigrade
e = water vapor pressure in millimeters of mercury
 σ = $1/\lambda$ = the wave number
 λ = average vacuum wavelength of the transmitted radiation in microns.

Both equations provide values of N which are accurate to better than ± 0.1 for air containing 0.03% by volume of carbon dioxide, for wavelengths between 0.4358 and 0.6438 microns, air pressure between 720 and 800 mm of Hg and temperature between 10° and 30°C. These limitations are not serious except for temperature, where for outdoor measurements the value is often below 10°C (50°F). The above formulas are recommended as the best available for use in this region also, although no experimental verification of their accuracy is known to exist. When maximum accuracy is required, measurements should be made for temperatures between 10° and 30°C.

Of course, high accuracy in the determination of n requires that wavelength, temperature, pressure, etc. be known with sufficient accuracy. To get an idea of what sort of accuracy is required in the determination of these quantities, let the error in n_G be expressed as:

$$\begin{aligned}\Delta n_G &= \Delta N_G \times 10^{-6} \\ &= \left[\frac{\partial N_G}{\partial t} \Delta t + \frac{\partial N_G}{\partial P} \Delta P + \frac{\partial N_G}{\partial e} \Delta e + \frac{\partial N_G}{\partial \lambda} \Delta \lambda \right] \times 10^{-6}\end{aligned}\tag{B-12}$$

where Δn_G = the error in group refractive index.

Δt = the error in the determination of the temperature at a given point along the ray path.

ΔP = the error in determination of the total air pressure in mm of Hg.

Δe = the error in the determination of the water vapor pressure in mm of Hg.

$\Delta \lambda$ = the error in the determination of the effective wavelength of the radiated signal in microns.

and the errors are assumed to be sufficiently small. Also, let the following typical values for the pertinent quantities be assumed:

$$P = 760 \text{ mm}$$

$$t = 20^\circ\text{C}$$

$$e = 10.4 \text{ mm (60\% Relative Humidity)}$$

$$\lambda = 0.6328 \text{ microns}$$

The graphs of Figures B1-B5 then indicate the values of the various partial derivatives included in Equation B-12. Special mention should be made of the method for evaluating $\frac{\partial N_G}{\partial t}$. This quantity will consist of the sum of two terms, one, obtained from Figure (B-1) is due to the density factor and the other, obtained from Figure (B-2), is due to the water vapor correction term. A similar situation occurs for $\frac{\partial N_G}{\partial \lambda}$ where contributions from both the dispersion relationship and the water vapor correction term exist. The latter quantity may be neglected, however, because of its small size. When the values of the derivatives are substituted into Equation (B-12), we obtain:

$$\Delta n_G = [-0.965 \Delta t + 0.368 \Delta P - 0.053 \Delta e - 34 \Delta \lambda] \times 10^{-6} \quad (\text{B-13})$$

In terms of standard deviations, σ , Equation (B-13) may be expressed as:

$$\sigma_{n_G} = \left[(0.956)^2 \sigma_t^2 + (.368)^2 \sigma_P^2 + (.053)^2 \sigma_e^2 + (34)^2 \sigma_\lambda^2 \right]^{1/2} \times 10^{-6} \quad (\text{B-14})$$

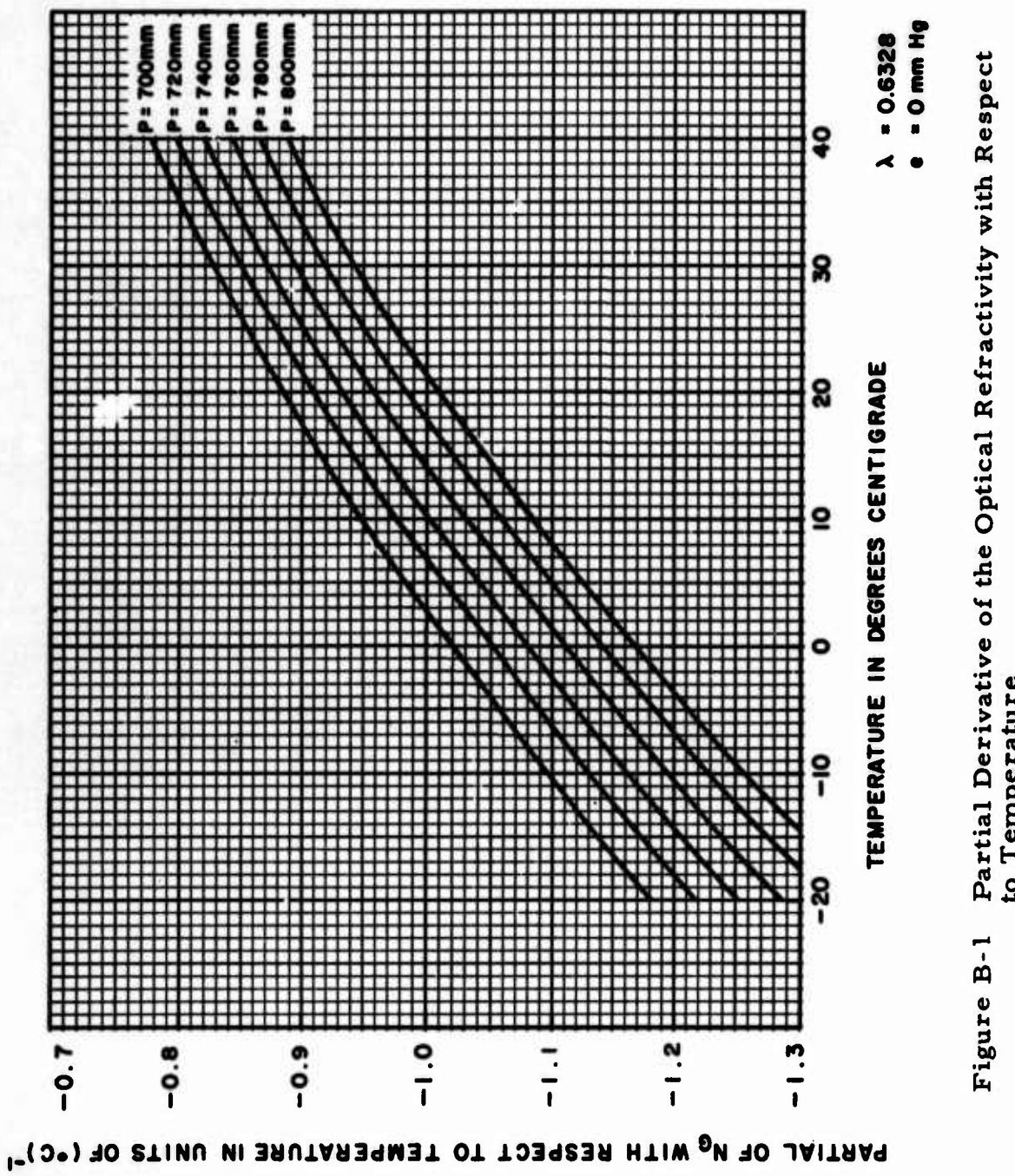


Figure B-1 Partial Derivative of the Optical Refractivity with Respect to Temperature

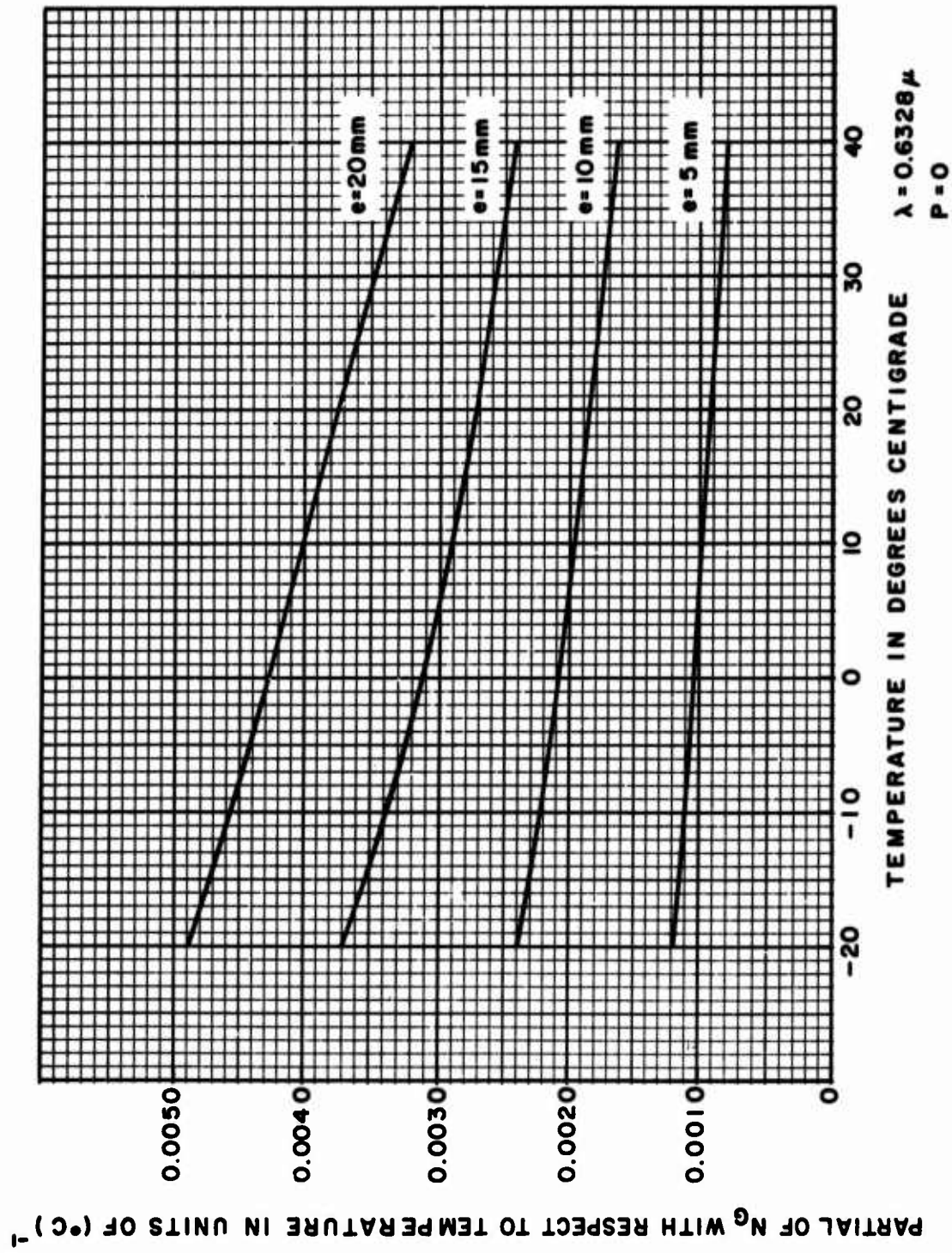


Figure B-2 Partial Derivative of the Optical Refractivity with Respect to Temperature

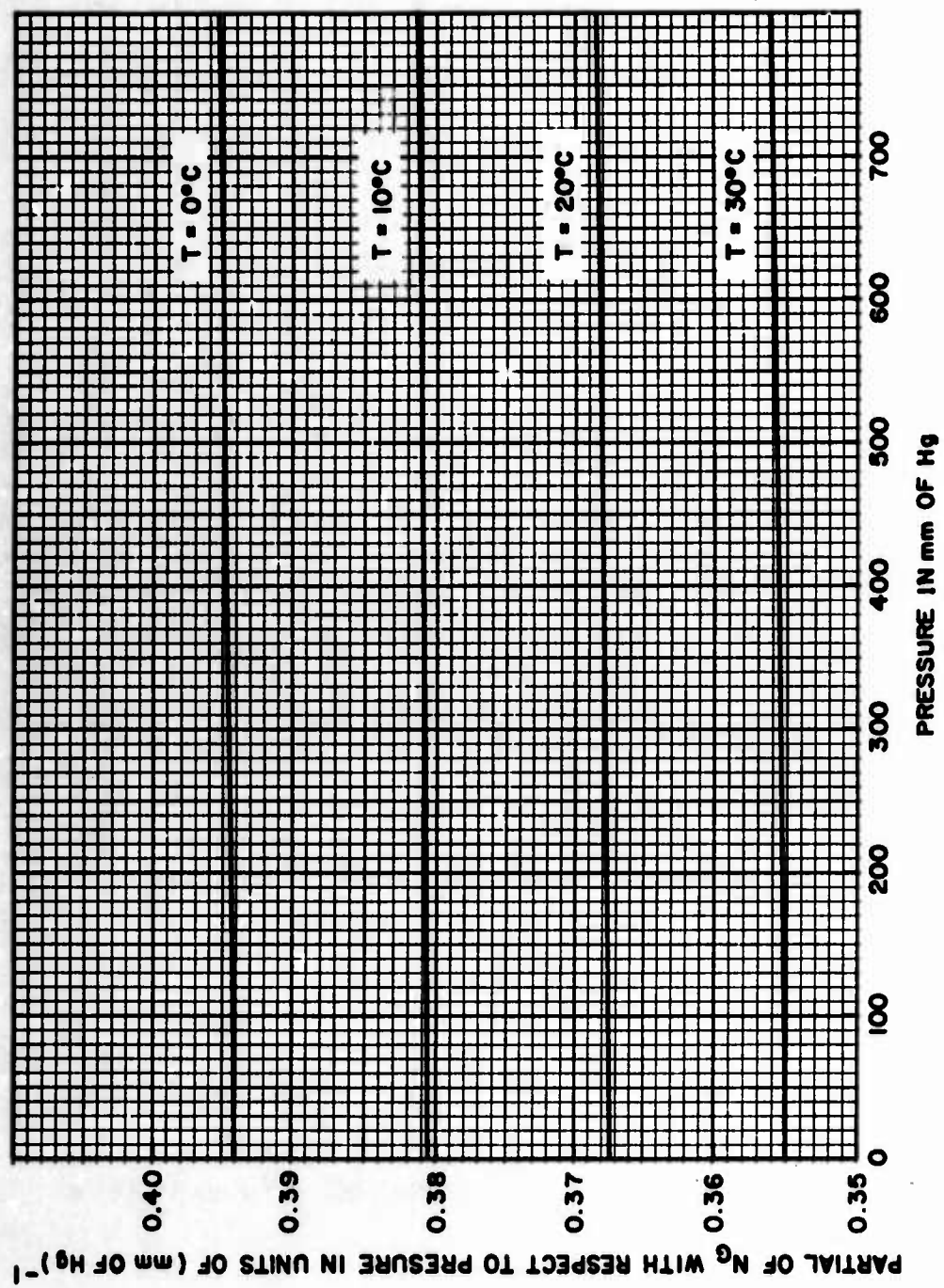


Figure B-3 Partial Derivative of the Optical Refractivity with Respect to Pressure

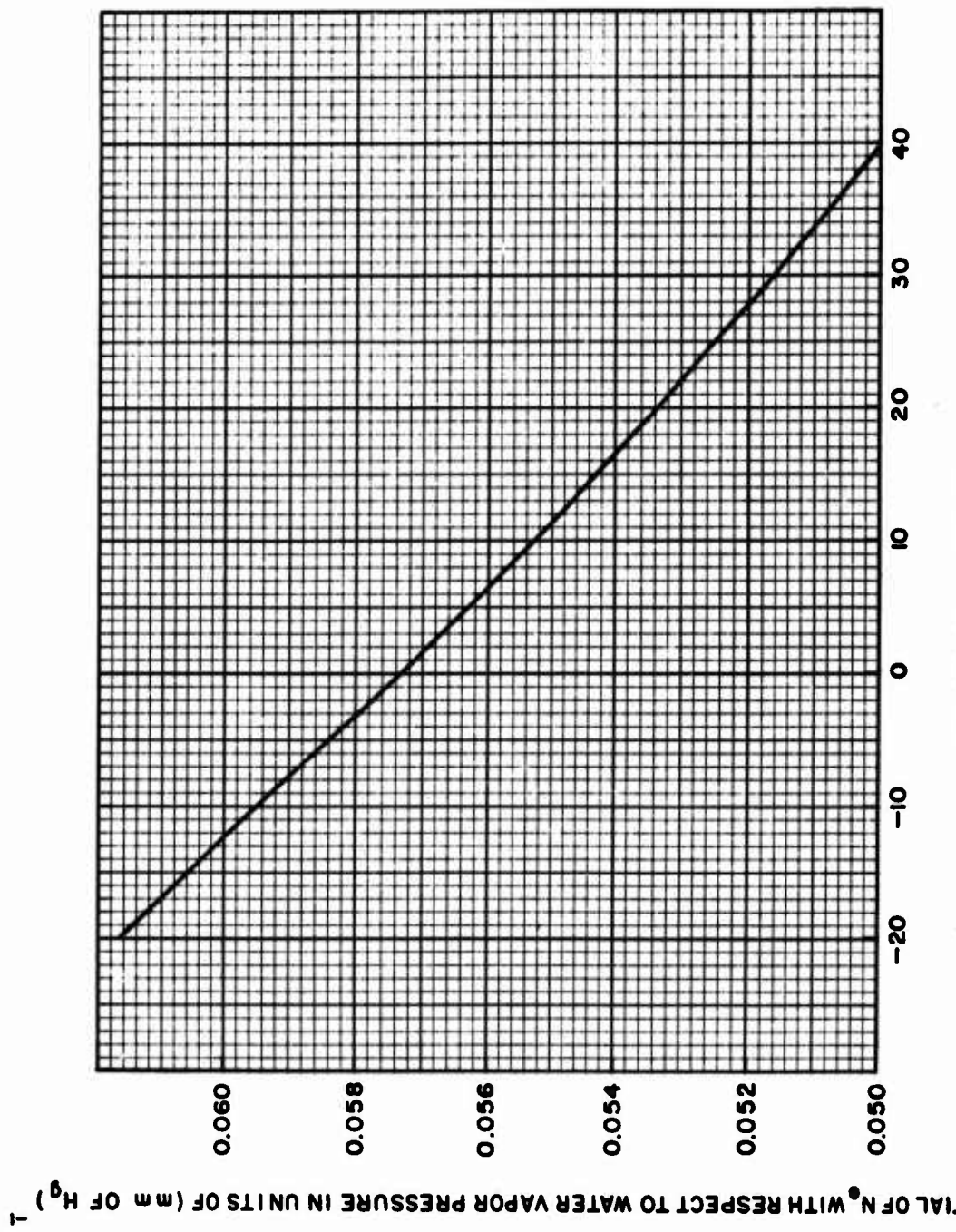


Figure B-4 Partial Derivative of the Optical Refractivity with Respect to Water Vapor Pressure

PARTIAL OF N_G WITH RESPECT TO WAVELENGTH IN UNITS OF (MICRONS)⁻¹

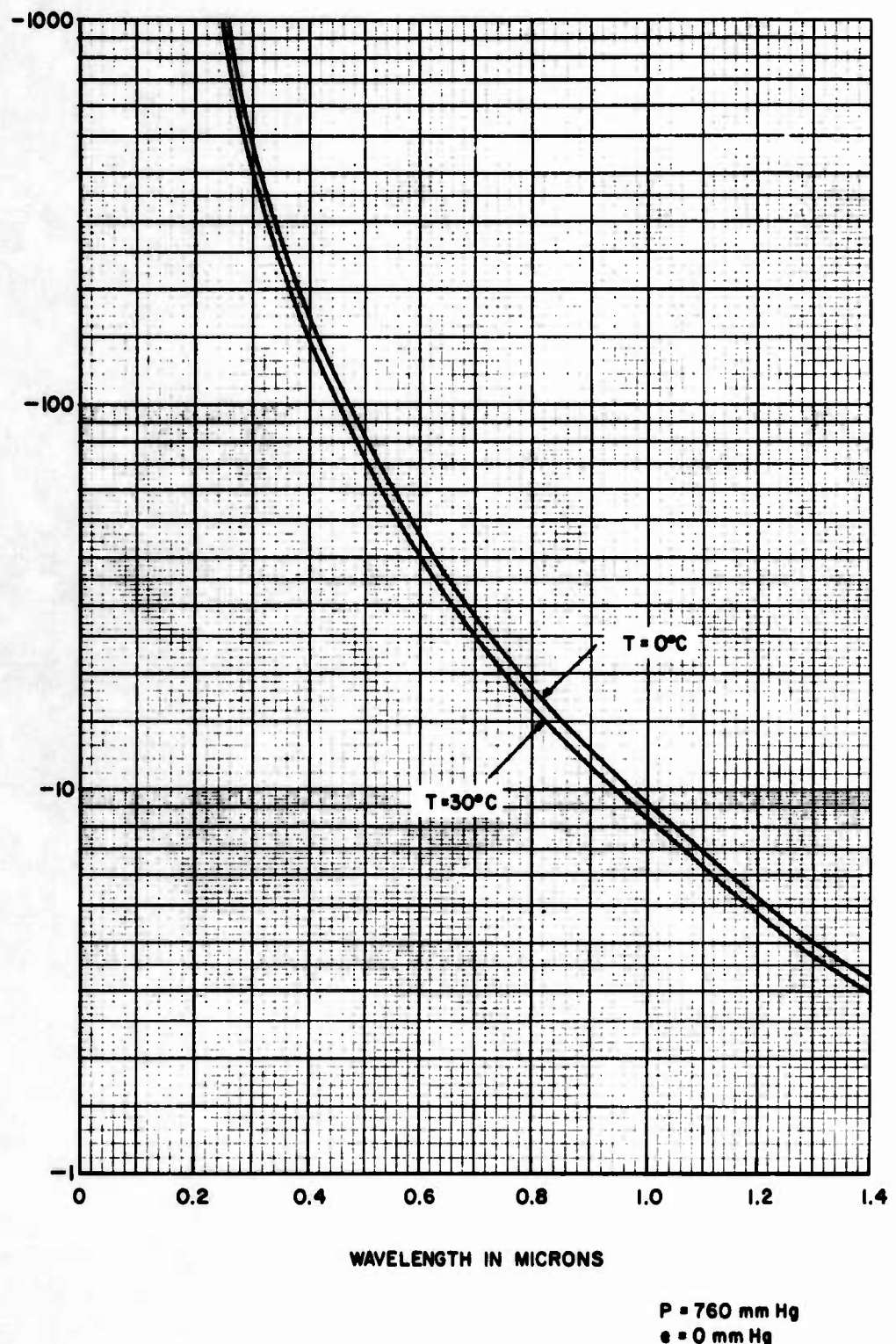


Figure B-5 Partial Derivative of the Optical Refractivity with Respect to Wavelength

where Δt , ΔP , Δe and $\Delta \lambda$ are assumed to be independent and have zero average values.

A study has been carried out to determine how small each of the error terms can be made without resorting to excessively complicated and expensive instrumentation. Typical values were found to be

$$\begin{aligned}\sigma_t &= 0.05^\circ\text{C} \\ \sigma_P &= 0.10 \text{ mm of Hg} \\ \sigma_e &= 1.0 \text{ mm of Hg} \\ \sigma_\lambda &= 10^{-4} \text{ microns}\end{aligned}$$

When these values are substituted into the above equation we get:

$$\begin{aligned}\sigma_{n_G} &= \left[23.28 \times 10^{-4} + 13.54 \times 10^{-4} + 28.09 \times 10^{-4} + 0.116 \times 10^{-4} \right]^{1/2} \times 10^{-6} \\ &= 0.0806 \times 10^{-6} \quad (\text{B-15})\end{aligned}$$

If Gaussian distributions with zero means, are assumed for all of the errors, then it can be said that for 68% of all determinations Δn_G will be less than 0.0806×10^{-6} . In 95% of all cases the error will be less than 0.161×10^{-6} .

An examination of the various factors contributing to Δn_G indicates that the temperature and pressure measurements are the most critical. If maximum accuracy is required, as for example while calibrating a standard baseline, then the use of sophisticated temperature and pressure measuring systems would be necessary. In such a case, the standard deviation of these measurements probably could be reduced to values somewhat below those listed above, thereby decreasing the error in n_G .

Once the refractive index has been determined at many

points along the ray path, it then becomes necessary to determine the average value. The best way to do this is to assume that the index varies in a linear manner between the sample points and to calculate an average based on this. If the samples are taken at M equally spaced points along the line, including the ends, then the average is given by:

$$\bar{n} = \frac{1}{M-1} \left[\frac{n_1 + n_M}{2} + \sum_{m=2}^{M-1} n_m \right] \quad (B-16)$$

where n_1 and n_M are the values obtained at the two ends of the line and \bar{n} is the refractive index averaged with respect to distance.

3. Determining the Refractive Index of the Atmosphere at Radio and Microwave Frequencies

In the microwave and radio frequency ranges, the refractive index of the atmosphere is a constant, independent of frequency. Therefore the group and phase indexes are the same and it is not necessary to make any distinction between them

Several means for measuring the refractive index are possible with the most accurate devices making use of small resonant cavities. Such devices, known as refractometers, are physically large, expensive and there is no real assurance that the atmosphere within the cavity is typical of that in the neighborhood of the device. Furthermore, the size of this device is such that its presence can result in undesirable temperature gradients.

As in the optical case, an alternative technique consists of measuring the temperature, pressure and constituents of the atmosphere and then calculating the effective index by means of an appropriate formula. Through the years a number of formulas have been developed for making such a determination and one was adopted by the International Association of Geodesy in 1960. This

expression, developed by Essen and Froome, may be written as:

$$N = (n-1) \times 10^6 = \frac{103.49}{T} P_d + \frac{86.26}{T} \left[1 + \frac{5748}{T} \right] e \quad (B-17)$$

where n = is the refractive index of the atmosphere

P_d = the dry air pressure in millimeters of mercury

e = the water vapor partial pressure in millimeters of mercury

T = the temperature in degrees Kelvin.

This formula will be used to determine the radio refractive index whenever it is required.

It should be mentioned that:

$$P = P_d + e$$

where P is the total air pressure measured with a barometer.

Equation (B-17) is a simplified version of the more complete formula:

$$N = (n-1) \times 10^6 = \frac{103.49 P_d}{T} + \frac{177.4 P_c}{T} + \frac{86.26}{T} \left[1 + \frac{5748}{T} \right] e \quad (B-18)$$

where P_c is the CO_2 partial pressure in mm and

$$P = P_c + P_d + e$$

When using Equation (B-17) the carbon dioxide term is ignored and the pressure, P_d , actually includes the CO_2 component. The same result would be obtained if the 177.4 factor in Equation (B-18) were changed to 103.49. This would produce a 42% change in the magnitude of the CO_2 factor. To get an idea of the effect of using Equation (B-17) rather than Equation (B-18), consider the following statistics concerning the composition of the atmosphere (exclusive of water vapor) (17) :

<u>Constituent</u>	<u>Content (percent by volume)</u>
Nitrogen	78.084 \pm 0.004
Oxygen	20.946 \pm 0.002
Carbon Dioxide	0.003 \pm 0.001

For a temperature of 15°C and P = 760 mm, the CO₂ pressure, P_c, would be approximately 0.25 mm and the CO₂ term in Equation (B-18) would be approximately 0.154. If Equation (B-17) were used instead, with the CO₂ pressure being included in the dry air term, the difference in N would be 0.064. For the purposes of this study, such a difference is negligible and therefore the simpler form of Equation (B-17) will be used.

A significant question at this point is: "How accurate is the Essen and Froome formula?" Unfortunately, the amount of experimental evidence available to verify this expression is not large. Through the years the index has been measured using several different techniques and the results have shown considerably more variation than was found in the optical region. Table (B-1) contains some of the values which have been obtained. Some of the measurements were actually made under different conditions of temperature and pressure and the results reduced to standard conditions for comparison. The third column indicates the value of N for dry air at 0°C temperature and 760 mm of pressure and the fourth column the value of N for an atmosphere of pure water vapor. In both cases, no carbon dioxide was present.

Examination of the table shows that the experimental results for dry air differ by as much as 15 N units, with most values being close to 288.099, the value obtained using Equation (B-17) (the first item in the table). On the basis of the data it is concluded that the formula is probably accurate to about one part in 10⁶ when used to determine the refractive index of air containing water vapor. This, of course, assumes that there is no significant

TABLE B-1

EXPERIMENTAL VALUES FOR RADIO REFRACTIVE INDEX

Author or Source	Frequency mhz	Year	$0^{\circ}\text{C}, 760\text{mm}$ $(n_{\text{air}} - 1) \times 10^6$	$T=20^{\circ}\text{C}, 10\text{mm}$ $(n_w - 1) \times 10^6$
Essen and Froome Formula			288.099	60.699
Sanger	1.0	1930		62.7
Watson	0.5	1934	288.2	
Stranathan	0.5	1935		61.3 \pm 0.4
Hector and Woernley	1.0	1946	283.7	
Crain	9000	1948	286	61.3
Lyons, Birnbaum, and Kryder	9000	1948	288.7	
Phillips	3000	1950	299.2	62.4
Birnbaum, Kryder, and Lyons	9000	1951	287.9 \pm 0.7	
Essen and Froome	24,000	1951	288.15 \pm 0.10	60.7 \pm 0.1
Barrell		1951	287.8 \pm 0.1	
Hughes and Armstrong	3000	1952	284.7 \pm 2.0	
Essen	9000	1953	288.2 \pm 0.1	60.7 \pm 0.2
Saito	9000	1955	287.2 \pm 1.25	

error in the determination of P_d , e and T.

It turns out however, that in practice the errors in P_d , T and especially e are often far from insignificant. If one takes partial derivatives of Equation (B-17) the following results are obtained at $P = 760$ mm, and $e = 10$ mm

$$\frac{\partial N}{\partial e} = 5.92$$

$$\frac{\partial N}{\partial P_d} = 0.36 \quad (B-19)$$

$$\frac{\partial N}{\partial T} = -1.15$$

If the standard deviations of the errors in measuring the atmospheric quantities are given by:

$$\sigma_T = 0.05^\circ C$$

$$\sigma_{P_d} = 0.2 \text{ mm of Hg} \quad (B-20)$$

$$\sigma_e = 0.3 \text{ mm of Hg}$$

then, as in the previous section, we may write that the standard deviation of the error in determining n (σ_n) is given by:

$$\begin{aligned} \sigma_n &= \left[(1.15)^2 \sigma_T^2 + (0.36)^2 \sigma_{P_d}^2 + (5.92)^2 \sigma_e^2 \right]^{1/2} \times 10^{-6} \\ &= 1.77 \times 10^{-6} \\ &= 1.77 \text{ N units} \end{aligned} \quad (B-21)$$

It is obvious that, under the conditions described here, the average radio refractive index along a baseline cannot be computed with an error whose standard deviation is less than one N unit even

if Equation (B-17) is completely accurate. In fact, it appears that errors of two or more N units are possible especially when one considers that the quantities are not measured at every point along the ray path, but rather are sampled at discrete points. The values of the index calculated at these points are combined statistically in the manner described in the previous section to obtain the average for the ray path.

When sections 2 and 3 of this appendix are considered, it is found that the atmospheric limitations which normally exist are such that electromagnetic distance measurements made using optical wavelengths can be about ten times as accurate as the best microwave measurements. It is for this reason that all new, highly accurate distance measuring devices operate in the visible region.

4. APPLICATION OF REFRACTIVE INDEX FORMULAS

The sort of correction which must be applied to measurements made with a particular electromagnetic instrument depends upon the manner in which the device was originally calibrated. For example, assume that the equipment was calibrated such that it produces an accurate indication of the distance when operating in a vacuum. When used in the atmosphere the equipment will provide a distance measurement, denoted by S, which is related to the true distance, D, by the equation:

$$D = \frac{S}{\bar{n}} \quad (B-22)$$

where $\bar{n} = 1 + \bar{N} \times 10^{-6}$ and \bar{N} is the average of the values obtained using either Equation (B-10), (B-11) or (B-17) depending upon the characteristics of the transmitted radiation. Most practical devices transmit a multi-frequency signal thereby requiring the use of the group refractive index given by either Equation (B-11) or (B-17).

For another device, assume that calibration has been carried out in such a way that accurate distance measurements are produced for $t = t_0$ °C., $P = P_0$ mm of Hg and $e = e_0$ mm of Hg. In this case the relationship between the measured value and the correct value is given by:

$$D = \frac{S n(t_0, P_0, e_0)}{\bar{n}} \quad (B-23)$$

Here also the indexes may be either the group or phase values depending upon the characteristics of the transmitted radiation.

REFERENCES

1. McNish, A G., "The Speed of Light", IRE Transactions on Instrumentation, Vol. 11, December 1962, pp. 138-148.
2. Bruins, C. J., Standard Base Loenermark, Publication of the Netherlands Geodetic Commission, 1964.
3. Heiskanen, W A , "Geodetic Standard Baselines and the Dimensions of the Earth," Estratto dal Bolletino di Geodesia e Scienze Affini, Rivista dell 'Istituto Geografico Militare, Anno XXII-N4-Ottobre-Novembre, 1963.
4. Heiskanen, W A ., "The Finnish 864m-Long Nurmela Standard Baseline Measured with Viäsälä Light Interference Comparator," Bulletin Geodesique, Vol. 17, 1950.
5. Kukkamaki, T J. and Honkasalo, T., "Measurement of the Standard Baseline of Buenos Aires with Väisälä Comparator," Bulletin Geodesique, No. 34, 1954.
6. Honkasalo, T., "Measurement of Standard Baseline with the Väisälä Light Interference Comparator", Journal of Geophysical Research, Vol. 65, #2, February, 1960.
7. Negri, Heliodoro, "Väisälä Light Interference Comparator-A Valuable Contribution to the Geodesy of Today," Am. Acad. Scient. Fennical A III, 1961.
8. Ditchburn, R.W., Light, John Wiley, 1963, p. 353.
9. Vali, V., Krogstad, R S. and Vali, W., "Measurement of Earth Tides and Continental Drift with Laser Interferometer," Proceedings of IEEE, July 1964, pp. 857-858.
10. Vali, V., Krogstad, R S. and Moss, R.W., "Laser Interferometer for Earth Strain Measurements," The Review of Scientific Instruments, Vol. 36, No. 9, September 1965, pp. 1352-1355.
11. Vali, V., Krogstad, R S. and Moss, R W., "Observation of Earth Tides Using a Laser Interferometer," Journal of Applied Physics, Vol. 37, No. 2, February 1966, pp. 580-582.
12. Simmons, L.G., "A Singular Geodetic Survey," Technical Bulletin No. 13, USC and GS, September, 1960.

13. USC and GS Special Bulletin No. 247, p. 9.
14. Sutton, O.G., Micrometeorology, McGraw-Hill, 1953.
15. Barrell, H. and J. E. Sears, "The Refraction and Dispersion of Air for the Visible Spectrum," Philosophical Transactions of the Royal Society of London A 238: 1-64, 1939.
16. Edlen, B., "The Dispersion of Standard Air," Journal of the Optical Society of America 43: 339-344, May 1953.
17. Handbook of Chemistry and Physics, 42nd Edition, 1960.

UNCLASSIFIED

Security Classification

DOCUMENT CONTROL DATA - R & D

(Security classification of title, body of abstract and indexing annotation must be entered when the overall report is classified)

1. ORIGINATING ACTIVITY (Corporate author) Syracuse University Research Corporation Merrill Lane Syracuse, New York 13210		2a. REPORT SECURITY CLASSIFICATION UNCLASSIFIED
		2b. GROUP N/A
3. REPORT TITLE RANGE AND ANGLE CALIBRATION FACILITY STUDY		
4. DESCRIPTIVE NOTES (Type of report and inclusive dates) Final		
5. AUTHOR(S) (First name, middle initial, last name) Dr. Robert L. Richardson		
6. REPORT DATE August 1968	7a. TOTAL NO. OF PAGES 210	7b. NO. OF REFS 17
8a. CONTRACT OR GRANT NO. AF 30(602)-4215	8c. ORIGINATOR'S REPORT NUMBER(S)	
8b. PROJECT NO. 6512	8d. OTHER REPORT NO(S) (Any other numbers that may be assigned this report) RADC-TR-68-300	
10. DISTRIBUTION STATEMENT This document is subject to special export controls and each transmittal to foreign governments or foreign nationals or their representatives may be made only with prior approval of RADC (EMASI), GAFB, NY 13440.		
11. SUPPLEMENTARY NOTES	12. SPONSORING MILITARY ACTIVITY Rome Air Development Center (EMASI) Griffiss Air Force Base, New York 13440	
13. ABSTRACT <p>Design criteria for a time delay and angle calibration facility was developed. A site survey was performed in Central New York and a site with a 2.5 mile line was located. Means for calibration of the line length and refractive index of the atmosphere are outlined. Measurements were taken on a 500 KM line at Ohio State University. These measurements tested the refractive index correction technique and the spectra physics model 30 Geodolite and AGA Corp. Model 4B Geodimeter.</p>		

DD FORM 1 NOV 68 1473

UNCLASSIFIED

Security Classification

UNCLASSIFIED

Security Classification

14. KEY WORDS	LINK A		LINK B		LINK C	
	ROLE	WT	ROLE	WT	ROLE	WT
Calibration Geodesy Optical Interferometer Temperature Measurement Propagation Correction						

UNCLASSIFIED

Security Classification